PDR

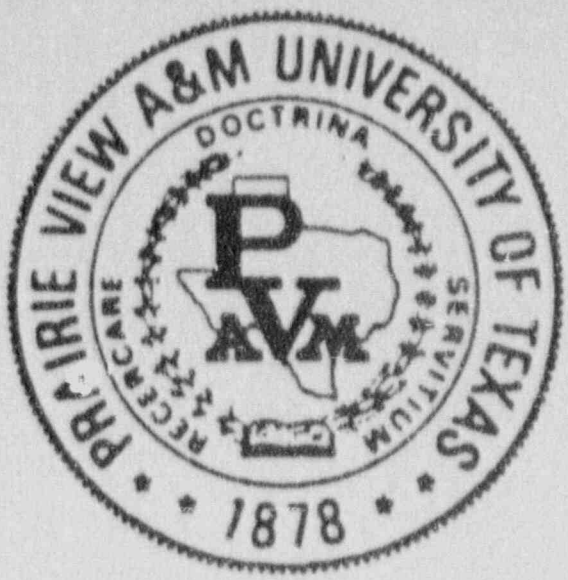

A

REPORT

FROM

THE

THERMAL SCIENCE RESEARCH CENTER (TSRC)

DIRECTOR: DR. RONALD D. BOYD, Ph.D., P.E.
HONEYWELL ENDOWED PROFESSOR OF ENGINEERING
P.O. Box 397
Prairie View A&M University
Prairie View, Texas 77446
(409) 857-4811 (2827 or 4023)

F03
0/1

SUBCOOLED FLOW BOILING MODEL ASSESSMENT AND DEVELOPMENT

INTERIM REPORT
December 20, 1992

TSRC – 2

Submitted to:

The U.S. Nuclear Regulatory Commission (NRC)

From the:

THERMAL SCIENCE RESEARCH CENTER(TSRC)

by

Xiaowei Meng (Graduate Student), and

Dr. Ronald D. Boyd (P.I.)
Honeywell Endowed Professor of Engineering and
Director of Thermal Science Research Center
College of Engineering and Architecture
Prairie View A&M University
Prairie View, TX 77446
(409) 857-4811, 4023, or 2827

Project No. NRC-04-91-364

SUBCOOLED FLOW BOILING MODEL ASSESSMENT AND DEVELOPMENT

INTERIM REPORT
December 20, 1992

TSRC – 2

PRAIRIE VIEW A&M UNIVERSITY
Thermal Science Research Center(TSRC)

Dr. Ronald D. Boyd, P. I.,
Honeywell Endowed Professor
and Director of the TSRC.

SUBCOOLED FLOW BOILING MODEL ASSESSMENT AND DEVELOPMENT

Xiaowei Meng[1], and Ronald D. Boyd[2]

EXECUTIVE SUMMARY

The physical phenomenon of forced convective boiling is probably one of the most interesting and complex transport phenomena. It has been under study for more than two centuries. Simply stated, forced convective subcooled boiling involves a locally boiling fluid: (1) whose mean temperature is below its saturation temperature, and (2) that flows over a surface exposed uniformly or non-uniformly to a high heat flux (HHF) . In physical cases where it is feasible, flow boiling is one of the most efficient techniques of transferring HHFs. A precise knowledge of subcooled flow boiling is essential in many engineering applications, which include research fission and fusion reactor components, high-power synchrotron and optical components, and advanced electronic component packaging. Such examples are characterized as HHF applications which can only be accommodated by subcooled flow boiling.

Accurate subcooled flow boiling conditions are usually represented by the boiling curve, which describes the relationship between the applied heat flux and the wall temperature, and hence the heat transfer coefficient for the given flow conditions. Complete and accurate representation of this curve for HHF applications requires the identification and characterization of various flow regimes and transition boundaries which include: (1) single-phase (sp) heat transfer regime, (2) onset to partial nucleate boiling (ONB), (3) partial nucleate boiling (pnb) heat transfer regime, (4) onset to fully developed boiling (OFDB), (5) fully developed boiling (FDB) heat transfer regime, and (6) the critical heat flux (CHF). Although much work in characterizing the boiling curve at low heat flux levels has been completed, there are still many uncertainties and inaccuracies in HHF applications.

---

[1] Graduate Student

[2] Honeywell Endowed Professor of Engineering and Director of the Thermal Science Research Center (TSRC)

The objective of this research is to assess and/or improve our present ability to predict local heat transfer and critical heat flux in the subcooled flow boiling regime for the case of uniformly heated coolant channels. This requires an accurate and complete representation of the boiling curve up to and including the critical heat flux.

This interim report is not intended to report all the work which has been completed or that is in progress. Rather, it is intended to represent some of the preliminary results. Certain sections in this report have only one section and are usually denoted by .1 (e.g., 4.1) in the text. The implication is that additional sections will be added to form the final report. Regular summaries of the progress of this research, which are enclosed in Appendix D, have been reported to the Nuclear Regulatory Commission.

Several existing heat transfer models were examined for: (1) accurate representation of the boiling curve, and (2) characterizing the local heat transfer under HHF conditions. Comparing with HHF data showed that major correlation modifications were needed in the pnb region. Since the slope of the boiling curve in this region is important to assure continuity of the HHF trends into the FDB region and up to CHF, accurate characterization in the pnb region is essential. Approximations for the asymptotic limits for the pnb region have been obtained and have been used to develop a new correlation. The developed correlation has been compared with 365 water data points. The agreement is encouraging. In predicting the local heat transfer coefficient, the over-all percent standard deviation (psd) with respect to the data was 19% for the high velocity water data. The over-all psd for the absolute wall temperature was less than 3.0%. The conditions for the water data included an exit pressure of 0.77 MPa, exit subcooling varying from 50 to 85 K, and Peclet number greater than 10^5.

In order to increase the range of the physical properties of the data, 155 freon-11 data points were also compared with the modified correlation. However, the freon data were obtained originally by making local circumferential outside wall temperature measurements on the test section. These measurements were numerically converted to values of the local inside wall temperature and local heat transfer coefficient. Prelimiary comparisons show that the absolute wall temperatures were predicted to less than 3.0%. However, additional improvements can be made to the numerical model for better correlation with the local heat transfer coefficient.

Many HHF devices have very narrow channels or employ heat transfer

enhancement schemes such twisted tapes, composite materials, and hyper-vapotrons. If effective flow parameters such as the Reynolds can be defined for these schemes, the present envolving modified correlation may prove to be applicable.

ACKNOWLEDGMENTS:

This study has been financially supported by the U. S. Nuclear Regulatory Commission under contract number NRC-04-91-364. The authors are appriciative especially to the Science and Engineering Alliance (SEA) and its director Dr. Robert L. Shepard for their support and suggestions. Finally the authors are appreciative to Mr. Robert Effinger, Mr. Bruce Cunningham, and the Prairie View A&M Research Foundation Staff for their continual support and assistance.

TABLE OF CONTENTS

TABLE OF FIGURES

NOMENCLATURE

A	area, m^2
A_c	cross section area of tube, m^2
A_s	external tube surface area, m^2
A_1	half node area in heat resistance formula, m^2
A_2	quarter node area in heat resistance formula, m^2
a	constant in Kandlikar's equation
Bi	Biot number, $\frac{hR_1}{k}$
Bo	Boiling number
b	constant in Kandlikar's equation
c_p	specific heat, $\frac{J}{kgK}$
D	inside diameter, m
f	friction factor in Petukhov's correlation
f_1	friction factor in Shah's correlation
G	mass velocity, $\frac{kg}{m^2 s}$
h	heat transfer coefficient, $\frac{W}{m^2 C}$
h_{lo}	heat transfer coefficient for total flow assumed to be liquid, $\frac{W}{m^2 C}$
h_{pb}	partial boiling heat transfer coefficient, $\frac{W}{m^2 C}$
h_{sp}	single phase heat transfer coefficient, $\frac{W}{m^2 C}$
h_{tp}	fully developed boiling heat transfer coefficient, $\frac{W}{m^2 C}$

$h(i)$	local circumferential heat transfer coefficient, $\frac{W}{m^2 \cdot C}$
i	enthalpy of fluid, $\frac{J}{kg}$
i_f	enthalpy of saturated liquid $\frac{J}{kg}$
i_{fg}	latent heat of vaporization, $\frac{J}{kg}$
i_{inlet}	inlet fluid enthalpy, $\frac{J}{kg}$
i_{exit}	exit fluid enthalpy, $\frac{J}{kg}$
$i_b(Z)$	local fluid enthalpy, $\frac{J}{kg}$
K_1	constant given in Petukhov's correlation
K_2	constant given in Petukhov's correlation
k	thermal conductivity of tube, $\frac{W}{m^\circ C}$
k_f	thermal conductivity of liquid, $\frac{W}{m^\circ C}$
L	length of channel, m
Nu_D	Nusselt number, $\frac{hD}{k}$
Nu_{sp}	Nusselt number in single phase
Pe	Peclet number, $\frac{GDc_p}{k}$
P_{exit}	exit pressure, MPa
Pr	Prandtl number, $\frac{c_p \mu}{k}$
Pr_f	Prandtl number for liquid
Q	total applied power, W
Ql	power loss, W

q	inner heat source, W
$q^{"}$	heat flux, $\frac{W}{m^2}$
$q^{"}_E$	heat flux at onset of fully developed boiling(FDB), $\frac{W}{m^2}$
$q^{"}_{FDB}$	heat flux at onset of fully developed boilind, $\frac{W}{m^2}$
$q^{"}_{ONB}$	heat flux at onset of nucleate boiling (ONB), $\frac{W}{m^2}$
$q^{"}_{PB}$	heat flux in partial boiling region, $\frac{W}{m^2}$
$q^{"}_{SP}$	heat flux in single-phase region, $\frac{W}{m^2}$
Re_D	Reynolds number, $\frac{GD}{\mu}$
R_1	inside radius, m
R_2	outside radius, m
R	ratio of radius to inside radius $\frac{r}{R_1}$
$R(i,j)$	heat resistance in r direction, $\frac{^\circ C}{W}$
$RC(i,j)$	heat resistance in φ direction, $\frac{^\circ C}{W}$
r	radial coordinate, m
Δr_{cop}	mesh size in copper, m
Δr_{ins}	mesh size in insulation, m
St	Stanton number, $\frac{Nu}{Pe} = \frac{q^{"}}{Gc_p\Delta T}$
T	temperature, $^\circ C(K)$
T_{inlet}	inlet temperature, $^\circ C$
T_b	bulk temperature, $^\circ C$

GREEK

ρ density, $\frac{kg}{m^3}$

μ viscosity, $\frac{N_s}{m^2}$

μ_b viscosity of bulk fluid, $\frac{N_s}{m^2}$

μ_w viscosity at wall temperature, $\frac{N_s}{m^2}$

φ circumferential coordinate

σ surface tension, $\frac{N}{m}$

ϵ temperature tolerance, $^\circ C$

SUBSCRIPTS

B	bulk liquid
b	bulk liquid
FC	forced convection
f	liquid or film
l	liquid
g	gas or vapor
w	wall
FDB or E	fully developed boiling
ONB	onset of nucleate boiling

ρ density, $\frac{kg}{m^3}$

μ viscosity, $\frac{N_s}{m^2}$

μ_b viscosity of bulk fluid, $\frac{N_s}{m^2}$

μ_w viscosity at wall temperature, $\frac{N_s}{m^2}$

φ circumferential coordinate

σ surface tension, $\frac{N}{m}$

ϵ temperature tolerance, $°C$

SUBSCRIPTS

B	bulk liquid
b	bulk liquid
FC	forced convection
f	liquid or film
l	liquid
g	gas or vapor
w	wall
FDB or E	fully developed boiling
ONB	onset of nucleate boiling
PB	partial nucleate boiling

SAT	saturation
SP	single-phase region
SC	single-phase

1. INTRODUCTION

Flow boiling heat transfer plays an important part in engineering and in today's high technology fields, such as space station energy system, microelectronic devices, and nuclear facilities. Based on theoretical and numerical analysis and the large amount of data, investigators have been able to create advanced software to both predictions of local heat transfer and experimental data reduction for single-phase flows in vertical channel geometries with uniform heat flux boundary conditions. Although it has been known for decades that flow boiling increases and enhances heat transfer, little or no attention has been given to advanced heat transfer development for subcooled flow boiling inside channels or ducts with uniform circumferential heating.

This work deals with improved ways to characterize the local heat transfer inside circular channels. The objectives of the present work are to assess: (1) and if need be to develop a composite correlation which can be used to predict local (axial only) heat transfer coefficients for turbulent subcooled flows with and without boiling in uniformly heated channels, and (2) the present capability of critical heat flux correlations and propose an approach for future development. Unless otherwise noted the local heat transfer coefficient is defined as

$$\frac{q''_{local}}{T_W(\varphi, Z) - T_b(Z)}. \qquad (1-1)$$

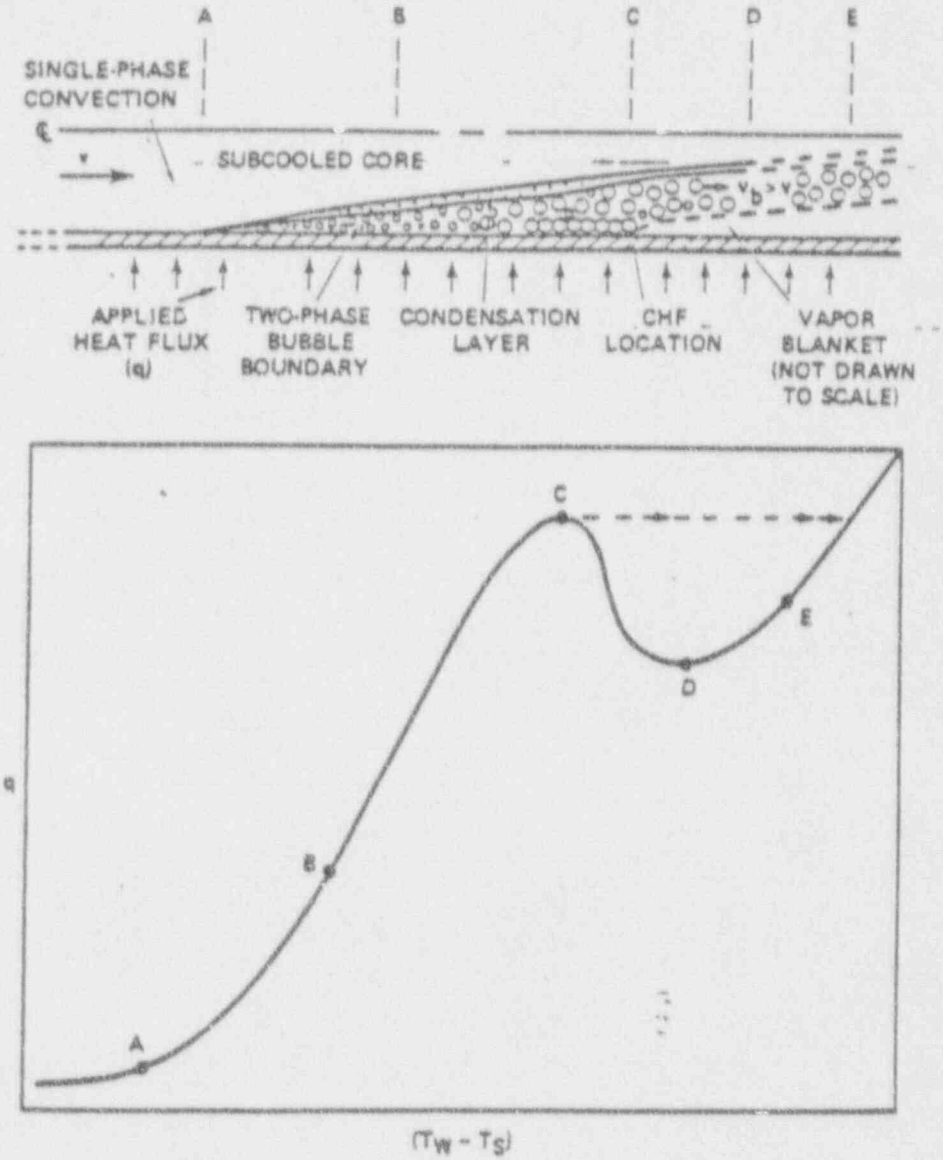

Figure 1.1 Typical Boiling Curve.

Boiling heat transfer is defined as a mode of heat transfer that occurs with a change in phase from liquid to vapor. There are two basic types of boiling: pool boiling and forced flow boiling. From the forced flow boiling point of view, the working fluid is defined in several regimes (see Figure 1.1): single-phase flow, subcooled boiling and many configurations of saturation boiling. Figure 1.1 shows a typical boiling curve which shows the change in the wall temperature superheat, $T_w - T_{sat}$, as the heat flux is increased. Much work has been done on each region of the boiling curve and each flow regime in the past five decades[1,9,18], and people are still investigating the mechanisms and behaviors of the fluids which are subjected to flow boiling.

Flow boiling has been applied not only in modern industries such as power and chemical process plants, but also in the high technology areas such as nuclear facilities, space station and electronic cooling. For such applications, it is not always convenient to use a limited family of fluids. Therefore, it is still very important to obtain knowledge and information for a variety of fluids, so that increased incite can gained in the energy transport mechanisms and the changes of flow regimes.

In Figure 1.2a, the region labeled "local boiling" includes single-phase and subcooled flow boiling. Subcooled boiling is an important regime of flow boiling which can be used to significantly enhance the heat transfer. The mechanism of phase change and transition from one region to another in highly subcooled boiling are so complicated and unstable that investigators have not understood them in the past. The present work provides investigators: (1) tools to predict local (axial) subcooled heat transfer coefficients, and (2) local (circumferential and axial) two dimensional (2-D) reduced data and mean data for the

heat transfer coefficient inside uniformly heated flow channels. The primary data sources are from: (1) the highly subcooled water flow boiling experiments of Boyd[6,7,15,28], (2) the Freon-11 flow boiling enhancement work of Smith and Boyd[30], and (3) the classical water flow boiling work of McAdams[13]. The range of flow parameters is given in Table 1.1. Since gravitational effects are negligible compared to inertial effects, quatitative comparisons of the local (axial) heat transfer coefficient and wall temperature are possible for the water data. Since such effects are not negligible for the freon-11 data, only qualitative comparisons are possible with the present predictive flow boiling model.

The present results will be extremely useful for heat transfer research and industrial design. For example, the composite subcooled flow boiling correlation should be applicable to any subcooled flow and any fluid as long as gravitational effects are not important. In addition, local (axial and circumferential) heat transfer coefficients have been obtained from local wall temperature data of Smith and Boyd[30] for case freon-11 flowing in uniformly heated smooth surface channels.

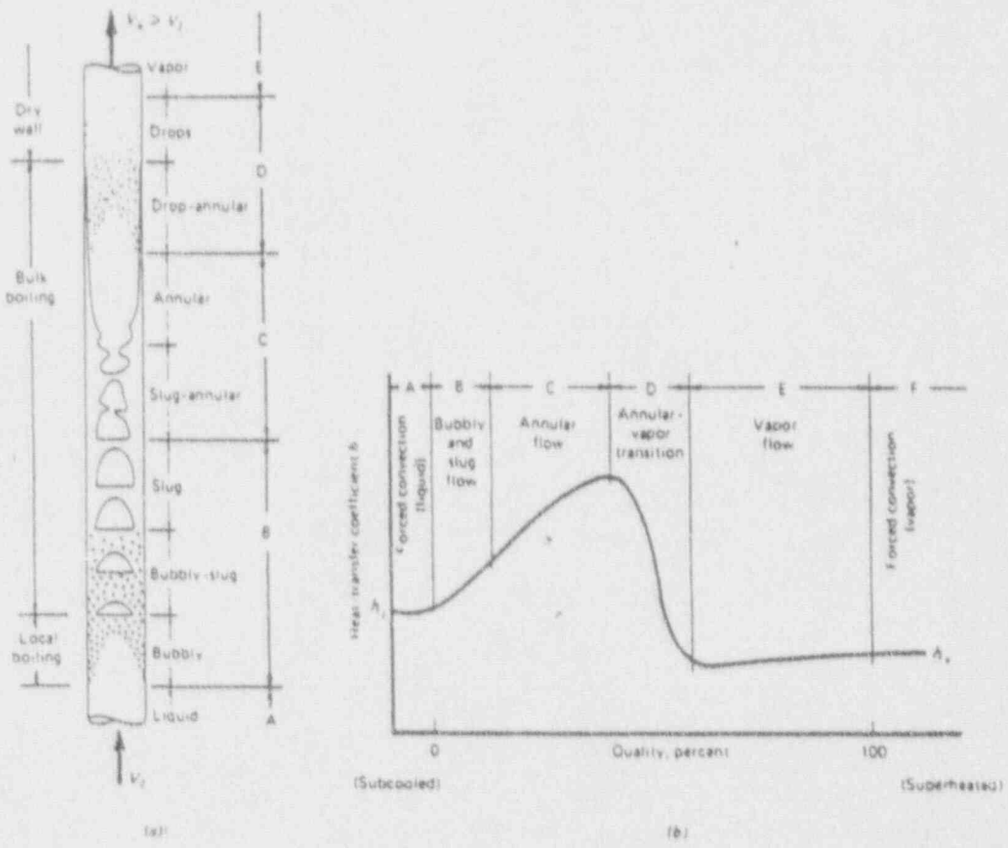

Fig. 1.2 Two-phase flow regimes for liquid forced flow boiling[1]

Table 1.1 Data Parameter Ranges

Parameter	Fluid		
	Water		Freon-11
* Mass velocity (Mg/m^2s)	4.4-36.0	1.22	0.21-0.281
* Exit Pressure (MPa)	0.77-1.66	4.1	0.186
* Inlet Temperature (°C)	20.0	116.8	22.2
* I.D. of Channel (cm)	0.3	0.064	1.07
*Channel Orientation (important?)	Horizontal (No)	Vertical (No)	Horizontal (Yes)
*Enhancement	Subcooling	Subcooling	Subcooling
*Type Heating of the Channel	Uniform	Uniform	Uniform
*Inside TW and h dependence	Z	Z	Z and phi
*Flow Regimes	Subcooled	Subcooled	Stratified and Subcooled
Data Source	Boyd[6]	McAdams[13]	Smith[30] and Boyd
Number of Data Points	354	9	155

2. LITERATURE SURVEY

The single-phase and flow boiling literature is voluminous. However, closer inspection of the literature related to subcooled flow boiling reveals a spare number of sources. Much of the literature covers saturated flow boiling which would include a large number of the flow regimes characterized in Figure 1.1a as "bulk boiling." Since the correlational development in the present work is restricted to subcooled flow boiling and single-phase heat transfer under the above noted conditions, our attention in this survey will be restricted accordingly. In the second part of this interim report, we seek to reduce the subcooled and bulk boiling data of Smith and Boyd[30].

2.1 SINGLE-PHASE CONVECTION AND FLOW BOILING

Because of the strong emphasis on subcooled flow or "local " boiling, only a representative number of literature sources will be summarized. These sources will be selected based on their foundamental nature, long history of use, or direct relationship to data summary shown in Table 1.1. In this section, the survey will characterize three subcooled regimes as well as any literature with single-side heating. The three subcooled regimes include: (1) the single phase (SP), (2) partial nucleate boiling, and (3) fully developed boiling (FDB) regimes.

2.1.1 *Single – Phase Heat Transfer*

A large number of papers have been published on single-phase heat transfer. Many

correlations are available for forced convection for a wide range of flow parameters (i.e. Pr, Re, Pe, etc.). Some currently used correlations include:

(a) Hausen's[2] correlation for developing laminar flow for an isothermal tube,

$$Nu_D = 3.66 + \frac{0.0668(\frac{D}{L})Re_D Pr}{1 + 0.4[(\frac{D}{L})Re_D Pr]^{\frac{2}{3}}}, \quad where \qquad (2.1.1-1)$$

$$T_{Ref} = \frac{T_{b_{inlet}} + T_{b_{outlet}}}{2} = T_{bm} = T_{b_{mean}}$$

(b) Dittus-Boelter's[3] correlation for fully developed turbulent flow,

$$Nu_D = 0.023 Re_D^{0.8} Pr^n, \quad where \qquad (2.1.1-2)$$

$$10^4 < Re < 10^6, \ 0.7 < Pr < 160,$$

$$n = 0.3 \ for heating \ \ the \ wall, \ n = 0.4 \ for \ cooling \ the \ wall$$

$$T_{Ref} = T_b$$

Although this correlation is not the most accurate, it is one of the widely used correlations.

(c) Sieder and Tate's[4] correlation for fully developed turbulent flow,

$$Nu_D = 0.027 Re_D^{0.8} Pr^{\frac{1}{3}} (\frac{\mu_b}{\mu_w})^{0.14}, \quad where \qquad (2.1.1-3)$$

$$T_{Ref} = T_b.$$

which is more accurate than the Dittus-Bolter correlation, applies for all values of $|T_W - T_b|$, and applies for the remaining parameter ranges given above for the Dittus-Bolter correlation;

(d) Petukhov's[5] correlation for fully developed turbulent flow, was admitted to give the best result for single-phase heat transfer in late 1980's,

$$Nu_D = \frac{(\frac{f}{8}) Re_D Pr}{1.07 + 12.7\sqrt{\frac{f}{8}}(Pr^{\frac{2}{3}} - 1)} (\frac{\mu_b}{\mu_w})^n, \qquad (2.1.1-4a)$$

$$f = (1.82 \log_{10} Re_D - 1.64)^{-2}, \quad where \qquad (2.1.1-4b)$$

$$n = \begin{cases} 0.11, & \text{for liquid when } T_W > T_b \\ 0.25, & \text{for liquid when } T_W < T_b \\ 0, & \text{for gases and constant heat flux boundary conditions, and} \end{cases}$$

$$T_{Ref} = \alpha(T_W - T_b) + T_b, \quad 0 < \alpha < 1$$

$$10^4 < Re_D < 5 \times 10^6, \quad and$$

where a is a function of Pr. Petuhkov's correlation is still the most accurate single-phase[2] turbulent correlation for fully developed flow. His correlation has been used exclusively in the work that follows for the condition of $n = 0$ for constant tube wall heat flux and $a = 0.5$.

Many heat transfer text books gave the incorrect reference temperature for Petukhov's correlation. Based on comparisons with high velocity data, Boyd and Meng[6] concluded that the reference temperature should be the film temperature for water. Figure 2.1, 2.2, and 2.3 show Petuhkov's correlation compared with Boyd's[7] high velocity single-phase data for two exit channel pressures for cases where the reference temperature is the inlet temperature[7], the mean bulk temperature[7], the local bulk temperature[7], and the local film temperature, $T_{film} = \frac{Tw(x)+T_b(x)}{2}$. The latter reference temperature clearly yields the better result. Figure 2.4 and 2.5 show examples of using Petuhkov's recommandation of the Prandle number depandence for the reference temperature, rather than the local film temperature. Again, the latter temperature gives better results.

Boyd and Meng[7] compared Petukhov's correlation with Dittus-Boelter's correlation for subcooled water (e.g. see, Figure 2.6), Petukhov's correlation with the above modifications gave more accurate results when comparing with the experimental data under conditions of $T_{inlet} = 20°C$, $G = 4.4$ to $30.5 Mg/m^2 s$, $P_{exit} = 0.77$ to $1.66 MPa$. This will be discussed in more detail below.

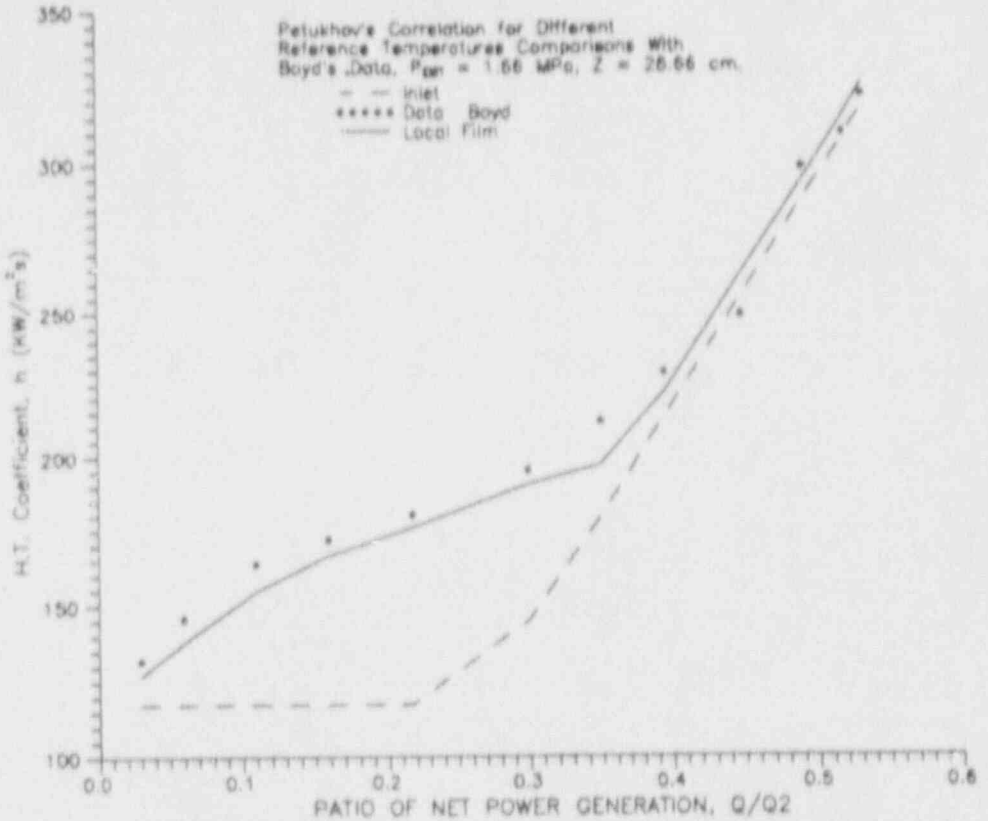

Figure 2.1 Petukhov's Correlation Comparisons With Inlet Temperature and Local Film Temperature as the Reference Temperature.

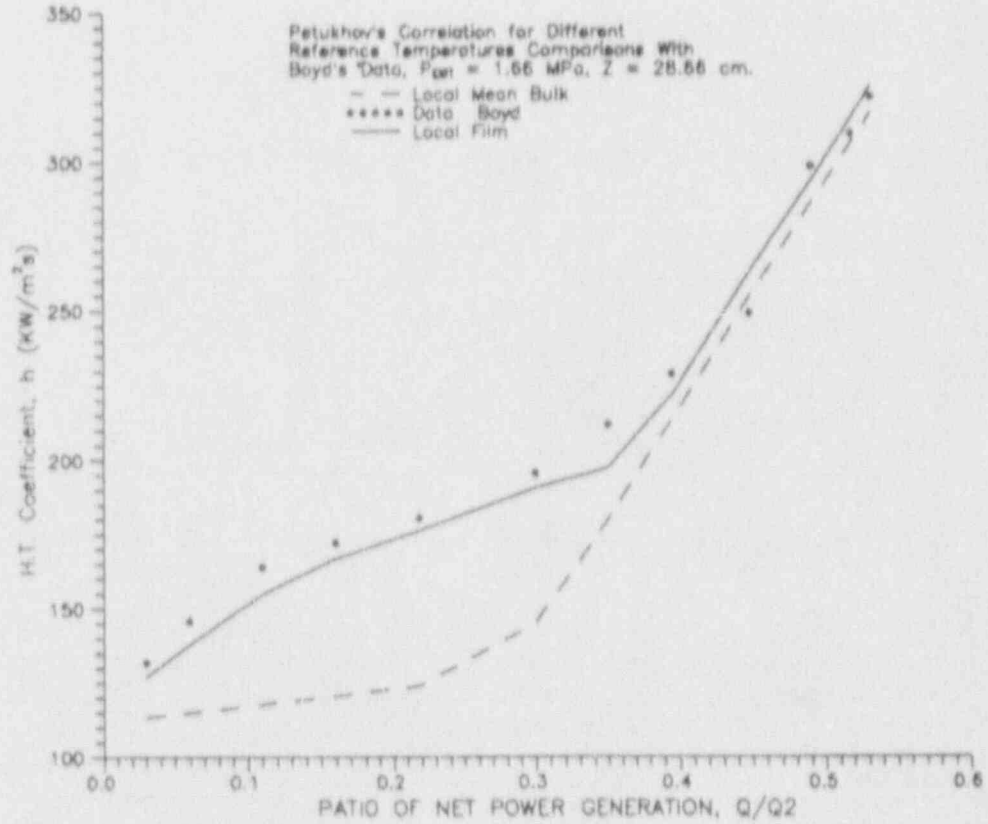

Figure 2.2 Petukhov's Correlation Comparisons With Local Mean Bulk temperature and Local Film Temperature as the Reference Temperature.

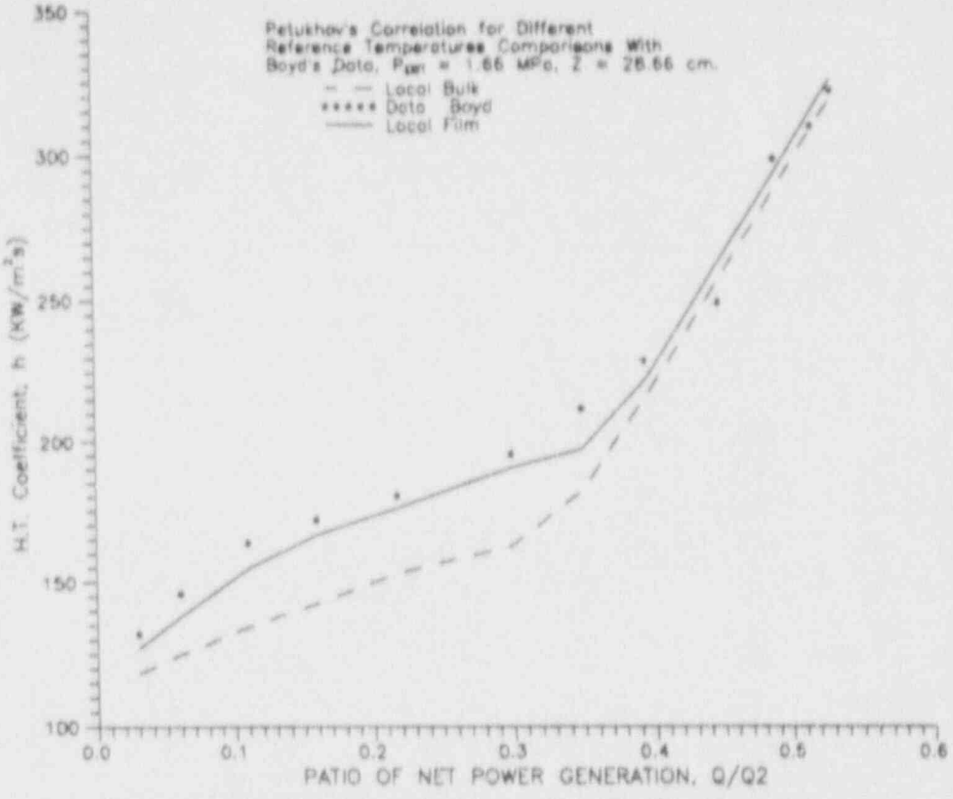

Figure 2.3 Petukhov's Correlation Comparisons With Local Bulk temperature and Local Film Temperature as the Reference Temperature.

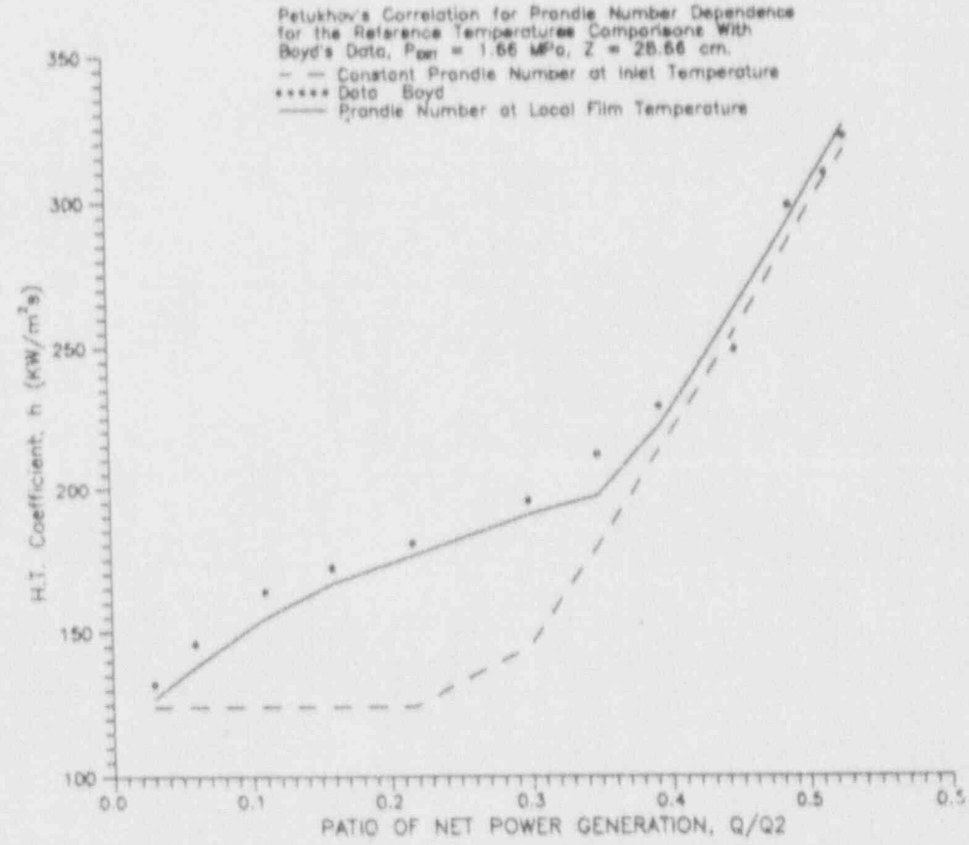

Figure 2.4 Petukhov's Correlation Comparisons With Prandle Number Dependence for the Reference Temperature for Exit Pressure 1.66 MPa

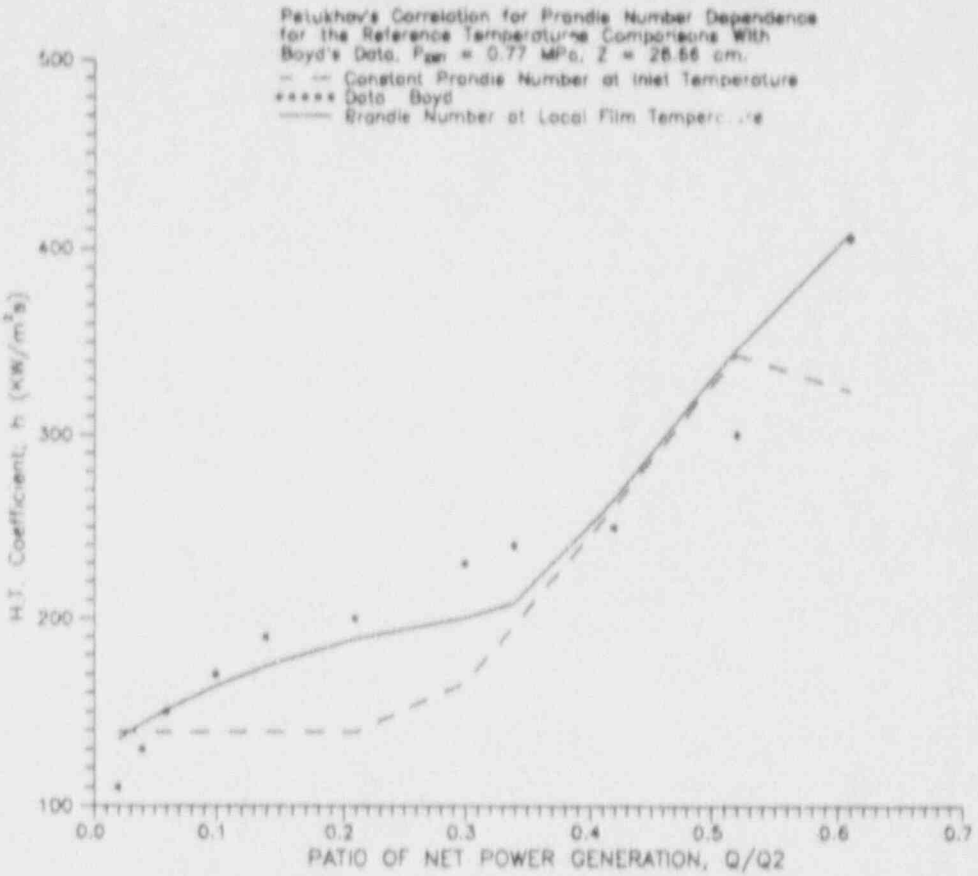

Figure 2.5 Petukhov's Correlation Comparisons With Prandle Number Dependence for the Reference Temperature for Exit Pressure 0.77 MPa.

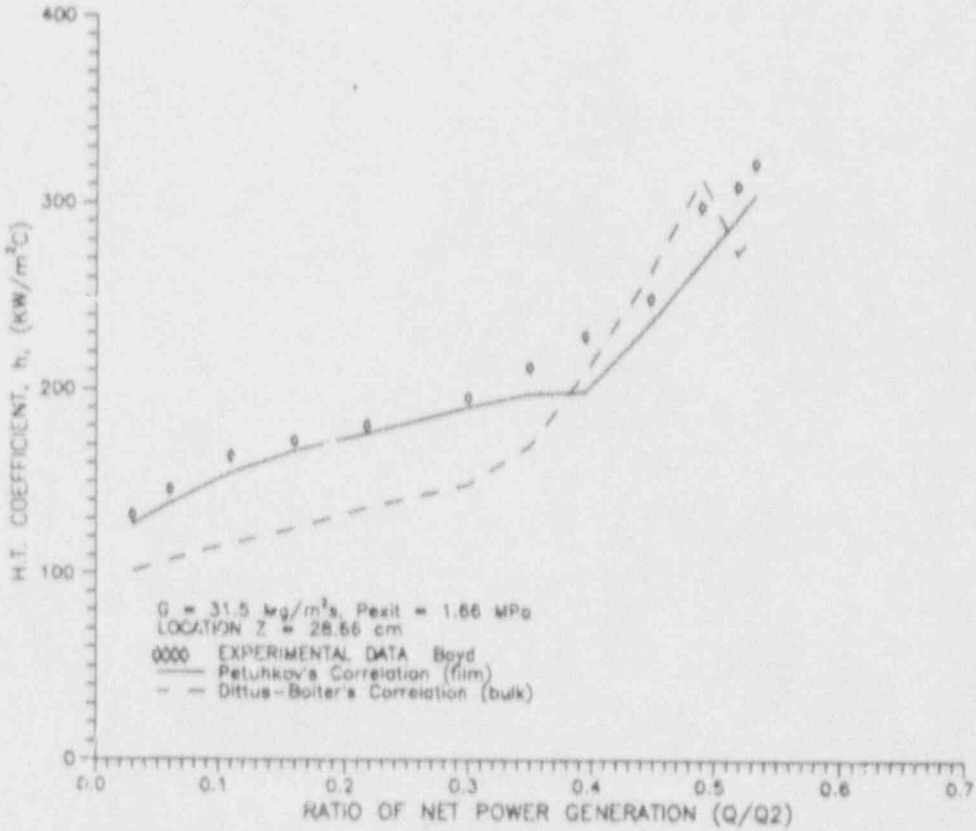

Figure 2.6 Comparisons With Petukhov's and Dittus-Boelter's Correlations in Single-Phase Regime for P_{exit}=1.66 MPa, Z=28.66 cm and G=31.5 Kg/m²s.

2.1.2 *Partial Boiling*

In 1964, Bergles and Rohsenow[8] introduced a simple interpolation formula for incipient boiling from a small amount of experimental information; i.e.,

$$q^{"} = q^{"}_{SP}[1 + \{\frac{q^{"}_{FDB}}{q^{"}_{SP}}(1 - \frac{q^{"}_{ONB}}{q^{"}_{FDB}})\}^2]^{\frac{1}{2}} \qquad (2.1.2-1)$$

Frost and Dzakowic[24] developed the following relationship between superheat and heat flux for the condition of ONB,

$$\Delta T_{sat,ONB} = [\frac{8\sigma q^{"}_{ONB} T_{sat}}{J i_{fg} k_f \rho_g}]^{0.5} Pr_f \qquad (2.1.2-2)$$

where J is always 1.0 in SI unit, and T_{sat} has the unit of K. This correlation can be used for many different fluids, including water and refrigerants. However, this correlation is not as accurate as the Bergles and Rohsenow at ONB for water. The Bergles and Rohsenow[8] correlation only applies for water, and is given as

$$\Delta T_{sat,ONB} = 0.556[\frac{q^{"}}{1082p^{1.156}}]^{0.463p^{0.0234}} \qquad (2.1.2-3)$$

Collier[9] summarized linear connections between single phase and fully developed boiling in his 1972 text.

An exponent equation which was intended to improve partial boiling fitting was given by Kandlikar[10] in 1988. The connecting line in partial boiling region is a non-linear relation between surface heat flux, $q^{"}$, and wall superheat, ΔT_{sat}. The equation is

$$q''_{PB} = a^* + b^*(\Delta T_{sat})^m \qquad (2.1.2-4a)$$

where "PB" denotes partial nucleate boiling.

$$b^* = \frac{(q''_E - q''_{onb})}{\Delta T_{sat,E} - \Delta T_{sat,ONB}} \qquad (2.1.2-4b)$$

$$a^* = q''_{ONB} - b^* \Delta T_{sat,ONB} \qquad (2.1.2-4c)$$

$$m = n + pq'' \qquad (2.1.2-4d)$$

$$p = \frac{1}{q''_E - q''_{ONB}} \qquad (2.1.2-4e)$$

$$n = 1 - pq''_{ONB} \qquad (2.1.2-4f)$$

Kandlikar noted that this approximate connection gave better results than Collier's linear connection. In June of 1991, Boyd[11] noticed abnormalities with the above expressions and noted the abnormalities to Kandlikar[11]. Boyd's[31] modification resulted in a more accurate approximation (this will be demonstrated below) which required the parameters a^* and b^* to be functions of the local heat flux; i.e.,

$$q''_{PB} = a + b(\Delta T_{sat})^m \qquad (2.1.2-5a)$$

$$b = \frac{(q''_E - q''_{onb})}{\Delta T^m_{sat,E} - \Delta T^m_{sat,ONB}} \qquad (2.1.2-5b)$$

$$a = q''_{ONB} - b\Delta T^m_{sat,ONB} \qquad (2.1.2-5c)$$

where a and b replace a^* and b^* in equation (2.1.2-4a). Further, the equations for m, p, and n are identical to those recommended by Kandlikar[10] above. The recommendations given by Kandlikar resulted in the discontinities at the intersection of partial boiling and fully developed boiling, which could severly effect the accuracy of the entire prediction. This will be demonstrated below.

Boyd's approximation has been tested via experimental data for water. The results were within 18.6% percentage diviation. In partial boiling region, Boyd's approximation improved the current correlations, and further modifications will be seen in this work and reference [7].

A number of correlations have been proposed in literature specifically for water. The equation provided by Jens and Lottes[9] is widely used; e.g.,

$$\Delta T_{sat} = 25 q''^{0.25} e^{-\frac{p}{62}}. \qquad (2.1.2-6a)$$

This correlation covers water temperatures from $115°C$ to $340°C$, mass velocities from 11 to $1.05 \times 10^4 kg/m^2 s$, and heat flux up to $12.5 MW/m^2$.

An improved correlation from Thom's was reported by Collier as

$$\Delta T_{sat} = 22.65 q''^{0.5} e^{-\frac{p}{87}}. \qquad (2.1.2-6b)$$

Here p is the absolute pressure in bar, ΔT_{sat} is in $°C$, and the heat flux q'' is in MW/m^2.

Bjorge et al[12] correlation covers subcooled and saturated boiling for water. In the region called subcooled and low quality region, the correlation was given as:

$$q = \{q_{FC}^2 + q_B^2[1 - (\frac{\Delta T_{sat,ib}}{\Delta T_{sat}})^3]^2\}^{0.5} \qquad (2.1.2-7a)$$

$$q_{FC} = h_{FC}(\Delta T_{sat} + \Delta T_{sc}) \qquad (2.1.2-7b)$$

The forced convective heat transfer coefficient, h_{FC}, for their correlation is calculated from following equation

$$\frac{h_{FC}D}{k_b} = 0.023 Re_f^{0.8}(\frac{\mu_f C_p}{k_b})^{\frac{1}{3}} \qquad (2.1.2-7c)$$

The subscript f and b indicate that property should be evaluated at the film temperature, T_{film}, and the liquid bulk temperature, T_b, respectively. $\Delta T_{sat,ib}$ is called the superheat at the incipient boiling point. It is related to the radius of the point of tangency, r_{tang};

for $r_{tang} > r_{max}$,

$$\Delta T_{sat,ib} = \frac{1}{1-N}(\frac{1}{4\Gamma N} - N\Delta T_{sc}); \qquad (2.1.2-7d)$$

for $r_{tang} < r_{max}$,

$$\Delta T_{sat,ib} = \frac{1}{2\Gamma}[1 + (1 + 4\Gamma\Delta T_{sc})^{0.5}], \qquad (2.1.2-7e)$$

where

$$r_{tang} = \frac{4T_{sat}v_{fg}}{h_{fg}\Delta sat,ib} \qquad (2.1.2-7f)$$

$$\Gamma = \frac{k_l h_{fg}}{8\Delta T_{sat} v_{fg} h_{FC}} \qquad (2.1.2-7g)$$

$$N = \frac{h_{FC} r_{max}}{k_l} \qquad (2.1.2-7h)$$

In the equations above, r_{max} is defined as 10^{-6} m.

Compared with the data of McAdams[13] and Latsch[12], Bjorge had good agreement in the partial boiling region.

Bergles and Rohsenow[8] summarized work done by McAdams[12], Kreith and Forster[8] and Engelberg-Forster and Greif[8] for fully developed boiling. They found that flow boiling data were not significantly affected by either velocity or subcooling. After comparing with pool boiling data, Bergles and Rohsenow used the fully developed pool boiling curve to test the asymptotic for the flow boiling curve in the fully developed nucleate boiling regime.

2.1.3 *Fully Developed Boiling*

Based on experimental data for water, refrigerants, and alcohols in fully developed boiling, Shah's correlation[13] can be express as:

$$\frac{h_{tp}}{h_{lo}} = [f_1(Bo) + \frac{x}{x^*}]^{-1} \qquad (2.1.3-1a)$$

where

$$f_1(Bo) = \begin{cases} 230Bo^{0.5}, & \text{Bo} > 3.0 \times 10^{-5}; \\ 1 + 46Bo^{0.5}, & \text{Bo} \leq 3.0 \times 10^{-5} \end{cases} \qquad (2.1.3-1b)$$

$$x^* = -\frac{q'' c_{pc}}{h_{sp} i_{lg}} = -\frac{Bo}{St} \qquad (2.1.3-1c)$$

Here, h_{lo} is the single phase heat transfer coefficient. Shah did point out that "single phase convection plays an important part in subcooled boiling heat transfer. The accuracy of single phase correlation limits the accuracy of boiling heat transfer correlation." Dittus-Boelter's correlation was suggested for h_{lo} at the time the article was published. However,

updated correlations, such as that by Petukhov, can be used instead. Shah also mentioned that the behavior of cavities, which is strongly affected by the tube surface condition, has generally been found "unpredictable due to the particular set of conditions such as pressure, temperature, heat flux, and mass flow rate."

The standard deviation reported by Shah was ±30% over 97% of the data points. The applied range of parameters are: pipe diameter from 2.4 to 27.1 mm; pipe materials include stainless steel, copper, nickel, and glass; reduced pressures ranged from 0.1 to 13.8 MPa; the subcooling (i.e., $T_b - T_{sat}$) ranged from 0 to 153°C; the heat flux ranged from 0.01 to 22.9 MW/m^2; and the mass flow rate ranged from 200 to 87 × 10^3 Mg/hm^2.

Typical curves for subcooled water boiling were given by Collier[9] and are presented in figures 2.7, and 2.8. Figure 2.7 is in the form of q'' vs. $T_W(Z) - T_b(Z)$ and consists of two straight lines on a semi-log scale with a significant slope change. These two lines intersect at ONB. As the flow rate increases, the curves shift upward in the single phase regime, but are almost identical in the fully developed boiling regime.

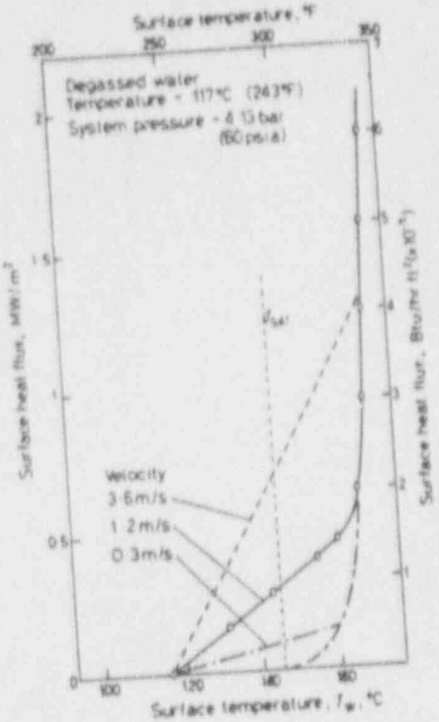

Fig. 2.7 Typical curves for subcooled boiling[9].

Figure 2.7 in form of q'' vs. T_{wall} and shows the transition from the single-phase to the fully developed boiling regime.

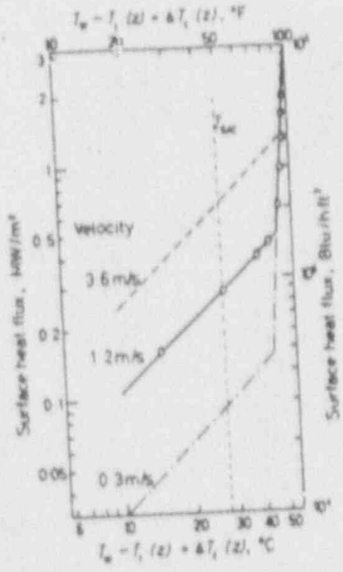

Fig. 2.8 Typical curves for subcooled boiling[9].

The wall temperature is truely effected by the flow rate, pressure and heat flux, but independent of the subcooling. Kreith and Summerfield[8] obtained this result based on the studies of both horizontal and vertical electrically heated tubes.

There were no correlations found for partial boiling regime only, all the correlations were applied for the nucleate boiling region.

3. BACKGROUND

Because of the diverse nature of the topics of subcooled flow boiling, a brief background will be present here. Further details can be found in reference [9].

3.1 SUBCOOLED BOILING REGIONS

In this work, subcooled boiling is defined as localized boiling regime between the single-phase heat transfer regime and the onset of saturation boiling regime. In other words, the nucleate subcooled boiling is the regime where the bulk equilibrium quality, x, is less than zero, 0.0.

During nucleate subcooled boiling, heat is transported to increase the enthalpy of the fluid, which has a bulk temperature below the saturation temperature, T_{sat}. The temperature of the fluid near the wall increases until it reaches the saturation temperature. Theoretically there are no bubbles created up to this point. However, when the wall temperature exceeds the saturation temperature by a certain amount (i.e., superheated), the fluid starts evaporating at the root of the nucleation site on the substrate. As the bubble grows while it is still attached to the wall, it experiences growth near its heated base but tends to shrink or grow much less due to condensation at the top of the bubble. Although the fluid is boiling locally, the bulk fluid is still in the subcooled condition. Since the bubble generation is periodic, the flow has an ability to transfer large amounts of energy from heated surface because of the large and energetic subcooled liquid core flow.

The nucleate subcooled boiling regime is loosly defined in terms of three regimes:

The nucleate subcooled boiling regime is loosly defined in terms of three regimes: the single-phase heat transfer regime, the nucleate partial boiling regime, and the fully developed nucleate boiling regime. The starting point for the nucleate partial boiling regime is called onset nucleate boiling (ONB), and the starting point for the fully developed nucleate boiling regime is called FDB in this work.

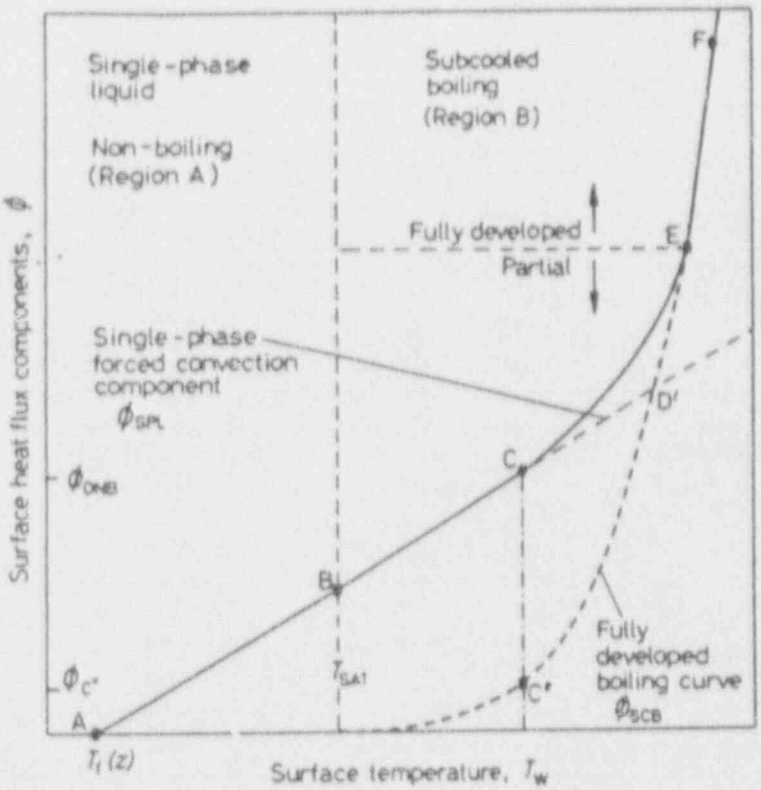

Fig. 3.1 Method of Bergles and Rohsenow[9].

The heat transfer coefficient increases with heat flux from the single-phase region to the fully developed boiling region. This increase is associated with mass flow rate, inlet subcooling, pressure and the properties of the fluid.

In figure 2.7, the typical curve for subcooled boiling was presented as a combination of two straight lines, which includes a single-phase line and a fully developed boiling line based on experimental data. Figure 3.1 shows a similar curve that has an almost constant slope and displays the nucleate subcooled boiling regions. The curve drawn though points A to point C represents the single-phase heat transfer. The curve between points C and F has an increasing slope from that for the single-phase regime up to the FDB region. This indicates that there is a higher heat transport ability as the fully developed nucleate boiling regime is approached. Point D', the intersection of single-phase curve and the fully developed boiling curve, is essential in finding the starting point of fully developed boiling region, point E. Bergles and Rohsenow gave $q"_E = 1.4q"_{D'}$, based on a large amount of experimental data. The ONB starts at point C, at which point the partial nucleate boiling regime proceeds up to point E. The entire curve representing the transition from single-phase to fully developed boiling can be approximated for any fluid and substrate provided characterizing correlations are available for at least the single-phase and the fully developed regimes.

4. PROBLEM DEFINITION

4.1 SUBCOOLED BOILING PROBLEM

The subcooled flow boiling model to be generated is for local heat transfer prediction for Freon-11 and water cooled channels. The flow through portions of the channel will be in the single-phase region, partial boiling region, and/or fully developed region. The basic flow parameters (see figure 4.1), which are assumed known, include: mass flow rate, inlet temperature, exit pressure, coolant channel geometry, and unform heating on the outside surface of the channel. Because of the availibility of numerous single-phase and two-phase correlations, existing correlations will be used where possible and modified where necessary to develop the model, which will be a composite correlation applicable over the full subcooled region prior to the critical heat flux. An attempt will be made to extend the models applicability to any fluid.

The basic motivation is to develop a better or more accurate technique for evaluations of existing systems or new designs for cooling systems where local heat transfer rates are required. Comparisons will be made between the developed model and existing single-phase and subcooled boiling experimental data, which includes both water and freon-11 as working fluids.

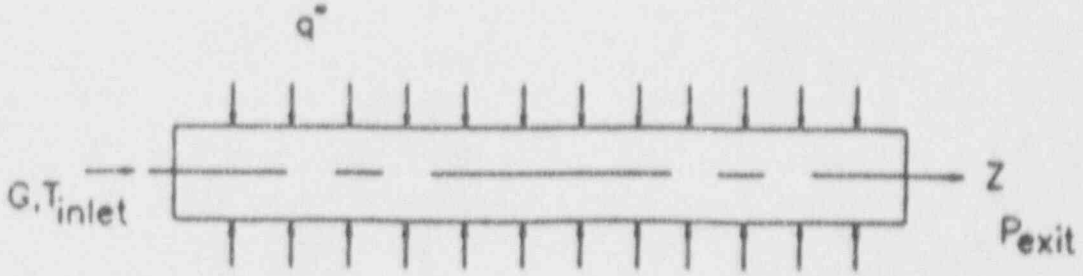

Fig. 4.1 Test section.

5. MODEL DEVELOPMENT

5.1 SUBCOOLED BOILING MODEL

There have been many investigations made of subcooled boiling, and there have been many correlations[9,18,19] given for each regime in the subcooled nucleate boiling region (see literature survey). Using selections from this previous work, an updated composite nucleate subcooled boiling model is proposed below. Among the recommended correlations in the literature survey, Petuhkov's[5], Shah's[14], Kandlikar's[10], and Boyd and Meng's[6] correlations were essential in the development of the present model.

The local (axial) heat transfer coefficient is defined as the ratio of local applied heat flux to the difference between the local inside wall temperature and the local fluid's bulk temperature; i.e.,

$$h(Z) = \frac{q''(Z)}{(t_w(Z) - t_b(Z))}. \qquad (5.1-1)$$

The local film temperature was used to evaluate all the thermophysical properties in all correlations; i.e.,

$$t_{film}(Z) = \frac{t_w(Z) + t_b(Z)}{2} \qquad (5.1-2)$$

Subroutines were developed for the temperature-dependent thermophysical properties of each fluid used in the correlational comparisons with experimental data. These subroutines are part of the computer programs that are given in Appendix A.1, A.2, and A.3-1 or A.3-2. The local mean bulk temperature is calculated from the First Law of Thermodynamics for given values of the: applied heat flux, q''; location, Z; mass flow rate, G; and inlet fluid

temperature, T_{inlet}. From the First Law,

$$i_b(Z) = i_{inlet} + \frac{q'' A_s(Z)}{GA_c} \qquad (5.1-3)$$

The local bulk temperature, $t_b(Z)$, is obtained from $i_b(Z)$ via the saturation table which are also a part of the temperature-dependent thermophysical property subroutines.

As a reference heat flux used in the presentation of this model, q_2 is introduced as the heat flux at which the fluid reaches the saturation liquid state at the exit of the channel (or $Z = L$); i.e.,

$$q_2 = \frac{GA_c}{A_s(L)}(i_{sat}(L) - i_{inlet}) \qquad (5.1-4)$$

Much of the results will be presented in terms of heat transfer coefficient, h, vs. net power generation ratio, $\frac{q}{q_2}$. When $\frac{q}{q_2} < 1$, the fluid is in the subcooled boiling condition.

5.1.1 *Single – Phase*

In single-phase region, Petukhov's correlation (equation 2.1.1-4) was used instead of Dittus-Boelter's(which was used by Kandlikar[10]) because it is much more accurate. The slight change in this correlation is that $n = 0$, and T_{Ref} for all fluids will be the local (axial) film temperature.

5.1.2 *Onset Nucleate Boiling (ONB)*

In cases where estimates of ONB were required, Bergles and Rohsenow's correlation (equation 2.1.2-3) was used. The theoretical correlation by Davis and Anderson could

also has been used for water. For other fluids other than water, the Frost and Dzakowic correlation can be used. In order to find heat transfer coefficient, one has to generate a group of points on boiling curve and then graphically find the exact $\Delta T_{sat,ONB}$ and q_{ONB} for given values of G, Z, T_{inlet} and P_{exit}.

5.1.3 *Partial Boiling*

Two models for the partial nucleate boiling region were developed by Boyd[31] and are used here to improve Kandlikar's model. Both of the present models are based equation (2.1.2-4) which was used by Kandlikar.

In the first model (referred to here after as the **"initial model"**), the corrected expressions for the parameters a^* and b^* were provided by equations (2.1.2-5b) and (2.1.2-5c) for a and b, respectively. This correction allowed : (1) $q"$ to approach $q"_{ONB}$ when T_W approched $T_{W,ONB}$, and (2) $q"$ to approach $q"_{FDB}$ when T_W approached $T_{W,FDB}$. Although they should have, Kandlikar's equations (2.1.2-4b) and (2.1.2-4c) did not satisfy thoes con litions. The "initial model" is dependent on one's ability to estimate ONB. Later comparisons with the available data base will show that if the ONB limit can be replaced with a more realistic asymptotic limit less than $T_{W,ONB}$: (1) the need to estimate ONB will be eliminated , and (2) the accuracy of model in the partial boiling regime will improve.

The second partial nucleate boiling model proposed by Boyd[31] uses the same relationship given in equation (2.1.2-5a) but all expressions for a, b and m are different. **The important point to note here is that no apriori assumptions were made for the relationship for m and the resulting correlation applies to all fluids. Further,**

the definitions for "a" and "b" will change because additional asymptotic approximations will be employed at both ends of the partial boiling region. These conditions for the determination of "a", "b", and "m" are:

$$(i)\ q''_{PB} = q''_{SP} \quad when T_W = T_{sat}; \tag{5.1.3.1a}$$

$$(ii)\ q''_{PB} = q''_{FDB} \quad when \quad \Delta T_{sat,PB} = \Delta T_{sat,FDB}; \quad and, \tag{5.1.3-1b}$$

$$(iii)\ \frac{\partial q''_{PB}}{\partial \Delta T_{sat}} = \frac{\partial q''_{FDB}}{\partial \Delta T_{sat}} \quad at \quad FDB \tag{5.1.3-1c}$$

These conditions, when applied to equation (2.1.3-5a), result in the following new forms for the parameters "a", "b", and "m":

$$a = h_{SP}(T_W = T_{sat})\Delta T_{sub} \tag{5.1.3-2}$$

$$b = \frac{q''_{FDB} - a}{\Delta T^m_{sat,FDB}}, \tag{5.1.3-3}$$

$$m = \frac{\epsilon \Delta T_{sat,FDB}}{q''_{FDB} - a}, \tag{5.1.3-4}$$

$$\epsilon = \frac{h_{SP}}{F})_{FDB}[1 - h_{SP}\frac{(T_W - T_b)g_1}{F^2 f_1^2}]^{-1}_{FDB} \tag{5.1.3-5}$$

$$F = [\frac{1}{f_1(Bo)} + X], \quad X = \frac{x}{x^*} \tag{5.1.3-6}$$

$$g_1 = \frac{\partial f_1}{\partial q''} = \begin{cases} 115 Bo^{0.5}_{FDB}\frac{1}{q''_{FDB}}, & \text{for Bo } > 3.0\times10^{-5}; \\ 23 Bo^{0.5}_{FDB}\frac{1}{q''_{FDB}}, & \text{for Bo} \leq 3.0\times10^{-5} \end{cases} \tag{5.1.3-7}$$

and f_1 is given by shah in equation (2.1.3-1b). Notice from the above that "m" is a function of q'' but **no assumptions or curve fits were made to adjust "a", "b", or "m"**. Therefore a "modified" or improved correlation now results and is in the form

$$q''_{PB} = a + b\Delta T^m_{sat,PB}, \quad where \tag{5.1.3-8}$$

"a", "b", and "m" are redefined (improved) in equations (5.1.3-2) through (5.1.3-7). This correlation will hence be referred to as the **"modified"** partial nucleate boiling correlation. This correlation modification was intended to increase the magnitude of the heat transfer coefficient relative to the values predicted by the **"initial"** model;i.e., equations (2.1.2-5b), (2.1.2-5c), (2.1.2-4d), (2.1.2-4e), and (2.1.2-4f). The modified correlation provides a better approximation for the asymptotic limit for the partial nucleate boiling region as ΔT_{sat} decreases.

In the discussion of the results where the above two models are compared with previous data, the terms, **"modified"** and **"initial"** will be used to refer equation (5.1.3-8) with the "modified" parameter equations (equations (5.1.3-2) through (5.1.3-7)) and the "initial" parameter equations as noted above.

5.1.4 *Onset of Fully Developed Boiling (OFDB)*

The onset of fully developed boiling (OFDB) is the starting point of fully developed boiling regime. The method summarized in Figure 3.1 is used to located point "E," which corresponds to OFDB. As Foster and Grief recommended, point "E" was assumed to correspond to a heat flux level, $q''_{FDB} = 1.4q''_D$. The corresponding heat transfer coefficient is,

$$h_{tp} = \frac{q''_{FDB}}{\Delta T_{sat,FDB} + \Delta T_{sub,FDB}} \qquad (5.1.4-1)$$

where

$$\Delta T_{sub,FDB} = -\frac{x i_{lg}}{c_{pl}}$$

$$x = \frac{i(Z) - i_{lg}}{i_{lg}}$$

5.1.5 *Fully Developed Boiling*

The fully developed boiling heat transfer begins at point E and can be characterized by Shah's correlation, which is given in equation (2.1.3-1).

5.1.6 *Wall Temperature*

In order to use film temperature as the reference temperature for temperature-dependent thermophysical properties, the wall temperature must be known for each of the above three regimes. A straight-forward trail-and-error method was used to find T_W as follows:

(1) compute the local (axial) bulk temperature from equation (5.1-3) for a given level of $q"$;

(2) assume a wall temperature and then estimate the film temperature using equation (5.1-2);

(3) (a)If $T_W < T_{sat}$, use equation (2.1.1-4) to compute h_{SP} and compute a revised estimate for T_W;

(b)If $q"$ is less than $q"_{FDB}$ use equations (5.1.3-2) through (5.1.3-8) to compute a new estimate for T_W; or

(c)If $q"$ is greater than or equal to $q"_{FDB}$, use equation (2.1.3-1) to compute $h_{tp}(Z)$

and then equation (5.1-1) to obtain a revised estimate for T_W;

(4) compare the revised wall temperature to the assumed or previously computed wall temperatrue. If the difference is greater than a desired value, let the new wall temperature equal to the assumed or previously computed wall temperature, and then repeat step (3).

Once the local wall temperature is accurate enough, the local (axial) heat transfer coefficient is the last computed value of h_{tp} (for the case of boiling). See Appendix A.4 for instructions on how to run the computer programs used for the above procedure.

5.2 NUMERICAL CONDUCTION MODEL

Based on the need of a data reduction capability for the freon-11 data, the governing steady-state energy equation, for thermal conduction can be written as

$$\frac{k}{r}\frac{\partial}{\partial r}(r\frac{\partial T}{\partial r}) + \frac{k}{r^2}\frac{\partial^2 T}{\partial \varphi^2} = 0 \qquad (5.2-1)$$

The governing equation will be solved by dividing the schematic in figure 4.2.2 into two domains with two different sets of boundary conditions (also see figures 5.1 and 5.2).

(a) Domain I (Insulation and Ambient;)

$$(1)\ at\ \varphi = 0\ , \frac{\partial T}{\partial \varphi} = 0; \qquad (5.2-2a)$$

$$(2)\ at\ \varphi = \pi\ , \frac{\partial T}{\partial \varphi} = 0; \qquad (5.2-2b)$$

$$(3)\ T(R2, \varphi) = T_W(\varphi); \qquad (5.2-2c)$$

$$(4)\ h_\infty[T(R2^{'}, \varphi) - T_\infty] + k\frac{\partial T(R2^{'}, \varphi)}{\partial r} = 0. \qquad (5.2-2d)$$

In condition (3), $T_W(\varphi)$ was measured experimentally (see Smith and Boyd[30]) and is the outside temperature of copper coolant channel.

(b) Domain II (Copper and bulk fluid;)

$$(1)\ at\ \varphi = 0,\ \frac{\partial T}{\partial \varphi} = 0; \qquad (5.2-2e)$$

$$(2)\ at \varphi = \pi,\ \frac{\partial T}{\partial \varphi} = 0; \qquad (5.2-2f)$$

$$(3)\ k\frac{\partial T(R1,\varphi)}{\partial r} = h(\varphi)[T(R1,T_b)];\ and \qquad (5.2-2g)$$

$$(4)\ T(R2,\varphi) = T_W(\varphi). \qquad (5.2-2h)$$

5.2.1 *Domain I*

The temperature profile in Domain I was determined by using the Gauss-Seidel iteration technique to the difference equations. This procedure has two major results: (1) computation of the temperature of the insulation first whole node (node (M+1,j) in figure 5.2) which is adjacent to the outside copper surface; and (2) total heat loss to the ambient. The computed nodal temperatures of the insulation are used as input for the difference equations which are used to determine the temperature variation in Domain II (the copper). These latter difference equations do not require iteration and were used to find the inside wall temperature of the copper channel. The local (axial and circumferential) heat transfer coefficient, $h(\varphi, z)$ was then computed using equation (1-1), where $q"_{local}$ was computed from the numerically computed temperatures from Domain II (figure 5.2) at node number (1,j) and (2,j), using the thermal resistance between those nodes. For this computation using equation (1-1) $T_b(z)$ was used and no attempt was made to define a $T_b(\varphi, z)$.

The complete difference formulation for the interior and exterior nodes is contained in Appendix B.3. All difference equations and all thermal resistance equations are given in Appendix B.3. $TT(i,j)$, and $T(i,j)$ represent the latest and previous estimates of nodal

temperatures, respectively for Domain I. $TT(i,j)$ is given by

$$TT(i,j) = \frac{\frac{T(i+1,j)}{R(i,j)} + \frac{T(i-1,j)}{R(i-1,j)} + \frac{T(i,j+1)}{RC(i,j)} + \frac{T(i,j-1)}{RC(i,j-1)}}{\frac{1}{R(i,j)} + \frac{1}{R(i,j-1)} + \frac{1}{RC(i,j)} + \frac{1}{RC(i,j-1)}}; \qquad (5.2-3)$$

where $|TT(i,j) - T(i,j)|$ must be $< \epsilon$ for all nodes before convergence is assumed. For Domain I, convergence always occurred when ϵ was $0.00001°C$. The sample conduction finite difference analysis in Appendix C demonstrated that there is a relationship between ϵ, and Δr, if adequate heat flux balances are to be achieved. From those results, ϵ must be less than $0.001°C$ and Δr must be less than $0.0001\ m$ as a basis of further computations.

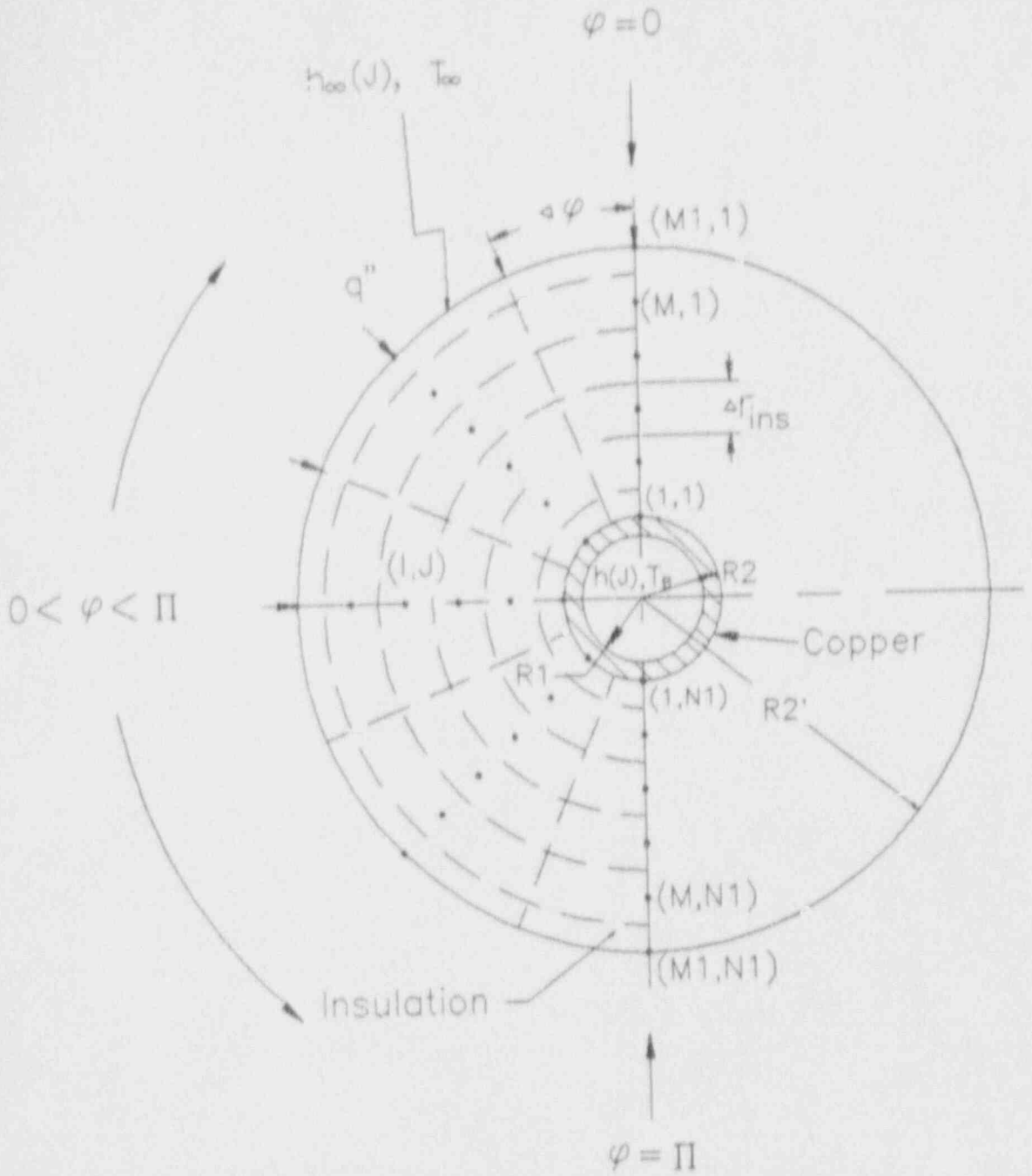

Figure 5.1 Mesh Diagram for Domain I: Insulation and Ambient

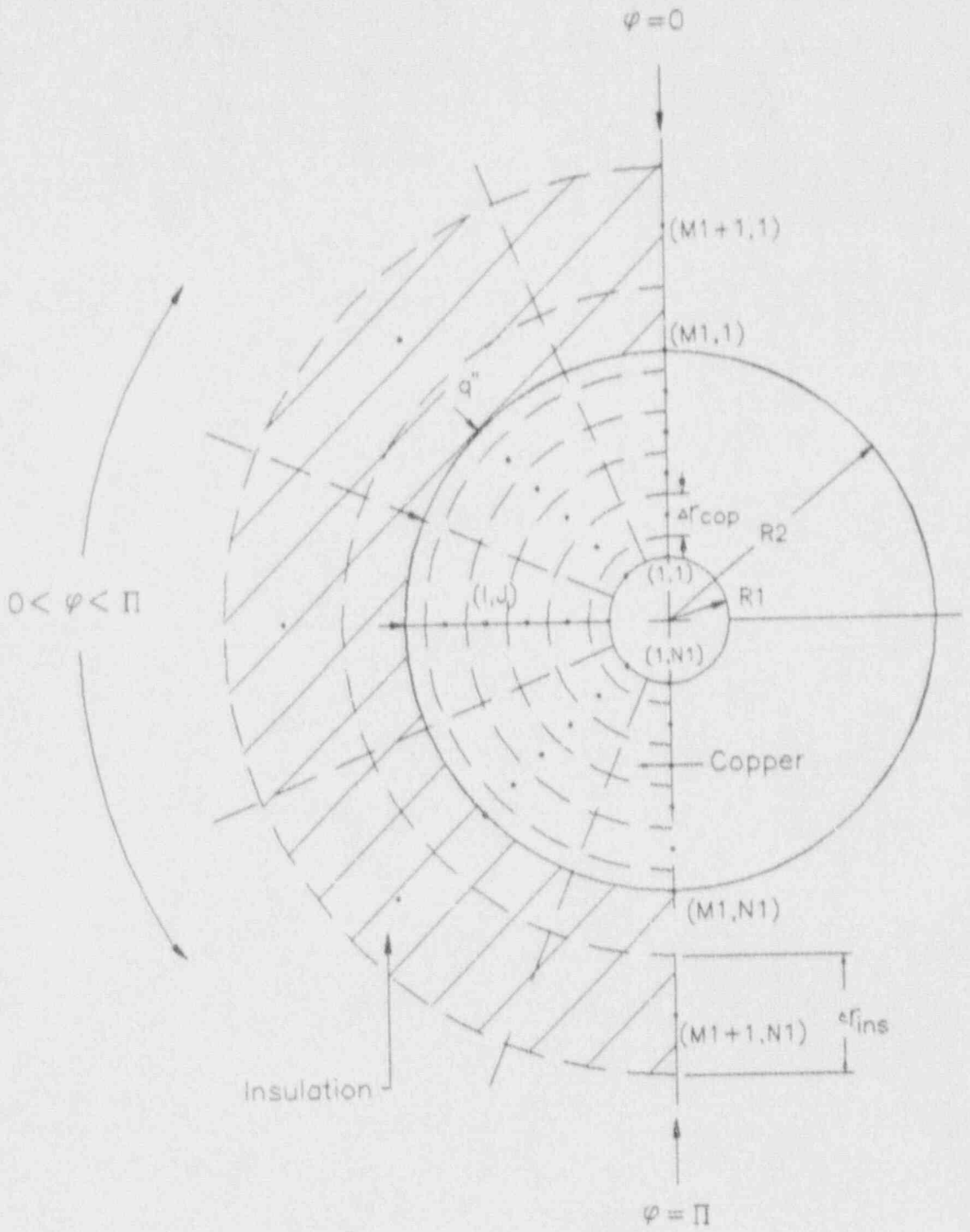

Figure 5.2 Mesh Diagram for Domain II: Copper Bulk Fluid and the First Layer Nodes in Insulation

Similarly, the nodal temperature estimates for $T(i-1,j)$ are determined from,

$$T(i-1,j) = T(i,j) - R(i-1,j)\left(\frac{T(i+1,j)-T(i,j)}{R(i,j)}\right.$$

$$\left. + \frac{T(i,j+1)-T(i,j)}{RC(i,j)} + \frac{T(i,j-1)-T(i,j)}{RC(i,j-1)}\right) \qquad (5.2-4)$$

This equation can be used as a basis to write specific equations for the both the internal and the boundary nodes.

The inside surface boundary temperatures ($T(1,J)$) are known * and are also the outside surface temperatures of Domain II (the copper channel). The interior nodal equations for Domain I correspond to $I = 2$ to M, $J = 1$ to $N1$, and are given as follows (see Figure 5.1):

(a) At $\varphi = 0$,

$$T(I,1) = \frac{\frac{T(I-1,1)}{R(I-1,1)} + \frac{T(I+1,1)}{R(I,1)} + 2\frac{T(I,2)}{RC(I,1)}}{\frac{1}{R(I-1,1)} + \frac{1}{R(I,1)} + \frac{2}{RC(I,1)}}; \qquad (5.2-5)$$

(b) At $0 < \varphi < \pi$,

$$T(I,J) = \frac{\frac{T(I-1,J)}{R(I-1,J)} + \frac{T(I+1,J)}{R(I,J)} + \frac{T(I,J-1)}{RC(I,J-1)} + \frac{T(I,J+1)}{RC(I,J)}}{\frac{1}{R(I-1,J)} + \frac{1}{R(I,J)} + \frac{1}{RC(I,J-1)} + \frac{1}{RC(I,J)}}; \quad and (5.2-6)$$

(c) At $\varphi = \pi$,

$$T(I,N1) = \frac{\frac{T(I-1,N1)}{R(I-1,N1)} + \frac{T(I+1,N1)}{R(I,N1)} + 2\frac{T(I,N)}{RC(I,N)}}{\frac{1}{R(I-1,N1)} + \frac{1}{R(I,N1)} + \frac{2}{RC(I,N)}}. \qquad (5.2-7)$$

---

* The measured thermocouple data of Smith and Boyd[30] will be reduced in the present work to produce local (axial and circumferential) variations in the heat transfer coefficient, $h(\varphi, z)$.

Similarlly, the nodal equations for the outside surface of the insulation (i.e., $I = M1$; see Figure 5.1) are,

(a) At $\varphi = 0$,

$$T(M1,1) = \frac{\frac{T(M,1)}{R(M,1)} + 2\frac{T(M1,2)}{RC(M1,1)} + T_\infty h_\infty A}{\frac{1}{R(M,1)} + \frac{2}{RC(M1,1)} + h_\infty A}; \qquad (5.2-8)$$

(b) At $0 < \varphi < \pi$,

$$T(M1,J) = \frac{\frac{T(M,J)}{R(M,J)} + \frac{T(M1,J-1)}{RC(M1,J-1)} + \frac{T(M1,J+1)}{RC(M1,J)} + T_\infty h_\infty A}{\frac{1}{R(M,J)} + \frac{1}{RC(M,J-1)} + \frac{1}{RC(M1,J)} + h_\infty A}; \text{ and} \qquad (5.2-9)$$

(c) At $\varphi = \phi$,

$$T(M1,N) = \frac{\frac{T(M,N1)}{R(M,N1)} + 2\frac{T(M1,N)}{RC(M1,N)} + T_\infty h_\infty A}{\frac{1}{R(M,N1)} + \frac{2}{RC(M1,N)} + h_\infty A}. \qquad (5.2-10)$$

The heat resistances in the above equations are for the:

(a) Radial Direction,

$$R(i,j) = \frac{\Delta r_{ins}}{k_{ins}\Delta\varphi(R_2 + (j-0.5))}; \text{ and} \qquad (5.2-11a)$$

(b) Circumferential Direction,

$$RC(i,j) = \frac{R(i)\Delta\varphi}{k_{ins}\Delta r_{ins}}, \qquad (5.2-11b)$$

where $\Delta r_{ins} = \frac{(R_2' - R_2)}{M}$ and $\Delta\varphi = \frac{\pi}{N}$.

In the above equations, h_∞ is given by Ozisik[42] as,

$$h_\infty = h_c + h_r, \quad where \tag{5.2-12a}$$

$$h_c = \frac{k_{air} Nu_D}{D}; \tag{5.2-12b}$$

$$Nu_D = \{0.6 + 0.387 Ra_D^{\frac{1}{6}} [1 + (\frac{0.599}{Pr})^{\frac{9}{16}}]^{-\frac{8}{27}}\}^2; \quad and, \tag{5.2-12c}$$

$$h_r = \sigma(Ts^2 + T_\infty^2)(Ts + T_\infty). \tag{5.2-12d}$$

Before an iterative solution to the above equation is obtained, the assumed values of $T(M1, j)$ are first to used to estimate h_∞. Then h_∞ and all other assumed (or previously computed) values of $T(i, j)$ are used to compute the new wall temperature ($TT(i, j)$), where r varies from $R_2 + \Delta r_{ins}$ to R_2'.

5.2.2 *Domain II*

After the nodal temperature and heat transfer computations have converged, the nodal temperatures, ($TT(2, j)$ for Domain I (insulation) are used as necessary boundary conditions for the Domain II (epoxy and copper *) nodal temperatures at locations $i = M$ (i.e. $r = R_2 - \Delta r_{cop}$) and j shown in Figure 5.2. Therefore, based on the measured copper outside temperatures, $T(M1, j)$, and calculated inside insulation temperatures,

* For simplicity the epoxy is not shown in Figures 5.1 and 5.2. The difference equations are similar to those for copper.

$TT(M1+1,j)$, the nodal temperatures * in the copper test section can be computed directly without iteration. For the first internal node next to the outside boundary ($i = M$) of Domain II, the nodal equations are:

(a) At $\varphi = 0$,

$$T(M,1) = T(M1,1) + R(M,1)(2\frac{T(M1,1) - T(M1\ 2)}{RC(M1,1)}$$

$$+\frac{T(M1,1) - T(M1+1,1)}{R(M1,1)} - \frac{Q}{L}); \qquad (5.2-13a)$$

(b) At $0 < \varphi < \pi$,

$$T(M,J) = T(M1,J) + R(M,J)(\frac{T(M1,J) - T(M1,J+1)}{RC(M1,J)}$$

$$+\frac{T(M1,J) - T(M1,J-1)}{RC(M1,J-1} + \frac{T(M1,J) - T(M1,J+1)}{RC(M1,J)}$$

$$--\frac{T(M1+1,J)}{R(M1,J)} - \frac{Q}{L}); \quad and \qquad (5.2-13b)$$

(c) At $\varphi = \pi$,

$$T(M,N1) = T(M1,N1) + R(M,N1)(2\frac{T(M1,N1) - T(M1,N)}{RC(M1,N)}$$

$$+\frac{T(M1,N1) - T(M1+1,N1)}{R(M1,N1)} - \frac{Q}{L}), \qquad (5.2-13c)$$

* In order to conserve space and simplify notation, the nodal temperatures for the copper in Domain II will be represented henceforth as $T(i,j)$ using the notation of Figure 5.2.

where the heating tape is considered to be the internal heat source of total power, Q. Further, the remaining internal nodes for Domain II ($i = 2$ to $M-1$, $j = 1$ to $N1$) have the following difference equations:

(a) At $\varphi = 0$,

$$T(I,1) = T(I+1,1) + R(I,1)\left(\frac{T(I+1,1) - T(I+2,1)}{R(I+1,1)}\right.$$
$$\left. +2\frac{T(I+1,1) - T(I+1,2)}{RC(I+1,1)}\right); \qquad (5.2-14a)$$

(b) At $0 < \varphi < \pi$,

$$T(I,J) = T(I+1,J) + R(I,J)\left(\frac{T(I+1,J) - T(I+2,J)}{R(I+1,J)}\right.$$
$$\left. +\frac{T(I+1,J) - T(I+1,J+1)}{RC(I+1,J)} + \frac{T(I+1,J) - T(I+1,J-1)}{RC(I+1,J-1)}\right); \quad \textit{and} \qquad (5.2-14b)$$

(c) At $\varphi = \pi$,

$$T(I,N1) = T(I+1,N1) + R(I,N1)\left(\frac{T(I+1,N1) - T(I+2,N1)}{R(I+1,N1)}\right.$$
$$\left. +2\frac{T(I+1,N1) - T(I+1,N)}{RC(I+1,N)}\right). \qquad (5.2-14c)$$

Similarly, the nodal equations for the first full nodes (i.e. at $r = R1 + \Delta r_{cop}$) adjacent inside boundary of Domain II are:

(a) At $\varphi = 0$,

$$T(1,1) = T(2,1) + R(1,1)\left(\frac{T(2,1) - T(3,1)}{R(2,1)} + 2\frac{T(2,1) - T(2,2)}{RC(2,1)}\right); \qquad (5.2-15a)$$

(b) At $0 < \varphi < \pi$,

$$T(1,J) = T(2,J) + R(1,J)(\frac{T(2,J) - T(3,J)}{R(2,J)}$$

$$+\frac{T(2,J) - T(2,J+1)}{RC(2,J)} + \frac{T(2,J) - T(2,J-1)}{RC(2,J-1)}); \quad and, \qquad (5.2-15b)$$

(c) At $\varphi = \pi$,

$$T(1,N1) = T(2,N1) + R(1,N1)(\frac{T(2,N1) - T(3,N1)}{R(2,N1)}$$

$$+2\frac{T(2,N1) - T(2,N)}{RC(2,N)}). \qquad (5.2-15c)$$

Finally, the circumferential heat transfer coefficient was computed from the difference equations for the nodes on the inside boundary (i.e., $r = R1$, or $i = 1$) and are given by:

(a) At $\varphi = 0$,

$$h(1)\Delta A = \frac{2\frac{T(1,1)-T(1,2)}{RC(1,1)} + \frac{T(1,1)-T(2,)}{R(1,1)}}{T(1,1) - Tb} -; \qquad (5.2-16a)$$

(b) At $0 < \varphi < \pi$,

$$h(J)\Delta A = \frac{\frac{T(1,J)-T(2,J)}{R(1,J)} + \frac{T(1,J)-T(1,J+1)}{RC(1,J)} + \frac{T(1,J)-T(1,J-1)}{RC(1,J-1)}}{T(1,J) - Tb}; \quad and, \qquad (5.2-16b)$$

(c) At $\varphi = \pi$,

$$h(N1)\Delta A = \frac{2\frac{T(1,N1)-T'1,N)}{RC(1,N)} + \frac{T(1,N1)-T(2,N1)}{R(1,N1)}}{T(1,N1) - Tb}. \qquad (5.2-16c)$$

where $\Delta A = \Delta r_{cop}\Delta\varphi$.

The form of the equations for the thermal resistances for the copper (Domain II) are the same as that in the insulation (Domain I), except

$$R(M1,j) = \frac{R(M1)\Delta\varphi}{k_{ins}\frac{\Delta r_{ins}}{2} + k_{cop}\frac{\Delta r_{cop}}{2}}. \tag{5.2.17}$$

The computer programs developed from the above difference equations for Domain I and II are contained in Appendix B.2. Appedix B.1 contains a partially computed computer program which can be used to compare with results[39] from a theoretical conduction formulation of the problem in Figure 4.2 for the case where the insulation is perfect. Appendix B.3 contains a detail difference formulation of all above difference equations and thermal resistances for Figure 5.1 and 5.2.

6. RESULTS

6.1 EXPERIMENTAL DATA BASE AND SUBCOOLED FLOW BOILING PREDICTIONS

Flow boiling predictions were made of the local (axial) heat transfer and wall temperature for both water and freon-11 for smooth tubes with a uniform heat flux. The flow conditions for both fluids are summarized in Tables 6.1.1; and 6.1.2. Because orientation effects were unimportant for the water data, direct comparisons can be made with the "modified" correlation. However, orientations effects were important for the freon-11 data; and, so only qualitative comparisons can be made with that data. This work will be summarized in a TSRC report[49] and technical paper.

The plots of the results were presented in the form of local heat transfer coefficient versus net power generation ratio, and power versus the local wall temperture. The predictions and the experimental data were compared, and standard deviations were tabulated for each mass velocity of each fluid and for all the data for each fluid.

Table 6.0-1 Water Data Matrix (orientation unimportant)

Flowrate G (Mg/m^2s)	Exit Pressure P (MPa)	Inlet Temperature Tin (°C)	Location* Z (cm)
4.4	1.66	20.0	*
13.3	1.66	20.0	*
20.0	1.66	20.0	*
24.9	1.66	20.0	*
31.5	1.66	20.0	*
4.6	0.77	20.0	*
13.5	0.77	20.0	*
26.9	0.77	20.0	*
36.0	0.77	20.0	*
* Axial Locations from the Inlet (cm): Z1 = 0.317, Z2 = 14.59, Z3 = 26.88			

Table 6.0-2 Freon-11 Data Matrix (orientation unimportant)

Flowrate G (Kg/m^2s)	Exit Pressure P (MPa)	Inlet Temperature Tin (°C)	Axial Location* Z (cm)
210.0	0.186	22.2	*
281.0	0.186	22.2	*
* Z2 = 20.32, Z3 = 40.64, Z4 = 60.96, Z5 = 81.28, Z6 = 101.60.			

6.1.1 *Water Results*

The results for water show that the initial idea of Boyd[6,7,11,13] seems sound. Both the "initial" and the "modified" models have good agreement with the data. The "modified" model was expected to improve the agreement with the data by raising the predictions in partial nucleate boiling region via an expanded approximation for the asymptotic limit below ONB. Improved predictions occured in many cases and can be varified by comparing, on a one-to-one basis, Figure 6.1.1 through 6.1.6 (for $P = 1.66\ MPa$ for Figures 6.1.1 to 6.1.3, and 0.77 MPa for Figures 6.1.4 to 6.1.6) for "initial" model with the "modified" model in Figures 6.1.7 through 6.1.12 ($P = 1.66\ MPa$ for Figures 6.1.7 to 6.1.9, and 0.77 MPa for Figures 6.1.10 to 6.1.12), respectively. These figures present $h(Z)$ as a function of the power ratio, Q/Q_2. In each case the comparison with the data seems good. The results from these comparisons are summarized in Tables 6.1.1-1 through 6.1.1-4. Both the percent and the actual standard deviation for the predictions of h with respect to the data are presented in the tables. The "modified" model has the best predictions at $P = 1.66\ MPa$ with an overall percent standard deviation (psd) of 12.5% compared to 13.7% for the "initial" model. In these cases, 185 data points were used in the comparison. However at a $0.77 MPa$ exit pressure, the overall psd increased to 19.0% for the "modified" model and that for the "initial" model increased to 18.6% for 169 data points. A more classical representatioin of the comparisons is the power (or heat flux) as a function of the wall temperature (or superheat). Similar comparisons were made for this representation. This will be presented below.

For most cases, the predictions are best at the channel exit (i.e., $Z = Z3 = 28.66\ cm$),

and worse at other upstream locations.

As shown in most plots, presented for upstream locations (i.e. Figures 6.1.2, 6.1.3, 6.1.5, 6.1.6, 6.1.8, 6.1.9, 6.1.11, and 6.1.12), the predictions are below the experimental data. This is due primarily to: (1) the heat transfer being thermally developing at upstream locations, and (2) the limiting condition used to match the single-phase and the partial boiling regoins must be replaced will a better estimate for the asymptotic limit. Although the data is for a horizontal flow channel, the Froude number was very large so that orientation effects were negligible. This latter point is also apparent from the above comparisons when one notes that the predictions apply primarilly to flows where gravitational effects are small. Had gravitational effects been consistently important, the data would have been below the predictions.

An examination of whether a better estimate for the asymptotic limit will result in better predictions of the wall temperature at a given heat flux can be made by comparing "initial" and "modified" models in terms of the power (or heat flux) as a fuction of the wall temperature (or superheat). These results for the "initial" model are contained in Figures 6.1.13 through 6.1.18, and the results for the "modified" model are contained in Figures 6.1.19 through 6.1.24. The results are presented, as before, for $P = 1.66$ and $0.77\ MPa$.

Since the data[15and28] were originally presentes in terms of $h(z)$ as a function of a dimensionless power ratio, the correspoding wall temperature was computed from $T_W(z) = T_b(z) + q"/h(z)$. A one-to-one comparison of the figures for each model (e.g., compare Figure 6.1.13 with 6.1.19, Figures 6.1.14 with 6.1.20, etc.) reveals that in each case, the "modified" model shifts, the predictions upwards towards the data for T_W. This

Table 6.1-1 Heat Transfer Coefficient Percent(%) Standard Deviation for the Water Predictions Using "Initial" Model (D = 0.3 cm).

Exit Pressure Pexit = 1.66 MPa				
Flowrate G (Mg/m^2s)	Location Z (cm)			Number of Data Points
	0.317	14.59	28.66	
4.4	29.7	22.5	14.4	9/11/14
13.3	13.1	7.9	10.8	15/16/12
20.0	9.7	7.9	7.5	13/12/14
24.9	N/A	23.9	8.0	-/15/13
31.5	8.9	15.1	6.3	14/15/12
Pressure Drop Effect	No	No	Yes	
Percent Deviation at Z	14.8	16.2	9.6	51/69/65
Overall Percent Standard Deviation: 13.7%				185
Exit Pressure Pexit = 0.77 MPa				
4.6	30.2	10.4	17.2	15/19/15
13.5	12.7	9.9	35.2	17/20/20
26.9	8.1	24.6	7.7	11/12/11
36.0	8.7	14.1	11.1	10/8/11
Pressure Drop Effect	No	No	Yes	
Percent Deviation at Z	18.0	14.3	22.9	53/59/57
Overall Percent Standard Deviation: 18.6%				169

Table 6.1-2 Heat Transfer Coefficient Standard(KW/m^2K) Deviation for the Water Predictions Using the "Initial" Model (D = 0.3cm).

Exit Pressure Pexit = 1.66 MPa				
Flowrate G (Mg/m^2s)	Location Z (cm)			Number of Data Points
	0.317	14.59	28.66	
4.4	6.6	10.9	5.6	9/11/14
13.3	16.7	8.7	12.2	15/16/12
20.0	10.2	12.2	11.0	13/12/14
24.9	N/A	49.7	14.5	-/15/13
31.5	23.7	36.4	15.0	14/15/12
Pressure Drop Effect	No	No	Yes	
Standard Diviation at Z	16.0	29.0	11.8	51/69/65
Overall Standard Deviation: 20.7 (KW/m^2K)				185
Exit Pressure Pexit = 0.77 MPa				
4.6	13.4	3.4	17.3	15/19/15
13.5	11.3	7.4	11.5	17/20/20
26.9	8.8	23.1	11.6	11/12/11
36.0	13.0	29.3	20.1	10/ 8/11
Pressure Drop Effect	No	No	Yes	
Standard Deviation at Z	11.5	15.1	14.7	53/59/57
Overall Standard Diviation: 13.9 (KW/m^2K)				169

Table 6.1-3 Heat Transfer Coefficient Percent(%) Standard Deviation for the Water Predictions Using the "Modified" Model (D = 0.3 cm).

Exit Pressure Pexit = 1.66 MPa				
Flowrate G (Mg/m^2s)	Location Z (cm)			Number of Data Points
	0.317	14.59	28.66	
4.4	17.5	20.6	16.6	9/11/14
13.3	19.3	5.0	9.2	15/16/12
20.0	7.9	4.6	5.9	13/12/14
24.9	N/A	21.1	6.7	-/15/12
31.5	11.9	11.1	4.1	14/15/12
Pressure Drop Effect	No	No	Yes	
Percent Deviation at Z	14.4	13.8	9.3	51/69/65
Overall Percent Percent Deviation: 12.5%				185
Exit Pressure Pexit = 0.77 MPa				
4.6	29.1	13.1	18.6	15/19/15
13.5	12.0	13.9	35.7	17/20/20
26.9	7.7	23.9	8.3	11/12/11
36.0	8.2	12.1	11.6	10/8/11
Pressure Drop Effect	No	No	Yes	
Percent Diviation at Z	17.2	15.6	23.5	53/59/57
Overall Percent Standard Deviation: 19.0%				169

Table 6.1-4 Heat Transfer Coefficient(KW/m^2K) Standard Deviation for the Water Predictions Using the "Modified" Model (D = 0.3 cm).

Exit Pressure Pexit = 1.66 MPa				
Flowrate G (Mg/m^2s)	Location Z (cm)			Number of Data Points
	0.317	14.59	28.66	
4.4	6.6	9.7	6.8	9/11/14
13.3	16.5	4.3	9.1	15/16/12
20.0	9.6	6.0	8.5	13/12/14
24.9	N/A	41.2	12.5	-/15/13
31.5	18.9	24.3	8.2	14/15/12
Pressure Drop Effect	No	No	Yes	
Standard Deviation at Z	14.1	22.3	8.9	51/69/65
Overall Standard Deviation: 16.3 (KW/m^2K)				185
Exit Pressure Pexit = 0.77 MPa				
4.6	12.9	4.8	17.6	15/19/15
13.5	10.5	12.4	13.6	17/20/20
26.9	8.0	20.5	14.9	11/12/11
36.0	11.4	22.1	23.2	10/8/11
Pressure Drop Effect	No	No	Yes	
Standard Deviation at Z	10.7	14.0	16.6	53/59/57
Overall Standard Deviation: 14.0 (KW/m^2K)				169

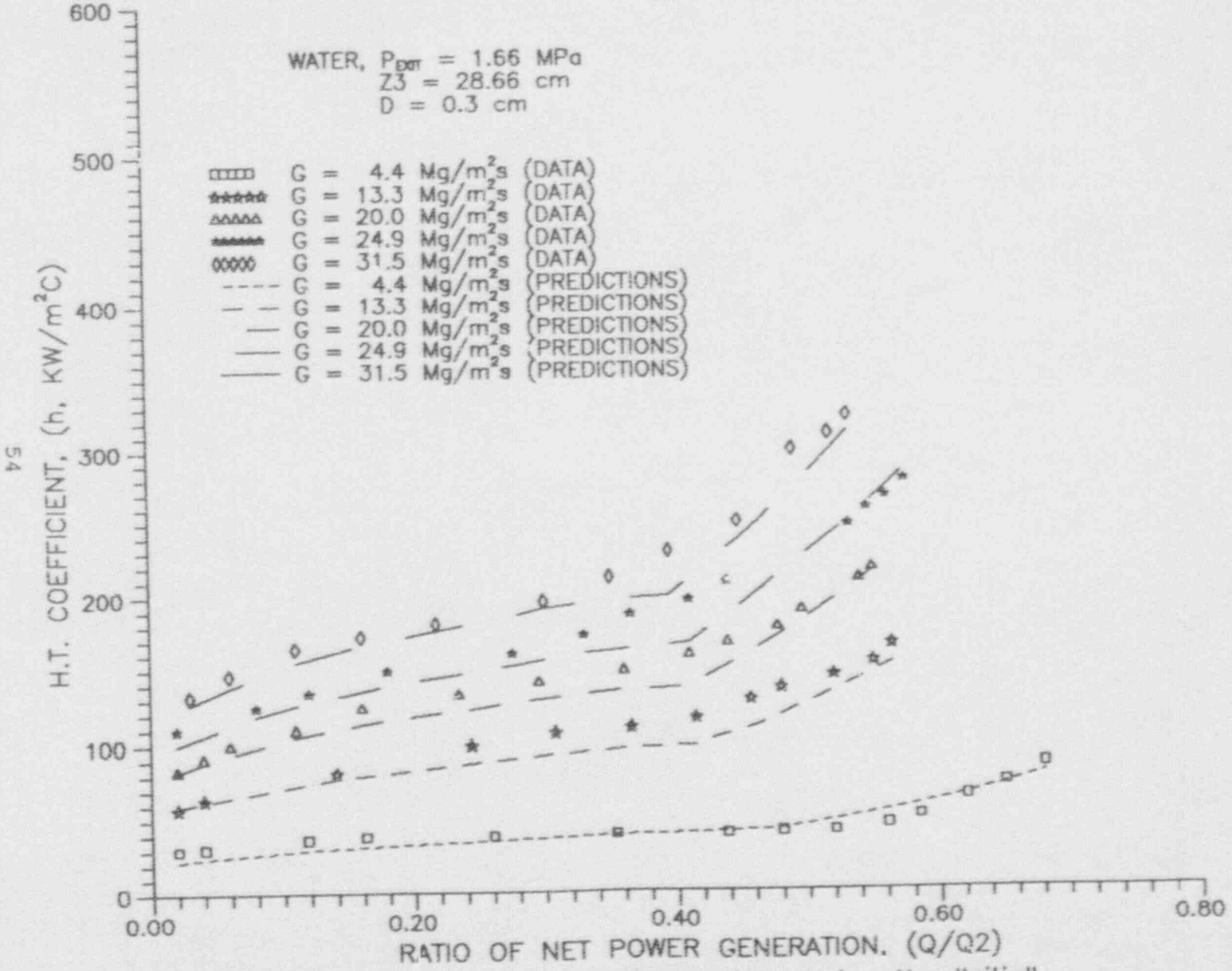

Fig. 6.1.1 Heat Transfer Coefficient Comparison Using the 'Initial' Model for Z = 28.66 cm (near the channel exit).

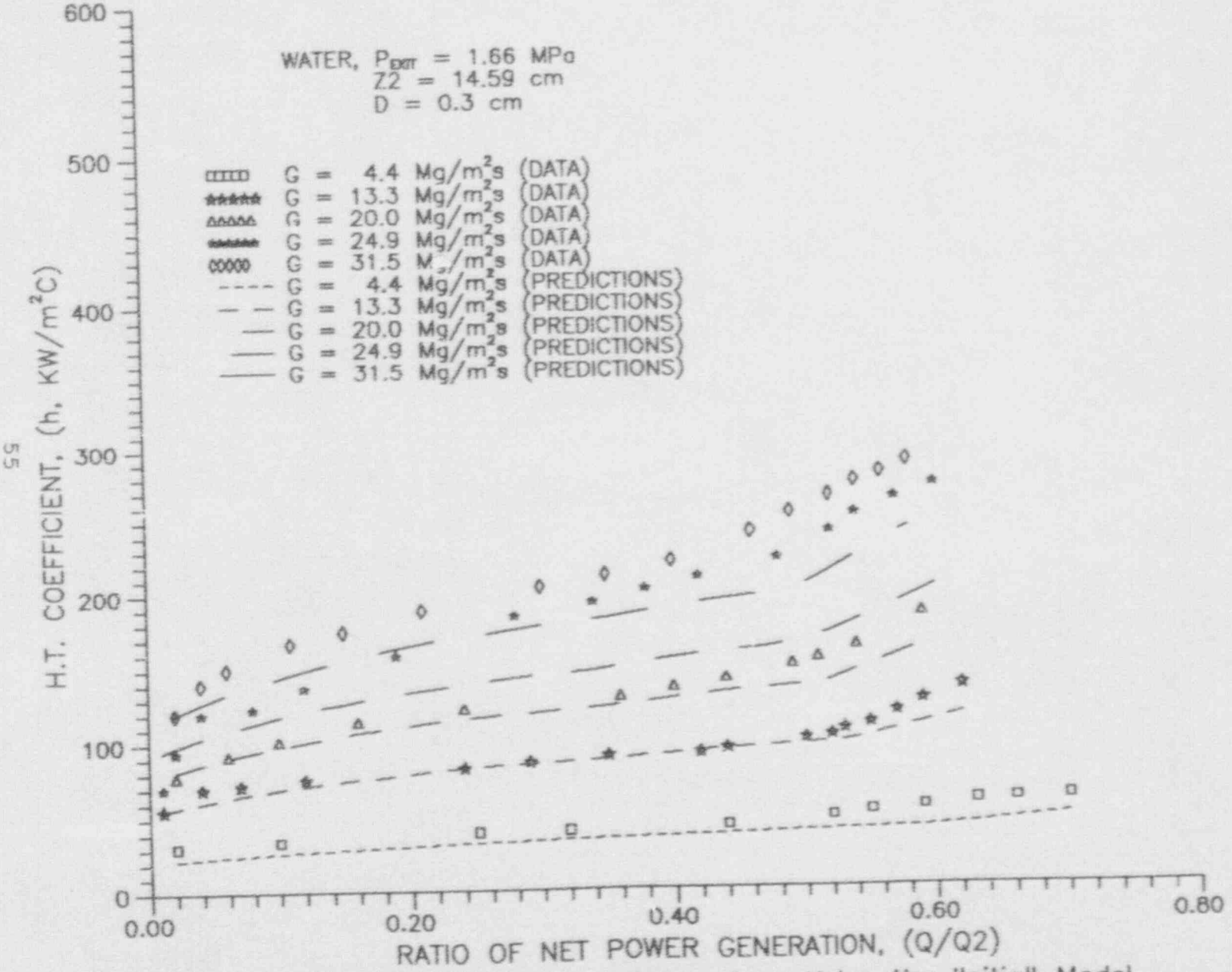

Fig. 6.1.2 Heat Transfer Coefficient Comparison Using the 'Initial' Model for Z = 14.59 cm (middle of the channel), and for P_{EXIT} = 1.66 MPa.

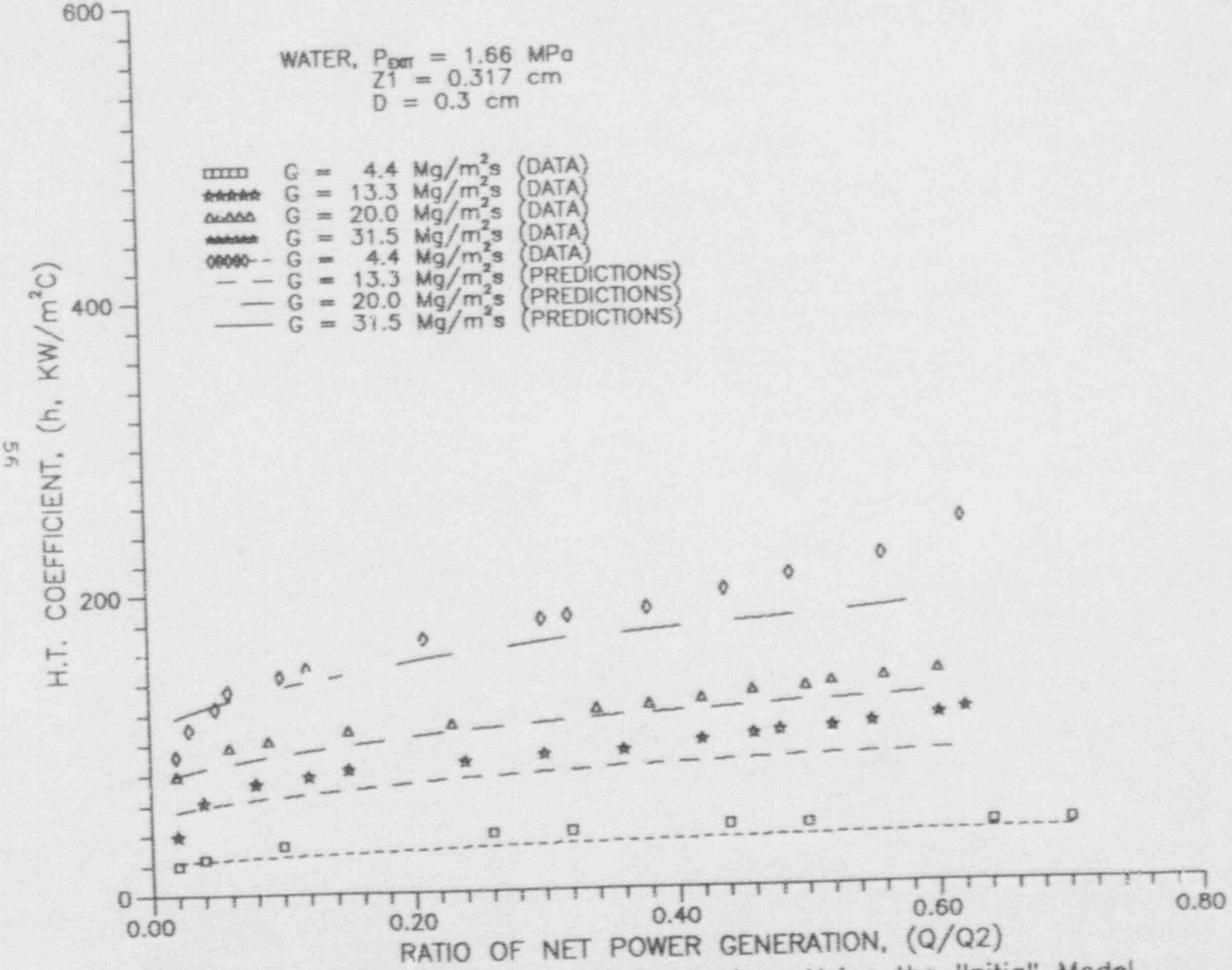

Fig. 6.1.3 Heat Transfer Coefficient Comparison Using the 'Initial' Model for Z = 0.317 cm (near the channel entrance), and for P_{EXIT} = 1.66 MPa.

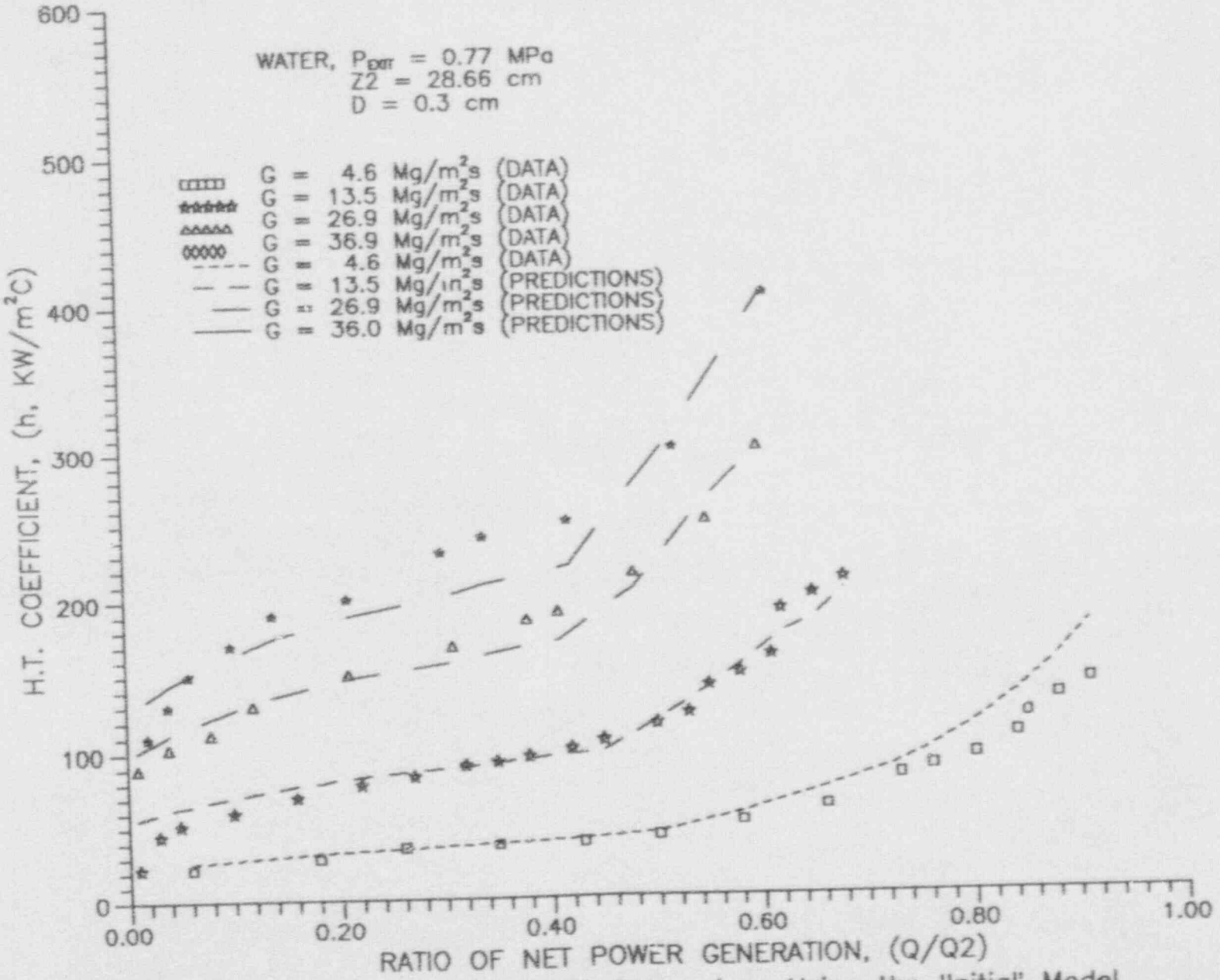

Fig. 6.1.4 Heat Transfer Coefficient Comparison Using the 'Initial' Model for Z = 28.66 cm (near the channel exit), and for P_{exit} = 0.77 MPa.

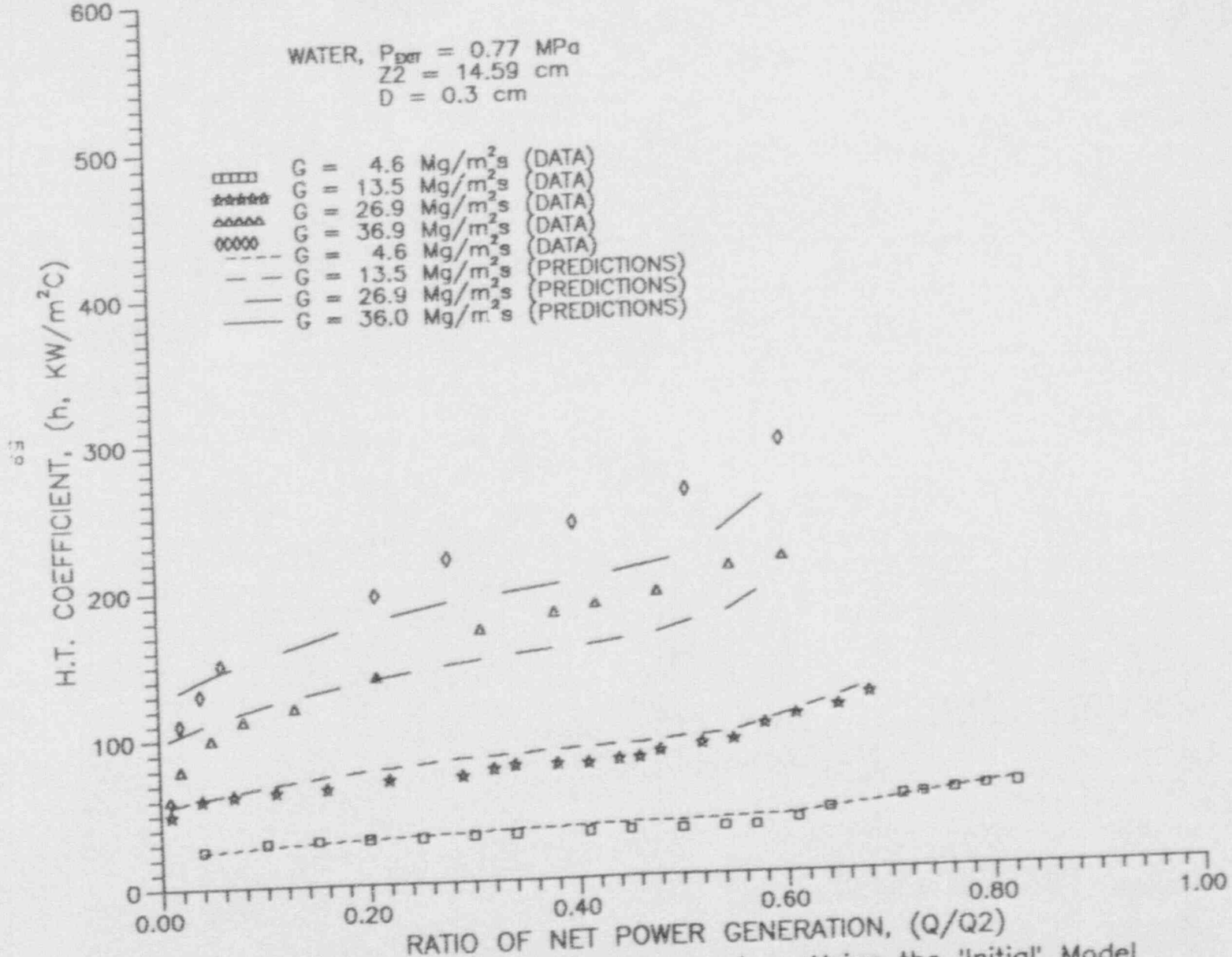

Fig. 6.1.5 Heat Transfer Coefficient Comparison Using the 'Initial' Model for Z = 14.59 cm (middle of channel), and for P_{EXIT} = 0.77 MPa.

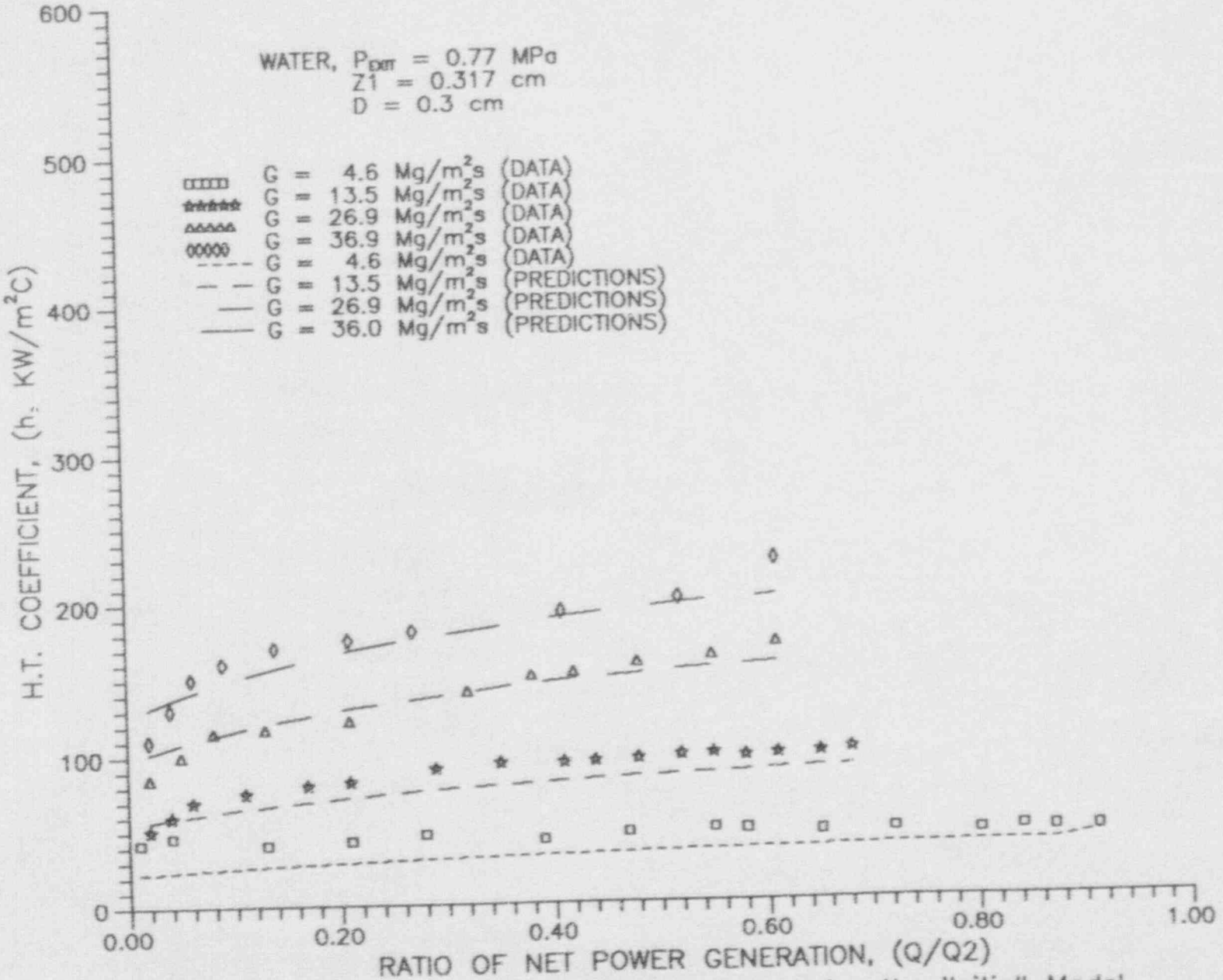

Fig. 6.1.6 Heat Transfer Coefficient Comparison Using the 'Initial' Model for Z = 0.317 cm (near the channel entrance), and for P_{EXIT} = 0.77 MPa.

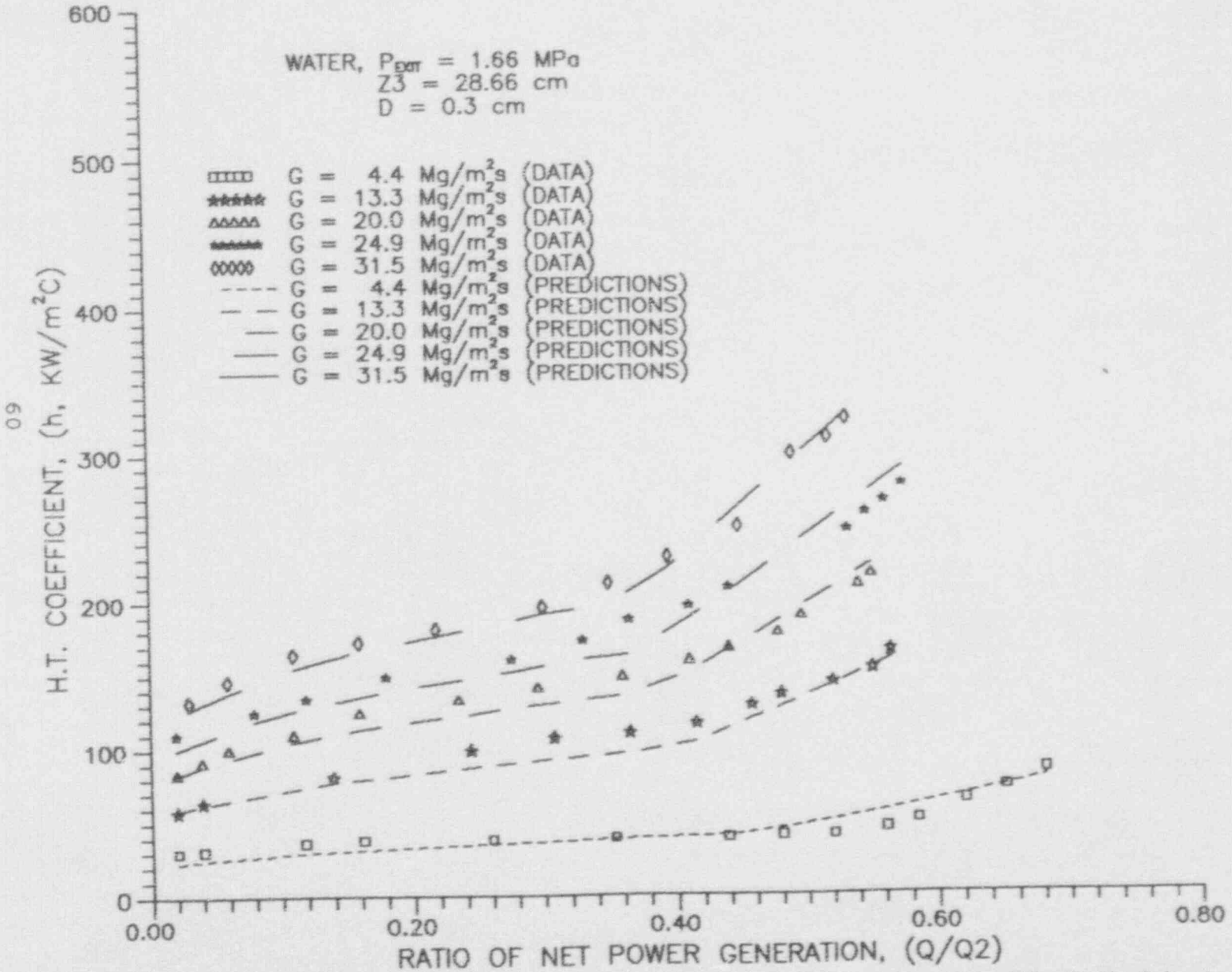

Fig. 6.1.7 Heat Transfer Coefficient Comparison Using the 'Modified' Model for Z = 28.66 cm (near the channel exit), and P_{EXIT} = 1.66 MPa.

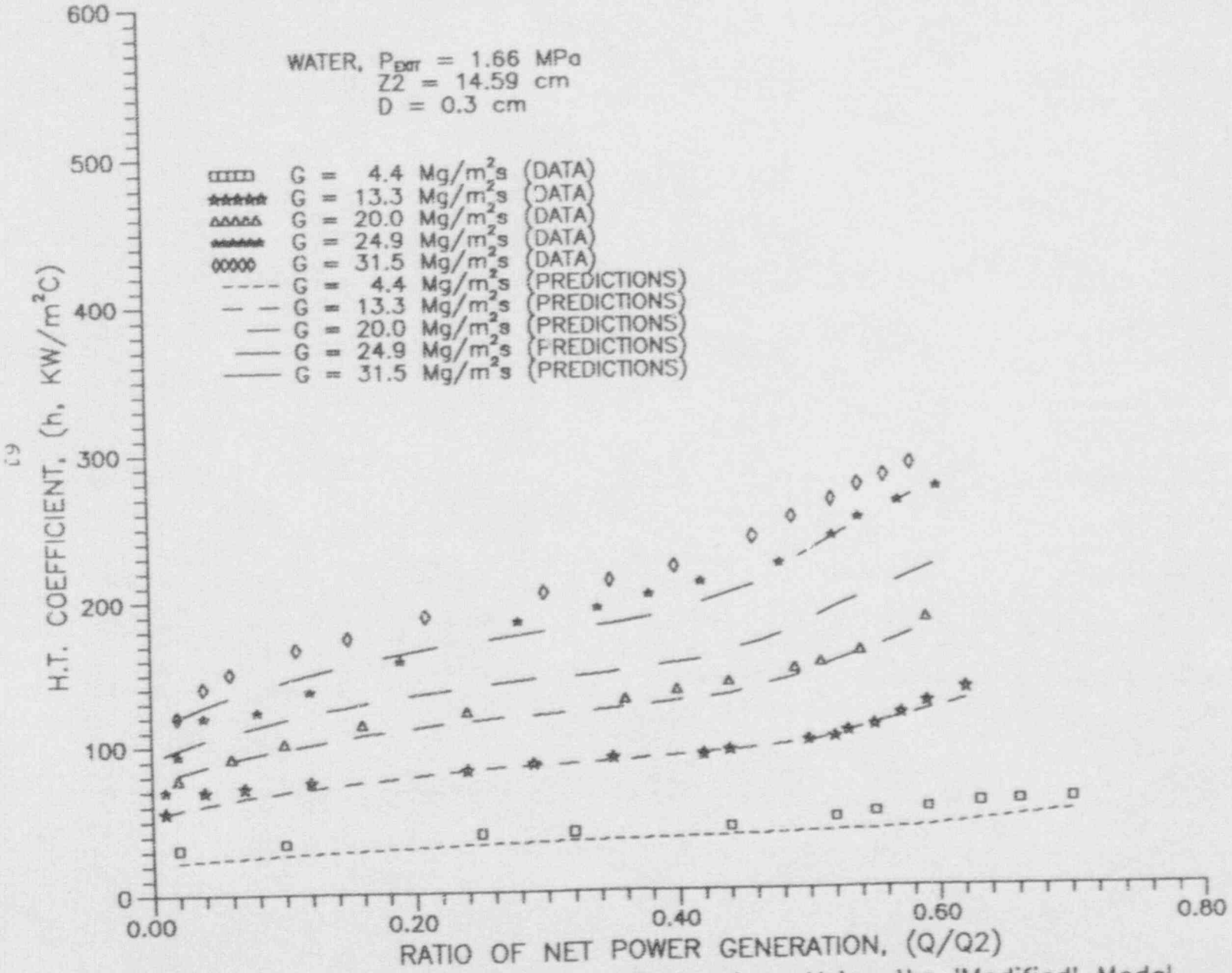

Fig. 6.1.8 Heat Transfer Coefficient Comparison Using the 'Modified' Model for Z = 14.59 cm (middle of channel), and P_{EXIT} = 1.66 MPa.

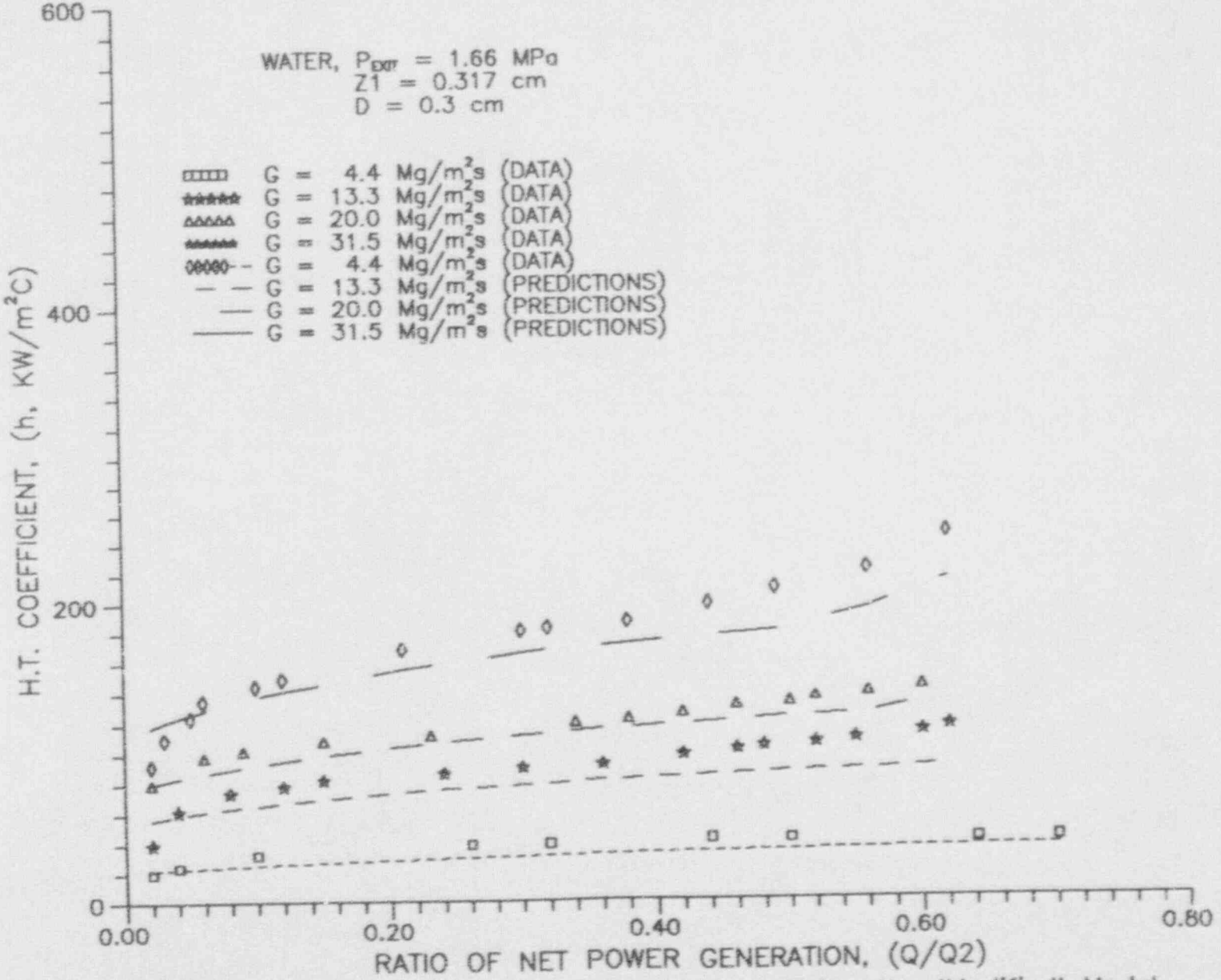

Fig. 6.1.9 Heat Transfer Coefficient Comparison Using the 'Modified' Model for Z = 0.317 cm (near the channel entrance), and P_{EXIT} = 1.66 MPa.

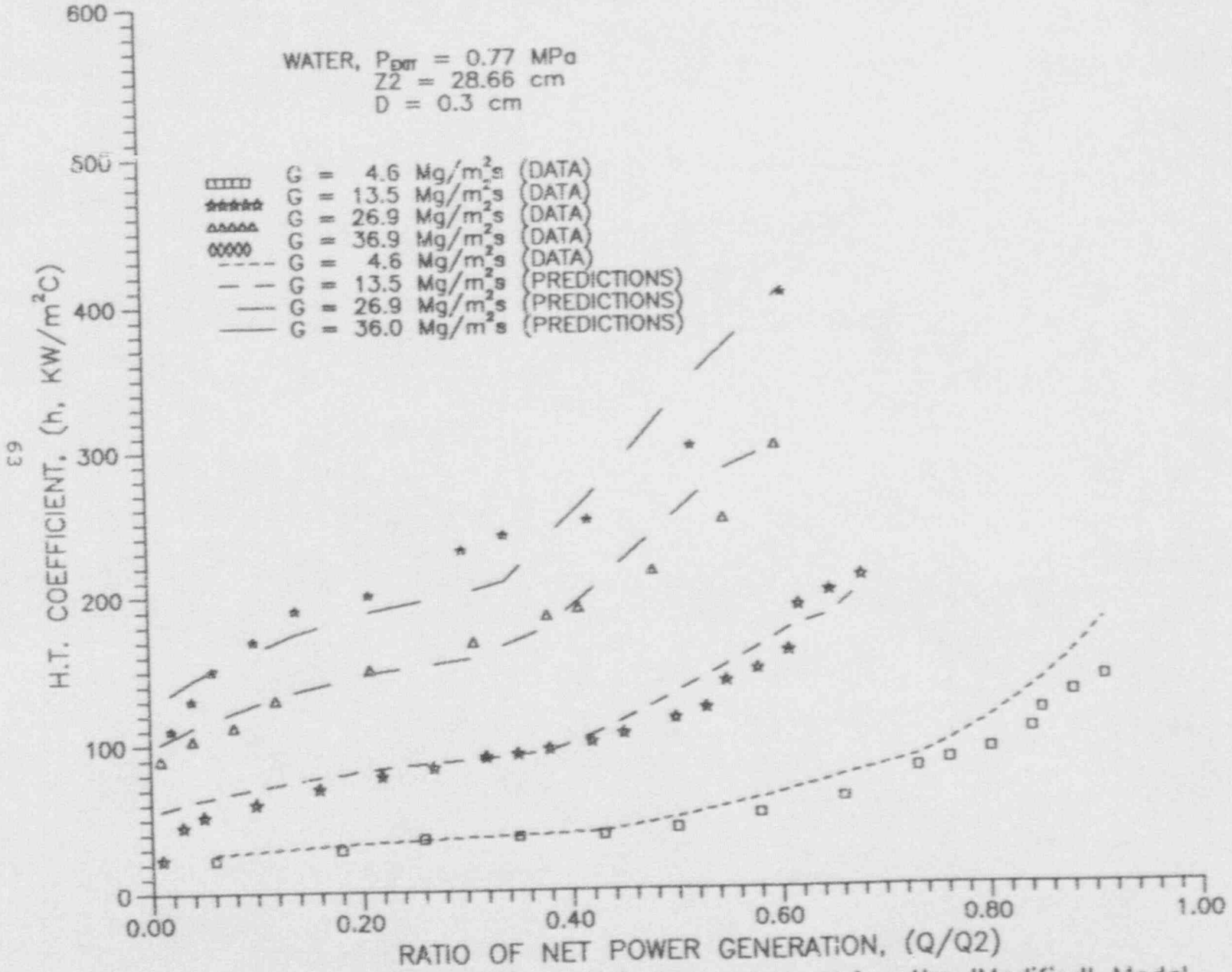

Fig. 6.1.10 Heat Transfer Coefficient Comparison Using the 'Modified' Model for Z = 28.66 cm (near the channel exit), and for P_{DET} = 0.77 MPa.

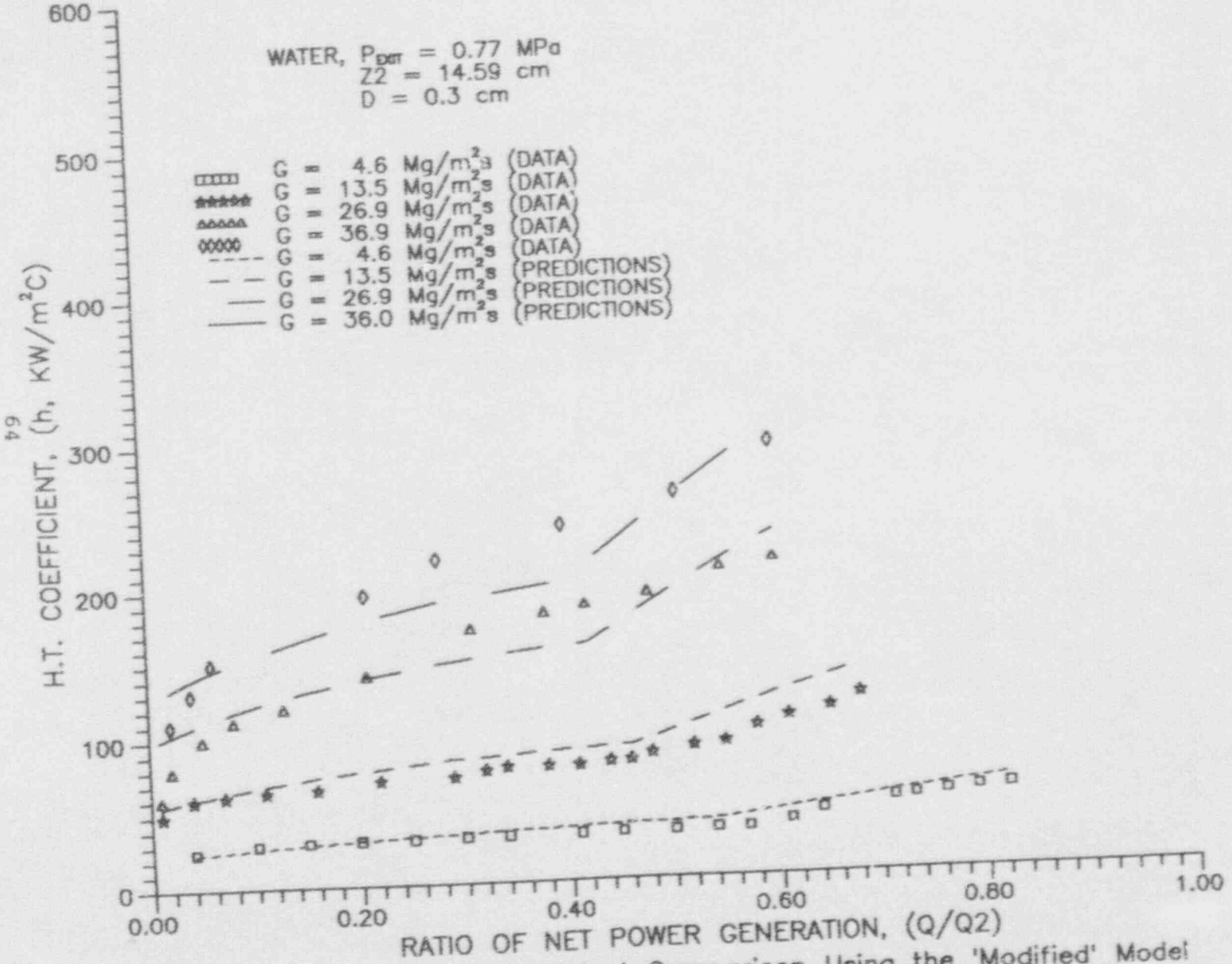

Fig. 6.1.11 Heat Transfer Coefficient Comparison Using the 'Modified' Model for Z = 14.59 cm (middle of channel), and for P_{EXIT} = 0.77 MPa.

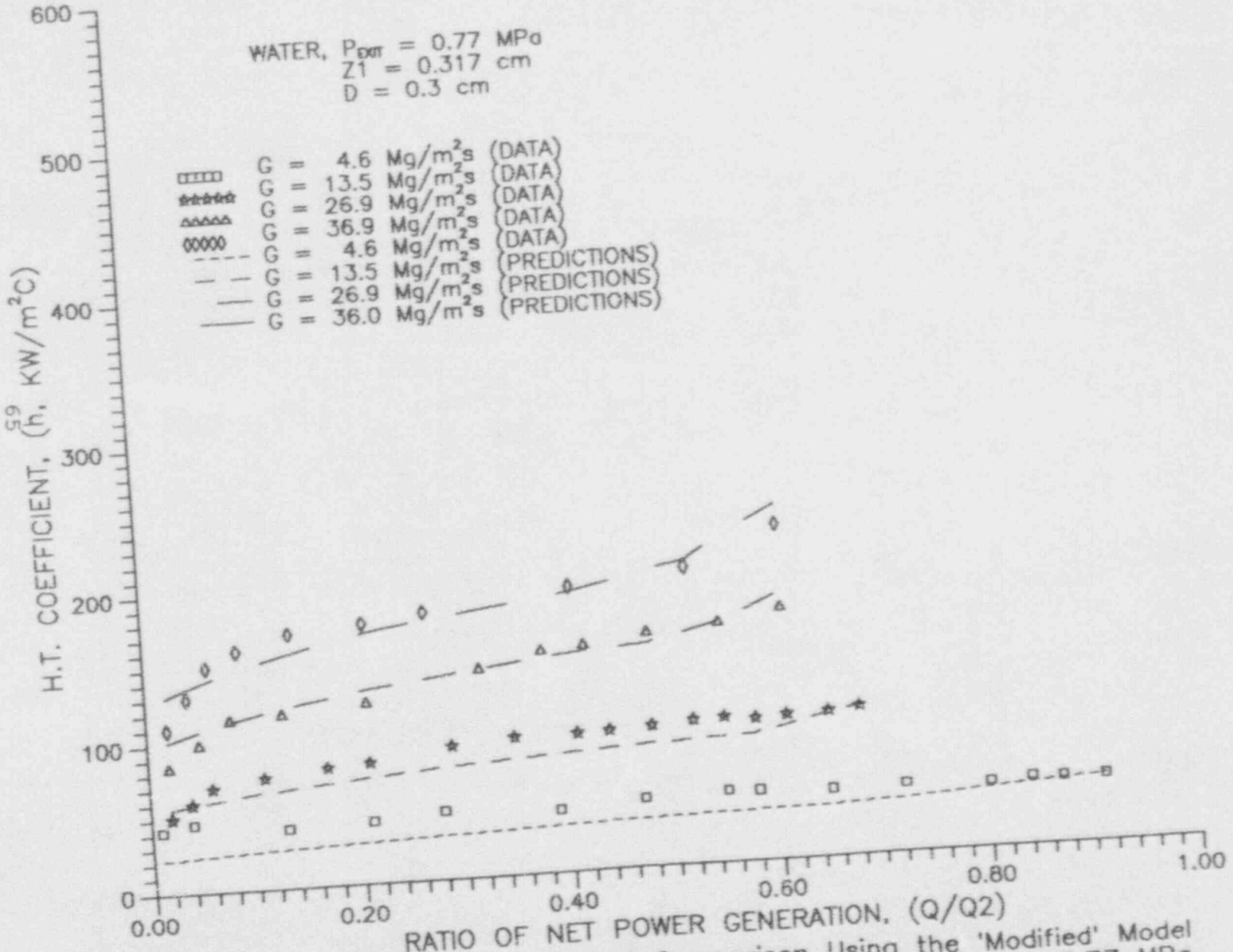

Fig. 6.1.12 Heat Transfer Coefficient Comparison Using the 'Modified' Model for Z = 0.317 cm (near the channel entrance), and for P_{EXIT} = 0.77 MPa.

demonstrates that a more accurate asymptotic limit would improve the predictions in the partial nucleate boiling region.

For the "initial" model, the asymptotic limit was assumed to occur at a wall temperature, $T_W = T_{sat} + \Delta T_{ONB}$, where ΔT_{ONB} was computed using Bergles and Rohsenow correlation and ranged from $7.4°C$ to $22.8°C$ for $P_{exit} = 1.66MPa$, and from $11.9°C$ to $35.8°C$ for $P_{exit} = 0.77\ MPa$. The improved results occured with the "modified" model by requiring the asymptotic limit for the wall temperature to be the saturation temperature T_{sat}. This latter limit eliminated the need to compute ΔT_{ONB}; and hence, the "modified" model does not require predictions of ONB.

Instead of being constant as was the case in Kandlikar's correlation, "a", "b", and "m" are varing in Boyd's correlations. These improved correlations result in both the slope and the shape of the boiling curve changing not only with the power level, ONB and FDB, but also with the local bulk temperature, local quality, and wall temperature as well. When more of these local characteristics are included, the accuracy improves.

In most practical analyses, the underlying task is to predict local value of T_W. In the above results, the predictions of T_W were made as a function of power, mass velocity, pressure, and local (axial) location. A summary of the psd and the standard deviation (sd) fot T_W is presented in Tables 6.1-5 and 6.1-6 for the "initial" model and Tables 6.1-7 and 6.1-8 for the "modified" model. One obvious observation is that for both methods, the psd for T_W is significantly smaller than that for h. The order of the magnitude of the sd was 12.0 K. Although the results show improvements occurred with the "modified" model, when compared with the "initial" model, they clearly show that there is a need for

Table 6.1-5 Inside Wall Temperature Percent(%) Standard Deviation for the Water Predictions Using "Initial" Model (D = 0.3 cm).

Flowrate G (Mg/m^2s)	Location Z (cm)			Number of Data Points
	0.317	14.59	28.66	
Exit Pressure Pexit = 1.66 MPa				
4.4	4.3	5.6	1.6	9/11/14
13.?	5.3	2.2	2.6	15/16/12
20.0	2.4	2.5	1.8	13/12/14
24.9	N/A	6.8	1.9	-/15/13
31.5	4.1	4.6	1.8	14/15/12
Pressure Drop Effect	No	No	Yes	
Percent Deviation at Z	4.1	4.6	1.9	51/69/65
Overall Percent Standard Deviation: 3.6%				185
Exit Pressure Pexit = 0.77 MPa				
4.6	6.5	2.4	1.9	15/19/15
13.5	3.1	2.2	1.3	17/20/20
26.9	1.4	2.7	1.7	11/12/11
36.0	1.5	3.1	1.7	10/8/11
Pressure Drop Effect	No	No	Yes	
Percent Deviation at Z	3.9	2.4	1.5	53/59/57
Overall Percent Standard Deviation: 2.7%				169

Table 6.1-6 Inside Wall Temperature (σ) Standard Deviation for the Water Predictions Using the "Initial" Model (D = 0.3cm).

Flowrate G (Mg/m^2s)	Location Z (cm)			Number of Data Points
	0.317	14.59	28.66	
Exit Pressure Pexit = 1.66 MPa				
4.4	17.2	25.9	7.9	9/11/14
13.3	22.5	10.5	12.1	15/16/12
20.0	10.9	11.6	8.2	13/12/14
24.9	N/A	30.0	9.0	-/15/13
31.5	18.3	21.2	8.0	14/15/12
Pressure Drop Effect	No	No	Yes	
Standard Diviation at Z	17.5	20.4	8.8	51/69/65
Overall Standard Deviation: 16.3 (K)				185
Exit Pressure Pexit = 0.77 MPa				
4.6	25.5	10.7	8.8	15/19/15
13.5	12.8	9.5	5.0	17/20/20
26.9	5.8	11.2	5.4	11/12/11
36.0	6.5	13.2	7.0	10/ 8/11
Pressure Drop Effect	No	No	Yes	
Standard Deviation at Z	15.5	10.5	6.5	53/59/57
Overall Standard Diviation: 11.2 (K)				169

Table 6.1-7 Inside Wall Temperature Percent(%) Standard Deviation for the Water Predictions Using "Modified" Model (D = 0.3 cm).

Exit Pressure Pexit = 1.66 MPa				
Flowrate G (Mg/m^2s)	Location Z (cm)			Number of Data Points
	0.317	14.59	28.66	
4.4	4.3	4.8	2.1	9/11/14
13.3	5.2	0.8	1.8	15/16/12
20.0	2.2	1.2	1.3	13/12/14
24.9	N/A	5.4	1.3	-/15/13
31.5	3.0	2.9	0.8	14/15/12
Pressure Drop Effect	No	No	Yes	
Percent Deviation at Z	3.4	2.7	1.7	51/69/65
Overall Percent Percent Deviation: 3.0%				185
Exit Pressure Pexit = 0.77 MPa				
4.6	5.6	2.9	2.2	15/19/15
13.5	2.7	3.2	1.6	17/20/20
26.9	1.2	2.1	1.3	11/12/11
36.0	1.0	2.1	1.7	10/8/11
Pressure Drop Effect	No	No	Yes	
Percent Diviation at Z	3.4	2.7	1.7	53/59/57
Overall Percent Standard Deviation: 2.7%				169

Table 6.1-8 Inside Wall Temperature (K) Standard Deviation for the Water Predictions Using "Modified" Model (D = 0.3 cm).

Exit Pressure Pexit = 1.66 MPa				
Flowrate G (Mg/m^2s)	Location Z (cm)			Number of Data Points
	0.317	14.59	28.66	
4.4	17.2	21.2	10.3	9/11/14
13.3	22.1	3.6	8.3	15/16/12
20.0	9.7	5.2	4.8	13/12/14
24.9	N/A	23.3	6.0	-/15/13
31.5	12.9	12.8	3.6	14/15/12
Pressure Drop Effect	No	No	Yes	
Standard Deviation at Z	15.8	14.8	6.7	51/69/65
Overall Standard Diviation: 12.9 (K)				185
Exit Pressure Pexit = 0.77 MPa				
4.6	21.4	13.4	10.0	15/19/15
13.5	10.9	14.4	6.8	17/20/20
26.9	4.6	8.4	5.6	11/12/11
36.0	4.1	8.6	7.2	10/8/11
Pressure Drop Effect	No	No	Yes	
Standard Deviation at Z	13.0	12.1	7.5	53/59/57
Overall Standard Deviation: 11.0 (K)				169

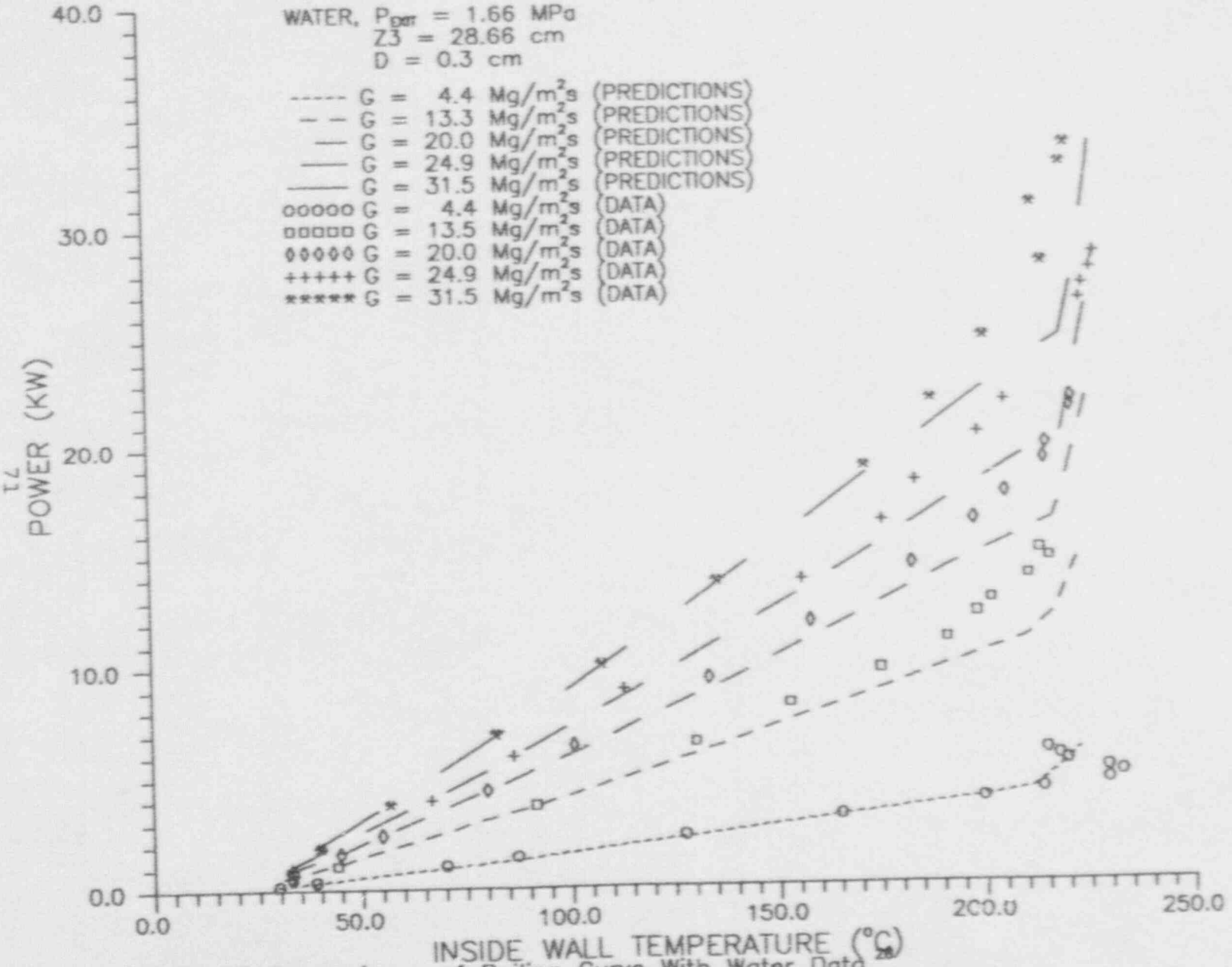

Fig. 6.1.13 Comparisons of Boiling Curve With Water Data Using the 'Initial' Model for Z = 28.66 cm (near the channel exit), and for P_{EXIT} = 1.66 MPa.

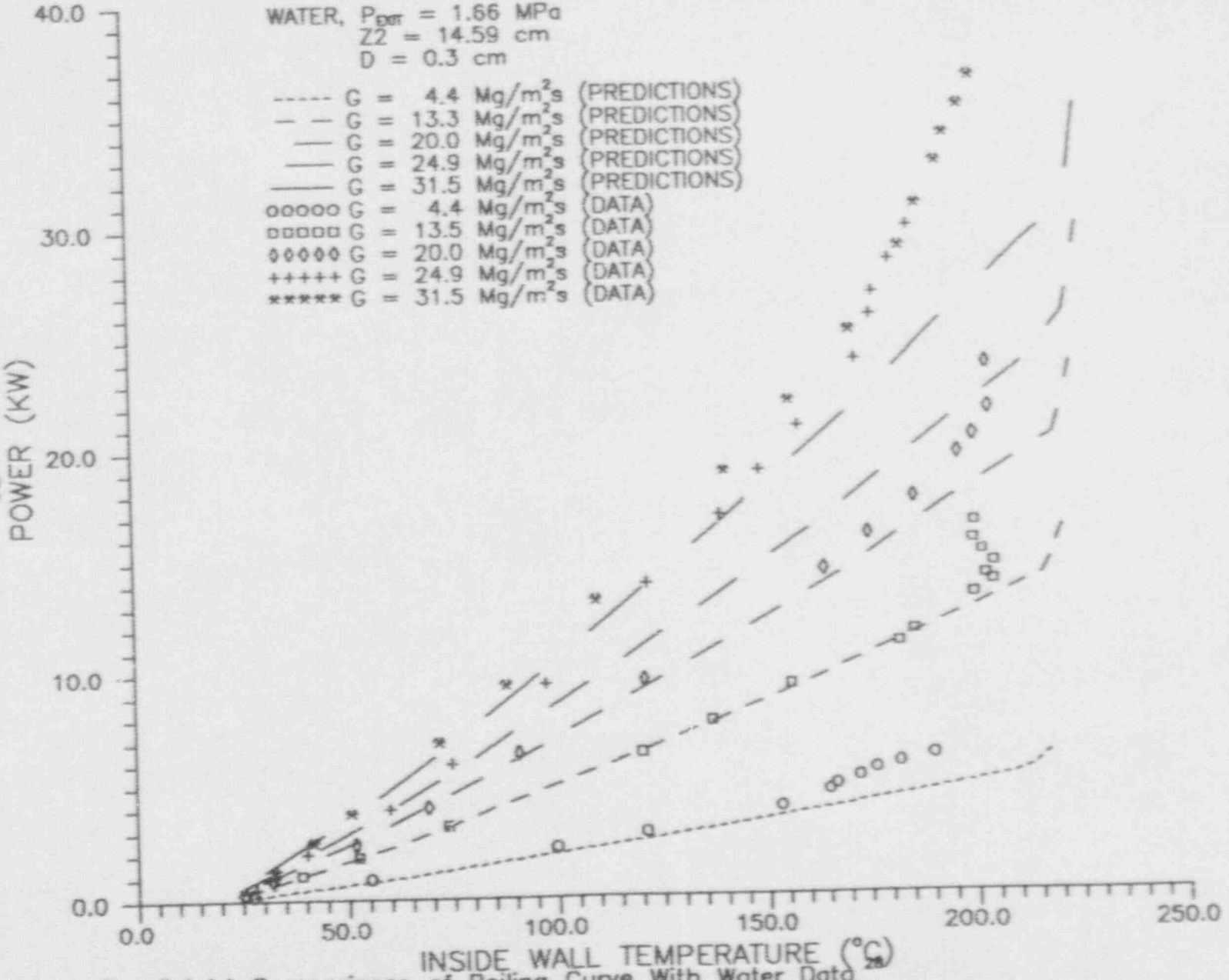

Fig. 6.1.14 Comparisons of Boiling Curve With Water Data Using the 'Initial' Model for Z = 14.59 cm (middle of channel), and for P_{EXIT} = 1.66 MPa.

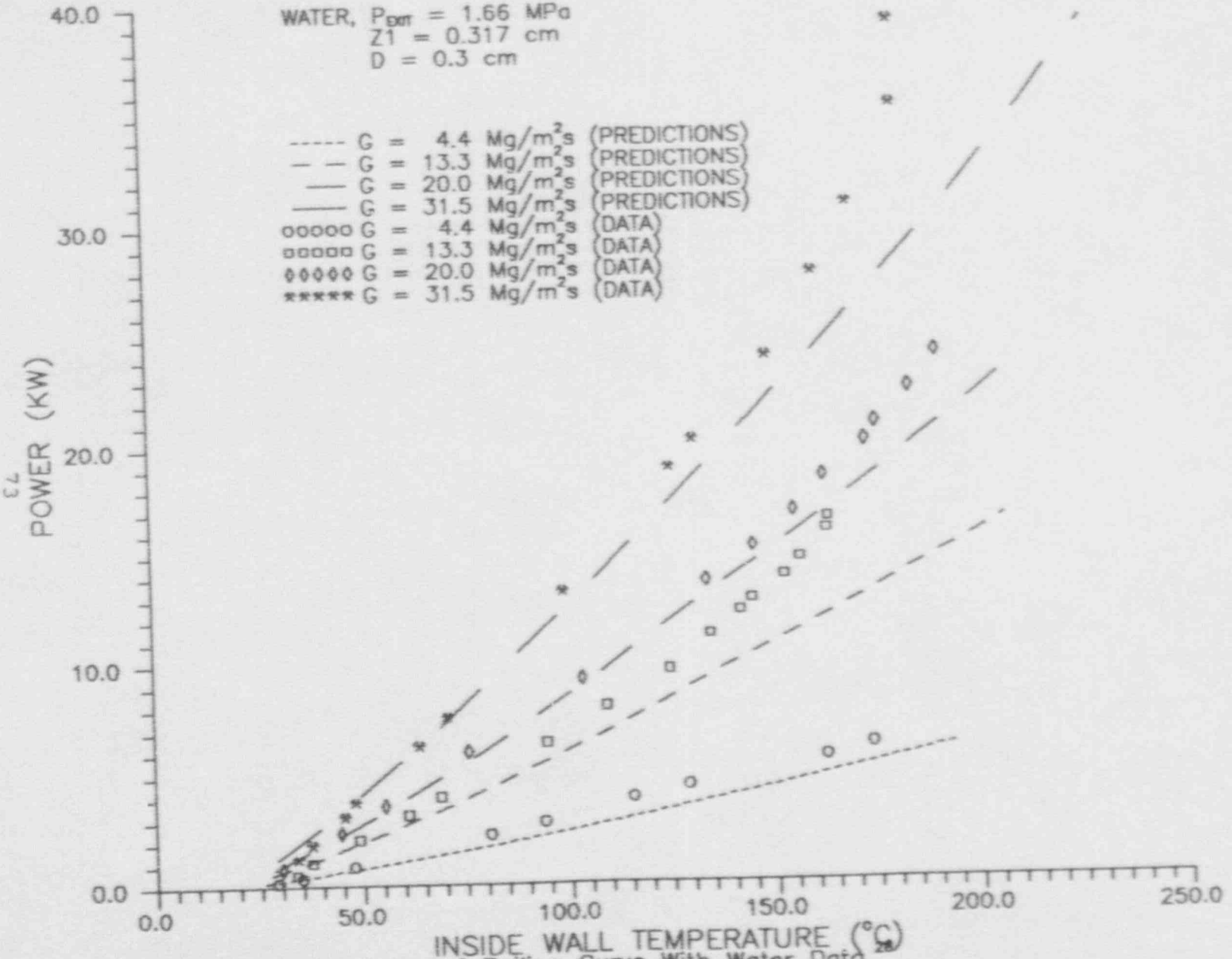

Fig. 6.1.15 Comparisons of Boiling Curve With Water Data Using the 'Initial' Model for Z = 0.317 cm (near the channel entrance), and for P_{EXIT} = 1.66 MPa.

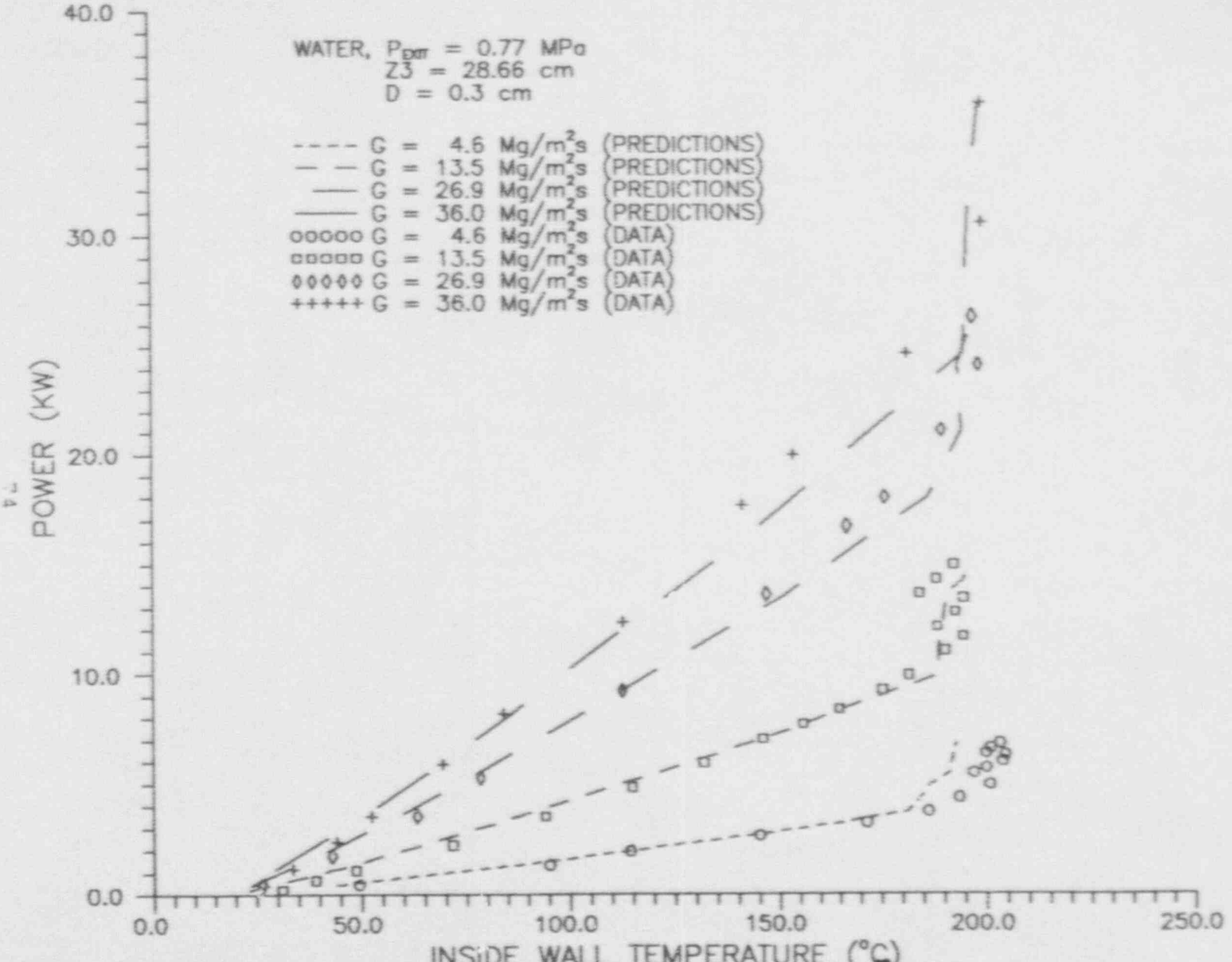

Fig. 6.1.16 Comparisons of Boiling Curve Predictions With Water Using the 'Initial' Model for Z = 28.66 cm (near the channel exit), and for P_{EXIT} = 0.77 MPa.

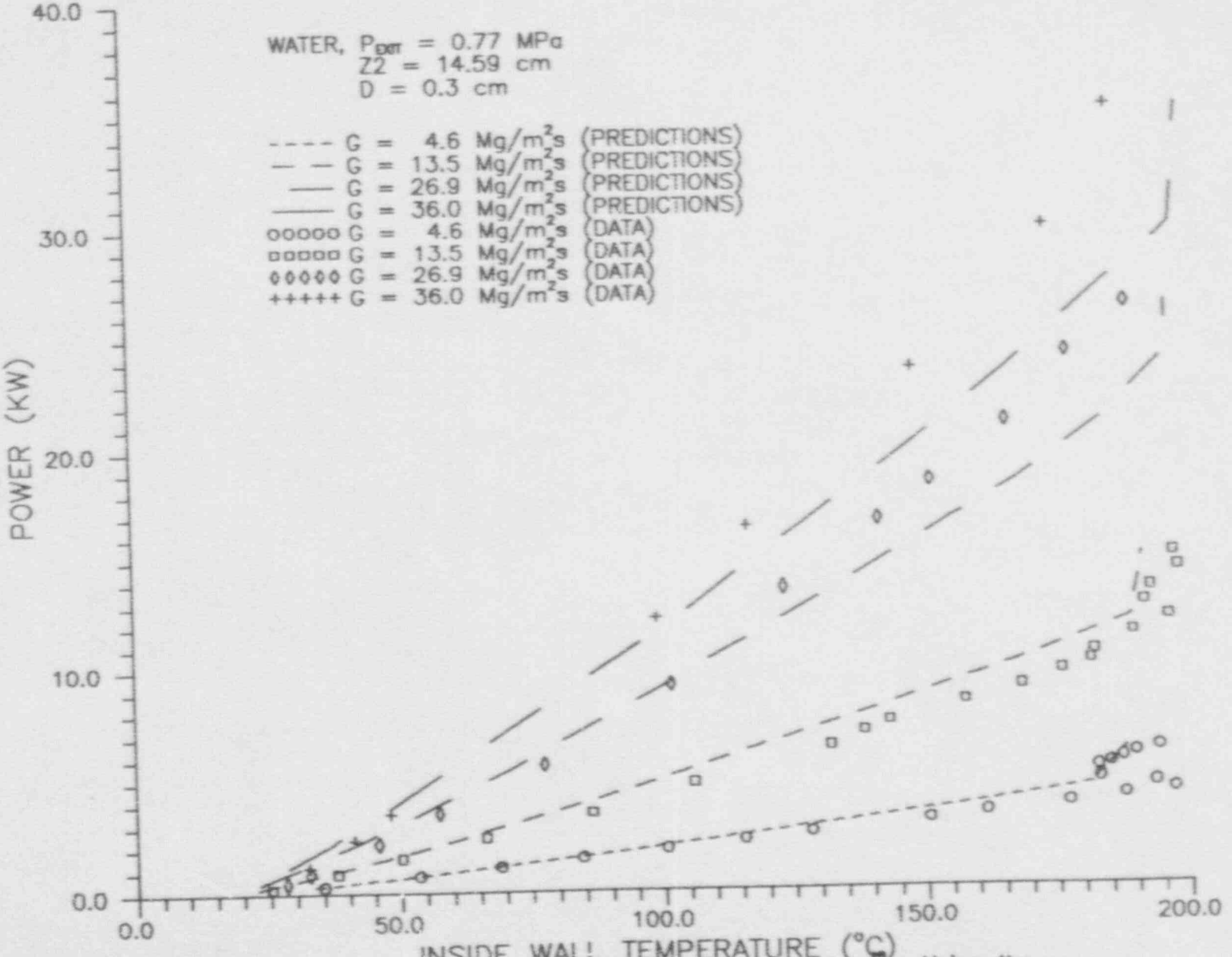

Fig. 6.1.17 Comparisons of Boiling Curve Predictions With Water Using the 'Initial' Model for Z = 14.59 cm (middle of channel), and for P_{EXIT} = 0.77 MPa.

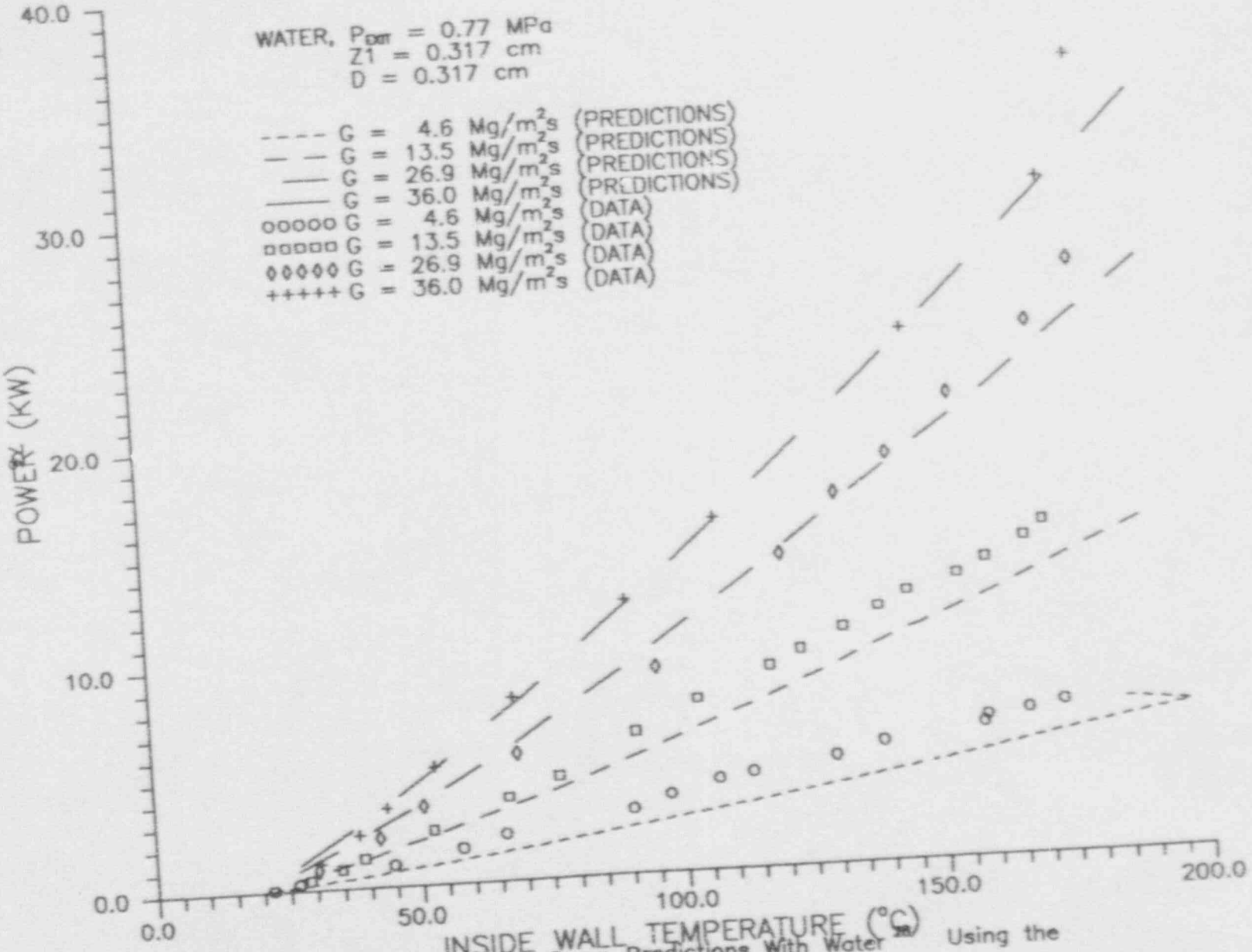

Fig. 6.1.18 Comparisons of Boiling Curve Predictions With Water Using the 'Initial' Model for Z = 0.317 cm (near the channel entrance), and for P_{EXIT} = 0.77 MPa.

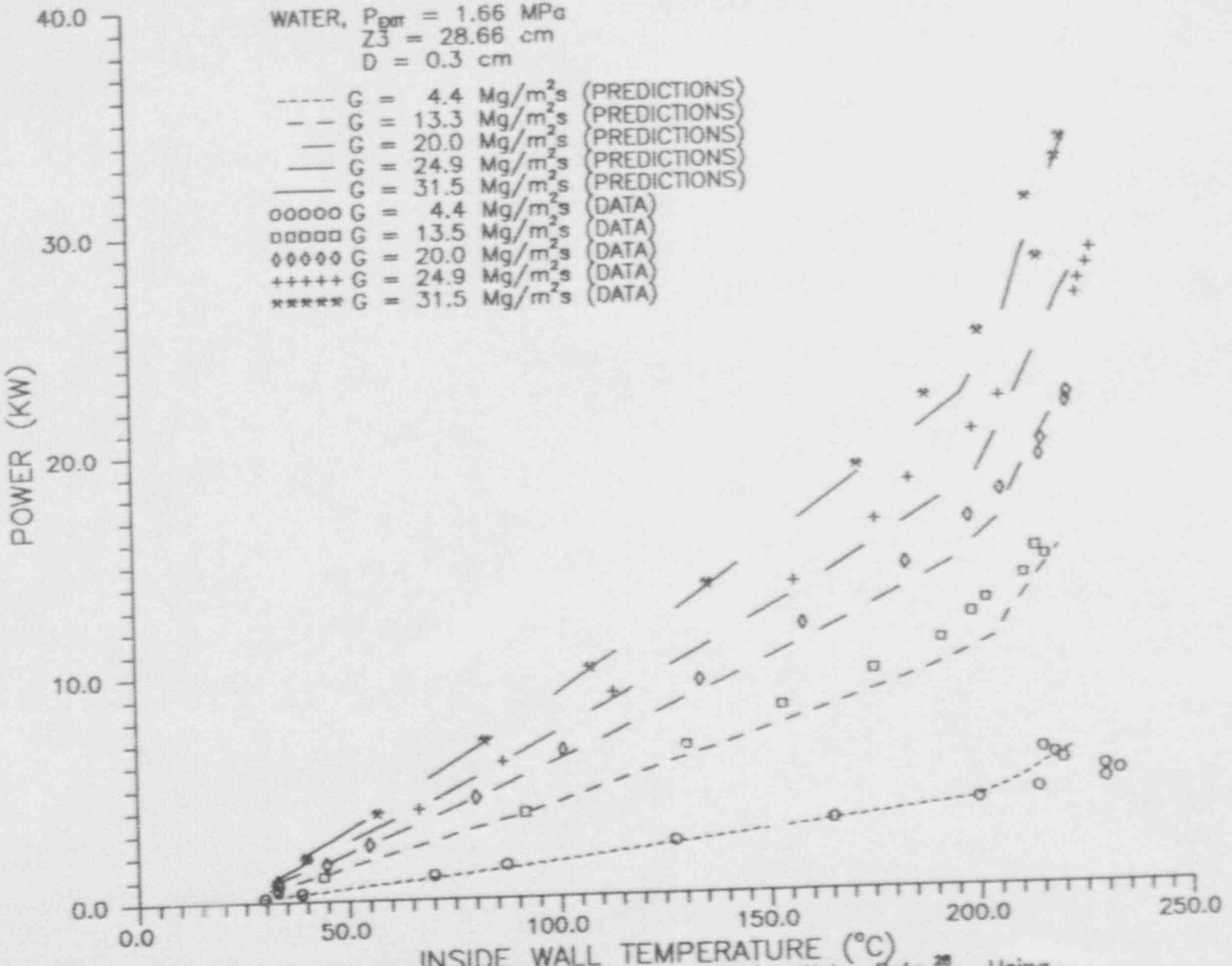

Fig. 6.1.19 Comparisons of Boiling Curve Predictions With Water Data [28] Using the 'Modified' Model for Z = 28.66 cm (near the channel exit). and for P_{EXIT} = 1.66 MPa.

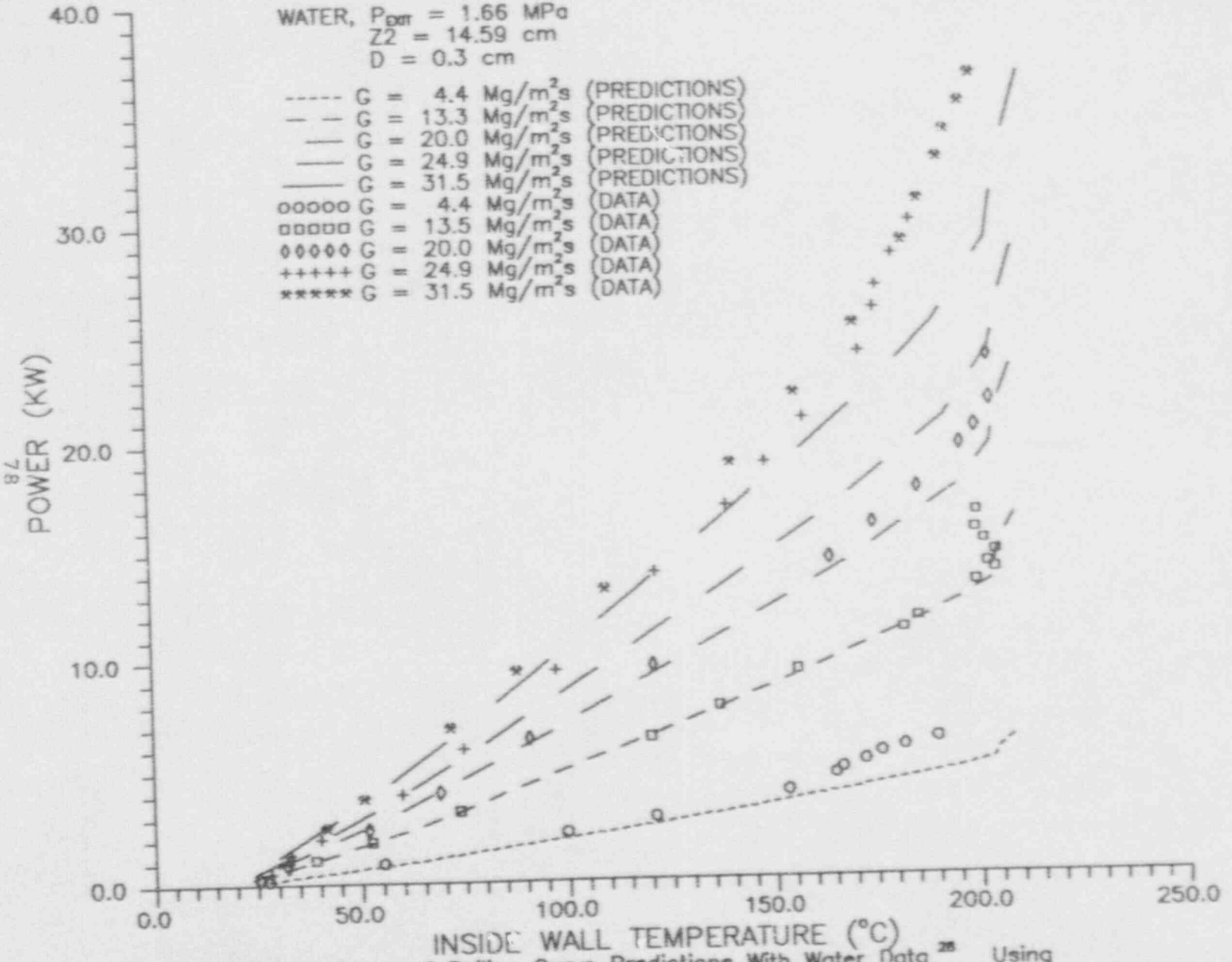

Fig. 6 1.20 Comparisons of Boiling Curve Predictions With Water Data [28] Using the 'Modified' Model for Z = 14.59 cm (middle of channel), and for P_{EXIT} = 1.66 MPa.

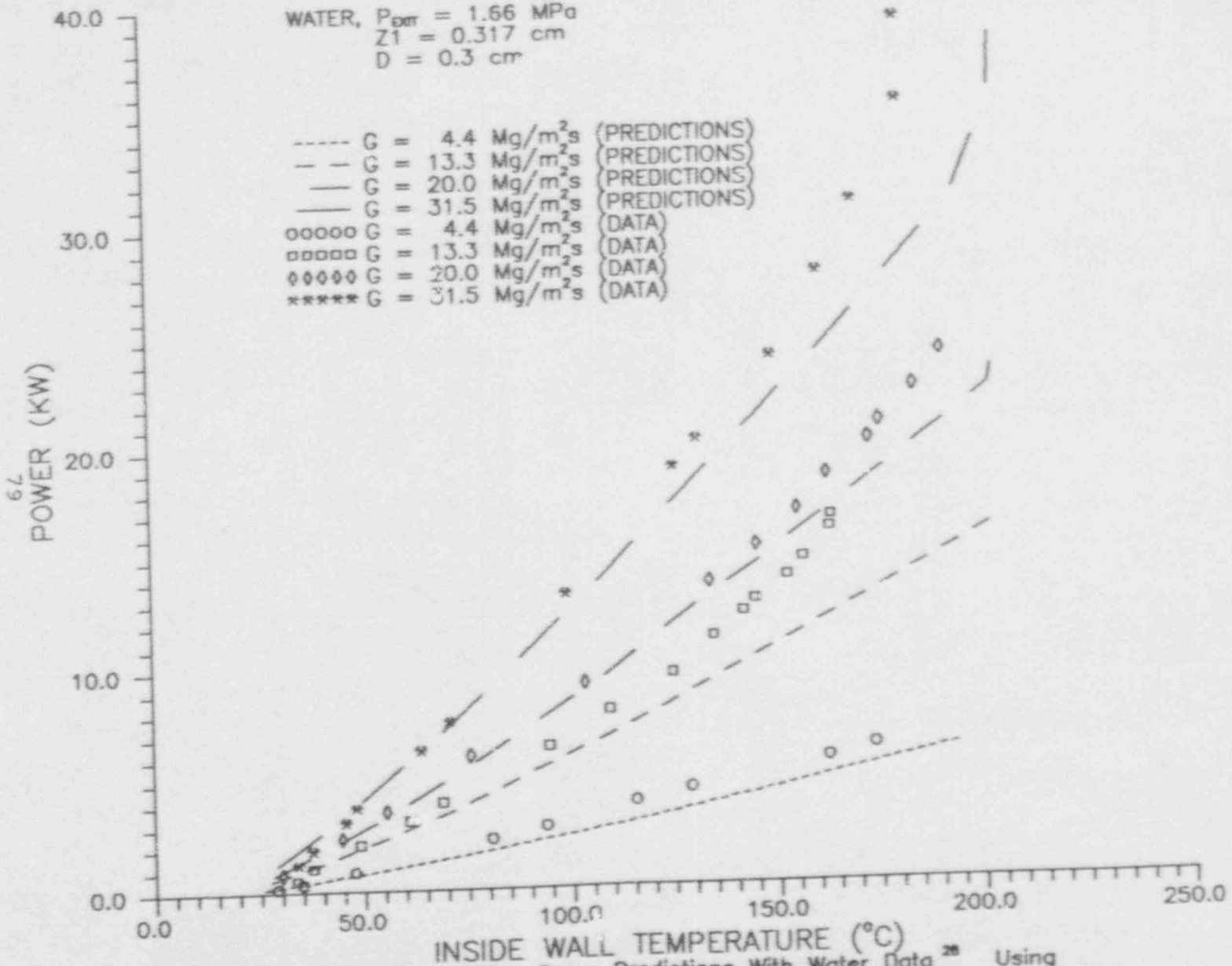

Fig. 6.1.21 Comparisons of Boiling Curve Predictions With Water Data [28] Using the 'Modified' Model for Z = 0.317 cm (near the channel entrance), and for P_{EXIT} = 1.66 MPa.

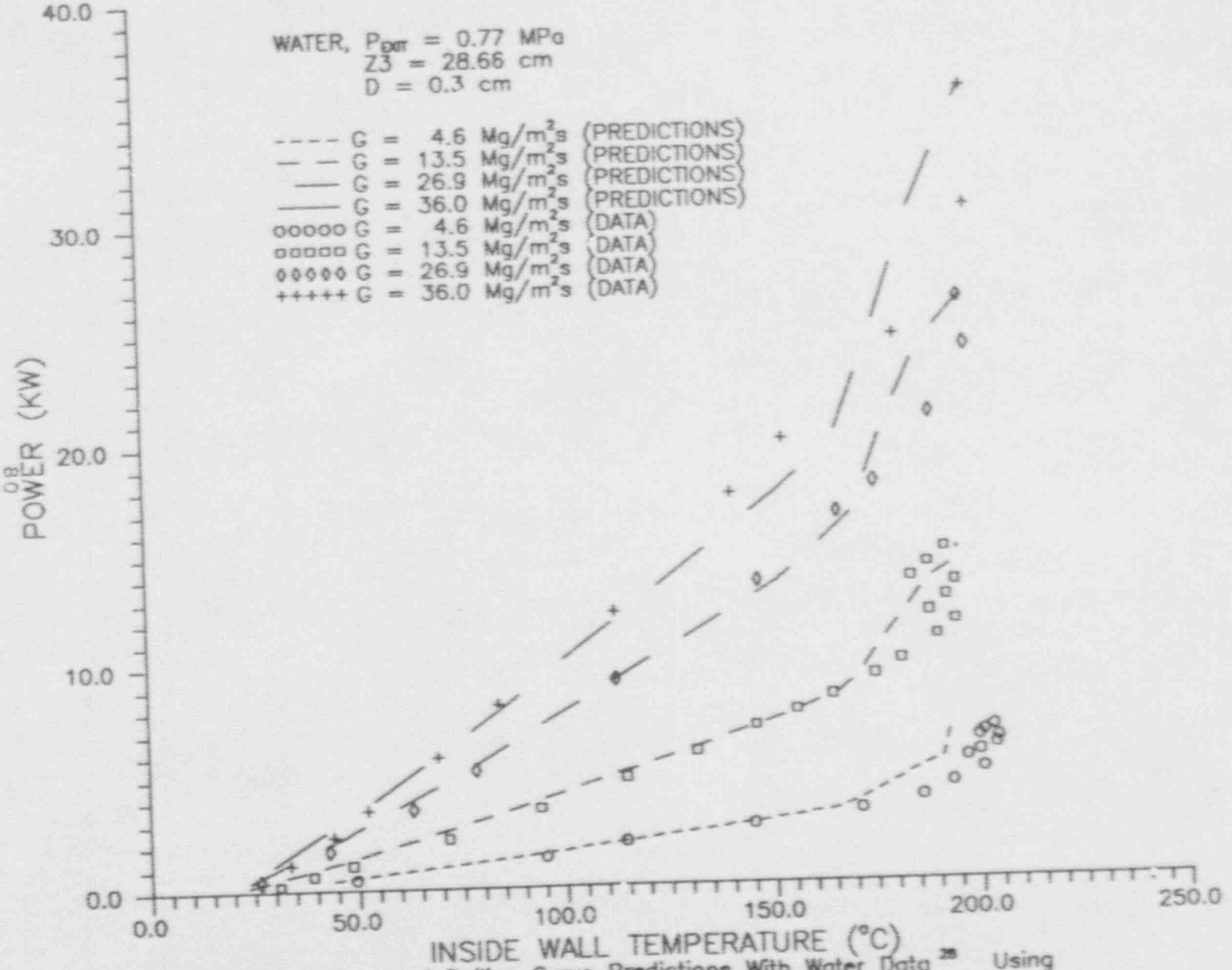

Fig. 6.1.22 Comparisons of Boiling Curve Predictions With Water Data [28] Using the 'Modified' Model for Z = 28.66 cm (near the channel exit), and for P_{EXIT} = 0.77 MPa.

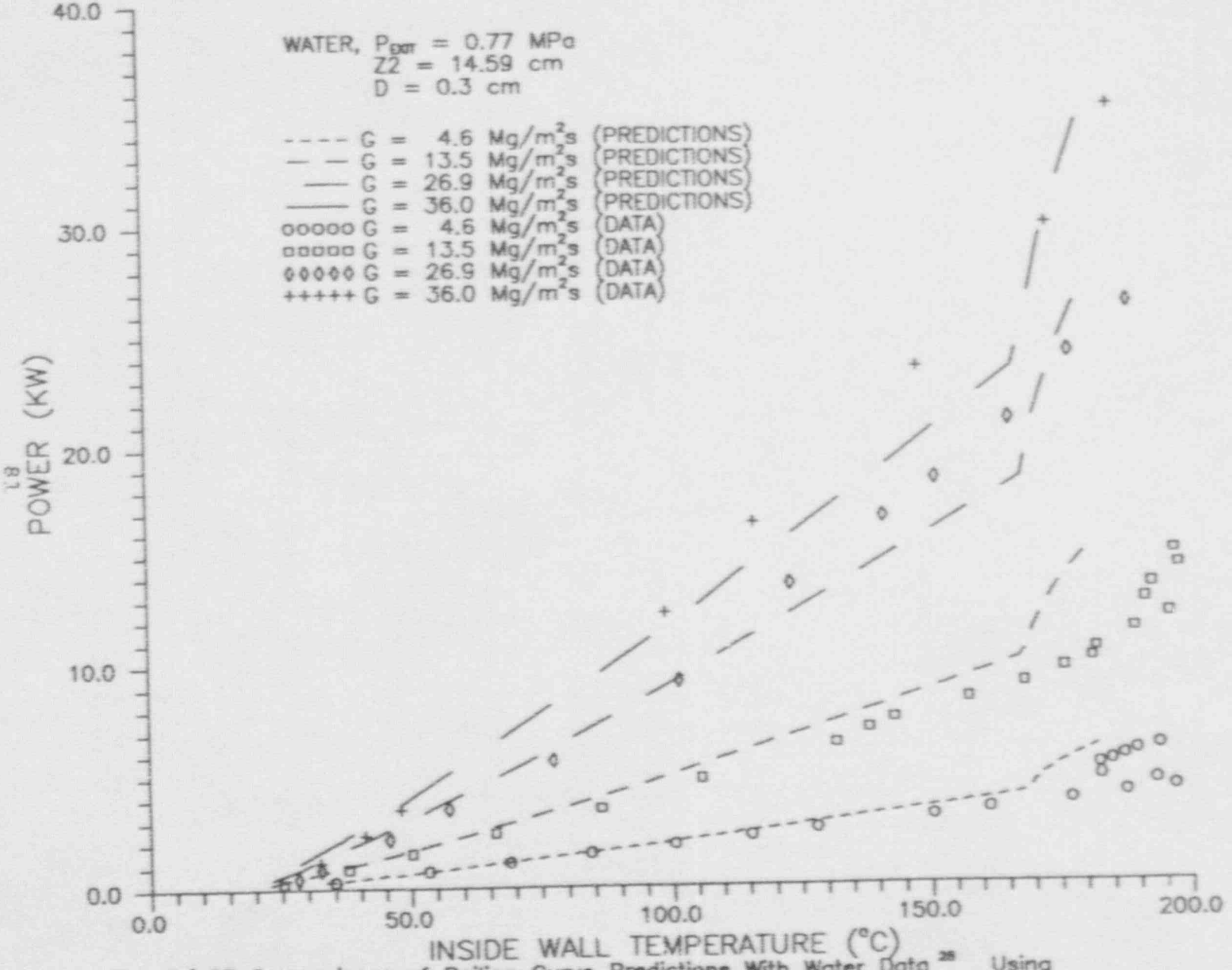

Fig. 6.1.23 Comparisons of Boiling Curve Predictions With Water Data [28] Using the 'Modified' Model for Z = 14.59 cm (middle of channel), and for P_{exit} = 0.77 MPa.

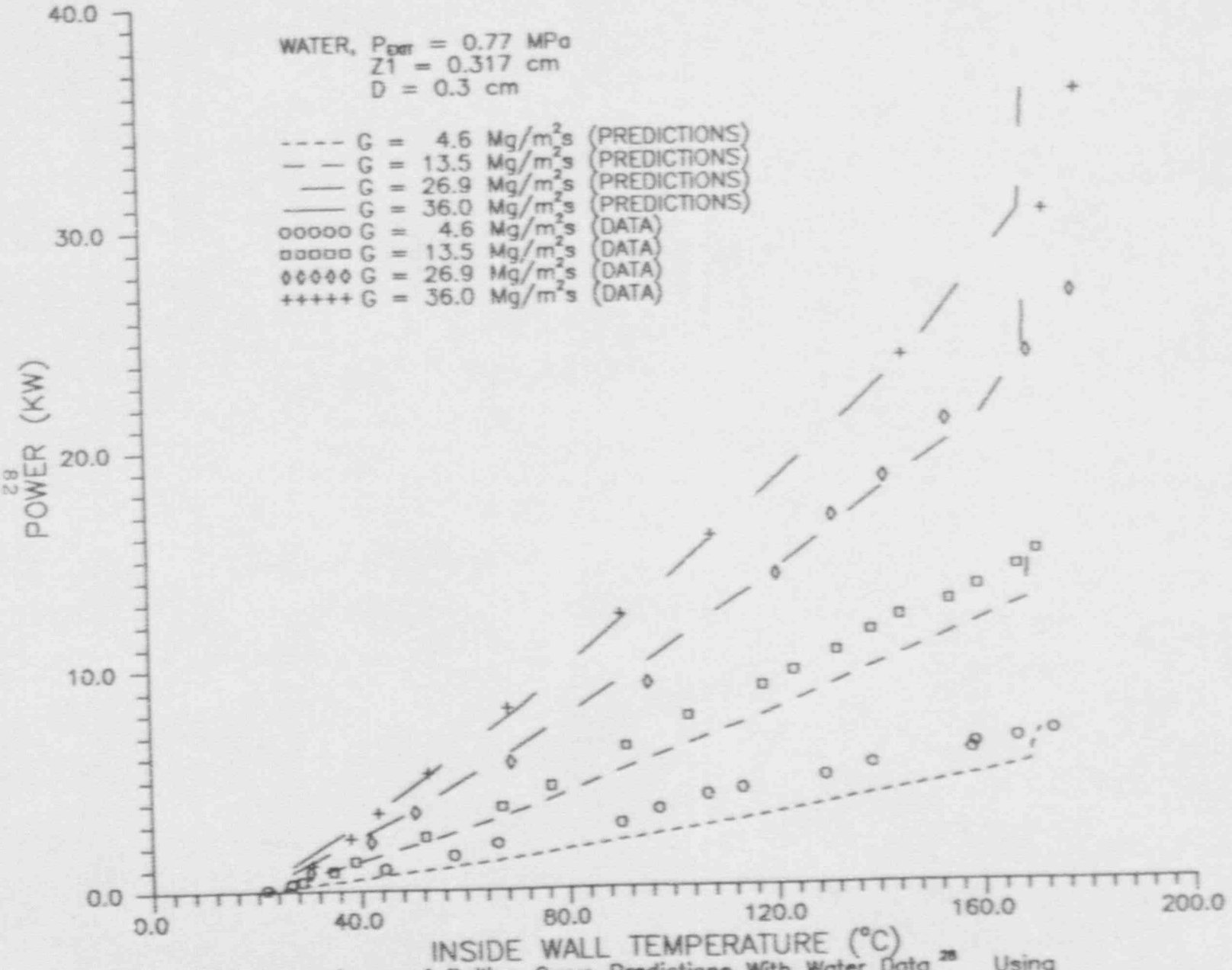

Fig. 6.1.24 Comparisons of Boiling Curve Predictions With Water Data [28] Using the 'Modified' Model for Z = 0.317 cm (near the channel entrance), and for P_{EXIT} = 0.77 MPa.

a more accurate asymptotic limit for the partial nucleate boiling region as the heat flux (σr power) decreases toward the single-phase limit.

A final set of comparisons were made with McAdams's water data[13] using both the "initial" and "modified" models. Figures 6.1.24-1a and 6.1.24-1b show the comparisons of predictions with McAdams's data for wall superheat and the heat transfer coefficient for water. The heat transfer coefficient comparison is presented in Figure 6.1.24-1a, and the boiling curve comparison is presented in Figures 6.1.24-1b for the "initial" and "modified" model respectively. The standard percent deviation is 17.3% for both the "initial" and the "modified" models for the heat transfer coefficient. For his widely referenced boiling curve, the standard percent deviation is 28.9% for both the "initial" and the "modified" models, for nine data points. The experimental parameters for this comparison are: $P_{exit} = 60\,psia$, $v = 4\ ft/sec$, inlet subcooling $50°F$, and a test section length of 3.75 in. The comparisons show that the "initial" and "modified" models are identical for this case.

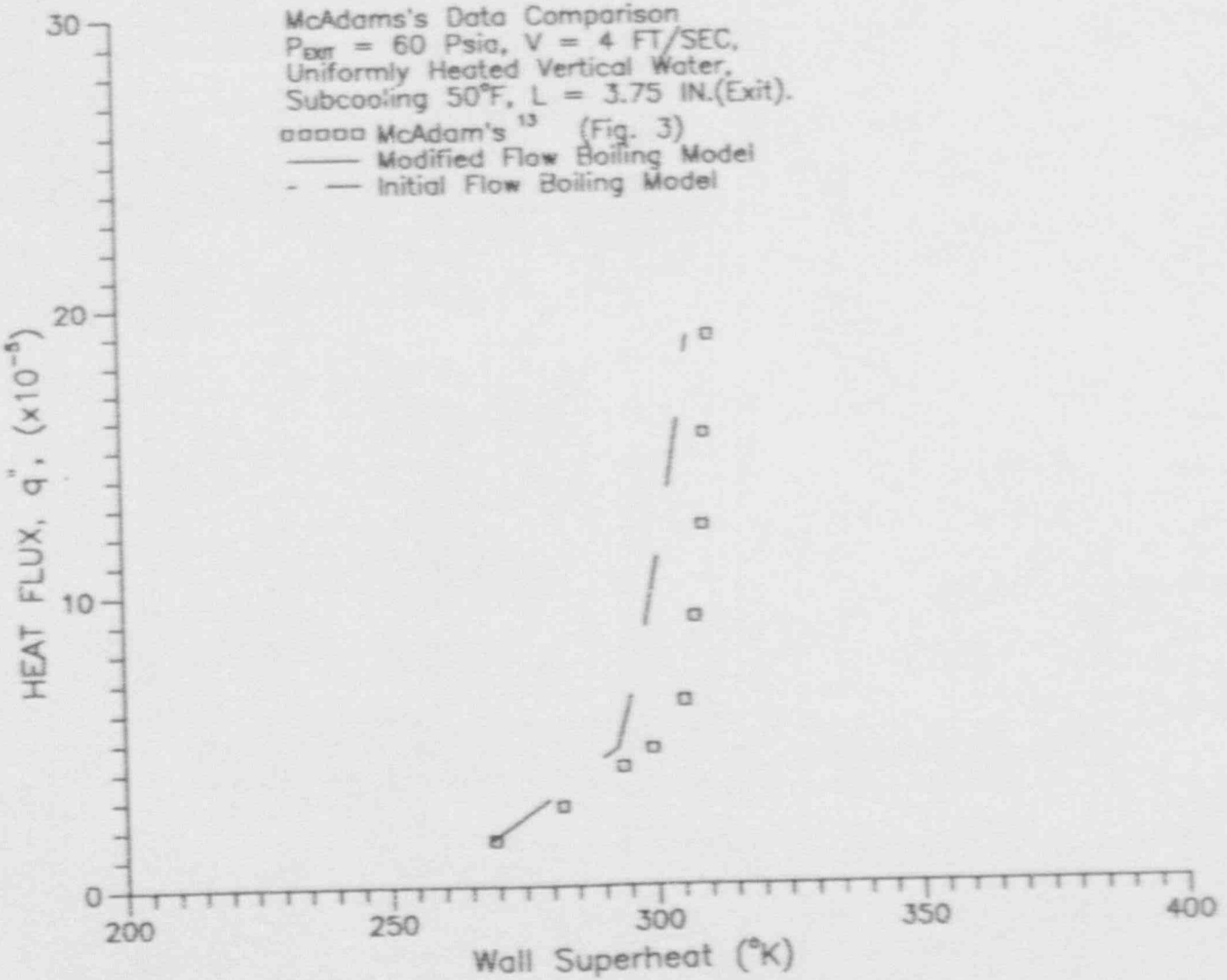

Figure 6.1.24–1b Comparisons of Boiling Curve With McAdam's Data Using the 'Initial' and 'Modified' Model.

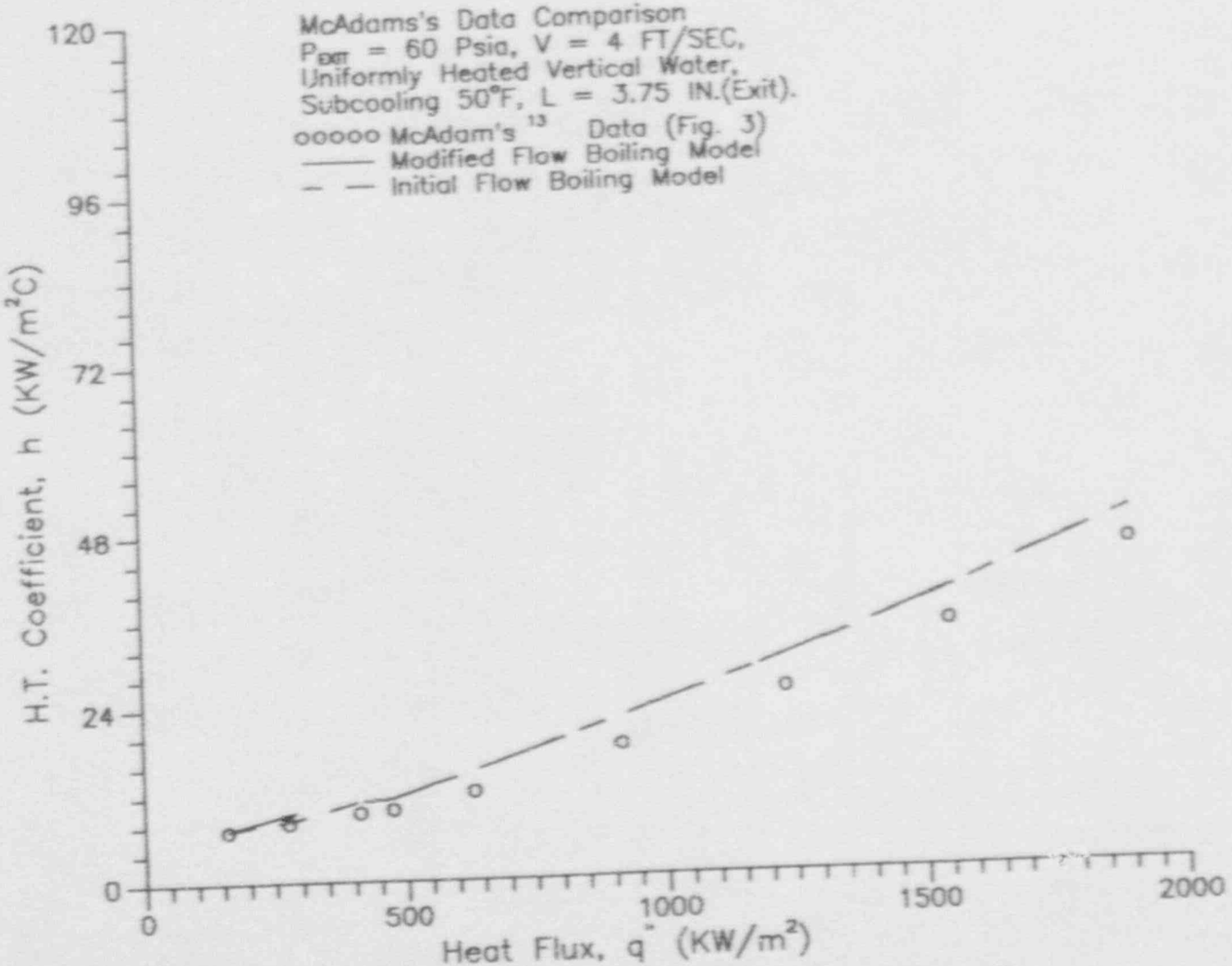

Figure 6.1.24–1a Comparisons of Heat Transfer Coefficient With McAdam's Data Using the 'Initial' Model.

6.1.3 *Freon – 11 Results*

Freon-11 comparisons were made with data produced by Smith and Boyd[30]. The data sets involved a horizontal test section and included two flow rate levels, five axial locations, and four circumferential locations with different enhancement, inlet subcoolings and inside diameter. All data involved either uniformly or top-side heated tubes. **Since the models apply only within the nucleate subcooled boiling region, data in the saturation boiling region ($q/q_2 \geq 1$ or $x \geq 0$) will not be reduced, and all predictions will be stopped beyond this region.** Further, predictive comparisons will be made with only the data from uniformly test sections.

The heat transfer coefficient behavior is quite different from that for water. In the single-phase regime, its magnitude is almost constant when the supplied power increases. However, after onset of nucleate boiling, the heat transfer coefficient inceases rapidly as supplied power increases. This behavior is due to the heat capacity and latent heat differences between Freon-11 and water. Both the heat capacity and latent heat of Freon-11 are much lower than that of water. Therefore, freon-11 reaches saturation must faster and has a short nucleate subcooled boiling region.

The heat transfer coefficient and wall temperature predictions were compared with the data reduced by Smith and Boyd using the one-dimensional Thermal Hydraulic Model (THM)[26]. In the last part of this work, Smith's and Boyd's outside wall temperature data will be reduced using a more accurate two-dimensional finite difference approximation of the top-side heated test section shown in Figure 4.2.

6.1.3. *A Freon – 11 Heat Transfer Predictions*

Comparison of the THM data with predictions of the local (axial) heat transfer coefficients for freon-11 are presented in: (1) Figures 6.1.25 through 6.1.29 for the "initial" model, and (2) Figures 6.1.30 through 6.1.34 for the "modified" model. It is essential to note that since the predictive models neglect gravitational effects, only qualitative comparisons can be made with THM data which applies to a horizontal uniformly heated flow channel. As noted with the comparisons with the water data, the predictive models strictly apply to thermally fully developed flows. Finally, the effect of pressure drop was neglected and the saturation temperature at the exit pressure was used in all computations.

With the above in mind, comparisons of both models show that the best agreement is obtained with the data when most of the above conditions are not violated. This occurs at the larger values of the axial coordinate, ($Z = Z5 = 81.28\ cm$, and $Z = Z6 = 101.60\ cm$) and higher mass velocities. This can be seen in Figures 6.1.28 and 6.1.29 for the "initial" model, and in Figures 6.1.33 and 6.1.34 for the "modified" model. Poorer agreement was obtained at upstream locations ($Z < 81.28\ cm$) and at the lower mass velocity. The percent standard deviations and standard deviations for the predictions for freon-11 are included in Tables 6.1-9 and 6.1-10 for the "initial" model, and Tables 6.1-11 and 6.1-12 for the "modified" model.

Table 6.1-9 Heat Transfer Coefficient Percent(%) Standard Deviation for the Freon-11 Predictions Using "Initial" Model (D = 1.07 cm).

Exit Pressure Pexit = 0.186 MPa						
Flowrate G (Kg/m^2s)	Location Z (cm)					Number of Data Points
	20.32	40.64	60.96	81.28	101.6	
210.0	107.1	155.4	312.6	64.1	129.7	13x5
281.0 *	22.7	20.3	47.7	13.1	99.9	10x5
281.0 **	22.8	29.9	63.4	21.2	20.2	8x5
Pressure Drop Effect	NO	NO	NO	NO	YES	
Percent Deviation at Z	69.9	100.2	202.2	43.5	99.3	31x5
Overall Percent Deviation: 114.6%						155

Table 6.1-10 Heat Transfer Coefficient Standard Deviation (W/m^2K) for the Freon-11 Predictions Using "Initial" Model (D = 1.07 cm).

Exit Pressure Pexit = 0.186 MPa						
Flowrate G (Kg/m^2s)	Location Z (cm)					Number of Data Points
	20.32	40.64	60.96	81.28	101.6	
210.0	183.8	209.6	296.3	201.4	363.7	13x5
281.0 *	82.0	77.1	320.0	60.8	170.0	10x5
281.0 **	72.2	315.4	161.8	93.9	115.7	8x5
Pressure Drop Effect	NO	NO	NO	NO	YES	
Standard Deviation at Z	130.5	206.7	268.9	139.5	256.0	31x5
Overall Standard Deviation: 205.7 (W/m^2K)						155

* - Smith and Boyd[30] run number #R0111.
** - Smith and Boyd[30] run number #R0423.

Table 6.1-11 Heat Transfer Coefficient Percent(%) Standard Deviation for the Freon-11 Predictions Using "Modified" Model (D = 1.07 cm).

Exit Pressure Pexit = 0.186 MPa						
Flowrate G (Kg/m^2s)	Location Z (cm)					Number of Data Points
	20.32	40.64	60.96	81.28	101.6	
210.0	121.9	170.9	307.9	65.3	88.0	13x5
281.0 *	22.8	20.3	47.7	13.1	99.9	10x5
281.0 **	22.8	29.9	63.4	21.2	78.8	8x5
Pressure Drop Effect	NO	NO	NO	NO	YES	
Percent Deviation at Z	79.0	109.8	199.3	43.2	78.8	31x5
Overall Percent Deviation: 113.5%						155

Table 6.1-12 Heat Transfer Coefficient Standard Deviation (W/m^2K) for the Freon-11 Predictions Using "Modified" Model (D = 1.07 cm).

Exit Pressure Pexit = 0.186 MPa						
Flowrate G (Kg/m^2s)	Location Z (cm)					Number of Data Points
	20.32	40.64	60.96	81.28	101.6	
210.0	189.3	202.2	261.9	173.7	172.6	13x5
281.0 *	82.0	77.1	320.0	60.8	175.9	10x5
281.0 **	78.2	315.4	161.8	93.9	115.7	8x5
Pressure Drop Effect	NO	NO	NO	NO	YES	
Standard Diviation at Z	133.7	203.8	254.2	123.7	156.4	31x5
Overall Standard Diviation: 178.7 (W/m^2K)						155

* - Smith and Boyd[30] run number #R0111.
** - Smith and Boyd[30] run number #R0423.

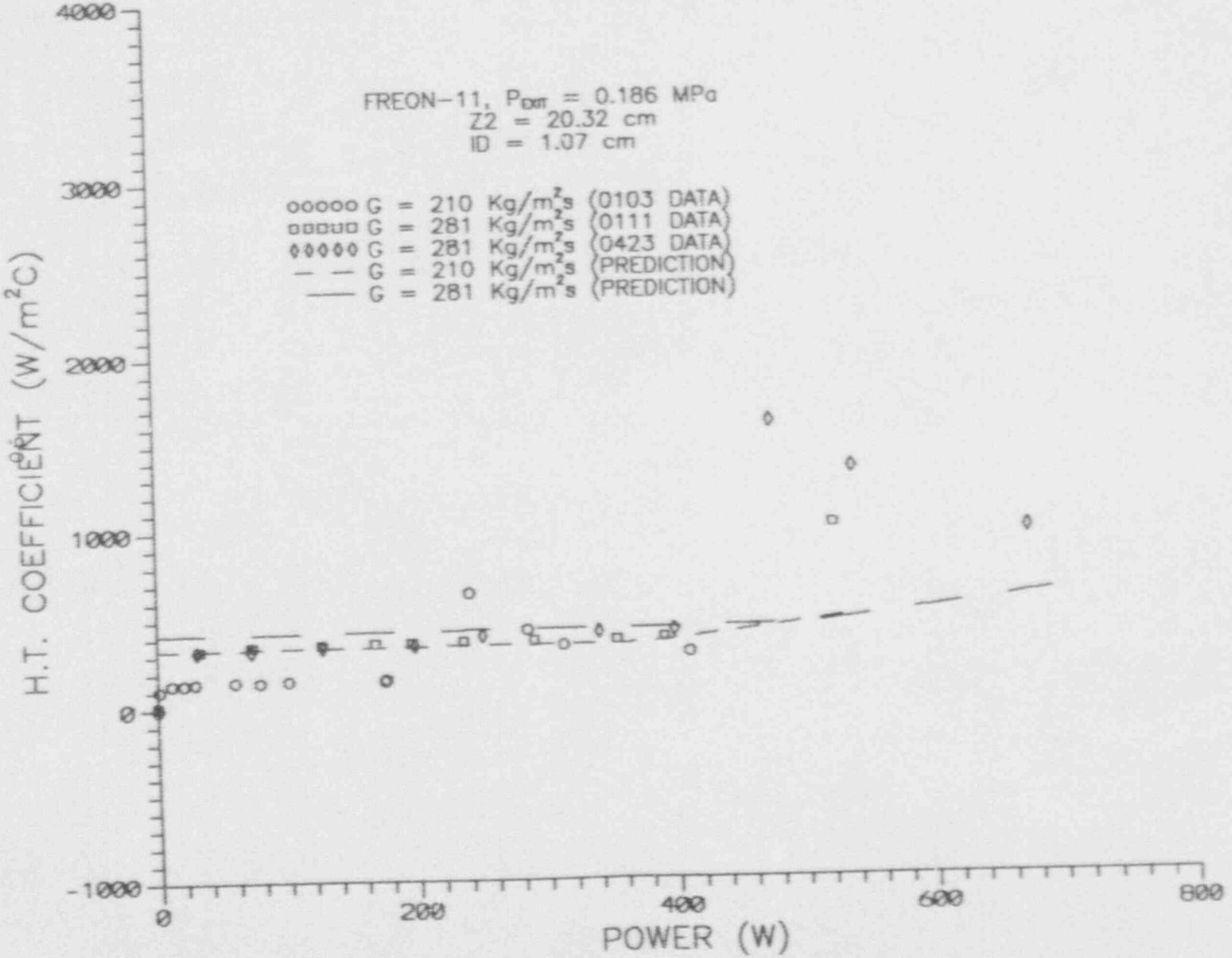

Fig. 6.1.25 Heat Transfer Coefficient Comparison Using the 'Initial' Model for Z = 20.32 cm (near entrance), and ID = 1.07 cm.

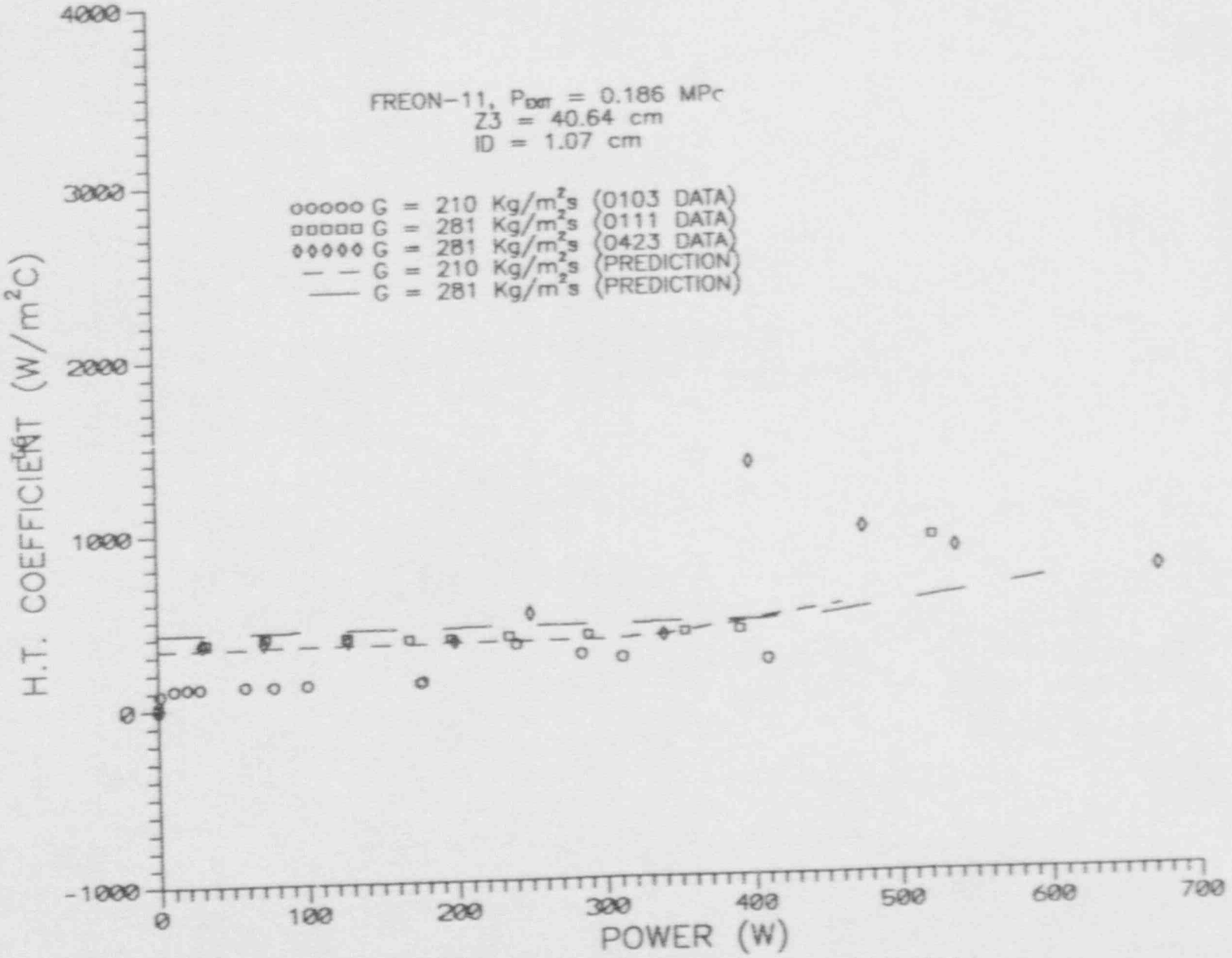

Fig. 6.1.26 Heat Transfer Coefficient Comparison Using the "Initial" Model for Z = 40.64 cm, and ID = 1.07 cm.

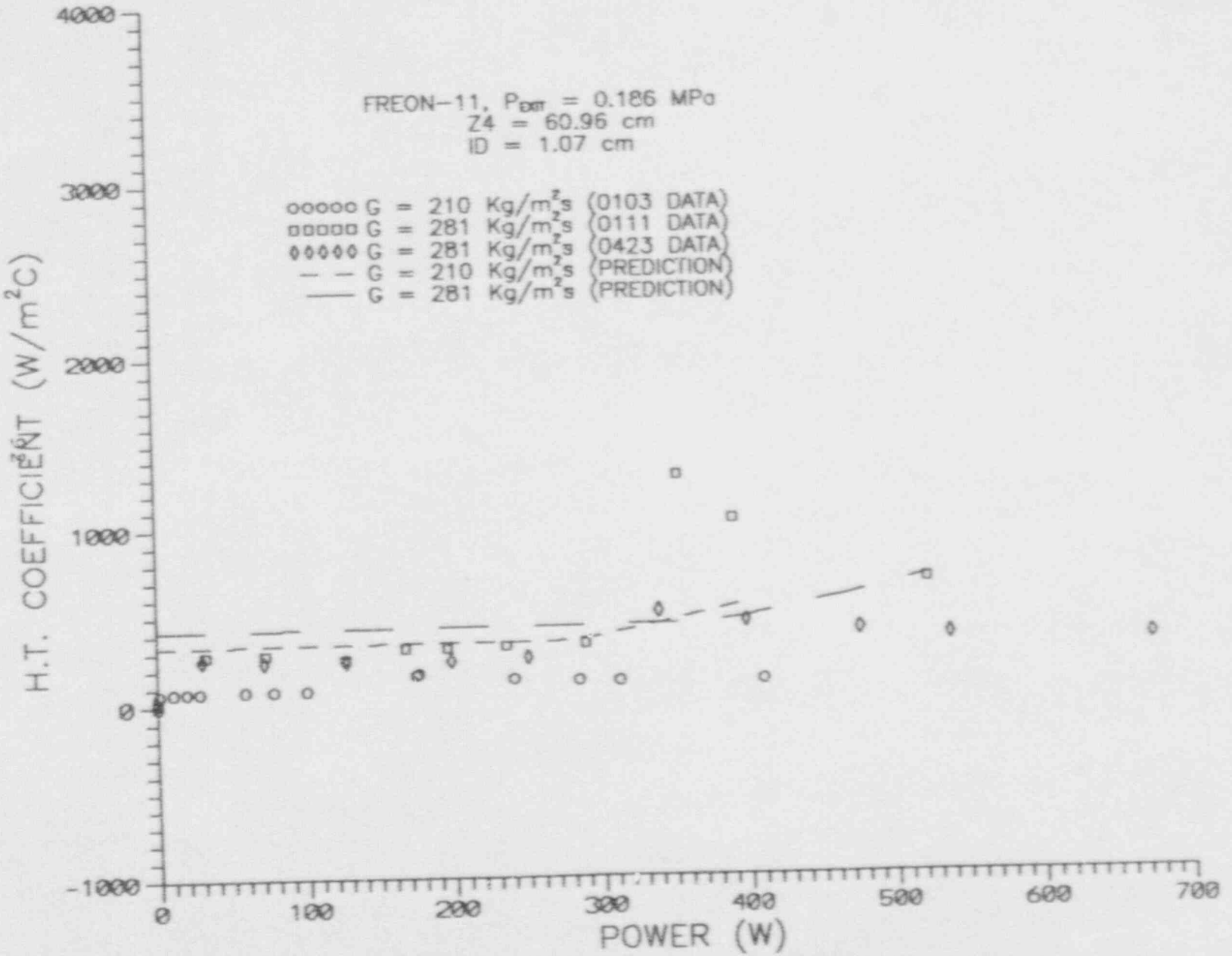

Fig. 6.1.27 Heat Transfer Coefficient Comparison Using the 'Initial' Model for Z = 60.96 cm, and ID = 1.07 cm.

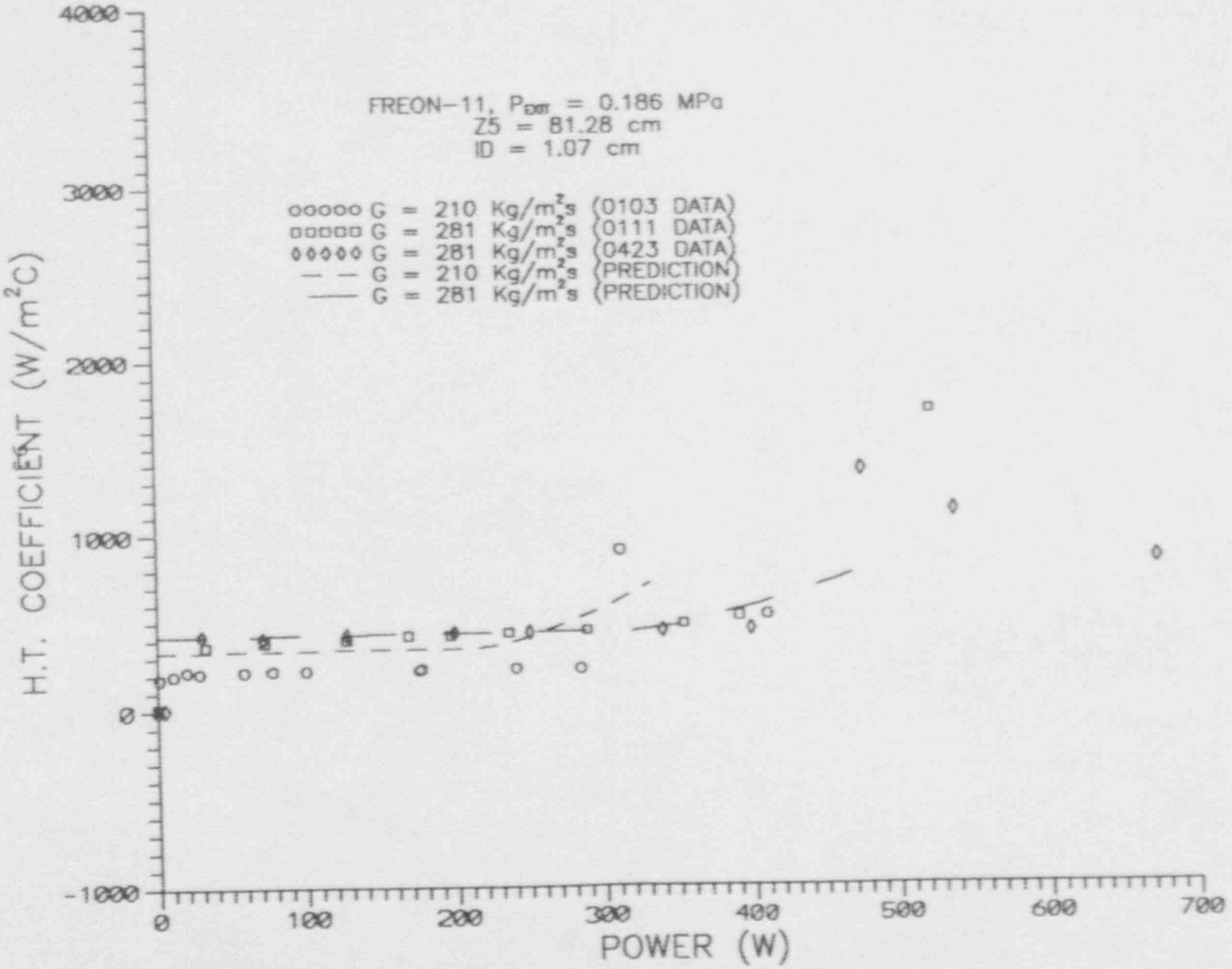

Fig. 6.1.28 Heat Transfer Coefficient Comparison Using the 'Initial' Model for Z = 81.28 cm, and ID = 1.07 cm.

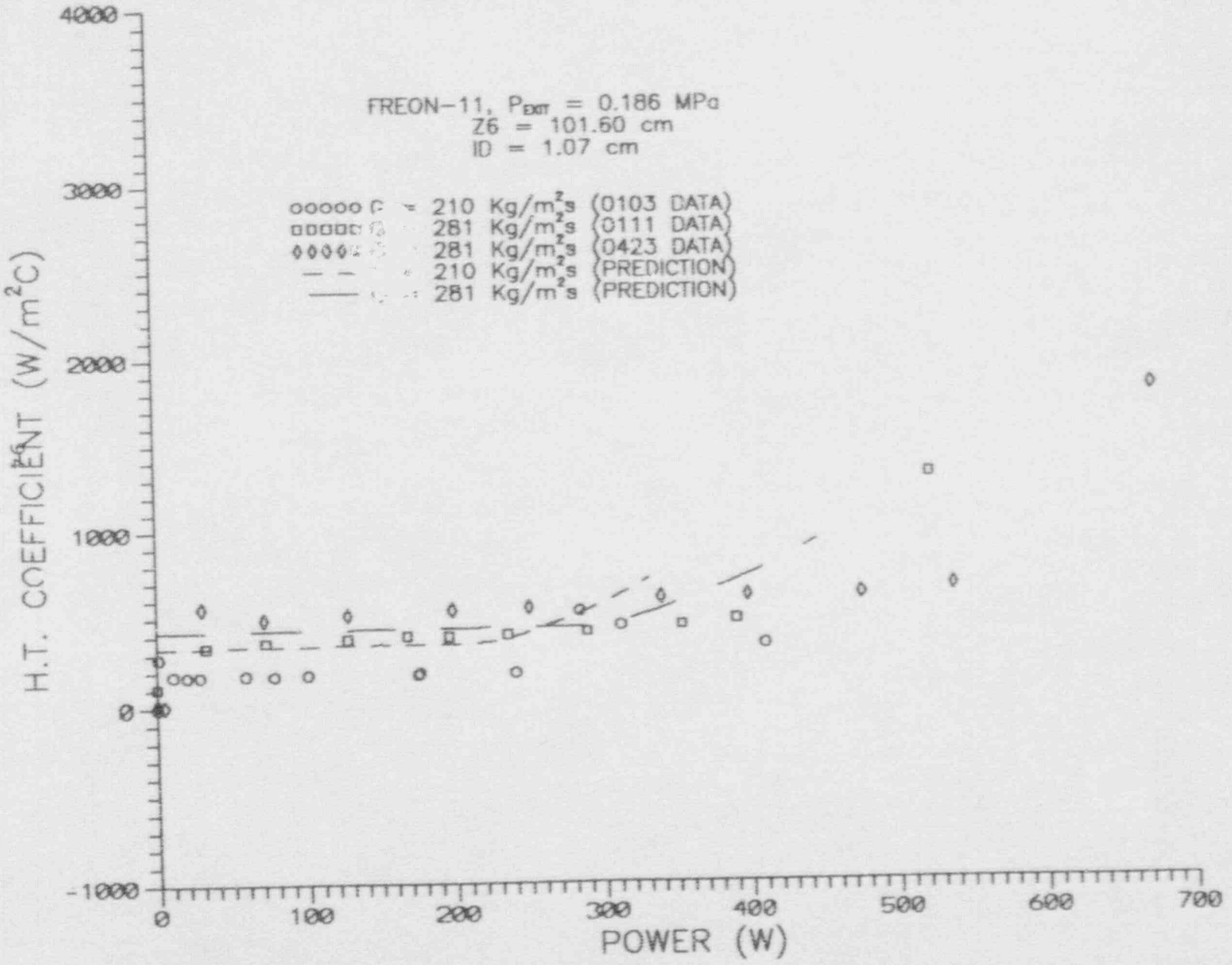

Fig. 6.1.29 Heat Transfer Coefficient Comparison Using the 'Initial' Model for Z = 101.6 cm (22.0 upstream of exit), and ID = 1.07 cm.

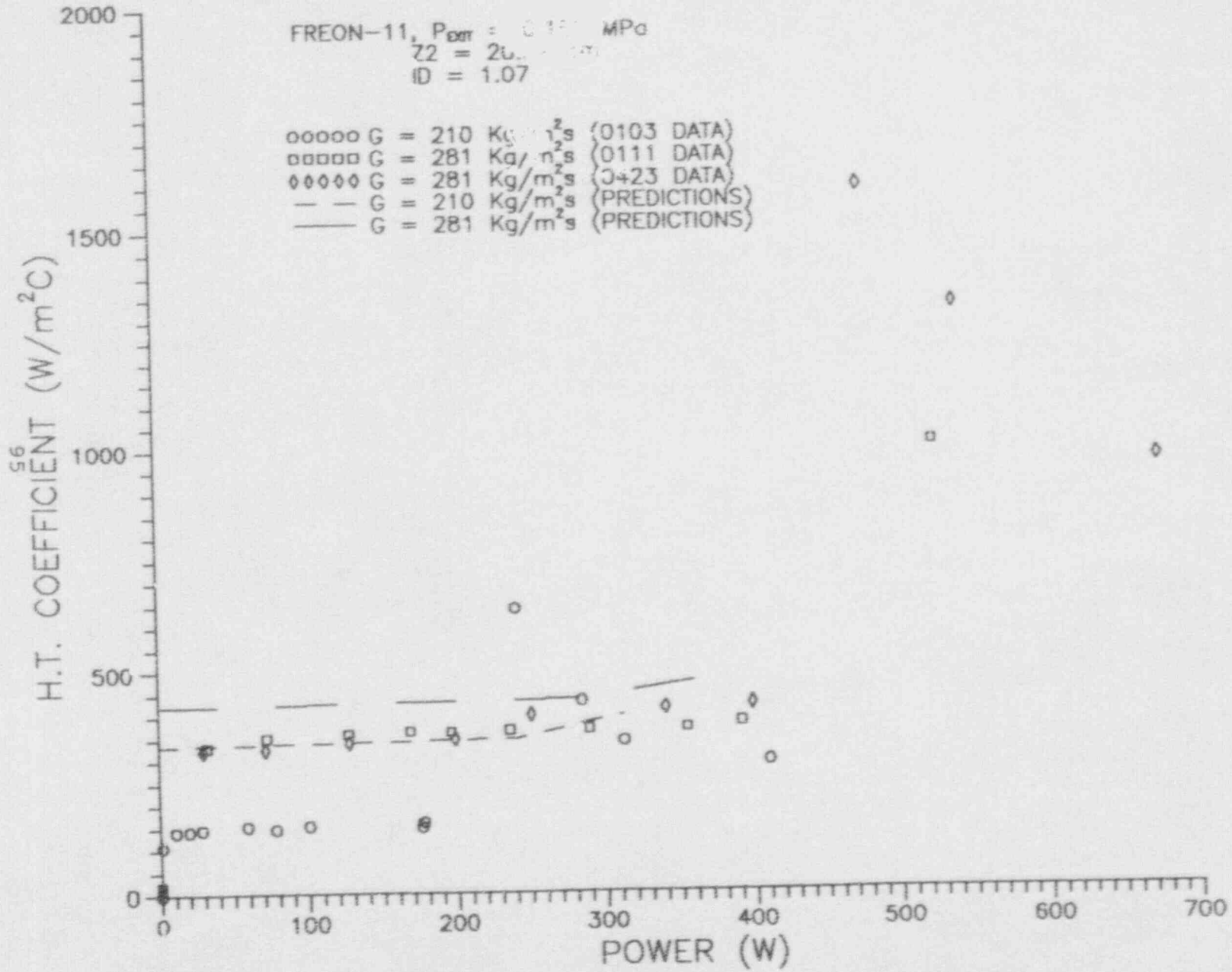

Fig. 6.1.30 Heat Transfer Coefficient Comparison Using the 'Modified' Model for Z = 20.32 cm (near entrance), and ID = 1.07 cm.

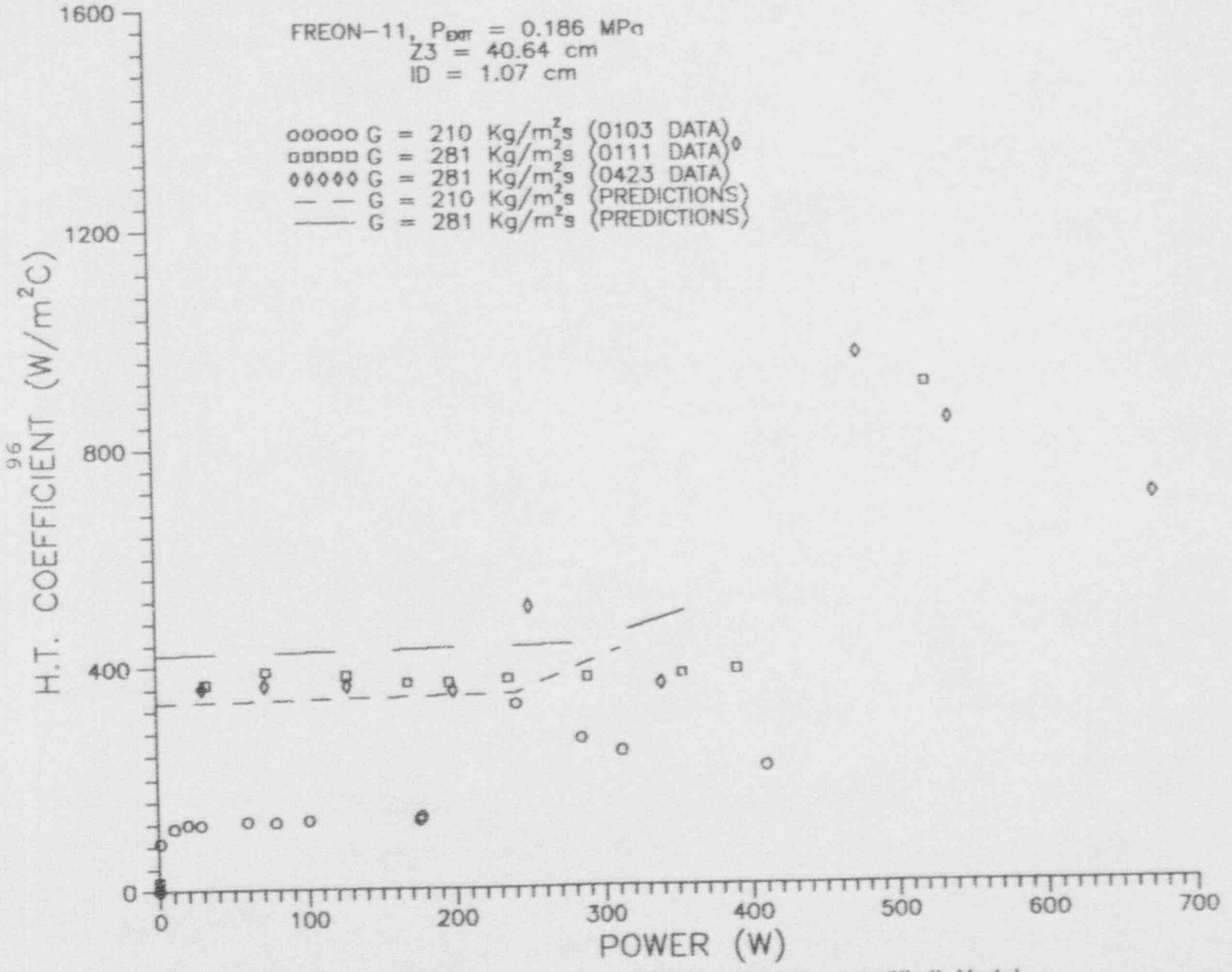

Fig. 6.1.31 Heat Transfer Coefficient Comparison Using the 'Modified' Model for Z = 40.64 cm, and ID = 1.07 cm.

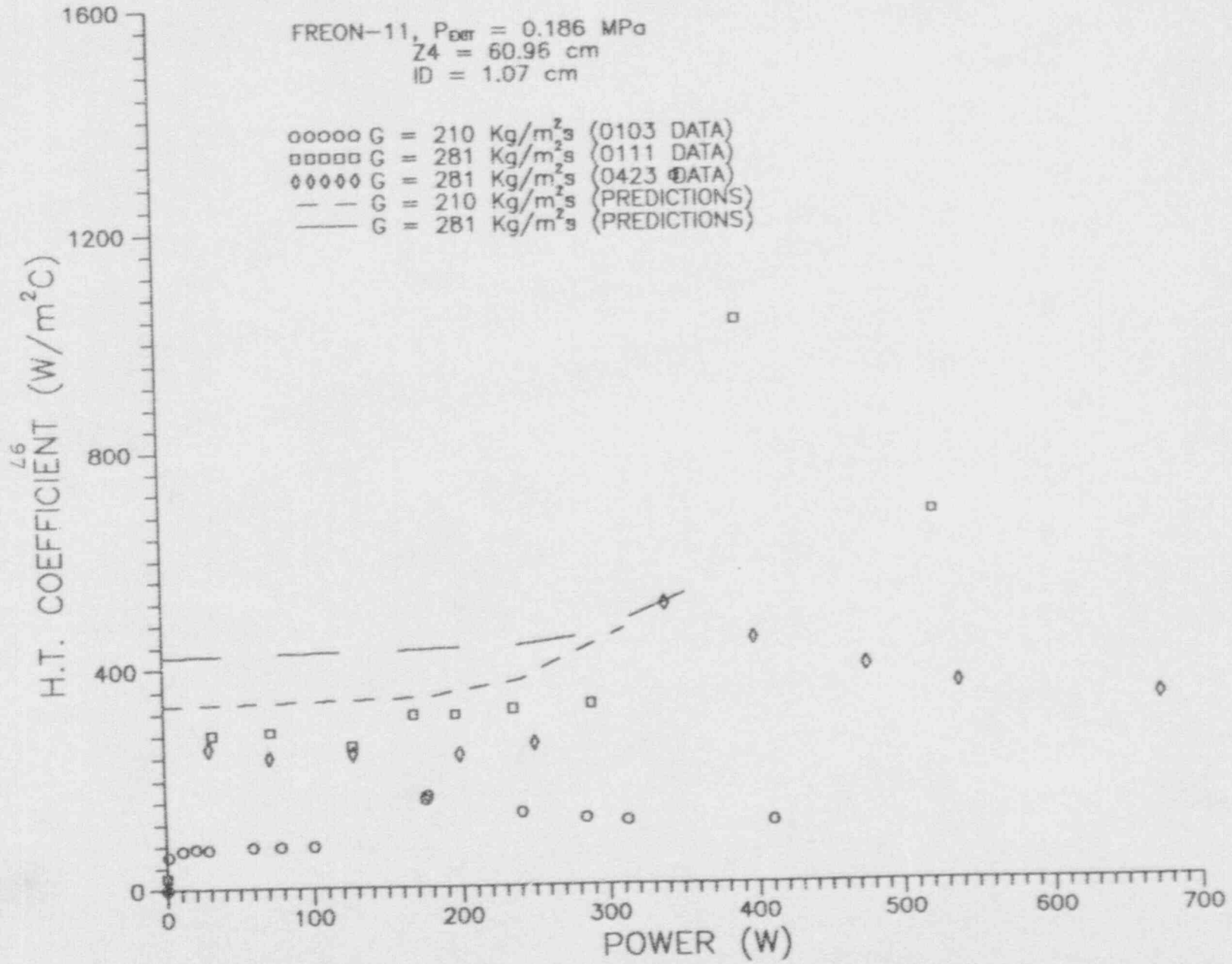

Fig. 6.1.32 Heat Transfer Coefficient Comparison Using the 'Modified' Model for Z = 60.96 cm, and ID = 1.07 cm.

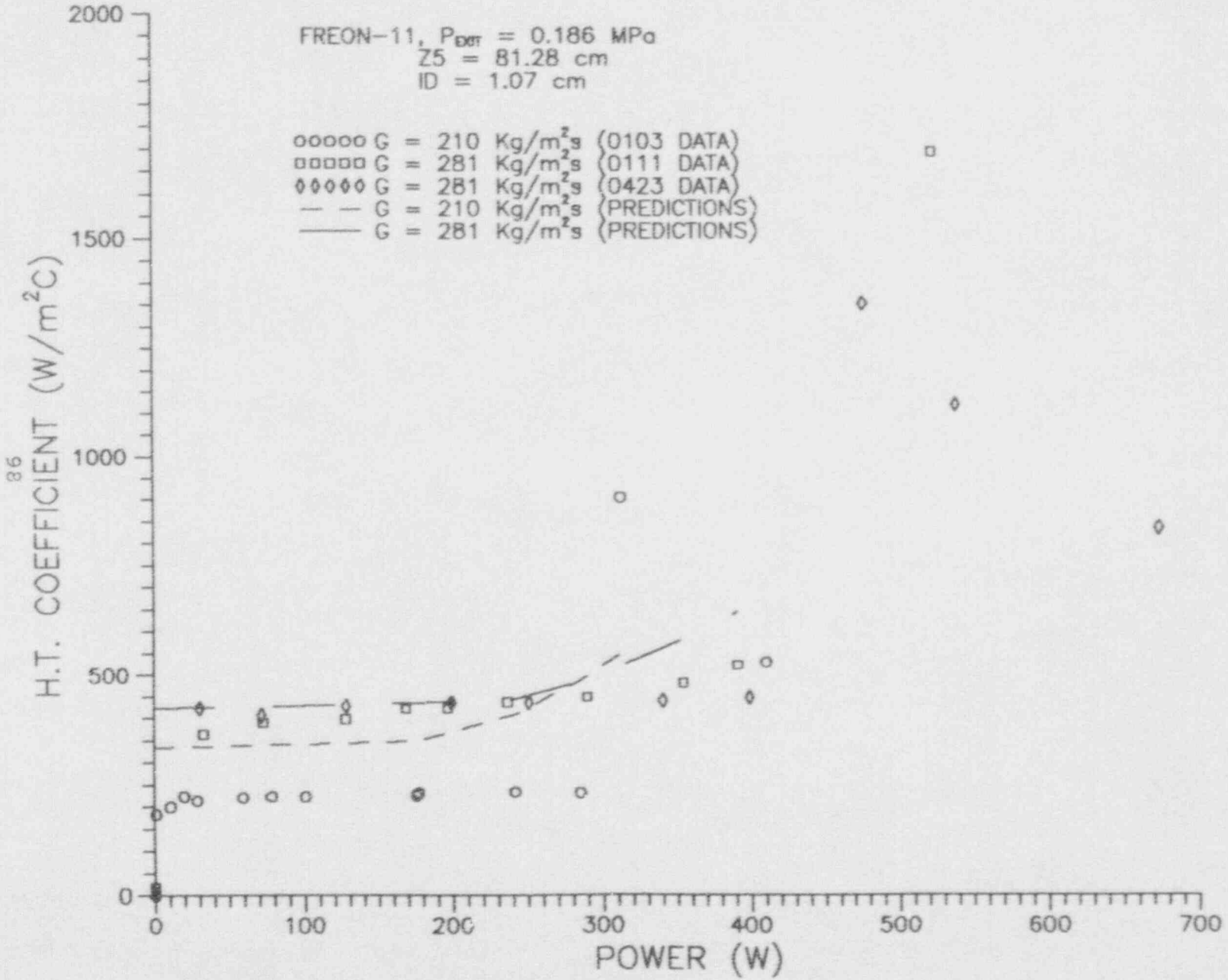

Fig. 6.1.33 Heat Transfer Coefficient Comparison Using the 'Modified' Model for Z = 81.28 cm, and ID = 1.07 cm.

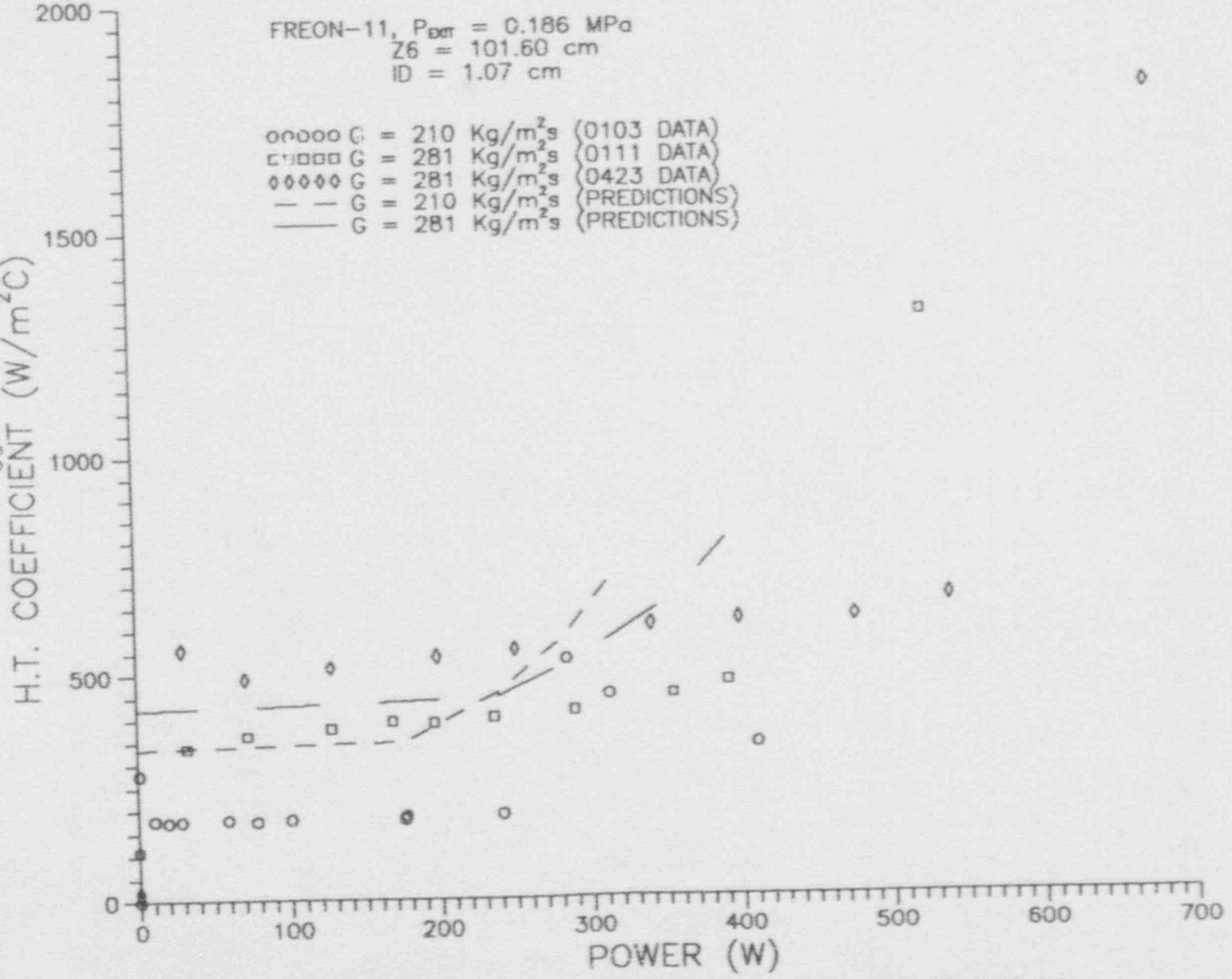

Fig. 6.1.34 Heat Transfer Coefficient Comparison Using the 'Modified' Model for Z = 101.6 cm (22.2 cm upstream of exit), and ID = 1.07 cm.

6.1.3B Inside Wall Temperature Predictions

Comparisons of the THM data with predictions of local inside wall temperature for freon-11 are presented in: (1) Figures 6.1.35 through 6.1.39 for the "initial" model, and (2) Figures 6.1.40 through 6.1.44 for the "modified" model.

For the higher flow rate, $G = 281\ Kg/m^2s$, the best agreement with the data occurs at the location near the entrance ($Z = 20.32\ and\ 40.64\ cm$), poorer agreement occurs at the location near the exit of the channel ($Z = 81.28\ and 101.6\ cm$) for both models which can be seen in Figures 6.1.35 and 6.1.39 for "initial" model, and Figures 6.1.40 and 6.1.44 for "modified" model.

For the lower flow rate, $G = 210\ Kg/m^2s$, the comparisons are just opposite. Through out the comparisons, for the same flow rate and location, the "modified" model gives better results than that of "initial" model. The percent standard deviations and standard deviations for freon-11 are included in Tables 6.1-13 and 6.1-14 for "initial" model, and Tables 6.1-15 and 6.1-16 for "modified" model.

Table 6.1-13 Inside Wall Temperature Percent(%) Standard Deviation for the Freon-11 Predictions Using "Initial" Model (D = 1.07 cm).

Exit Pressure Pexit = 0.186 MPa						
Flowrate G (Kg/m^2s)	Location Z (cm)					Number of Data Points
	20.32	40.64	60.96	81.28	101.6	
210.0	2.7	4.2	8.5	2.1	3.1	13x5
281.0 *	1.0	1.0	1.7	0.5	1.1	10x5
281.0 **	0.7	1.6	1.8	0.9	0.6	8x5
Pressure Drop Effect	NO	NO	NO	NO	YES	
Percent Deviation at Z	1.8	2.8	5.5	1.4	2.1	31x5
Overall Percent Deviation: 3.1%						155

Table 6.1-14 Inside Wall Temperature (K) Standard Deviation for the Freon-11 Predictions Using "Initial" Model (D = 1.07 cm).

Exit Pressure Pexit = 0.186 MPa						
Flowrate G (Kg/m^2s)	Location Z (cm)					Number of Data Points
	20.32	40.64	60.96	81.28	101.6	
210.0	8.7	14.0	31.3	7.0	0.3	13x5
281.0 *	3.1	3.1	5.5	1.6	3.7	10x5
281.0 **	2.1	4.9	5.9	3.1	2.0	8x5
Pressure Drop Effect	NO	NO	NO	NO	YES	
Standard Deviation at Z	5.8	9.4	20.2	4.8	6.9	31x5
Overall Standard Deviation: 10.8 (K)						155

* - Smith and Boyd[30] run number #R0111.
** - Smith and Boyd[30] run number #R0423.

Table 6.1-15 Inside Wall Temperature Percent(%) Standard Deviation for the Freon-11 Predictions Using "Modified" Model (D = 1.07 cm).

Exit Pressure Pexit = 0.186 MPa						
Flowrate G (Kg/m^2s)	Location Z (cm)					Number of Data Points
	20.32	40.64	60.96	81.28	101.6	
210.0	2.5	3.5	6.6	2.0	2.4	13x5
281.0 *	1.0	1.0	1.7	0.5	1.1	10x5
281.0 **	0.7	1.6	1.8	0.9	0.6	8x5
Pressure Drop Effect	NO	NC	NO	NO	YES	
Percent Deviation at Z	1.7	2.4	4.4	1.4	1.7	31x5
Overall Percent Deviation: 2.5%						155

Table 6.1-16 Inside Wall Temperature (K) Standard Deviation for the Freon-11 Predictions Using "Modified" Model (D = 1.07 cm).

Exit Pressure Pexit = 0.186 MPa						
Flowrate G (Kg/m^2s)	Location Z (cm)					Number of Data Points
	20.32	40.64	60.96	81.28	101.6	
210.0	7.9	11.4	23.1	6.6	7.9	13x5
281.0 *	3.1	3.1	5.5	1.6	3.7	10x5
281.0 **	2.1	4.9	5.9	3.1	2.0	8x5
Pressure Drop Effect	NO	NO	NO	NO	YES	
Standard Diviation at Z	5.4	7.8	15.2	4.5	5.5	31x5
Overall Standard Diviation: 8.5 (K)						155

* - Smith and Boyd[30] run number #R0111.
** - Smith and Boyd[30] run number #R0423.

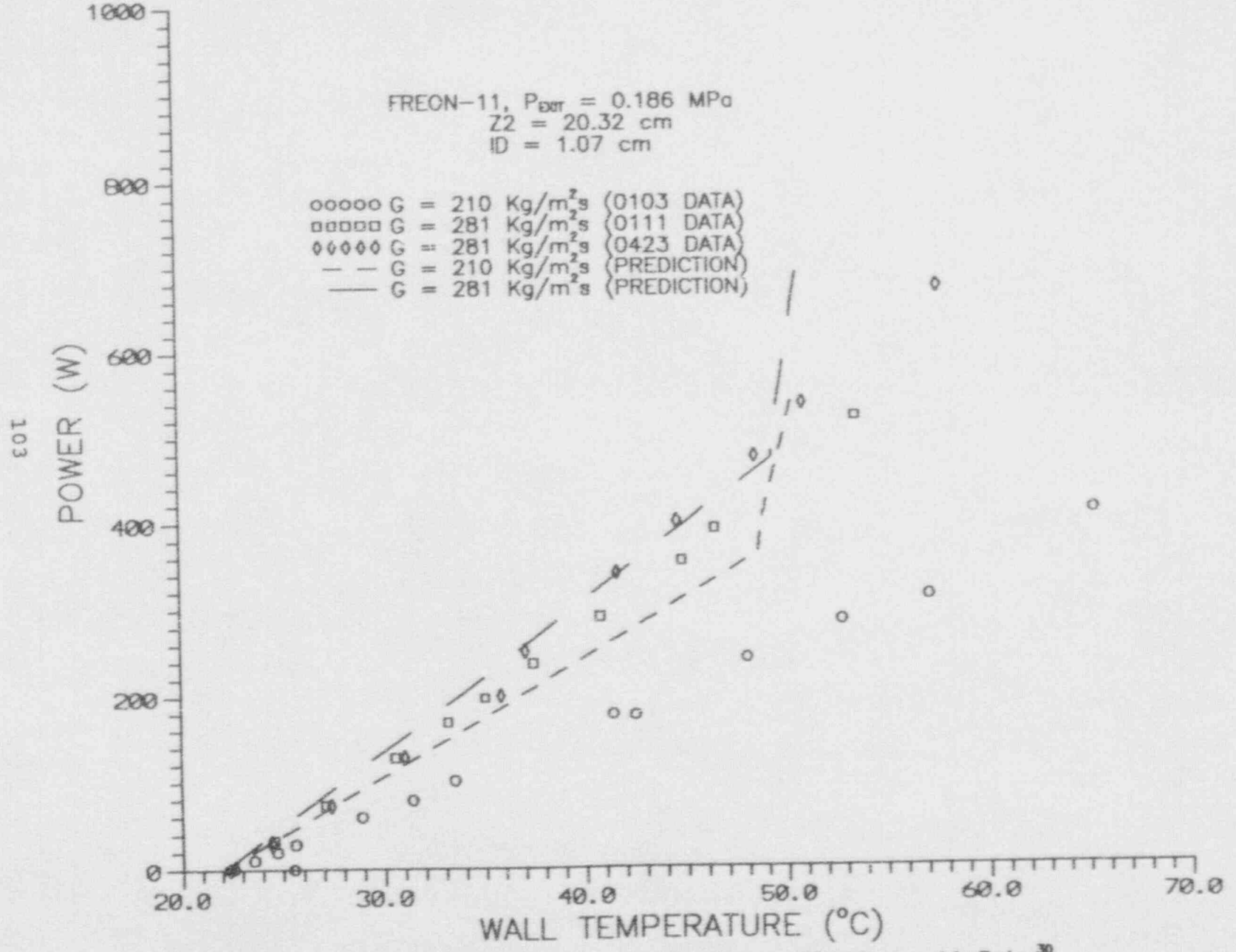

Fig. 6.1.35 Comparisons of Boiling Curve Predictions With Freon-11 Data[30] Using the 'Initial' Model for Z = 20.32 cm (near entrance), and ID = 1.07 cm.

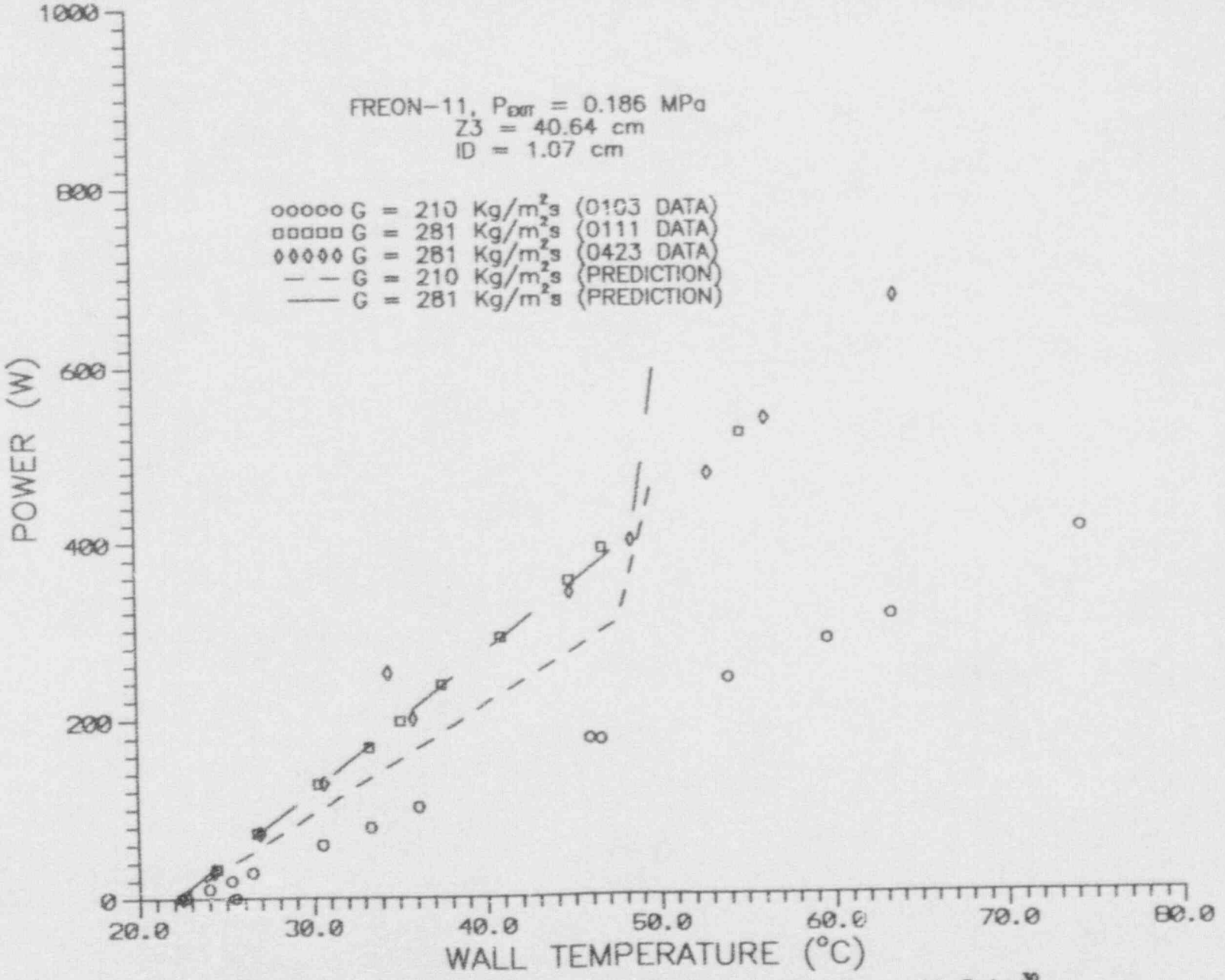

Fig. 6.1.36 Comparisons of Boiling Curve Predictions With Freon-11 Data [30] Using the 'Initial' Model for Z = 40.64 cm, and ID = 1.07 cm.

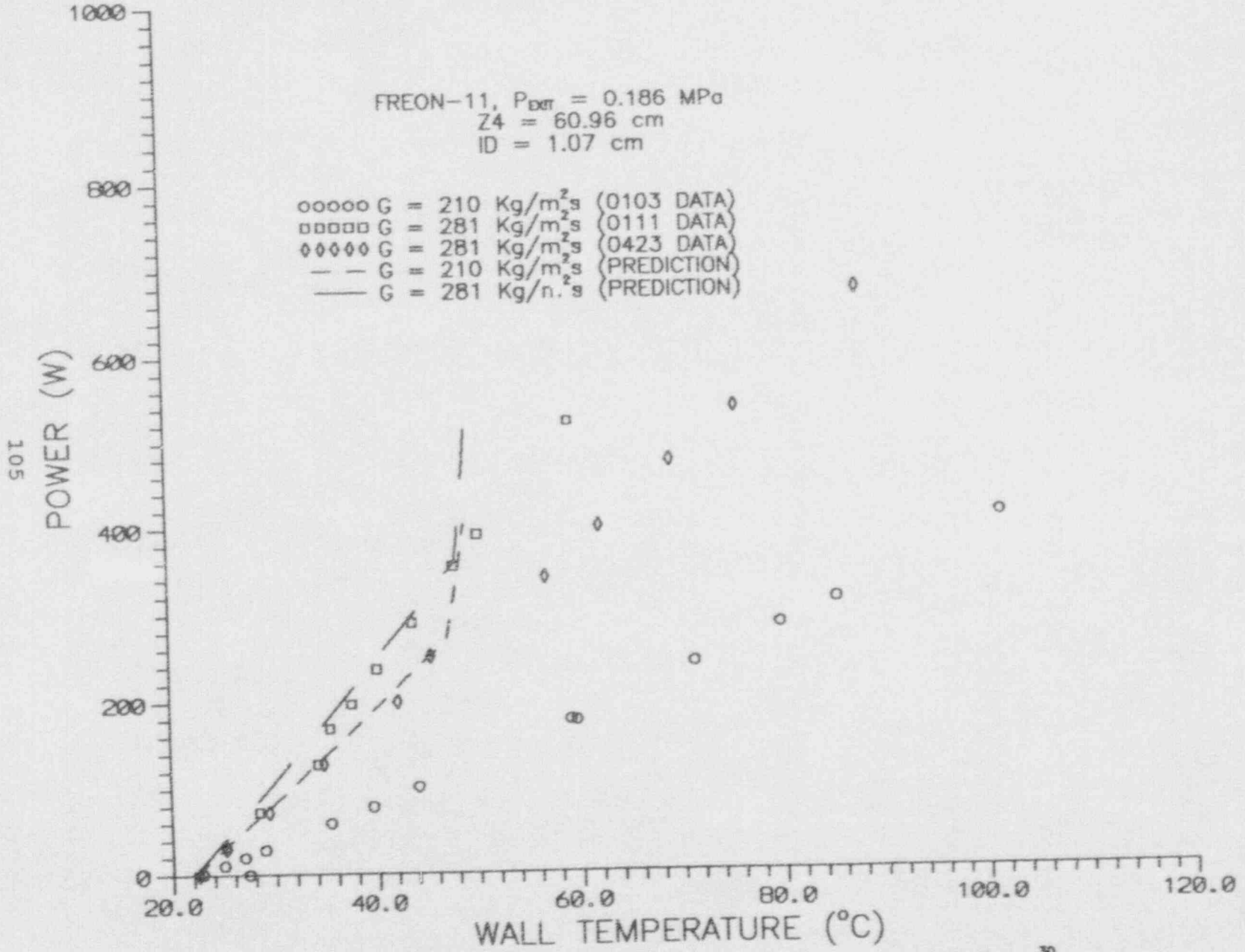

Fig. 6.1.37 Comparisons of Boiling Curve Predictions With Freon-11 Data [30] Using the 'Initial' Model for Z = 60.96 cm, and ID = 1.07 cm.

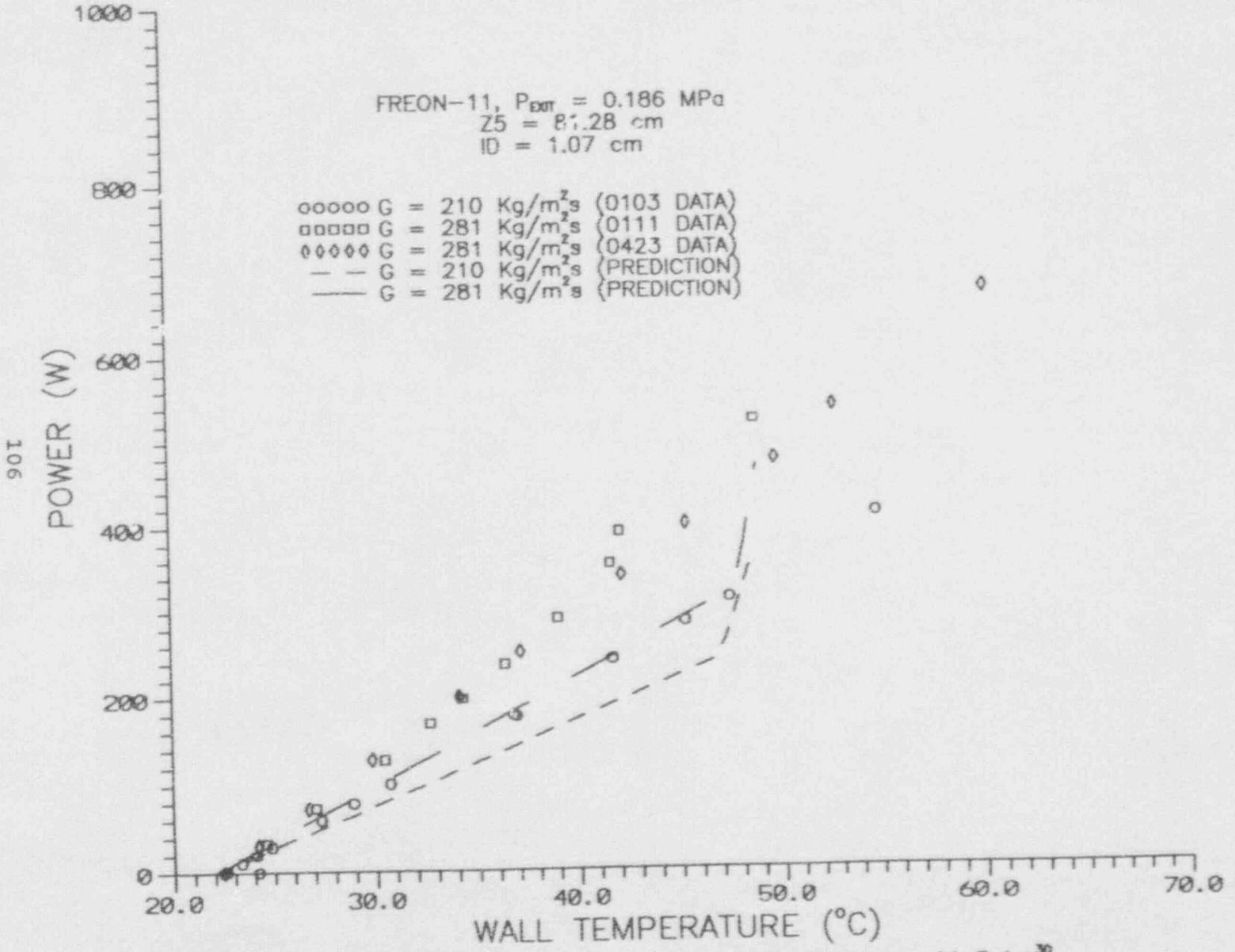

Fig. 6.1.38 Comparisons of Boiling Curve Predictions With Freon-11 Data [30] Using the 'Initial' Model for Z = 81.28 cm, and ID = 1.07 cm.

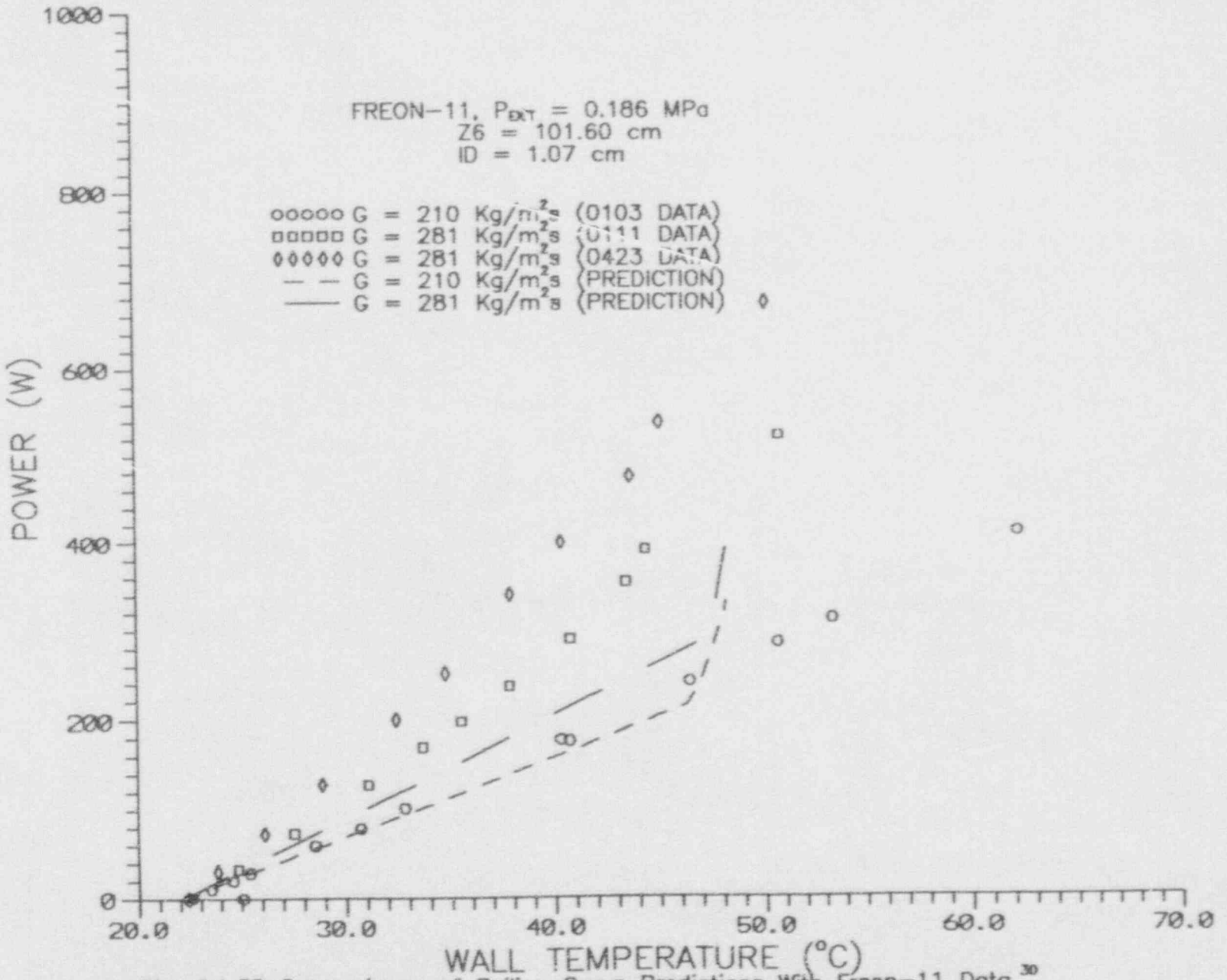

Fig. 6.1.39 Comparisons of Boiling Curve Predictions With Freon-11 Data [30] Using the 'Initial' Model for Z = 101.6 cm(22 cm upstream to exit), and ID = 1.07 cm.

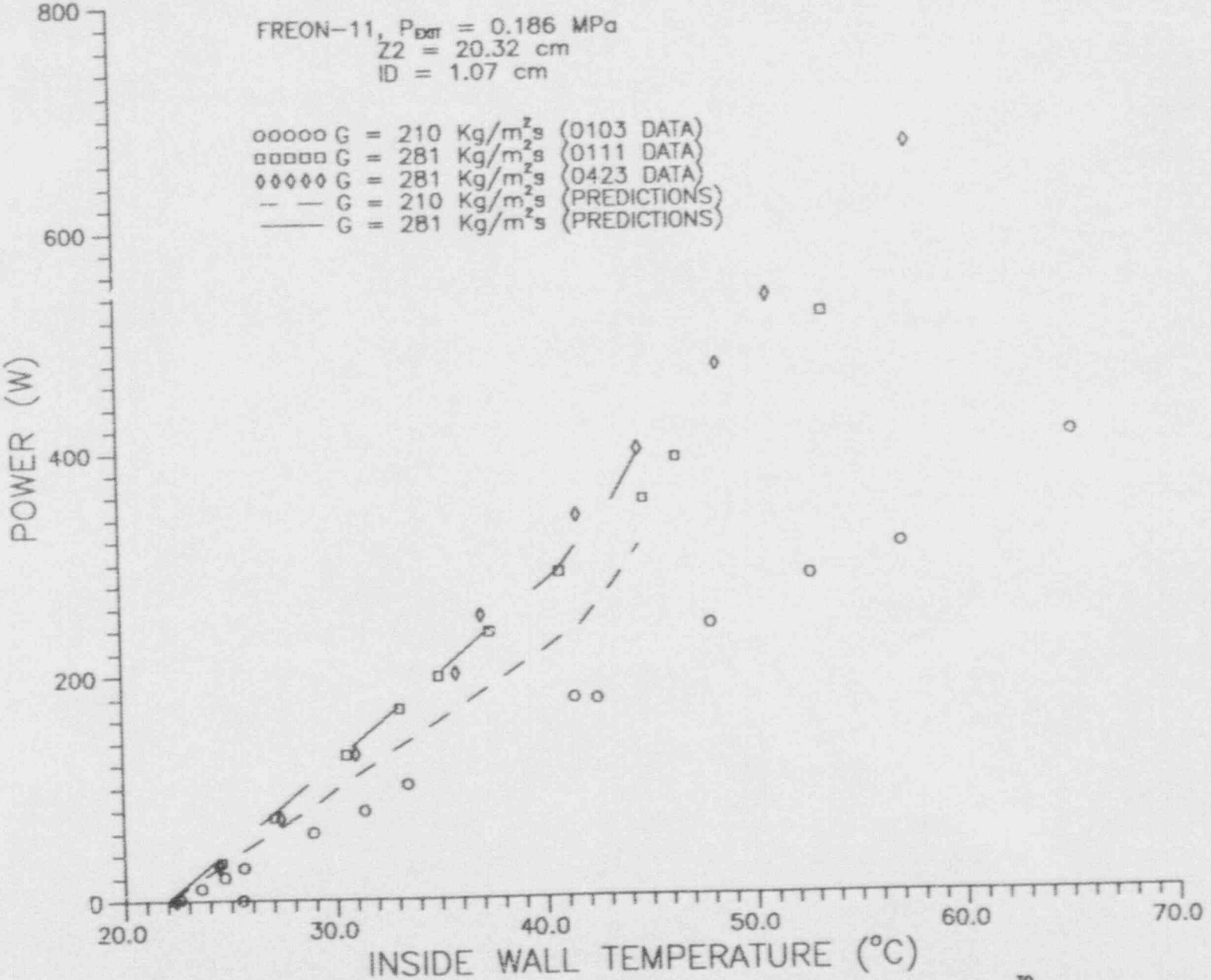

Fig. 6.1.40 Comparisons of Boiling Curve Predictions With Freon-11 Data [30] Using the 'Modified' Model for Z = 20.32 cm (near entrance), and ID = 1.07 cm.

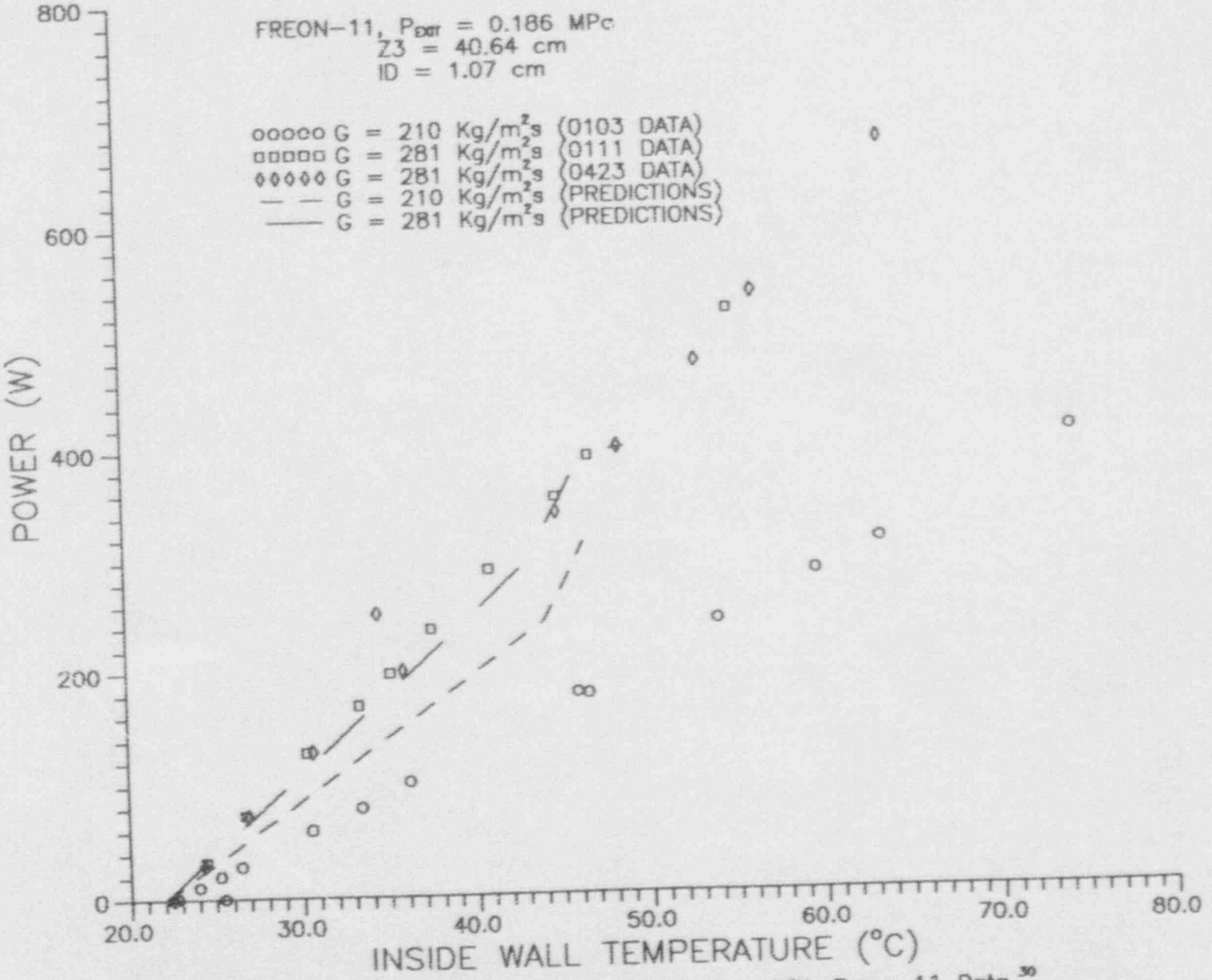

Fig. 6.1.41 Comparisons of Boiling Curve Predictions With Freon-11 Data [30] Using the 'Modified' Model for Z = 40.64 cm, and ID = 1.07 cm.

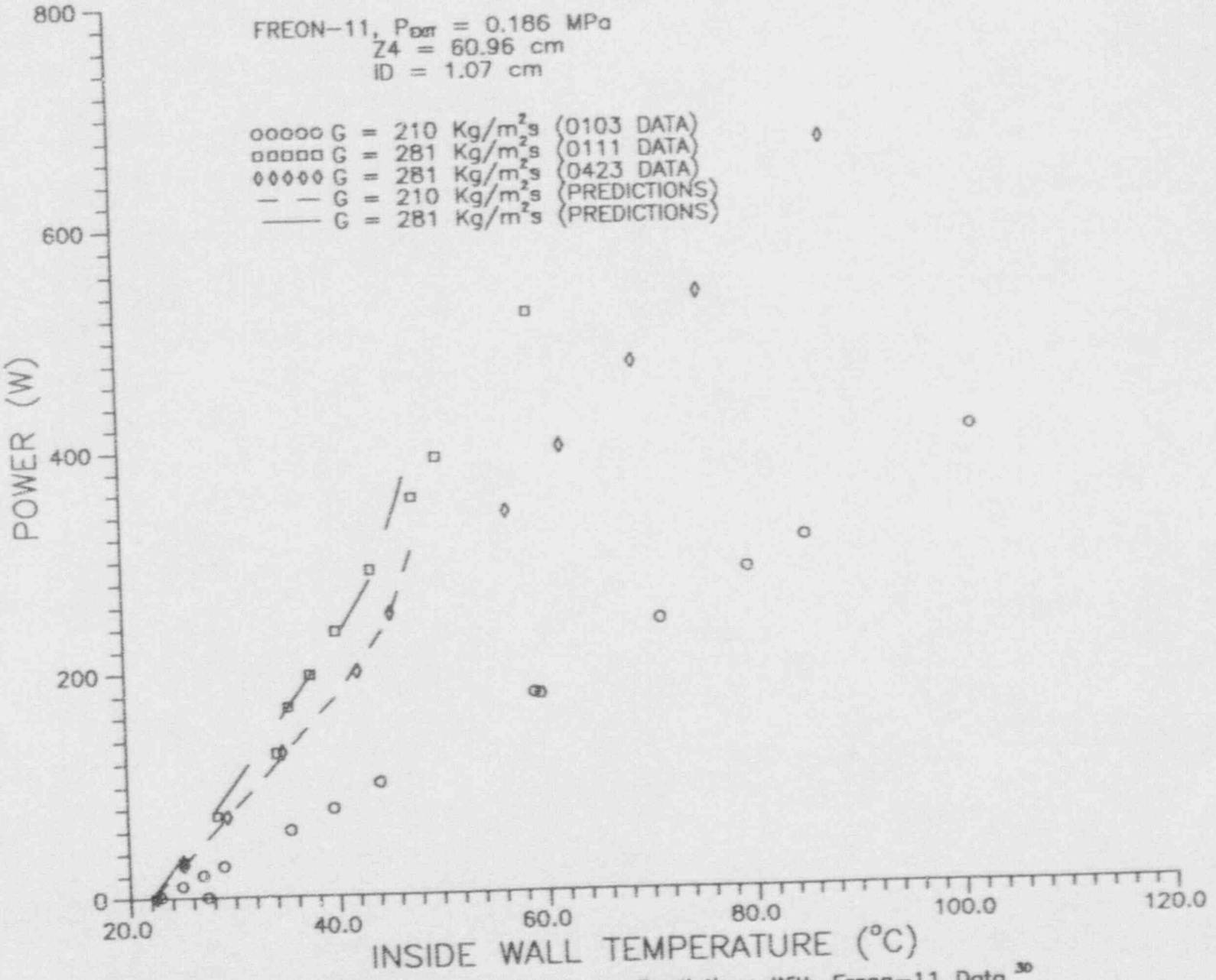

Fig. 6.1.42 Comparisons of Boiling Curve Predictions With Freon-11 Data [30] Using the 'Modified' Model for Z = 60.96 cm, and ID = 1.07 cm.

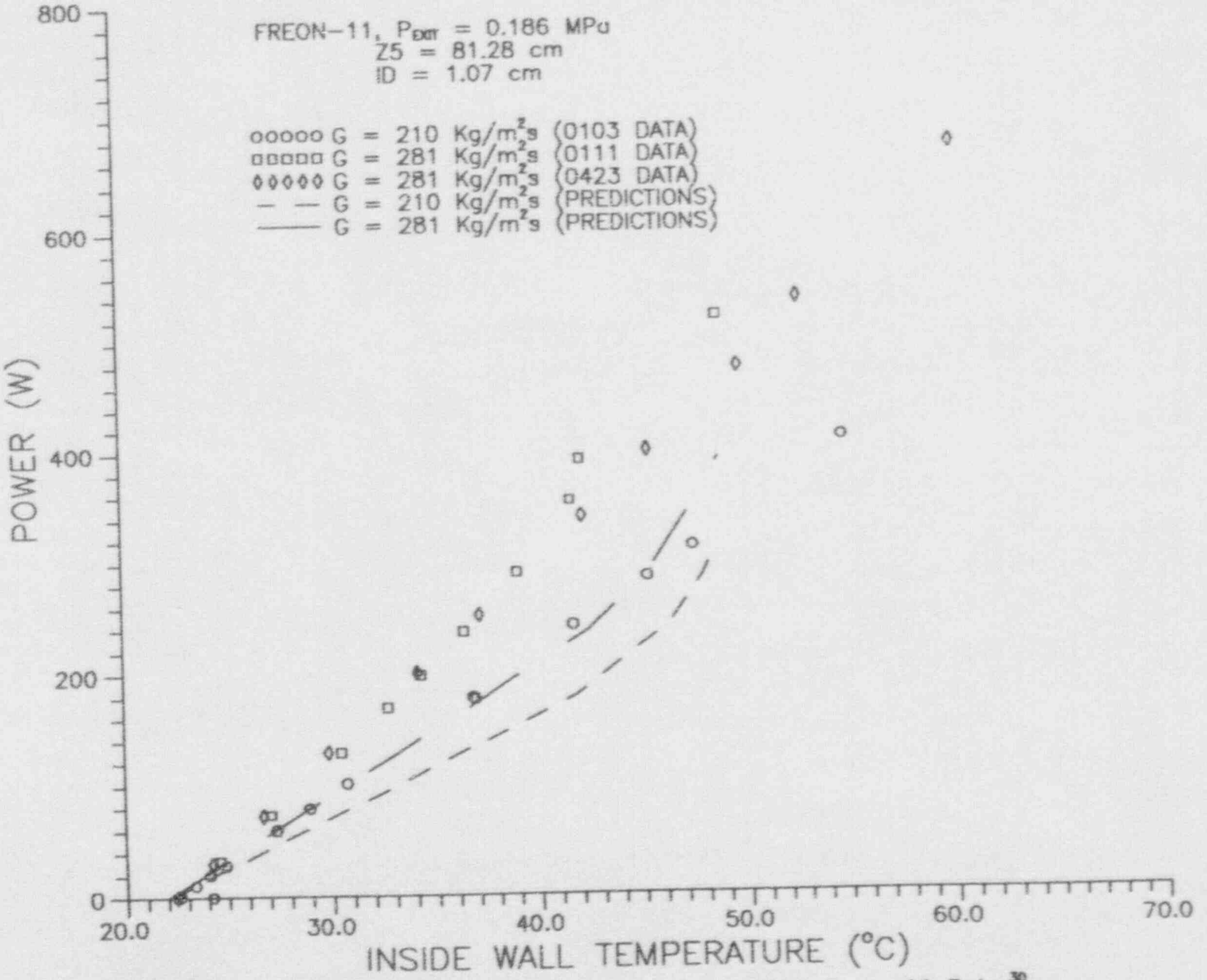

Fig. 6.1.43 Comparisons of Boiling Curve Predictions With Freon-11 Data [30] Using the 'Modified' Model for Z = 81.28 cm, and ID = 1.07 cm.

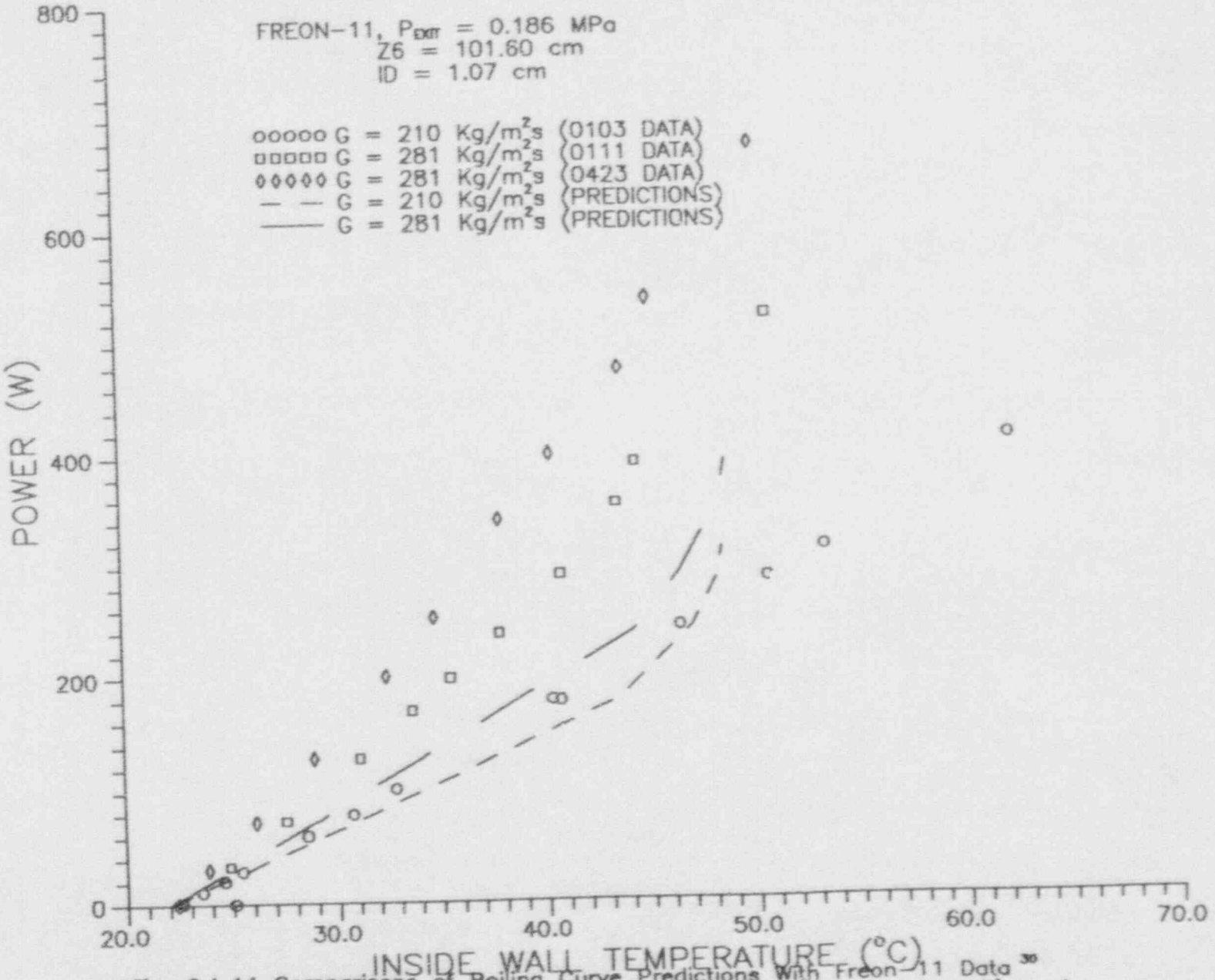

Fig. 6.1.44 Comparisons of Boiling Curve Predictions With Freon-11 Data [30] Using the 'Modified' Model for Z = 101.6 cm (22 cm upstream to exit), and ID = 1.07 cm.

7. CONCLUSIONS AND RECOMMENDATIONS

The flow boiling models are presented for predicting the local heat transfer coefficient. The findings may be summarized as follows:

(1) The flow boiling models can be used to evaluate the local heat transfer coefficient and local inside wall temperature for most fluids. For the system with less important gravitational effects, both heat transfer coefficient and wall temperature predictions are quantitive. For the system with important gravitational effects, the wall temperature and heat transfer coefficient predictions are qualitative. The flow boiling models do not apply in the saturation regime.

(2) The "Modified" model gives better predictions than the "Initial" model in the nucleate partial boiling regime. The over-all percent standard deviation from the water data is less than 19% for both models.

(3) Although the "Modified model" is more difficult to use, it is recommended because it appears to be independent of fluid and the ONB. The "Initial model" is restricted to water and depends on ONB.

(4) Additional observations and results are summarized in the regular progress reports which are contained in Appendix D.

The ongoing work includes formulating the turbulent flow model and assessing critical heat flux models.

REFERENCES

Subcooled Boiling

1. Burmeister, L.C., *Convective Heat Transfer, John Wiley and Sons*, 1983.
2. Chapman, A., *Fundamentals of Heat Transfer, Macmillan*, 1987.
3. Dittus, F. W. and L. M. K. Boelter, Univ. Calif. Publ. Eng. Vol. 2, 1930, p. 443.
4. Sieder, E. N and E. G. Tate, "Heat Transfer and Pressure Drop of Liduids in Tubes," Ind. Eng. Chem., Vol. 28, 1936, p. 1429
5. Petukhov, B.S., "Heat Transfer and Friction in Turbulent Pipe Flow with Variable Physical Properties", Advances in Heat Transfer, Vol. 6, pp. 503-564, 1970.
6. Boyd, R. D. and X. Meng, "Local Heat Transfer for Subcooled Flow Boiling With Water", Fusion Tech. 1992 (accepted for publication).
7. Boyd. R. D., and X. Meng, "——", In preparation.
8. Bergles, A. E., and W. M. Rohsenow, "The Determination of Forced-Convection Surface-Boiling Heat Transfer," J. of Heat Transfer , Aug. 1964, p. 365.
9. Collier, J.G., *Convective Boiling and Condensation, McGraw – Hill*, 1981.
10. Kandlikar, S.G., "A General Correlation for Saturated Two-Phase Flow Boiling Heat Transfer Inside Horizontal and Vertical Tubes", Jornal of Heat Transfer, Vol. 112, pp. 219-228, Feb. 1990.
11. Boyd, R. D. Private Communication with S.G. Kandlikar, June, 1991.
12. Bjorge, R.W., Hall, G.R., Rohsenow, W.M., "Correlation of Forced Convection Boiling Heat Transfer Data", J. Heat Mass Transfer. Vol. 25, pp753-757, 1982.
13. McAdams, W. H., et al., "Heat Transfer at High Rates to Water With Surface Boil-

ing," Ind. Eng. Chem., Vol. 41, 1949, p. 1945 -1953

14. Shah, M. M., "A General Correlation for Heat Transfer During Subcooled Boiling in Pipes and Annuli", ASHRAE Transactions, Vol. 83, pp. 202-215, 1970.

15. Boyd, R.D., "Subcooled Water Flow Boiling Experiments Under Uniform High Heat Flux Conditions", *Fusion Technology*, *Vol.*13, *Jan.*1988.

16. Chen, J.C., "A Correlation for Boiling Heat Transfer to Saturated Fluids in Convective Flow", Industrail and Engineering Chemistry, Process Design and Development, Vol. 5 No. 3, pp 322-329, 1966.

17. Kandlikar, S.G., "Flow Boiling Maps for Water, R-22, and R-134a in the Saturated Region," International Heat Transfer Conference, Jeru-salem, 1990.

18. Tong, L.S., "Boiling Heat Transfer and Two-Phase Flow", John Wiley and Sons, 1965.

19. Hsu, Y.Y., Graham, R.W., *Transport Processes in Boiling and Two -- Phase Systems*, $McGraw - Hill$, 1976.

20. DuPont, "Thermodynamic Properties of Freon-11", E.I. DuPont De Nemours and Company, 1965.

21. Kreith, F. *Fluid Flow Data Book*, *Genium Publishing Corporation*, *Section* 411, 1988.

22. Rohsenow, W.M., Harnett, J.P., Ganic, E.K., "Handbook of Heat Transfer Fundamentals", 2nd Edition, McGraw-Hill, 1985.

23. Vargaftik, N.B., "Table on the Thermophysical Properties of Liquids and Gases", John Willy and Sons, 1975.

24. Nishiguchi, A, Ohuchi, Tomihisa, Konn, K., "Boiling Heat Transfer with Forced

Convection of LiBr-Water Solutin in Horizontal Tube", ASME/JSME Thermal Engineerinng Proceedings, Vol. 2, ASME 1991.

25. Yoshida S., Mori H., Matsunaga T., Ohishi K., "Heat Transfer to Non-Azeotropic Mixturee of Refrigerants in Flowing in a Horizontal Evaporator Tube", ASME/JSME Thermal Engineering Proceedings, Vol. 2, ASME 1991.

26. Turknett, J.C. Jr. and Boyd, R. D., "Forced Convection and Flow Boiling with and without Enhancement Devices for Top-Side-Heated Horizontal Channels", MS Thesis, Mechanical Engineering Department, Prairie View, A&M University, Feb. 1989.

27. Boyd, R.D., "Subcooled Water Flow Boiling in a Horizontal Coolant Channel at $0.45MPa$ for Fusion Application", Submitted to Center of Space Power (NASA), Project RF 25000-14, Oct. 1989.

28 Boyd, R.D., "Experimental Subcooled Flow Boiling for High Heat Flux Applications", Submitted to Sandia National Laboratories, Project RF-90-092, Sep. 1989.

29 Boyd, R.D., "Flow Boiling with Enhancement Devices for Cold Plate Coolant Channel Design", Submitted to NASA, Contract NO. NAG 9-310, Aug. 1989.

30. Smith, A. and Boyd, R. D., "Subcooled Freon-11 Flow Boiling Heat Transfer With and Without Enhancement Devices for Top-Heated Horizontal Coolent Channels" MS Thesis, May, 1992, Prairie View A& M University.

31 Boyd R. D. Private Communication, 1991 and 1992.

*Numerical Conduction**

32. Shih, T.M., *Numerical Heat Transfer*, *Hemisphere Publishing Corporation*, 1984.

* Also see Appendix B.3

33. Jaluria, Y., Torrance, K.E., *Computational Heat Transfer*, *Hemisphere* Publishing Corporation, 1986.

34. Minkowycz, W.J., Sparrow, E.M., Slchneider, G.E., Pletcher, R.H., "Handbook of Numerical Heat Transfer", John Wiley and Sons, 1988.

35. Farnia, K., Beck, J.V., "Numerical Solution of Transient Heat Conduction Equation for Heat-Treatable Alloye Whose Thermal Properties Change with Time and Temperature", J. of Heat Transfer, Vol. 99, Aug. 1977, pp 471-478.

36. Warming, R.F., Hyett, B.J., "The Modified Equation Approach to the Stability and Accuracy Analysis of Finite-Difference Methods.", J. of Computational Physics, Vol. 14, 1974, pp 159-179.

37. Barakat, H.Z., Clark, J.A., "On the Solution of the Diffusion Equations by Numerical Methods", J. of Heat Transfer, Vol. 87-88, 1966, pp 421-428.

38. Maron, M.J., "Numerical Analysis, A Practical Approach", Macmillan, 1982.

39. Boyd R.D., "Flow Boiling with Enhancement Devices for Cold Plate Coolant Channel Design", Submitted to NASA (JSC), Contract No. NAG 9-310, Dec. 1991.

40. Kahaner D., Moler C., Nash S.,"Numerical Methods and Software", Prentice-Hall, 1989.

41. Schmid E.W., Spitz, G., Losch W., "Theoretical Physics on the Personal Computer", Springer-Verlag, 1988.

42. Ozisik M.N., *Heat Transfer A Basic Approach*, *McGraw – Hill*, 1985.

43. Boyd, R.D., "Flow Boiling with and without Enhancement Devices for Horizontal, Top-Heate, Coolant Channels for Cold Plate Design Applications (TASK-5)", Sub-

mitted to NASA, Contract No. 9-16899, Dec. 1986.

44. Whitaker S., "Fundamental Principles of Heat Transfer", Pergamon Press, Inc. 1977.

45. Carslaw, H.S., Jaeger, J.C., *Conduction of Heat in Solids*, *Oxford University* Press, 1959.

46. Schneider, P.J., *Conduction HeatTransfer*, *Addison – Wesley Publishing* Company, 1957.

47. Holman, J.P., *Heat Transfer*, *McGraw – Hill 5th*, 1981.

48. Myers, G.E., *Analytical Methods in Conduction Heat Transfer*, McGraw-Hill, 1971.

49. Meng, X., and Boyd, R. D., "Heat Transfer Predictions and Numerical Data Reduction for Freon-11 Flow Boiling in Enhanced and Smooth Wall Channels," Thermal Science Research Center (TSRC) Report #12-92-1, Prairie View A& M University, December, 1992.

DISTRIBUTION:

1. Division of Contracts
   US Nuclear Regulatory Commission
   Office of Nuclear Regulatory Research
   Wasnington, D.C. 20555

2. U.S. Nuclear Regulatory Commission (3)
   Office of Nuclear Regulatory Research
   Attn: Dr. Frank Odar, Mail Stop NLS-353
   Washington, DC 20555

3. U.S. Nuclear Regulatory Commission (2)
   Division of Technical Information and Document Control
   Document Management Branch
   Washington, D.C. 20555

4. S. Crampton, ADM/CABI
   U.S. Nuclear Regulatory Commission
   Washington, D.C. 20555

5. Dr. Ronald D. Boyd (20)
   Honeywell Professor of Engineering and
   Director of the Thermal Science Research Center
   Prairie View A&M University
   Prairie View, Texas 77446

6. Mr. Bruce Cunningham
   Prairie View A&M Research Foundation
   P.O. Box 3578
   College Station, Texas 77343

7. Mr. Xiaowei Meng
   Graduate Student

8. Dr. Robert L. Shepard,
   Director
   Science and Engineering Alliance
   1522 K Street, N. W., Suite 210
   Washington, D.C. 20005

9. Mr. Dennis Tarner
   Division of Contracts and
   Property Management
   Office of Administration
   U.S. Nuclear Regulatory Commission
   Washington, D.C. 20555

APPENDIX A.1

List of the program for generating single-phase curve, ONB curve and FDB cuve.

```
*       THE  CALCULATION      FOR  Pexit=1.66MPa
*       find  the  point  D  by  using  equ.  19  &  equ.  30
*       q:  heat  flux,  Q/(3.14*d*l),      W/m.
*       c:  specific  heat  of  water,      J/kgC.      20C  &  1.66MPa
*       u:dynamic  viscosity,      kg/ms.
*      k:  thermal  conductivity      of  water,    W/mC.
*       Pr:  Prandtle  number  of  water
*       i146:  enthalpy  of  water  at  saturation,        J/kg.
*       i129:  enthalpy  of  water  at  20C                J/kg.
*      cigma:surface      tension  of  water
*       g:  mass  flux  kg/m  s.
*       d:inside  diameter  of  tube,  m
*       Re:  Reynolds  number  based  on  all  flow  as  liquid.
*       hlo:  heat  transfer  coefficient  with  only  liquid,    w/mC
*      xstar:  quality  at  the  location  where  T=T  dimensionless
*      Bo:  boiling  number.


       real  i148,i129,k,g,hlo,htp,htpc,htpn,htpn1,htpc1
       real  hfd,ii148,htpf,i,iz
       open(5,file='a:men05.dat',status='new')
       open(6,file='a:men06.dat',status='new')
       open(7,     'a:men07.dat',status='new')
       open(1,file='a:inp01.dat',status='old')
       c=4525.
       u=0.0001309
       rof=861.08
       rog=8.312
       Tsat1=203.
       Tin=20.
       k=.665
       pr=0.9
       i148=1928.51*1000.
       ii148=856.99*1000.0
       i129=83.860*1000.0
       cigma=56.80*.001
       d=0.30*0.01
       p=16.6
       read(1,*)n
       do  2  i=1,n
       read(1,*)g,z
       g=g*1000.
       as=3.14*d*z
       ac=3.14*(d**2)/4.
       l=d*96.6

       q2=g*(ii148-i129)*ac/(3.14*d*l)
       dq=0.02*q2
       q=0
*      write(*,*)'q2=',q2
       do  10  j=1,40
       q=q+dq

       iz=(i129+(q*as)/(g*ac))/1000.
       call  bulk(iz,tb)
```

```
      Tw1=250
 20   Tf1=0.50*(Tw1-tb)+Tb
      call   prop(tf1,c,cigma,u,pr,k,rof,rog)
      call   propb(tb,ub)
      call   propw(tw1,uw)
      Re=g*D/u
      f=1.0/((1.82*alog10(Re)-1.64)**2.0)
      c1=1.+3.4*f
      c2=11.7+1.8/(Pr**0.333)
      o=c1+c2*((P.**0.67)-1.0)*((f/8.0)**0.5)
      hlo=(Re*Pr/o)*(f/8.)*k/d*((ub/uw)**0.00)
      hlo1=0.023*(Re**0.8)*(Pr**0.4)*k/d
      Tw=20.+q*((4.*z)/(g*c*d)+1./hlo)
*     write(*,*)'Tw1=',Tw1,'                Tw=',Tw
*     write(*,*)'hlo=',hlo,'             f=',f
      if  (abs(Tw-Tw1).gt.0.10)         then
          Tw1=tw
          goto   20
      endif
*     Tf=(Tb+Tw)/2.
      Tf=0.50*(Tw-Tb)+Tb
      write(*,*)'              Tfilm=',Tf
 80   call   prop(tf,c,cigma,u,pr,k,rof,rog)
      call   propw(tw,uw)
      call   propb(tb,ub)
      Znb=g*c*d*0.25*(183./q-1./hlo)
      Zsc=g*d*(il148-il29)/(4.*q)
*     write(*,*)'Znb=',Znb,'           Zsc=',Zsc

      s=0.463*(p**0.0234)
      tww=250.
 70   Q5=hlo*(tww-tb)
      delt=0.556*((q5/(1082.*(p**1.156)))**.6)
      if  (abs(delt-(tww-203.)).gt.0.1)             then
      tww=delt+203.
*     write(*,*)'tww=',tww,'                tb=',tb
          goto    70
      endif
      delt=tww-203.
*     delt=pr*((8*cigma*q5*(203+273.15)/(il48*k*rog))**.5)
*     write(*,*)'delt=',delt

      z1=g*c*d/4.*((183.+delt)/q-1./hlo)
      z2=g*c*d/4.*(1/hlo-delt/q)
      L=d*96.6
      Pexit=1.66
      c1=0.97
      c2=0.28
      c3=6.13/z2
      c4=6.13*z1/z2
      dPfo=3.72822*0.001*((g/1000.)**1.85)*(1.0-z/l)
      dd=c3*l+c4
      ddd=c3*(l-z)-c4
*     dPscb=dPfo*(c1*(l-z)+c2/c3*(exp(c3*(L-Z)-C4)))
      Pz=(Pexit+dPscb)
*     write(*,*)'Pz=',Pz
*     call   drop(pz,Tsat1,i148,il148)
*     I148=I148*1000.
*     il148=il148*1000.
*     write(*,*)'Tsat1=',Tsat1
*     write(*,*)'i148=',i148
      Bo=q/(g*i148)
```

```
      $tio=hio/(g*c)

      tw3=250.
100   tf3=0.5*(tw-tb)+tb
      call   prop(tf3,c,sigma,u,pr,k,rof,rog)
      xstar=-g*c/(hio*i148)
      x=(as*q/(g*ac)-il148+i129)/i148
      deltsu=-x*i148/c
*     write(*,*)'x=',x,'              deltsu=',deltsu
      if  (Bo.LE.0.00003)       then
            fbo=1.+46.*(Bo**0.5)
      else
        fbo=230.*(Bo**.5)
      endif
      htpf=hio/(1.0/fbo+x/xstar)
      tw=q/htpf+tb
      if  ((abs(tw-tw3)).gt.0.10)          then
      tw3=tw
      goto   100
      endif

      delts1=q/hio-deltsu
      delts2=q*(1./fbo+x/xstar)/hio-deltsu
      htpf=hio/(1./fbo+x/xstar)
      dxstar=delT*c/i148
      xonb=xstar+dxstar
      Twall1=delts1+Tsat1
      Twall2=delts2+Tsat1
      write(5,*)delts1,q/1000.
      write(6,*)delts2,q/1000.
      write(7,*)delt,q/1000.
10    continue
      write(5,*)
      write(6,*)
      write(7,*)
2     continue
      stop
      end


      subroutine     drop(p1,Tsat1,i148,il148)
      dimension     p(10),T(10)
      real       i(10),il(10),i148,il148
      integer    j
      data   p/1.56,1.66,1.92,2.32,2.8,3.35,3.98,4.7,5.5,6.4/
      data   t(1),t(2),t(3),t(4)/200,203,210,220/
      data   t(5),t(6),t(7),t(8)/230,240,250,260/
      data   t(9),t(10)/270,280/
      data   i(1),i(2),i(3),i(4)/1940.6,1928.5,1900.3,1858.3/
      data   i(5),i(6),i(7)/1811.7,1765.4,1715.2/
      data   i(8),i(9),i(10)/1661.0,1604.8,1543.2/
      data   il(1),il(2),il(3)/852.4,856.9,897.7/
      data   il(4),il(5),il(6)/943.7,990.3,1037.6/
      data   il(7),il(8),il(9),il(10)/1085.8,1135.0,1185.2,1236.8/
      do  5  k=1,10
       if(p1.le.p(k))       then
       goto   4
      endif
5     continue
4     Tsat1=t(k)+(p1-p(k))/(p(k)-p(k-1))*(t(k)-t(k-1))
      i148=i(k)+(p1-p(k))/(p(k)-p(k-1))*(i(k)-i(k-1))
      il148=il(k)+(p1-p(k))/(p(k)-p(k-1))*(il(k)-il(k-1))
```

```
      return
      end

      subroutine     bulk(i1,tb)
      real   i1,i(15),t(15)
      integer    j
      data   i(1),i(2),i(3),i(4)/83.86,125.66,167.47,209.3/
      data   i(5),i(6),i(7),i(8)/251.1,293.,334.9,376.9/
      data   i(9),i(10),i(11),i(12)/419.,461.,503.7,546./
      data   i(13),i(14),i(15)/589.3,632.2,675.5/
      data   t(1),t(2),t(3),t(4),t(5),t(6)/20,30,40,50,60,70/
      data   t(7),t(8),t(9),t(10),t(11)/80,90,100,110,120/
      data   t(12),t(13),t(14),t(15)/130,140,150,160/
      do  9  k=1,15
      if  (i1.le.i(k))       then
      goto   3
      endif
9         continue
3         tb=t(k)+(i1-i(k))/(i(k)-i(k-1))*(t(k)-t(k-1))
      write(*,*)'i1==',i1,'                tb==',tb
      return
      end

      subroutine     prop(tfi,c,cigma,u,Pr,k,rof,rog)
      dimension     b(28),z(28),d(28),pn(28),f(28),r(28),q(28)
      real   t(28),k
      data   t(1),t(2),t(3),t(4),t(5),t(6)/20,30,40,50,60,70/
      data   t(7),t(8),t(9),t(10),t(11)/80,90,100,110,120/
      data   t(12),t(13),t(14),t(15)/130,140,150,160/
      data   t(16),t(17),t(18),t(19)/170,180,190,200/
      data   t(20),t(21),t(22),t(23),t(24)/210,220,230,240,250/
      data   t(25),t(26),t(27),t(28)/260.,270.,280.,290./
      data   b(1),b(2),b(3),b(4)/4182.,4179.,4179.,4181./
      data   b(5),b(6),b(7),b(8)/4185.,4191.,4198.,4207./
      data   b(9),b(10),b(11),b(12)/4218.,4230.,4244.,4262./
      data   b(13),b(14),b(15),b(16)/4282.,4306.,4334.,4366./
      data   b(17),b(18),b(19),b(20)/4403.,4446.,4494.,4550./
      data   b(21),b(22),b(23),b(24)/4613.,4685.,4769.,4866./
      data   b(25),b(26),b(27),b(28)/4985.,5134.,5307.,5520./
      data   z(1),z(2),z(3),z(4)/72.78,71.23,69.61,67.93/
      data   z(5),z(6),z(7),z(8)/66.19,64.40,62.57,60.69/
      data   z(9),z(10),z(11),z(12)/58.78,56.83,54.85,52.83/
      data   z(13),z(14),z(15),z(16)/50.79,48.70,46.59,44.44/
      data   z(17),z(18),z(19),z(20)/42.26,40.05,37.81,35.53/
      data   z(21),z(22),z(23),z(24)/33.23,30.90,28.56,26.19/
      data   z(25),z(26),z(27),z(28)/23.82,21.44,19.07,16.71/
      data   d(1),d(2),d(3),d(4)/1002.,798.3,653.9,547.8/
      data   d(5),d(6),d(7),d(8)/467.3,404.8,355.4,315.6/
      data   d(9),d(10),d(11),d(12)/283.1,254.8,231.0,210.9/
      data   d(13),d(14),d(15),d(16)/194.1,179.8,167.7,157.4/
      data   d(17),d(18),d(19),d(20)/148.5,140.7,133.9,127.9/
      data   d(21),d(22),d(23),d(24)/122.4,117.5,112.9,108.7/
      data   d(25),d(26),d(27),d(28)/104.8,101.1,97.5,94.1/
      data   pn(1),pn(2),pn(3),pn(4),pn(5)/6.9,5.4,4.3,3.5,3./
      data   pn(6),pn(7),pn(8),pn(9),pn(10)/2.5,2.2,1.9,1.7,1.5/
      data   pn(11),pn(12),pn(13),pn(14),pn(15)/1.4,1.3,1.2,1.1,1./
      data   pn(16),pn(17),pn(18),pn(19),pn(20)/1.,.96,.93,.91,.89/
      data   pn(21),pn(22),pn(23),pn(24)/.87,.86,.85,.859/
      data   pn(25),pn(26),pn(27),pn(28)/.866,.882,.902,.932/
      data   f(1),f(2),f(3),f(4),f(5)/.603,.618,.631,.643,.653/
      data   f(6),f(7),f(8),f(9),f(10)/.662,.67,.676,.681,.684/
      data   f(11),f(12),f(13),f(14),f(15)/.687,.688,.688,.687,.684/
```

```
      data   f(16),f(17),f(18),f(19),f(20)/.681,.677,.671,.664,.657/
      data   f(21),f(22),f(23),f(24)/.648,.639,.628,.616/
      data   f(25),f(26),f(27),f(28)/.603,.589,.574,.558/
      data   r(1),r(2),r(3),r(4),r(5)/998.2,995.6,992.1,988.1,983.3/
      data   r(6),r(7),r(8),r(9),r(10)/978.5,971.8,966.2,958.8,951.5/
      data   r(11),r(12),r(13),r(14),r(15)/943.,935.,926.,917.,907./
      data   r(16),r(17),r(18),r(19),r(20)/897.,887.,876.,865.,853./
      data   r(21),r(22),r(23),r(24)/840.,827.,813.,799./
      data   r(25),r(26),r(27),r(28)/784.,767.8,750.7,732.3/
      data   q(1),q(2),q(3),q(4),q(5)/.017,.03,.051,.083,.13/
      data   q(6),q(7),q(8),q(9),q(10)/.198,.29,.42,.598,.826/
      data   q(11),q(12),q(13),q(14),q(15)/1.12,1.5,1.97,2.5,3.3/
      data   q(16),q(17),q(18),q(19),q(20)/4.1,5.2,6.4,7.87,9.6/
      data   q(21),q(22),q(23),q(24)/11.63,14.08,16.95,20.0/
      data   q(25),q(26),q(27),q(28)/23.72,28.09,33.18,39.16/
      do  7  k1=1,28
      if  (tfi.le.t(k1))       then
      goto   6
      endif
7        continue
6          c=b(k1)+(tfi-t(k1))/(t(k1)-t(k1-1))*(b(k1)-b(k1-1))
      cigma=z(k1)+(tfi-t(k1))/(t(k1)-t(k1-1))*(z(k1)-z(k1-1))
      u=d(k1)+(tfi-t(k1))/(t(k1)-t(k1-1))*(d(k1)-d(k1-1))
      Pr=pn(k1)+(tfi-t(k1))/(t(k1)-t(k1-1))*(pn(k1)-pn(k1-1))
      k=f(k1)+(tfi-t(k1))/(t(k1)-t(k1-1))*(f(k1)-f(k1-1))
      rof=r(k1)+(tfi-t(k1))/(t(k1)-t(k1-1))*(r(k1)-r(k1-1))
      rog=q(k1)+(tfi-t(k1))/(t(k1)-t(k1-1))*(q(k1)-q(k1-1))
      cigma=cigma*0.001
      u=u*0.000001
*     write(*,*)'c=',c,'            cigma=',cigma,'            u=',u
*     write(*,*)'pr=',pr,'          k=',k,'        rof=',rof,'        rog=',rog
      return
      end


      subroutine     propw(ts,uw)
      dimension     w(28),s(28)
      data   w(1),w(2),w(3),w(4)/20.,30.,40.,50./
      data   w(5),w(6),w(7),w(8)/60.,70.,80.,90./
      data   w(9),w(10),w(11),w(12)/100.,110.,120.,130./
      data   w(13),w(14),w(15),w(16)/140.,150.,160.,170./
      data   w(17),w(18),w(19),w(20)/180.,190.,200.,210./
      data   w(21),w(22),w(23),w(24)/220.,230.,240.,250./
      data   w(25),w(26),w(27),w(28)/260.,270.,280.,290./
      data   s(1),s(2),s(3),s(4)/1002.,798.3,653.9,547.8/
      data   s(5),s(6),s(7),s(8)/467.3,404.8,355.4,315.6/
      data   s(9),s(10),s(11),s(12)/283.1,254.8,231.,210.9/
      data   s(13),s(14),s(15),s(16)/194.1,179.8,167.7,157.4/
      data   s(17),s(18),s(19),s(20)/148.5,140.7,133.9,127.9/
      data   s(21),s(22),s(23),s(24)/122.4,117.5,112.9,108.7/
      data   s(25),s(26),s(27),s(28)/104.8,101.1,97.5,94.1/


      do  3  m=1,28
      if  (ts.le.w(m))      then
      goto   4
      endif
3     continue
4     uw=s(m)+(ts-w(m))/(w(m)-w(m-1))*(s(m)-s(m-1))
      uw=uw*0.000001
      return
      end
```

```
      subroutine     propb(ts,ub)
      dimension     w(28),s(28)
      data   w(1),w(2),w(3),w(4)/20.,30.,40.,50./
      data   w(5),w(6),w(7),w(8)/60.,70.,80.,90./
      data   w(9),w(10),w(11),w(12)/100.,110.,120.,130./
      data   w(13),w(14),w(15),w(16)/140.,150.,160.,170./
      data   w(17),w(18),w(19),w(20)/180.,190.,200.,210./
      data   w(21),w(22),w(23),w(24)/220.,230.,240.,250./
      data   w(25),w(26),w(27),w(28)/260.,270.,280.,290./
      data   s(1),s(2),s(3),s(4)/1002.,798.3,653.9,547.8/
      data   s(5),s(6),s(7),s(8)/467.3,404.8,355.4,315.6/
      data   s(9),s(10),s(11),s(12)/283.1,254.8,231.,210.9/
      data   s(13),s(14),s(15),s(16)/194.1,179.8,167.7,157.4/
      data   s(17),s(18),s(19),s(20)/148.5,140.7,133.9,127.9/
      data   s(21),s(22),s(23),s(24)/122.4,117.5,112.9,108.7/
      data   s(25),s(26),s(27),s(28)/104.8,101.1,97.5,94.1/


      do  3  m=1,28
      if  (ts.le.w(m))      then
      goto   4
      endif
3     continue
4     ub=s(m)*(ts-w(m))/(w(m)-w(m-1))*(s(m)-
      ub=ub*0.000001
      return
      end
```

APPENDIX A.2

List of program for finding the intersections of single-phase curve, ONB curve and FDB curve.

```
*       THIS   PROGRAM    IS  FOR  COMPUTING     THE  STATUSES     AT  ONB,   AND  FDB
        DIMENSION     T1(80),T2(80),T3(80),Q1(80),Q2(80),Q3(80)
        REAL   TC,TD,TE,QC,QD,QE
        OPEN   (2,FILE='A:INP01.DAT',STATUS='OLD')
        OPEN   (3,FILE='A:MEN05.DAT',STATUS='OLD')
        OPEN   (4,FILE='A:MEN07.DAT',STATUS='OLD')
        OPEN   (5,FILE='A:MEN06.DAT',STATUS='OLD')
        OPEN   (8,FILE='A:INP02.DAT',STATUS='NEW')
        READ(2,*)N
        WRITE(8,*)N
        DO  5  J=1,N
        READ(2,*)G,Z
        DO  10  I=1,47
        write(*,*)'j      =  ',j,'      i  =  ',i
        READ(3,*)T1(I),Q1(I)
        READ(4,*)T2(I),Q2(I)
        READ(5,*)T3(I),Q3(I)
10      CONTINUE
        DO  20  K=1,47
        IF  ((T1(K)-T3(K)).GT.0.00)          THEN
        GOTO   100
        ENDIF
20      CONTINUE
100     A=(T3(K-1)-T1(K-1))/(T1(K)-T1(K-1)-T3(K)+T3(K-1))
        Td=A*(T3(K)-T3(K-1))+T3(K-1)
        B=(Q3(K)-Q3(K-1))/(T3(K)-T3(K-1))
        Qd=Q3(K-1)+(B*(Td-T3(K-1)))
        Qfdb=1.4*Qd
        DO  30  M=1,47
        IF  ((Qfdb-Q3(M)).LT.0.00)          THEN
        GOTO   200
        ENDIF
30      CONTINUE
200     C=(T3(M)-T3(M-1))/(Q3(M)-Q3(M-1))
        Tfdb=C*(Qfdb-Q3(M-1))+T3(M-1)
        DO  40  L=1,47
        IF  ((T2(L)-T1(L)).LT.0.00)          THEN
        GOTO   300
        ENDIF
40      CONTINUE
300     D=(T2(L-1)-T1(L-1))/(T1(L)-T1(L-1)+T2(L-1)-T2(L))
        Tonb=(D*(T2(L)-T2(L-1)))+T2(L-1)
        E=(Q2(L)-Q2(L-1))/(T2(L)-T2(L-1))
        Qonb=((Tonb-T2(L-1))*E)+Q2(L-1)
        WRITE(8,*)G,Z
        WRITE(8,*)Tonb,Qonb
        WRITE(8,*)Tfdb,Qfdb
        WRITE(8,*)
 5      CONTINUE
        STOP
        END
```

APPENDIX A.3-1

List of the program for calculating heat transfer results for "initial" model.

```
      real   m,n,htp,hlo,htpc1,htpn1,htpc,htpn,htpp,htpf,HHPP
      real   k,il148,i129,i148,kg,l,pz,iz,i1,Nu
      open(9,file='a:men083.dat',status='new')
      open(21,file='a:qvstwd.dat',status='new')
      open(26,file='a:mx0753.dat',status='new')
      open(2,file='a:inp02.dat',status='old')
      open(5,file='a:datanz.dat',status='old')
      open(4,file='a:inati.dat',status='old')
      open(6,file='a:predict.dat',status='new')
      read(4,*)Tsat1,       il148,    i148,   p
      c=4525.
      u=0.0001309
      ug=0.00001582
      k=.665
      kg=0.03812
      pr=0.9
      il148=il148*1000.
      i148=i148*1000.
      i129=83.86*1000.
      cigma=38.80*.001
      d=0.30*.01
      L=d*96.6
      read(2,*)n1
c     n1=2
      do  55  j=1,n1
      read(2,*)g,z
      g=g*1000.
      as=3.14*d*z
      ac=3.14*(d**2)/4.
      q2=g*(il148-i129)*ac/(3.14*d*l)
      write(*,*)'q2=',q2
      rog=8.312
      rol=998.2

      read(2,*)delto,qonb
      read(2,*)delte,qe
      qonb=qonb*1000.
      qe=qe*1000.
      Read(5,*)IA
      write(21,*)IA
      write(6,*)IA
      Do  1000   INEW=   1,  IA
      Read(5,*)QQ2,HHDATA
      q=QQ2*q2
      dq=qonb/11.
*     q=dq
      do  2  i=1,1
*     write(*,*)'q=',q,'             q2=',q2
*     call   prs(g,q,z,pz)
*     call   drop(Pz,Tsat1,i148,il148)
      if(q   .ge.   qonb)   then
      go  to  160
      endif
      iz=(i129+(q*as)/(g*ac))/1000.
      iss=1
```

```
      call   bulk(iz,tb)
      Tw1=250.
42    Tf1=0.50*(Tw1-Tb)+Tb
      call   prop(tf1,e,cigma,u,pr,k,rof,rog)
      call   propb(tb,ub)
      call   propw(tw1,uw)
      Re=g*d/u
      f=1.0/((1.82*alog10(Re)-1.64)**2.)
      c1=1.+3.4*f
      c2=11.7+1.8/(Pr**0.333)
      o=c1+c2*((Pr**0.67)-1.)*((f/8.)**0.5)
      hlo1=(Re*Pr/o)*(f/8.)*k/d*((ub/uw)**0.00)
      hlo=0.023*(Re**0.8)*(Pr**0.4)*k/d
      Tw=20.+q*((4.*z)/(g*c*d)+1./hlo1)
      if  (abs(Tw-Tw1).gt.0.10)          then
      Tw1=Tw
*     write(*,*)'Re=',Re
      goto   42
      endif
      Tf=0.50*(Tw-Tb)+Tb
      call   prop(tf,e,cigma,u,pr,k,rof,rog)
      call   propb(tb,ub)
      call   propw(tw,uw)
*     call   film(tf,i148,il48)
      hlo=0.023*(Re**0.8)*(pr**0.4)*k/d
      hlo1=(Re*Pr/o)*(f/8.0)*k/d*((ub/uw)**0.00)
      x=(as*q/(g*ac)-il48+i129)/i148
      delts1=q/hlo1+x*i148/c
      Twall1=delts1+Tsat1
      Pe=Re*Pr
      Nu=hlo1*d/k
      St=Nu/Pe
      Twp=Twall1
      HHPP=hlo1/1000.
      write(9,*)Pe/100000,St
      write(26,*)q/q2,hlo1/1000.
      IF  (HLO.LE.0.0)      THEN
      WRITE(*,*)'      HLO=',HLO
      ENDIF
*     q=q+dq
2     continue
      write(*,*)'     END   OF   THE   FIRST   PART'
      dq=(qe-qonb)/10.
*     q=q+dq
      GO  TO  101
160   if(q   .ge.   qe)   then
      go  to  170
      endif
      iss=2
      do    10  i=1,1
      p=1./(qe-qonb)
      n=1.-p*qonb
      m=n+p*q
      m=m*10000.
      im1=int(m)
      m=im1/10000.
      b=(qe-qonb)/((delte**m)-(delto**m))
      a=qonb-b*(delto**m)
      m=1.0/m
      m=m*10000.
      im=int(m)
      m=im/10000.
```

```
      delt=((q-a)/b)**m
*     call   prs(g,q,z,pz)
*     call   drop(Pz,Tsat1,i148,ii148)
      iz=(i129+(q*as)/(g*ac))/1000.
      call   bulk(iz,tb)
      Tw2=250.
 43   Tf2=0.50*(Tw-Tb)+Tb
      call   prop(tf2,c,cigma,u,pr,k,rof,rog)
      Re=g*d/u
      http=q/(delt-x*i148/c)
      Tw=20.+q*((4.*z)/(g*c*d)+1./http)
      if  (abs(Tw2-Tw).gt.0.10)          then
      Tw2=Tw
      goto   43
      endif
*     write(*,*)'Tww=',tw

      tw=delt+tsat1
      Tf=0.50*(Tw-Tb)+Tb
*     write(*,*)'     Tf=',Tf,'        TWW=',tw
      call   prop(tf,c,cigma,u,pr,k,rof,rog)
*     call   film(tf,i148,ii148)
      x=(as*q/(g*ac)-ii148+i129)/i148
      Twall=delt+Tsat1
      htpp=q/(delt-x*i148/c)
      Re=g*d/u
      Nu=htpp*d/k
      Pe=Pr*Re
      St=Nu/Pe
      write(9,*)Pe/100000.,St
      write(26,*)q/q2,htpp/1000.
      Twp=Twall
      HHPP=htpp/1000.
*     q=q+dq
10    continue
      write(*,*)'     END  OF  THE  SECOND   PART'
*     q=qe
      qlmt=q2*0.8
*     do  15  i=1,1
*     q=q+dq
*     call   prs(g,q,z,pz)
*     call   drop(Pz,Tsat1,i148,ii148)
      GO  TO  101
170   iss=3
      iz=(i129+(q*as)/(g*ac))/1000.
      call   bulk(iz,tb)
      Tw3=250.
 44   Tf3=0.50*(Tw3-Tb)+Tb
      call   prop(tf3,c,cigma,u,pr,k,rof,rog)
      call   propb(tb,ub)
      call   propw(tw3,uw)
      Re=g*d/u
      f=1.0/((1.82*alog10(Re)-1.64)**2.)
      c1=1.+3.4*f
      c2=11.7+1.8/(Pr**0.333)
      o=c1+c2*((Pr**0.67)-1.0)*((f/8.0)**0.5)
      hlo=(Re*Pr/o)*(f/8.0)*k/d*((ub/uw)**0.00)
      Twsp=20.+q*((4.*z)/(g*d*c)+1.0/hlo)
      If  (abs(Tw3-Twsp).gt.0.10)          then
      Tw3=Twsp
      goto   44
      endif
```

```
      x=(as*q/(g*ac)-il148+i129)/i148
      xstar=-q*c/(hlo*i148)
      Bo=q/(g*i148)
      if  (bo.le.0.00003)       then
        fbo=1.+46.*(bo**0.5)
      else
        fbo=230.*(bo**0.5)
      endif
      htpf=hlo/(1./fbo+x/xstar)
      hlo1=0.023*(Re**0.8)*(pr**0.4)*k/d
      Tw=20.+q*((4.*z)/(g*d*c)+1./htpf)
*     if  (abs(Tw-Tw3).gt.0.10)          then
*     Tw3=Tw
*     goto  44
*     endif
 45   Tf=0.50*(Tw-Tb)+Tb
      call   prop(tf,c,cigma,u,pr,k,rof,rog)
*     call   film(tf,i148,il148)
      x=(as*q/(g*ac)-il148+i129)/i148
*     if  (q.ge.qlmt)     then
*      goto  11
*     endif
      Bo=q/(g*i148)
      if  (Bo.LE.    0.00003)     then
        fbo=1.+46.*(Bo**0.5)
      else
        fbo=230.*(Bo**0.5)
      endif
      Re=g*d/u
      xstar=-q*c/(hlo*i148)
      delt2=q*(1./fbo+x/xstar)/hlo+x*i148/c
      Twall2=delt2+Tsat1
      If(abs(Twall2-Tw).gt.0.10)           then
      Tw=Twall2
      goto  45
      endif

      htpf=hlo/(1/fbo+x/xstar)
      Nu=htpf*d/k
      Pe=Re*Pr
      St=Nu/Pe
      write(9,*)Pe/100000.,St
*15   write(*,*)
 15   write(26,*)q/q2,htpf/1000.
      Twp=Twall2
      HHPP=htpf/1000.
11    write(*,*)
 101  CONTINUE
      WRITE(*,*)'END      OF  THE   THIRD   PART'
      Twd=tb+(q/(1000.*HHDATA))
      write(21,*)Twp,q/1000000.,Twd
      Write(6,*)QQ2,HHPP
      write(6,*)
1000  continue
 55   CONTINUE
      write(*,*)     ' HERE   YOU   GO  !!!'
      stop
      end

      subrouiine     prs(g,q,z,pz)
      real   i148,il148,l,hlo,k
      c=4525.0
```

```
      d=0.30*0.01
      k=.665
      rof=861.08
      rog=8.312
      cigma=38.80*0.001
      i148=1928.51*1000.
      u=0.0001309
      Pr=0.9
      Re=g*d/u
      delt=(8*cigma*q*(203.+273.15)/(i148*k*rog))**.5*pr
      hlo=.023*(Re**0.8)*(pr**0.4)*k/d
      z1=g*c*d/4.*((183.+delt)/q-1./hlo)
      z2=g*c*d/4.*(1/hlo-delt/q)
      L=d*96.6
      Pexit=1.66
      c1=0.97
      c2=0.28
      c3=6.13/z2
      c4=6.13*z1/z2
      dPfo=3.72822*0.001*((g/1000.)**1.85)
      dPscb=dPfo*(c1*(l-z)+c2/c3*(exp(c3*(l-z)-c4)))
      Pz=Pexit+dPscb
      write(*,*)'dpfo=',dpfo,'             dpscb=',dpscb
      return
      end

      subroutine     film(t1,i148,il148)
      dimension    t(17)
      real   i(17),il(17),i148,il148
      integer    j
      data   t(1),t(2),t(3),t(4)/50.,60.,70.,80./
      data   t(5),t(6),t(7),t(8)/90.,100.,110.,120./
      data   t(9),t(10),t(11),t(12)/130.,140.,150.,160./
      data   t(13),t(14),t(15),t(16),t(17)/170.,180.,190.,200.,210./
      data   i(1),i(2),i(3),i(4)/2382.7,2357.9,2333.,2308.1/
      data   i(5),i(6),i(7),i(8)/2283.1,2256.9,2229.7,2202.3/
      data   i(9),i(10),i(11),i(12)/2173.7,2144.9,2114.8,2082.5/
      data   i(13),i(14),i(15),i(16)/2049.9,2014.9,1978.5,1940.6/
      data   i(17)/1900.3/
      data   il(1),il(2),il(3),il(4)/209.3,251.1,293.,334.9/
      data   il(5),il(6),il(7),il(8)/376.9,419.1,461.3,503.7/
      data   il(9),il(10),il(11),il(12)/546.3,589.1,632.2,675.5/
      data   il(13),il(14),il(15),il(16)/719.1,763.1,807.5,852.4/
      data   il(17)/897.7/
      do  5  k=1,17
      if  (t1.le.t(k))      then
       goto   4
       endif
5     continue
4       i148=i(k)+(t1-t(k))/(t(k)-t(k-1))*(i(k)-i(k-1))
        il148=il(k)+(t1-t(k))/(t(k)-t(k-1))*(il(k)-il(k-1))
      i148=i148*1000.
      il148=il148*1000.
      return
      end


      subroutine     bulk(i1,tb)
      real   i1,i(20),t(20)
      integer    j
      data   i(1),i(2),i(3),i(4)/83.86,125.66,167.47,209.3/
      data   i(5),i(6),i(7),i(8)/251.1,293.,334.9,376.9/
```

```
      data   i(9),i(10),i(11),i(12)/419.,461.,503.7,546./
      data   i(13),i(14),i(15),i(16)/589.3,632.2,675.5,719.1/
      data   i(17),i(18),i(19),i(20)/763.1,807.5,852.4,897.7/
      data   t(1),t(2),t(3),t(4),t(5),t(6)/20,30,40,50,60,70/
      data   t(7),t(8),t(9),t(10),t(11)/80,90,100,110,120/
      data   t(12),t(13),t(14),t(15),t(16)/130,140,150,160,170/
      data   t(17),t(18),t(19),t(20)/180,190,200,210/
      do  9  k=1,20
      if  (i1.le.i(k))       then
      goto   3
      endif
 9        continue
 3        tb=t(k)+(i1-i(k))/(i(k)-i(k-1))*(t(k)-t(k-1))
*     write(*,*)'i1==',i1,'                tb==',tb
      return
      end

      subroutine     prop(tfi,c,cigma,u,Pr,k,rof,rog)
      dimension    b(28),z(28),d(28),pn(28),f(28),r(28),q(28)
      real   t(28),k
      data   t(1),t(2),t(3),t(4),t(5),t(6)/20,30,40,50,60,70/
      data   t(7),t(8),t(9),t(10),t(11)/80,90,100,110,120/
      data   t(12),t(13),t(14),t(15)/130,140,150,160/
      data   t(16),t(17),t(18),t(19)/170,180,190,200/
      data   t(20),t(21),t(22),t(23),t(24)/210,220,230,240,250/
      data   t(25),t(26),t(27),t(28)/260,270,280,290/
      data   b(1),b(2),b(3),b(4)/4182.,4179.,4179.,4181./
      data   b(5),b(6),b(7),b(8)/4185.,4191.,4198.,4207./
      data   b(9),b(10),b(11),b(12)/4218.,4230.,4244.,4262./
      data   b(13),b(14),b(15),b(16)/4282.,4306.,4334.,4366./
      data   b(17),b(18),b(19),b(20)/4403.,4446.,4494.,4550./
      data   b(21),b(22),b(23),b(24)/4613.,4685.,4769.,4866./
      data   b(25),b(26),b(27),b(28)/4985.,5134.,5307.,5520./
      data   z(1),z(2),z(3),z(4)/72.78,71.23,69.61,67.93/
      data   z(5),z(6),z(7),z(8)/66.19,64.40,62.57,60.69/
      data   z(9),z(10),z(11),z(12)/58.78,56.83,54.85,52.83/
      data   z(13),z(14),z(15),z(16)/50.79,48.70,46.59,44.44/
      data   z(17),z(18),z(19),z(20)/42.26,40.05,37.81,35.53/
      data   z(21),z(22),z(23),z(24)/33.23,30.90,28.56,26.19/
      data   z(25),z(26),z(27),z(28)/23.82,21.44,19.07,16.71/
      data   d(1),d(2),d(3),d(4)/1002.,798.3,653.9,547.8/
      data   d(5),d(6),d(7),d(8)/467.3,404.8,355.4,315.6/
      data   d(9),d(10),d(11),d(12)/283.1,254.8,231.0,210.9/
      data   d(13),d(14),d(15),d(16)/194.1,179.8,167.7,157.4/
      data   d(17),d(18),d(19),d(20)/148.5,140.7,133.9,127.9/
      data   d(21),d(22),d(23),d(24)/122.4,117.5,112.9,108.7/
      data   d(25),d(26),d(27),d(28)/104.8,101.1,97.5,94.1/
      data   pn(1),pn(2),pn(3),pn(4),pn(5)/6.9,5.4,4.3,3.5,3./
      data   pn(6),pn(7),pn(8),pn(9),pn(10)/2.5,2.2,1.9,1.7,1.5/
      data   pn(11),pn(12),pn(13),pn(14),pn(15)/1.4,1.3,1.2,1.1,1./
      data   pn(16),pn(17),pn(18),pn(19),pn(20)/1.,.96,.93,.91,.89/
      data   pn(21),pn(22),pn(23),pn(24)/.87,.86,.85,.859/
      data   pn(25),pn(26),pn(27),pn(28)/.866,.882,.902,.932/
      data   f(1),f(2),f(3),f(4),f(5)/.603,.618,.631,.643,.653/
      data   f(6),f(7),f(8),f(9),f(10)/.662,.67,.676,.681,.684/
      data   f(11),f(12),f(13),f(14),f(15)/.687,.688,.688,.687,.684/
      data   f(16),f(17),f(18),f(19),f(20)/.681,.677,.671,.664,.657/
      data   f(21),f(22),f(23),f(24)/.648,.639,.628 .616/
      data   f(25),f(26),f(27),f(28)/.603,.589,.574,.558/
      data   r(1),r(2),r(3),r(4),r(5)/998.2,995.6,992.1,988.1,983.3/
      data   r(6),r(7),r(8),r(9),r(10)/978.5,971.8,966.2,958.8,951.5/
      data   r(11),r(12),r(13),r(14),r(15)/943.,935.,926.,917.,907./
```

```
      data   r(16),r(17),r(18),r(19),r(20)/897.,887.,876.,865.,853./
      data   r(21),r(22),r(23),r(24)/840.,827.,813.,799./
      data   r(25),r(26),r(27),r(28)/784.,767.8,750.7,732.3/
      data   q(1),q(2),q(3),q(4),q(5)/.017,.03,.051,.083,.13/
      data   q(6),q(7),q(8),q(9),q(10)/.198,.29,.42,.598,.826/
      data   q(11),q(12),q(13),q(14),q(15)/1.12,1.5,1.97,2.5,3.3/
      data   q(16),q(17),q(18),q(19),q(20)/4.1,5.2,6.4,7.87,9.6/
      data   q(21),q(22),q(23),q(24)/11.63,14.08,16.95,20.0/
      data   q(25),q(26),q(27),q(28)/23.73,28.09,33.18,39.16/
      do  7  k1=1,24
      if  (tfi.le.t(k1))       then
      goto   6
      endif
7        continue
6          c=b(k1)+(tfi-t(k1))/(t(k1)-t(k1-1))*(b(k1)-b(k1-1))
      cigma=z(k1)+(tfi-t(k1))/(t(k1)-t(k1-1))*(z(k1)-z(k1-1))
      u=d(k1)+(tfi-t(k1))/(t(k1)-t(k1-1))*(d(k1)-d(k1-1))
      Pr=pn(k1)+(tfi-t(k1))/(t(k1)-t(k1-1))*(pn(k1)-pn(k1-1))
      k=f(k1)+(tfi-t(k1))/(t(k1)-t(k1-1))*(f(k1)-f(k1-1))
      rof=r(k1)+(tfi-t(k1))/(t(k1)-t(k1-1))*(r(k1)-r(k1-1))
      rog=q(k1)+(tfi-t(k1))/(t(k1)-t(k1-1))*(q(k1)-q(k1-1))
      cigma=cigma*0.001
      u=u*0.000001
*     write(*,*)'c=',c,'              cigma=',cigma,'              u=',u
*     write(*,*)'pr=',pr,'            k=',k,'         rof=',rof,'         rog=',rog
      return
      end


      subroutine     propw(ts,uw)
      dimension     w(28),s(28)
      data   w(1),w(2),w(3),w(4)/20.,30.,40.,50./
      data   w(5),w(6),w(7),w(8)/60.,70.,80.,90./
      data   w(9),w(10),w(11),w(12)/100.,110.,120.,130./
      data   w(13),w(14),w(15),w(16)/140.,150.,160.,170./
      data   w(17),w(18),w(19),w(20)/180.,190.,200.,210./
      data   w(21),w(22),w(23),w(24)/220.,230.,240.,250./
      data   w(25),w(26),w(27),w(28)/260.,270.,280.,290./
      data   s(1),s(2),s(3),s(4)/1002.,798.3,653.9,547.8/
      data   s(5),s(6),s(7),s(8)/467.3,404.8,355.4,315.6/
      data   s(9),s(10),s(11),s(12)/283.1,254.8,231.,210.9/
      data   s(13),s(14),s(15),s(16)/194.1,179.8,167.7,157.4/
      data   s(17),s(18),s(19),s(20)/148.5,140.7,133.9,127.9/
      data   s(21),s(22),s(23),s(24)/122.4,117.5,112.9,108.7/
      data   s(25),s(26),s(27),s(28)/104.8,101.1,97.5,94.1/


      do  3  m=1,28
      if  (ts.le.w(m))       then
      goto   4
      endif
3     continue
4     uw=s(m)+(ts-w(m))/(w(m)-w(m-1))*(s(m)-s(m-1))
      uw=uw*0.000001
      return
      end

      subroutine     propb(ts,ub)
      dimension     w(28),s(28)
      data   w(1),w(2),w(3),w(4)/20.,30.,40.,50./
      data   w(5),w(6),w(7),w(8)/60.,70.,80.,90./
      data   w(9),w(10),w(11),w(12)/100.,110.,120.,130./
```

```
      data   w(13),w(14),w(15),w(16)/140.,150.,160.,170./
      data   w(17),w(18),w(19),w(20)/180.,190.,200.,210./
      data   w(21),w(22),w(23),w(24)/220.,230.,240.,250./
      data   w(25),w(26),w(27),w(28)/260.,270.,280.,290./
      data   s(1),s(2),s(3),s(4)/1002.,798.3,653.9,547.8/
      data   s(5),s(6),s(7),s(8)/467.3,404.8,355.4,315.6/
      data   s(9),s(10),s(11),s(12)/283.1,254.8,231.,210.9/
      data   s(13),s(14),s(15),s(16)/194.1,179.8,167.7,157.4/
      data   s(17),s(18),s(19),s(20)/148.5,140.7,133.9,127.9/
      data   s(21),s(22),s(23),s(24)/122.4,117.5,112.9,108.7/
      data   s(25),s(26),s(27),s(28)/104.8,101.1,97.5,94.1/


      do  3  m=1,28
      if  (ts.le.w(m))      then
      goto   4
      endif
3     continue
4     ub=s(m)+(ts-w(m))/(w(m)-w(m-1))*(s(m)-s(m-1))
      ub=ub*0.000001
      return
      end
```

APPENDIX A.3-2

List of program for calculating the heat transfer results for "Modified" Model.

```
      real   m,n,htp,hlo,htpc1,htpn1,htpc,htpn,htpp,htpf,HHPP,izf
      real   k,il148,i129,i148,kg,l,pz,iz,i1,Nu
      open(9,file='a:qvstwd.dat',status='new')
      open(26,file='a:mx0753.dat',status='new')
      open(2,file='a:inp02.dat',status='old')
      open(4,file='a:ineti.dat',status='old')
      open(5,file='a:datanz.dat',status='old')
      open(6,file='a:predict.dat',status='new')
      read   (4,*)Tsat1,      il148,    i148,    p
      c=4525.
      u=0.0001309
      ug=0.00001582
      k=.665
      kg=0.03812
      pr=0.9
      il148=il148*1000.
      i148=i148*1000.
      i129=83.86*1000.
      cigma=38.80*.001
      d=0.30*.01
      L=d*96.6
      read(2,*)n1
c     n1=2
      do  55  j=1,n1
      read(2,*)g,z
      g=g*1000.
      as=3.14*d*z
      ac=3.14*(d**2)/4.
      q2=g*(il148-i129)*ac/(3.14*d*l)
      rog=8.312
      rol=998.2

      read(2,*)delto,qonb
      read(2,*)delte,qe
      qonb=qonb*1000.
      qe=qe*1000.
      Read(5,*)IA
      write(9,*)IA
      write(6,*)IA
      Do  1000   INEW=   1,  IA
      Read(5,*)QQ2,HHDATA
      q=QQ2*q2
      dq=qonb/11.
*     q=dq
      do  2  i=1,1
*     write(*,*)'q=',q,'              q2=',q2
*     call   prs(g,q,z,pz)
*     call   drop(Pz,Tsat1,i148,il148)
      if(q   .ge.   qonb)   then
      go  to  160
      endif
      iz=(i129+(q*as)/(g*ac))/1000.
      iss=1
```

```
      call   bulk(iz,tb)
      Tw1=250.
42    Tf1=0.50*(Tw1-Tb)+Tb
      call   prop(tf1,c,cigma,u,pr,k,rof,rog)
      call   propb(tb,ub)
      call   propw(tw1,uw)
      Re=g*d/u
      f=1.0/((1.82*alog10(Re)-1.64)**2.)
      c1=1.+3.4*f
      c2=11.7+1.8/(Pr**0.333)
      o=c1+c2*((Pr**0.67)-1.)*((f/8.)**0.5)
      hlo1=(Re*Pr/o)*(f/8.)*k/d*((ub/uw)**0.00)
      hlo=0.023*(Re**0.8)*(Pr**0.4)*k/d
      Tw=20.+q*((4.*z)/(g*c*d)+1./hlo1)
      if  (abs(Tw-Tw1).gt.0.10)          then
      Tw1=Tw
*     write(*,*)'Re=',Re
      goto   42
      endif
      if  (tw.ge.tsat1)       then
      goto   160
      endif
      Tf=0.50*(Tw-Tb)+Tb
      call   prop(tf,c,cigma,u,pr,k,rof,rog)
      call   propb(tb,ub)
      call   propw(tw,uw)
*     call   film(tf,i148,ii148)
      hlo=0.023*(Re**0.8)*(pr**0.4)*k/d
      hlo1=(Re*Pr/o)*(f/8.0)*k/d*((ub/uw)**0.00)
      x=(as*q/(g*ac)-ii148+i129)/i148
      delts1=q/hlo1+x*i148/c
      Twall1=delts1+Tsat1
      Pe=Re*Pr
      Nu=hlo1*d/k
      St=Nu/Pe
      Twp=Twall1
      HHPP=hlo1/1000.
*     write(9,*)Pe/100000,St
      write(26,*)q/q2,hlo1/1000.
      IF  (HLO.LE.0.0)      THEN
      WRITE(*,*)'     HLO==',HLO
      ENDIF
*     q=q+dq
2     continue
      write(*,*)'     END   OF   THE   FIRST    PART'
      dq=(qe-qonb)/10.
*     q=q+dq
      GO  TO  101
160   if(q   .ge.   qe)   then
      go  to  170
      endif
      iss=2
      do    10  i=1,1
      tfonb=0.5*(tsat1+tb)
      twonb=delto+tsat1
      call   prop(tfonb,c,cigma,u,pr,k,rof,rog)
      call   propb(tb,ub)
      call   propw(tw1,uw)
      Re=g*d/u
      f=1.0/((1.82*alog10(Re)-1.64)**2.)
      c1=1.+3.4*f
      c2=11.7+1.8/(Pr**0.333)
```

```
      o=c1+c2*((Pr**0.67)-1.)*(f/8.)**0.5)
      hlo1=(Re*Pr/o)*(f/8.)*k  *((ub/uw)**0.00)
      twonb=tsat1+delto
      a=hlo1*(tsat1-tb)
      if  ((q-a).le.0.)       then
      goto   101
      endif
      izf=(i129+(qe*as)/(g*ac))/1000.
      call   bulk(izf,tbf)
      twfdb=tsat1+delte
      tffdb=0.5*(twfdb+tbf)
      call   prop(tffdb,c,cigma,u,pr,k,rof,rog)
      Re=g*d/u
      f=1.0/((1.82*alog10(Re)-  1.)
      c1=1.+3.4*f
      c2=11.7+1.8/(Pr**0.333)
      o=c1+c2*((Pr**0.67)-1.)*(f/8.)**0.5)
      hlfdb=(Re*Pr/o)*(f/8.)*k/d*((ub/uw)**0.00)
      x=(as*qe/(g*ac)-il148+i129)/i148
      xstar=qe*c/(hlfdb*i148)
      Bof=qe/(g*i148)
      if  (bof.le.0.00003)        then
        fbo=1.+46.*(bof**0.5)
      else
        fbo=230.*(bof**0.5)
      endif
      if  (bof.le.0.00003)        then
        gbo=23.*(bof**0.5)/qe
      else
        gbo=115.*(bof**0.5)/qe
      endif
      sh=1./fbo+x/xstar
      ee=(hlfdb/sh)/((1.-(hlfdb*(twfdb-tbf)*gbo)/((sh*fbo)**2.)))
      m=(ee*delte)/(qe-a)
      b=(qe-a)/((delte**m))
      write(*,*)'m=',m,'            sh=',sh
      write(*,*)'q=',q,'         a=',a,'       b=',b
      m=1./m
      delt=((q-a)/b)**m
*     call   prs(g,q,z,pz)
*     call   drop(Pz,Tsat1,i148,il148)
      iz=(i129+(q*as)/(g*ac))/1000.
      call   bulk(iz,tb)
      Tw2=250.
 43   Tf2=0.50*(Tw2-Tb)+Tb
      call   prop(tf2,c,cigma,u,pr,k,rof,rog)
      Re=g*d/u
      x=(as*q/(g*ac)-il148+i129)/i148
      http=q/(delt-x*i148/c)
      Tw=20.+q*((4.*z)/(g*c*d)+1./http)
      if  (abs(Tw2-Tw).gt.0.10)         then
      Tw2=Tw
      goto   43
      endif
*     write(*,*)'Tww=',tw

      tw=delt+tsat1
      Tf=0.50*(Tw-Tb)+Tb
*     write(*,*)'     Tf=',Tf,'       TWW=',tw
      call   prop(tf,c,cigma,u,pr,k,rof,rog)
*     call   film(tf,i148,il148)
      x=(as*q/(g*ac)-il148+i129)/i148
```

```
      Twall=delt+Tsat1
      htpp=q/(delt-x*i148/c)
      Re=g*d/u
      Nu=htpp*d/k
      Pe=Pr*Re
      St=Nu/Pe
*     write(9,*)Pe/100000.,St
      write(26,*)q/q2,htpp/1000.
      Twp=Twall
      HHPP=htpp/1000.
*     q=q+dq
10    continue
      write(*,*)'     END  OF  THE  SECOND   PART'
*     q=qe
      qlmt=q2*0.8
*     do  15  i=1,1
*     q=q+dq
*     call   prs(g,q,z,pz)
*     call   drop(Pz,Tsat1,i148,ii148)
      GO  TO  101
170   iss=3
      iz=(i129+(q*as)/(g*ac))/1000.
      call   bulk(iz,tb)
      Tw3=250.
 44   Tf3=0.50*(Tw3-Tb)+Tb
      call   prop(tf3,c,cigma,u,pr,k,rof,rog)
      call   propb(tb,ub)
      call   propw(tw3,uw)
      Re=g*d/u
      f=1.0/((1.82*alog10(Re)-1.64)**2.)
      c1=1.+3.4*f
      c2=11.7+1.8/(Pr**0.333)
      o=c1+c2*((Pr**0.67)-1.0)*((f/8.0)**0.5)
      hlo=(Re*Pr/o)*(f/8.0)*k/d*((ub/uw)**0.00)
      Twsp=20.+q*((4.*z)/(g*d*c)+1.0/hlo)
      if  (abs(Tw3-Twsp).gt.0.10)          then
      Tw3=Twsp
      goto   44
      endif

      x=(as*q/(g*ac)-ii148+i129)/i148
      xstar=-q*c/(hlo*i148)
      Bo=q/(g*i148)
      if  (bo.le.0.00003)        then
        fbo=1.+46.*(bo**0.5)
      else
        fbo=230.*(bo**0.5)
      endif
      htpf=hlo/(1./fbo+x/xstar)
      hlo1=0.023*(Re**0.8)*(pr**0.4)*k/d
      Tw=20.+q*((4.*z)/(g*d*c)+1./htpf)
*     if  (abs(Tw-Tw3).gt.0.10)          then
*     Tw3=Tw
*     goto   44
*     endif
 45   Tf=0.50*(Tw-Tb)+Tb
      call   prop(tf,c,cigma,u,pr,k,rof,rog)
*     call   film(tf,i148,ii148)
      x=(as*q/(g*ac)-ii148+i129)/i148
*     if  (q.ge.qlmt)      then
*      goto   11
*     endif
```

```
      Bo=q/(g*i148)
      if  (Bo.LE.    0.00003)    then
        fbo=1.+46.*(Bo**0.5)
      else
        fbo=230.*(Bo**0.5)
      endif
      Re=g*d/u
      xstar=-q*c/(hlo*i148)
      delt2=q*(1./fbo+x/xstar)/hlo+x*i148/c
      Twall2=delt2+Tsat1
      if(abs(Twall2-Tw).gt.0.10)           then
      Tw=Twall2
      goto   45
      endif

      htpf=hlo/(1/fbo+x/xstar)
      Nu=htpf*d/k
      Pe=Re*Pr
      St=Nu/Pe
*     write(9,*)Pe/100000.,St
*15   write(*,*)
 15   write(26,*)q/q2,htpf/1000.
      Twp=Twall2
      HHPP=htpf/1000.
11    write(*,*)
 101  CONTINUE
      WRITE(*,*)'END       OF   THE   THIRD    PART'
      Write(6,*)QQ2,HHPP
      Twd=tb+(q/(1000.*HHDATA))
      write(9,*)Twp,q/1000000.,Twd
1000  continue
 55   CONTINUE
      write(*,*)     '  HERE   YOU   GO   !!!'
      stop
      end

      subroutine     prs(g,q,z,pz)
      real   i148,il148,l,hlo,k
      c=4525.0
      d=0.30*0.01
      k=.665
      rof=861.08
      rog=8.312
      cigma=38.80*0.001
      i148=1928.51*1000.
      u=0.0001309
      Pr=0.9
      Re=g*d/u
      delt=(8*cigma*q*(203.+273.15)/(i148*k*rog))**.5*pr
      hlo=.023*(Re**0.8)*(pr**0.4)*k/d
      z1=g*c*d/4.*((183.+delt)/q-1./hlo)
      z2=g*c*d/4.*(1/hlo-delt/q)
      L=d*96.6
      Pexit=1.66
      c1=0.97
      c2=0.28
      c3=6.13/z2
      c4=6.13*z1/z2
      dPfo=3.72822*0.001*((g/1000.)**1.85)
      dPscb=dPfo*(c1*(1-z)+c2/c3*(exp(c3*(1-z)-c4)))
      Pz=Pexit+dPscb
      write(*,*)'dpfo=',dpfo,'            dpscb=',dpscb
```

```
      return
      end

      subroutine     film(t1,i148,ii148)
      dimension     t(17)
      real   i(17),ii(17),i148,ii148
      integer    j
      data   t(1),t(2),t(3),t(4)/50.,60.,70.,80./
      data   t(5),t(6),t(7),t(8)/90.,100.,110.,120./
      data   t(9),t(10),t(11),t(12)/130.,140.,150.,160./
      data   t(13),t(14),t(15),t(16),t(17)/170.,180.,190.,200.,210./
      data   i(1),i(2),i(3),i(4)/2382.7,2357.9,2333.,2308.1/
      data   i(5),i(6),i(7),i(8)/2283.1,2256.9,2229.7,2202.3/
      data   i(9),i(10),i(11),i(12)/2173.7,2144.9,2114.8,2082.5/
      data   i(13),i(14),i(15),i(16)/2049.9,2014.9,1978.5,1940.6/
      data   i(17)/1900.3/
      data   ii(1),ii(2),ii(3),ii(4)/209.3,251.1,293.,334.9/
      data   ii(5),ii(6),ii(7),ii(8)/376.9,419.1,461.3,503.7/
      data   ii(9),ii(10),ii(11),ii(12)/546.3,589.1,632.2,675.5/
      data   ii(13),ii(14),ii(15),ii(16)/719.1,763.1,807.5,852.4/
      data   ii(17)/897.7/
      do  5  k=1,17
      if  (t1.le.t(k))      then
       goto   4
       endif
 5     continue
 4       i148=i(k)+(t1-t(k))/(t(k)-t(k-1))*(i(k)-i(k-1))
         ii148=ii(k)+(t1-t(k))/(t(k)-t(k-1))*(ii(k)-ii(k-1))
      i148=i148*1000.
      ii148=ii148*1000.
      return
      end


      subroutine     bulk(i1,tb)
      real   i1,i(20),t(20)
      integer    j
      data   i(1),i(2),i(3),i(4)/83.86,125.66,167.47,209.3/
      data   i(5),i(6),i(7),i(8)/251.1,293.,334.9,376.9/
      data   i(9),i(10),i(11),i(12)/419.,461.,503.7,546./
      data   i(13),i(14),i(15),i(16)/589.3,632.2,675.5,719.1/
      data   i(17),i(18),i(19),i(20)/763.1,807.5,852.4,897.7/
      data   t(1),t(2),t(3),t(4),t(5),t(6)/20,30,40,50,60,70/
      data   t(7),t(8),t(9),t(10),t(11)/80,90,100,110,120/
      data   t(12),t(13),t(14),t(15),t(16)/130,140,150,160,170/
      data   t(17),t(18),t(19),t(20)/180,190,200,210/
      do  9  k=1,20
      if  (i1.le.i(k))       then
      goto   3
      endif
 9        continue
 3        tb=t(k)+(i1-i(k))/(i(k)-i(k-1))*(t(k)-t(k-1))
*     write(*,*)'i1==',i1,'                tb==',tb
      return
      end

      subroutine     prop(tfi,c,cigma,u,Pr,k,rof,rog)
      dimension     b(28),z(28),d(28),pn(28),f(28),r(28),q(28)
      real   t(28),k
      data   t(1),t(2),t(3),t(4),t(5),t(6)/20,30,40,50,60,70/
      data   t(7),t(8),t(9),t(10),t(11)/80,90,100,110,120/
      data   t(12),t(13),t(14),t(15)/130,140,150,160/
```

```
      data   t(16),t(17),t(18),t(19)/170,180,190,200/
      data   t(20),t(21),t(22),t(23),t(24)/210,220,230,240,250/
      data   t(25),t(26),t(27),t(28)/260,270,280,290/
      data   b(1),b(2),b(3),b(4)/4182.,4179.,4179.,4181./
      data   b(5),b(6),b(7),b(8)/4185.,4191.,4198.,4207./
      data   b(9),b(10),b(11),b(12)/4218.,4230.,4244.,4262./
      data   b(13),b(14),b(15),b(16)/4282.,4306.,4334.,4366./
      data   b(17),b(18),b(19),b(20)/4403.,4446.,4494.,4550./
      data   b(21),b(22),b(23),b(24)/4613.,4685.,4769.,4866./
      data   b(25),b(26),b(27),b(28)/4985.,5134.,5307.,5520./
      data   z(1),z(2),z(3),z(4)/72.78,71.23,69.61,67.93/
      data   z(5),z(6),z(7),z(8)/66.19,64.40,62.57,60.69/
      data   z(9),z(10),z(11),z(12)/58.78,56.83,54.85,52.83/
      data   z(13),z(14),z(15),z(16)/50.79,48.70,46.59,44.44/
      data   z(17),z(18),z(19),z(20)/42.26,40.05,37.81,35.53/
      data   z(21),z(22),z(23),z(24)/33.23,30.90,28.56,26.19/
      data   z(25),z(26),z(27),z(28)/23.82,21.44,19.07,16.71/
      data   d(1),d(2),d(3),d(4)/1002.,798.3,653.9,547.8/
      data   d(5),d(6),d(7),d(8)/467.3,404.8,355.4,315.6/
      data   d(9),d(10),d(11),d(12)/283.1,254.8,231.0,210.9/
      data   d(13),d(14),d(15),d(16)/194.1,179.8,167.7,157.4/
      data   d(17),d(18),d(19),d(20)/148.5,140.7,133.9,127.9/
      data   d(21),d(22),d(23),d(24)/122.4,117.5,112.9,108.7/
      data   d(25),d(26),d(27),d(28)/104.8,101.1,97.5,94.1/
      data   pn(1),pn(2),pn(3),pn(4),pn(5)/6.9,5.4,4.3,3.5,3./
      data   pn(6),pn(7),pn(8),pn(9),pn(10)/2.5,2.2,1.9,1.7,1.5/
      data   pn(11),pn(12),pn(13),pn(14),pn(15)/1.4,1.3,1.2,1.1,1./
      data   pn(16),pn(17),pn(18),pn(19),pn(20)/1.,.96,.93,.91,.89/
      data   pn(21),pn(22),pn(23),pn(24)/.87,.86,.85,.859/
      data   pn(25),pn(26),pn(27),pn(28)/.866,.882,.902,.932/
      data   f(1),f(2),f(3),f(4),f(5)/.603,.618,.631,.643,.653/
      data   f(6),f(7),f(8),f(9),f(10)/.662,.67,.676,.681,.684/
      data   f(11),f(12),f(13),f(14),f(15)/.687,.688,.688,.687,.684/
      data   f(16),f(17),f(18),f(19),f(20)/.681,.677,.671,.664,.657/
      data   f(21),f(22),f(23),f(24)/.648,.639,.628,.616/
      da     (25),f(26),f(27),f(28)/.603,.589,.574,.558/
      da     ,r(2),r(3),r(4),r(5)/998.2,995.6,992.1,988.1,983.3/
      data   r(  ,r(7),r(8),r(9),r(10)/978.5,971.8,966.2,958.8,951.5/
      data   r(11),r(12),r(13),r(14),r(15)/943.,935.,926.,917.,907./
      data   r(16),r(17),r(18),r(19),r(20)/897.,887.,876.,865.,853./
      data   r(21),r(22),r(23),r(24)/840.,827.,813.,799./
      data   r(25),r(26),r(27),r(28)/784.,767.8,750.7,732.3/
      data   q(1),q(2),q(3),q(4),q(5)/.017,.03,.051,.083,.13/
      data   q(6),q(7),q(8),q(9),q(10)/.198,.29,.42,.598,.826/
      data   q(11),q(12),q(13),q(14),q(15)/1.12,1.5,1.97,2.5,3.3/
      data   q(16),q(17),q(18),q(19),q(20)/4.1,5.2,6.4,7.87,9.6/
      data   q(21),q(22),q(23),q(24)/11.63,14.08,16.95,20.0/
      data   q(25),q(26),q(27),q(28)/23.73,28.09,33.18,39.16/
      do  7  k1=1,24
      if  (tfi.le.t(k1))       then
      goto   6
      endif
7        continue
6           c=b(k1)+(tfi-t(k1))/(t(k1)-t(k1-1))*(b(k1)-b(k1-1))
      cigms=z(k1)+(tfi-t(k1))/(t(k1)-t(k1-1))*(z(k1)-z(k1-1))
      u=d(k1)+(tfi-t(k1))/(t(k1)-t(k1-1))*(d(k1)-d(k1-1))
      Pr=pn(k1)+(tfi-t(k1))/(t(k1)-t(k1-1))*(pn(k1)-pn(k1-1))
      k=f(k1)+(tfi-t(k1))/(t(k1)-t(k1-1))*(f(k1)-f(k1-1))
      rof=r(k1)+(tfi-t(k1))/(t(k1)-t(k1-1))*(r(k1)-r(k1-1))
      rog=q(k1)+(tfi-t(k1))/(t(k1)-t(k1-1))*(q(k1)-q(k1-1))
      cigma=cigma*0.001
      u=u*0.000001
```

```
*       write(*,*)'c=',c,'              cigma=',cigma,'              u=',u
*       write(*,*)'pr=',pr,'            k=',k,'         rof=',rof,'         rog=',rog
        return
        end


        subroutine      propw(ts,uw)
        dimension     w(28),s(28)
        data   w(1),w(2),w(3),w(4)/20.,30.,40.,50./
        data   w(5),w(6),w(7),w(8)/60.,70.,80.,90./
        data   w(9),w(10),w(11),w(12)/100. 110.,120.,130./
        data   w(13),w(14),w(15),w(16)/140.,150.,160.,170./
        data   w(17),w(18),w(19),w(20)/180.,190.,200.,210./
        data   w(21),w(22),w(23),w(24)/220.,230.,240.,250./
        data   w(25),w(26),w(27),w(28)/260.,270.,280.,290./
        data   s(1),s(2),s(3),s(4)/1002.,798.3,653.9,547.8/
        data   s(5),s(6),s(7),s(8)/467.3,404.8,355.4,315.6/
        data   s(9),s(10),s(11),s(12)/283.1,254.8,231.,210.9/
        data   s(13),s(14),s(15),s(16)/194.1,179.8,167.7,157.4/
        data   s(17),s(18),s(19),s(20)/148.5,140.7,133.9,127.9/
        data   s(21),s(22),s(23),s(24)/122.4,117.5,112.9,108.7/
        data   s(25),s(26),s(27),s(28)/104.8,101.1,97.5,94.1/


        do  3  m=1,28
        if  (ts.le.w(m))      then
        goto   4
        endif
3       continue
4       uw=s(m)+(ts-w(m))/(w(m)-w(m-1))*(s(m)-s(m-1))
        uw=uw*0.000001
        return
        end

        subroutine      propb(ts,ub)
        dimension     w(28),s(28)
        data   w(1),w(2),w(3),w(4)/20.,30.,40.,50./
        data   w(5),w(6),w(7),w(8)/60.,70.,80.,90./
        data   w(9),w(10),w(11),w(12)/100.,110.,120.,130./
        data   w(13),w(14),w(15),w(16)/140.,150.,160.,170./
        data   w(17),w(18),w(19),w(20)/180.,190.,200.,210./
        data   w(21),w(22),w(23),w(24)/220.,230.,240.,250./
        data   w(25),w(26),w(27),w(28)/260.,270.,280.,290./
        data   s(1),s(2),s(3),s(4)/1002.,798.3,653.9,547.8/
        data   s(5),s(6),s(7),s(8)/467.3,404.8,355.4,315.6/
        data   s(9),s(10),s(11),s(12)/283.1,254.8,231.,210.9/
        data   s(13),s(14),s(15),s(16)/194.1,179.8,167.7,157.4/
        data   s(17),s(18),s(19),s(20)/148.5,140.7,133.9,127.9/
        data   s(21),s(22),s(23),s(24)/122.4,117.5,112.9,108.7/
        data   s(25),s(26),s(27),s(28)/104.8,101.1,97.5,94.1/


        do  3  m=1,28
        if  (ts.le.w(m))      then
        goto   4
        endif
3       continue
4       ub=s(m)+(ts-w(m))/(w(m)-w(m-1))*(s(m)-s(m-1))
        ub=ub*0.000001
        return
        end
```

APPENDIX A.4

FREON-11 MODEL INSTRUCTION:

(1) Prepare the input data file: INP01.DAT in format of:

n

$G1$,$Z(i)$

$G2$,$Z(i)$

.....

.....

Gn, $Z(i)$

Where n in the number of flowrate $Z(i)$ is the location in unit of m, $G1, G2, \cdots Gn$ are the flowrates in unit of Mg/m^2S. In order to run Freon-11 model for the different locations, one needs to chang $Z(i)$ to the desired values.

(2) Run program listed in Appendix A.1

As the result of F11A.FOR, the single phase boiling data will be in file MEN07.DAT, FDB data will be in MENO6.DAT, and ONB data will be in MEN05.DAT. Note that these three data files are used for finding the computed values of heat flux and superheat at ONB and FDB. As the output files of F11A.FOR, they are also the input data files for F11B.FOR.

(3) Run program listed in Appendix A.2

The output data file of F11B.FOR is called INP02.DAT in format of:

n

$G1$,$Z(i)$

$\Delta T_{SAT,ONB,1}$, $q_{ONB,1}$

$\Delta T_{SAT,FDB,1}$, $q_{FDB,1}$

$G2$, $Z(i)$

$\Delta T_{SAT,ONB,2}$, $q_{ONB,2}$

$\Delta T_{SAT,FDB,2}$, $q_{FDB,2}$

.....

.....

Gn, $Z(i)$

$\Delta T_{SAT,ONB,n}$, $q_{ONB,n}$

$\Delta T_{SAT,FDB,n}$, $q_{FDB,n}$

The data file INP02.DAT will be the input file for F11C.FOR.

(4) Run program listed in Appendix A.3-1 or 3-2

This program requires an additional disk in drive B. The final results will be installed into drive B named as MX075P.DAT and MEN08P.DAT respectively. The MX075P.DAT and MEN08P.DAT present the relations between the local heat transfer coefficient to the ratio of het power generation and Stanton number to Peclet number respectively for location $Z(i)$ and given flowrates.

APPENDIX B.1

List of program INSU.FOR and COPP.FOR for Freon-11 data reduction in Domain I and Domain II.

(a) Domain I Computer Program:

```
* *       PROGRAM    FOR  INSULATION     CALCULATION
        REAL   K,I2,IIN,A,A1,A2,hinf,hr,hin(30),LEN
        DIMENSION     RR(45),TS(30),Tf(30),hrr(30),QLO(30)
        DIMENSION     TSS(30),ANG(30)
        DOUBLE    PRECISION     DT(30,30),DTT(30,30),DR(30,30)
        DOUBLE    PRECISION     DRC(30,30)
           OPEN(1,FILE='A:INS1.DAT',STATUS='OLD')
          OPEN(2,FILE='A:INS2.DAT',STATUS='OLD')
          OPEN(3,FILE='A:AS11.DAT',STATUS='NEW')
        OPEN(4,FILE='A:ANSH.DAT',STATUS='NEW')
          OPEN(5,FILE='A:INC1.DAT',STATUS='NEW')
          OPEN(6,FILE='A:POLE.DAT',STATUS='OLD')
          OPEN(7,FILE='A:TOLE.DAT',STATUS='NEW')
        WRITE(*,*)'INPUT       NUMBER    OF  MESHES    IN  RADIAL    DIRECTION     '
        READ(*,*)M
        WRITE(*,*)'INPUT       NUMBER    OF  MESHES    IN  CIRCU.    DIRECTION     '
        READ(*,*)N
        WRITE(*,*)'INPUT       THE   ACCURACY,     E'
        READ(*,*)     E
        READ(6,*)LLL
        WRITE(7,*)M,N,E,LLL
        READ(2,*)R1,R2,K,LEN
        DO  101   MM=1,5
        DO  100   II=1,LLL
        READ(1,*)Q,Tin,Tinf,Z
        READ(1,*)(TSS(I),         I=1,4)
        Q=Q*(LEN/1.2192)
*       WRITE(*,*)'Q=',Q,'          Tinf   =  ',Tinf
*       WRITE(*,*)('TS(I)=',TS(I),           I=1,5)
*       WRITE(*,*)'II=',II
        IT=0

        N1=N+1
        M1=M+1
        Drr=(R2-R1)/M
        PHI=3.1416/N
        D=R2*2.
        RR(1)=R1*100.
        RR(M1)=R2*100.

        DO  44  J=1,N1
        ANG(J)=180*(J-1)/N
        IF  (ANG(J).LE.45)       THEN
        TS(J)=TSS(1)+((ANG(J)-0)/(45-0))*(TSS(2)-TSS(1))
        ENDIF
        IF  (ANG(J).GT.45)       THEN
        TS(J)=TSS(2)+((ANG(J)-45)/(135-45))*(TSS(3)-TSS(2))
        ENDIF
        IF  (ANG(J).GT.135)       THEN
        TS(J)=TSS(3)+((ANG(J)-135)/(180-135))*(TSS(4)-TSS(3))
        ENDIF
 44     CONTINUE
```

```
      DO  5  I=1,M1
      DO  8  J=1,N1
      DT(I,J)=1.1*Tinf
      DT(1,J)=TS(J)
      DTT(1,J)=TS(J)
8        CONTINUE
5        CONTINUE

      WRITE(4,*)
      WRITE(4,*)
      WRITE(4,*)'       INPUT     CHECK   LIST     FOR    INSULATION       PROGRAM'
      WRITE(4,*)
      WRITE(4,*)
      WRITE(4,*)'       OUTSIDE     INSULATION      RADIUS    (R2):    ',R2,'    m'
      WRITE(4,*)'       INSIDE    INSULATION      RADIUS    (R1):    ',R1,'    m'
      WRITE(4,*)'       CONDUCTIVITY      OF  INSULATION      (K):',K,'     W/mK'
      WRITE(4,*)
      WRITE(4,*)'       AMBIENT     TEMPERATURE      (Tinf):     ',Tinf,'     K'
      WRITE(4,*)'       POWER    SUPPLIED     TO  TEST   SECTION     (Q):   ',Q,'    W'
      WRITE(4,*)'       MEASURED     INSIDE    INSULATION     TEMP.    (T(1,J))     (K):'
      WRITE(4,*)(DTT(1,J),          J=1,N1)
      WRITE(4,*)
      WRITE(4,*)'       NODE   NUMBER    IN  RADIAL    DIRECTION      (M1):',    M1
      WRITE(4,*)'       NODE   NUMBER    IN  CIRCUMFERENTICAL        DIRECTION     (N1):',N1
      WRITE(4,*)
      DO  20  N2=2,M
      RR(N2)=RR(1)+(N2-1)*Drr*100.
20       CONTINUE

      DO  10  JJ=1,M
      J=M1-JJ
      DO  15  J1=1,N
      DR(J,J1)=Drr/(PHI*(R1+(J-0.5)*Drr)*K*LEN)
      DR(J,N1)=Drr/(PHI*(R1+(J-0.5)*Drr)*K*LEN)
      DRC(J,J1)=(PHI*RR(J)/100.)/(K*Drr*LEN)
      DRC(1,J1)=(PHI*RR(1)/100.)/(K*0.5*Drr*LEN)
      DRC(M1,J1)=(PHI*RR(M1)/100.)/(K*0.5*Drr*LEN)
15       CONTINUE
10       CONTINUE

      write(*,*)'POWER       LEVEL    =  ',II,'          LOCATION     =  ',MM
25    IT=IT+1
         DO  30  I1=1,M-1
      I=M1-I1
      DO  35  J=2,N
      A=PHI*R2
      DT(M1,1)=DTT(M1,1)
      DT(M1,J)=DTT(M1,J)
      DT(M1,N1)=DTT(M1,N1)
      DT(I,1)=DTT(I,1)
      DT(I,J)=DTT(I,J)
      DT(I,N1)=DTT(I,N1)

*     WRITE(*,*)'DT(M1,1)         =  ',DT(M1,1)
      ST=DT(M1,1)
      Tff=0.5*(Tinf+ST)
*     WRITE(*,*)'Tff       =  ',Tff,'         ST  =  ',ST
      CALL   PROP(Tff,Kair,Gama,Pr)
      CALL   HEAT(Kair,Gama,Pr,ST,Tinf,D,hinf,hr)
      hrr(1)=hr
      hin(1)=hinf
      DTT(M1,1)=DT(M,1)/DR(M,1)+2.*DT(M1,2)/DRC(M1,1)+Tinf*hinf*A*LEN
```

```
      DTT(M1,1)=DTT(M1,1)/(1./DR(M,1)+2./DRC(M1,1)+hinf*A*LEN)
*     IF  (DTT(M1,1).LE.Tinf)        THEN
*     DT(M1,1)=1.1*Tinf
*     ENDIF

*     WRITE(*,*)'DTT(M1,1)        = ',DTT(M1,1),'       DT(M1,1)    = ',DT(M1,1)
      ST=DT(M1,J)
      Tff=0.5*(Tinf+ST)
*     WRITE(*,*)'Tff      = ',Tff,'       ST  = ',ST
      CALL   PROP(Tff,Kair,Gama,Pr)
      CALL   HEAT(Kair,Gama,Pr,ST,Tinf,D,hinf,hr)
      hrr(J)=hr
      hin(J)=hinf
      DTT(M1,J)=DT(M,J)/DR(M,J)+DT(M1,J-1)/DRC(M1,J-1)
      DTT(M1,J)=DTT(M1,J)+DT(M1,J+1)/DRC(M1,J)+Tinf*hinf*A*LEN
      Y=LEN
      DTT(M1,J)=DTT(M1,J)/(1/DR(M,J)+1/DRC(M1,J-1)+1/DRC(M1,J)+hinf*A*Y)
*     IF  (DTT(M1,J).LE.Tinf)        THEN
*     DT(M1,J)=1.1*Tinf
*     ENDIF
*     WRITE(*,*)'DTT(M1,J)        = ',DTT(M1,J)
      ST=DT(M1,N1)
      Tff=0.5*(Tinf+ST)
*     WRITE(*,*)'Tff      = ',Tff,'       ST  = ',ST
      CALL   PROP(Tff,Kair,Gama,Pr)
      CALL   HEAT(Kair,Gama,Pr,ST,Tinf,D,hinf,hr)
      hrr(N1)=hr
      hin(N1)=hinf
      DTT(M1,N1)=DT(M,N1)/DR(M,N1)+2.*DT(M1,N)/DRC(M1,N)+Tinf*hinf*A*LEN
      DTT(M1,N1)=DTT(M1,N1)/(1./DR(M,N1)+2./DRC(M1,N)+hinf*A*LEN)
*     IF  (DTT(M1,N1).LE.Tinf)        THEN
*     DT(M1,N1)=1.1*Tinf
*     ENDIF

      DTT(I,1)=DT(I-1,1)/DR(I-1,1)+DT(I+1,1)/DR(I,1)
      DTT(I,1)=DTT(I,1)+2.*DT(I,2)/DRC(I,1)
      DTT(I,1)=DTT(I,1)/(1./DR(I-1,1)+1./DR(I,1)+2./DRC(I,1))
      DTT(I,J)=DT(I-1,J)/DR(I-1,J)+DT(I+1,J)/DR(I,J)
      DTT(I,J)=DTT(I,J)+DT(I,J-1)/DRC(I,J-1)+DT(I,J+1)/DRC(I,J)
      DTT(I,J)=DTT(I,J)/(1/DR(I-1,J)+1/DR(I,J)+1/DRC(I,J-1)+1/DRC(I,J))
      DTT(I,N1)=DT(I-1,N1)/DR(I-1,N1)+DT(I+1,N1)/DR(I,N1)
      DTT(I,N1)=DTT(I,N1)+2.*DT(I,N)/DRC(I,N)
      DTT(I,N1)=DTT(I,N1)/(1./DR(I-1,N1)+1./DR(I,N1)+2./DRC(I,N))
 35   CONTINUE
 30   CONTINUE

      DO  40  I1=1,M
      I=M1-I1+1
      DO  45  J=1,N1
      IF  (ABS(DTT(I,J)-DT(I,J)).GT.E)          GOTO  25
 45   CONTINUE
 40   CONTINUE
      write(*,*)'     ITERATION     NUMBER    = ',IT

*     WRITE(*,*)(hrr(J),        J=1,N1)
      QL=0.
      DO  77  J=1,N1
      QLO(J)=hin(J)*A*(DTT(M1,J)-Tinf)*LEN
      QLO(1)=hin(1)*A*(DTT(M1,1)-Tinf)*0.5*LEN
      QLO(N1)=hin(N1)*A*(DTT(M1,N1)-Tinf)*LEN*0.5
      QL1=QLO(J)
      QL=QL+QL1
```

```
 77     CONTINUE
        Preal=Q*2.*QL
        Qloss=2.*QL
*       WRITE(*,*)'REAL       POWER   =  ',Preal,'          LOSS   POWER   =  ',Qloss
        WRITE(5,*)Q,Drr,Preal,LEN,Qloss,Z
        WRITE(5,*)(TS(J),         J=1,N1)
        WRITE(5,*)(DTT(2,J),          J=1,N1)

        RR(1)=R1*100.
        RR(M1)=R2*100.
        DO  85  N3=2,M
        RR(N3)=RR(1)+(N3-1)*Drr*100.
 85     CONTINUE
*       WRITE(*,*)(RR(N4),         N4=1,M1)
        DO  80  J=1,N1
        DO  90  I=1,M1
*       WRITE(3,*)RR(I),DTT(I,J),I,J
 90       CONTINUE
 80       CONTINUE

 100    CONTINUE
 101    CONTINUE
        STOP
        END


        SUBROUTINE      PROP(T1,Kair,Gama,Pr)
        REAL    Kair,Gama,A(21),G(21),T(21),P(21),B(21)
        DATA    T(1),T(2),T(3),T(4),T(5)/10,20,30,40,50/
        DATA    T(6),T(7),T(8),T(9),T(10)/60,70,80,90,100/
        DATA    T(11),T(12),T(13),T(14),T(15)/110,120,130,140,150/
        DATA    T(16),T(17),T(18),T(19),T(20)/160,170,180,190,200/
        DATA    A(1),A(2),A(3),A(4),A(5)/24.87,25.64,26.38,27.10,27.81/
        DATA    A(6),A(7),A(8),A(9),A(10)/28.52,29.22,29.91,30.59,31.27/
        DATA    A(11),A(12),A(13),A(14),A(15)/31.94,32.61,33.28,33.94,34.59/
        DATA    A(16),A(17),A(18),A(19),A(20)/35.25,35.89,36.54,37.18,37.81/
        DATA    G(1),G(2),G(3),G(4),G(5)/14.19,15.09,16.01,16.96,17.92/
        DATA    G(6),G(7),G(8),G(9),G(10)/18.9,19.9,20.92,21.96,23.02/
        DATA    G(11),G(12),G(13),G(14),G(15)/24.1,25.19,26.31,27.44,28.58/
        DATA    G(16),G(17),G(18),G(19),G(20)/29.75,30.93,32.13,33.34,34.57/
        DATA    P(1),P(2),P(3),P(4),P(5)/.716,.713,.712,.710,.709/
        DATA    P(6),P(7),P(8),P(9),P(10)/.708,.707,.706,.705,.704/
        DATA    P(11),P(12),P(13),P(14),P(15)/.704,.703,.702,.702,.701/
        DATA    P(16),P(17),P(18),P(19),P(20)/.701,.700,.700,.699,.699/

        T1=T1-273.15
*       WRITE(*,*)'         T1    =     ',T1

        IF  (T1.LE.20.)      THEN
        T1  =  20.
        ENDIF

        DO  10  L  =  1,20
        IF  (T1.LE.T(L))      THEN
        GOTO   11
        ENDIF
 10     CONTINUE
 11     Kair=A(L)+(T1-T(L))/(T(L)-T(L-1))*(A(L)-A(L-1))
        Gama=G(L)+(T1-T(L))/(T(L)-T(L-1))*(G(L)-G(L-1))
        Pr=P(L)+((T1-T(L))/(T(L)-T(L-1)))*(P(L)-P(L-1))
        Kair=Kair/1000.
        Gama=Gama/1000000.
```

```
*       WRITE(*,*)'Kair       = ',Kair,    '      Gama   = ',Gama,'       Pr  = ',Pr
        RETURN
        END

        SUBROUTINE      HEAT(Kair1,Gama1,Pr1,ST1,Tinf1,D1,hinf,hr)
        REAL   Kair1,Gama1,hr,hc,hinf,gra,Nu
*       write(*,*)'gama1        = ',gama1,'          st1   = ',st1
        Beta1=1./Tinf1
        gra=9.8
        SIGMA=5.670E-8
        hr=SIGMA*(ST1**2.+Tinf1**2.)*(ST1+Tinf1)
        Ra=(Beta1*gra*(ABS(ST1-Tinf1))*(D1**3.))*Pr1/(Gama1**2.)
        U1=((1.+((0.599/Pr1)**(9./16.)))**(-8./27.))
*       WRITE(*,*)'      U1  =  ',U1
        Nu=((0.6+0.387*(Ra**(1./6.))*U1)**2.)
*       WRITE(*,*)'      Nu  =  ',Nu
        hc=(Kair1*Nu)/D1
        hinf=hc+hr
*       WRITE(4,*)'hc                  hr                      hinf'
*       WRITE(4,*)hc,hr,hinf
*       WRITE(*,*)'hc       = ',hc,'      hr  =  ',hr
        RETURN
        END
```

(b) Domain II Computer Program

```
* *       PROGRAM    FOR  H.T.  COEFFI.    INSIDE   OF  COPPER.
        REAL   K,iZ,iIN,A,A1,A2,Kins,L1,LEN
        DIMENSION     RR(45),TS(30),TF(30),QU(30),Tins(30)
        DOUBLE    PRECISION     Dh(45),DT(30,30),DTT(30,30),DR(30,30)
        DOUBLE    PRECISION     DRC(30,30),Dhh(30),DPre(30)
        DOUBLE    PRECISION     DPrealB,DhavgA,DhavgM,DTavg
        DOUBLE    PRECISION     DPrea,DPPPA
         OPEN(1,FILE='A:INC1.DAT',STATUS='OLD')
         OPEN(2,FILE='A:INC2.DAT',STATUS='OLD')
        OPEN(3,FILE='A:AS41.DAT',STATUS='NEW')
        OPEN(4,FILE='A:INSHC.DAT',STATUS='NEW')
        OPEN(5,FILE='A:AS43.DAT',STATUS='NEW')
        OPEN(6,FILE='A:TOLE.DAT',STATUS='OLD')
        OPEN(7,FILE='A:HAVL.DAT',STATUS='NEW')

        READ(6,*)M,N,E,LLL
        READ(2,*)R2,R1,K,Kins,WOT,iIN,G,L1
        Ac=3.1416*(R1**2.)
        AS=2.*3.1416*R2*L1/100.
        Tsat=41.65
        N1=N+1
        M1=M+1
        DO  101   MM=1,5
        DO  100   II=1,LLL
        WRITE(*,*)'POWER        LEVEL    =  ',II,'          LOCATION     =  ',MM
        READ(1,*)Qq,DRins,Preal,LEN,Qloss,Z
        READ(1,*)(TS(I),        I=1,N1)
        READ(1,*)(Tins(I),         I=1,N1)
        IT=0
        Q=Qq
        Q1=Qq*6.

        i2=iIN+(Q1*Z/(10000.*G*Ac*L1))
        CALL   FLUID(iZ,Tb)
        IF  (Tb.GT.Tsat)      THEN
        Tb=Tsat
        ENDIF
        WRITE(*,*)'FLUID        TEMP    =  ',Tb
        DO  11  J=1,N1
        TF(J)=Tb+273.15
11        CONTINUE
        WRITE(*,*)(TF(J),         J=1,N1)
        Drr=(R2-R1)/M
        PHI=3.1416/N
        COUNT=WOT/(2.*R2*PHI)
        A1=PHI*R1
        A2=PHI*R1/2.
```

```
      RR(1)=R1*100.
      RR(M1)=R2*100.

      WRITE(4,*)'         INPUT   CHECK   LIST   FOT   COPPER    PROGRAM'
      WRITE(4,*)
      WRITE(4,*)
      WRITE(4,*)'       OUTSIDE    COPPER    RADIUS    (R2):    ',R2,'    m'
      WRITE(4,*)'       INSIDE    COPPER    RADIUS    (R1):    ',R1,'    m'
      WRITE(4,*)'       CONDUCTIVITY      OF  INSULATION      (Kins):    ',Kins,'W/mK'
      WRITE(4,*)'       CONDUCTIVITY      OF  COPPER    (Kcop):    ',K,'    W/mK'
      WRITE(4,*)'       FLOWRATE    OF  FREON-11    (G):    ',G,'    Kg/m*m    s'
      WRITE(4,*)'       POWER    SUPPLIED    TO  TEST   SECTION    (Q):    ',Qq,'    W'
      WRITE(4,*)'       REAL   POWER   CALCULATED     (Preal):     ',Preal,'     W'
      WRITE(4,*)'       INLET   ENTHALPY     AT  Tin=22.2    C:  ',iIN,'KJ/Kg'
      WRITE(4,*)'       WIDTH   OF  THE  HEATING    TAPE:    ',WOT,'m'
      WRITE(4,*)'       LENGTH    OF  THE   TEST   SECTION:     ',L1,'    cm'
      WRITE(4,*)'       LOCAL   Z  OF  THE   TEST   SECTION:     ',Z,'    cm'
      WRITE(4,*)


      DO  5  I=1,M1
      DO  8  J=1,N1
      DT(I,J)=23.5+273.15
      DT(M1,J)=TS(J)
      DTT(M1,J)=TS(J)
 8       CONTINUE
 5       CONTINUE

      DO  20  N2=2,M
      RR(N2)=RR(1)+(N2-1)*Drr*100.
 20       CONTINUE

      DO  10  JJ=1,M
      J=M1-JJ
      DO  15  J1=1,N1
      P=1.0
      IF  (J1.EQ.N1)     THEN
      P=0.5
      ENDIF
      IF  (J1.EQ.1)     THEN
      P=0.5
      ENDIF
*        P=1.0
      DR(J,J1)=Drr/(PHI*P*(R1+(J-0.5)*Drr)*K*LEN)
      DR(J,N1)=Drr/(PHI*(R1+(J-0.5)*Drr)*K*LEN)
      DR(M1,J1)=DRins/(PHI*P*(R2+0.5*DRins)*Kins*LEN)
      DRC(J,J1)=(PHI*RR(J)/100.)/(K*Drr*LEN)
      DRC(1,J1)=(PHI*RR(1)/100.)/(K*0.5*Drr*LEN)
      DRC(M1,J1)=(PHI*RR(M1)/100.)/((K*0.5*Drr+Kins*0.5*DRins)*LEN)
 15       CONTINUE
 10       CONTINUE
*         WRITE(*,*)(RR(J),        J=1,M1)
*         DO  1  K1=1,M1
*         DO  2  K2=1,N1
*         WRITE(4,*)DR(K1,K2),DRC(k1,k2),'              M=',k1,'       N=',k2
* 2         CONTINUE
* 1         CONTINUE

 25       IT=IT+1
      DO  30  I1=2,M
      I=M1-I1
*         QU(1)=Q*PHI
```

```
      QU(1)=Q/(2.*N)
      DO  35  J=2,N
*        QU(J)=Q*PHI
      C1=(0.5*WOT)/(R2*(J-0.5)*PHI)
      IF  (C1.GE.0.5)      THEN
*        QU(J)=Q*C1*PHI
      QU(J)=Q*C1/(2.*N)
      ENDIF
      IF  (C1.GE.1.)      THEN
*        QU(J)=Q*PHI
      QU(J)=Q/(2.*N)
      ENDIF
      IF  (C1.LT.0.)      THEN
      QU(J)=0.
      ENDIF
*        QU(N1)=Q*PHI
      CN1=(0.5*WOT)/(R2*N*PHI)
      IF  (CN1.GE.0.5)      THEN
*        QU(N1)=Q*CN1*PHI
      QU(N1)=Q*CN1/(2.*N)
      ENDIF
      IF  (CN1.GE.1.)      THEN
*        QU(N1)=Q*PHI
      QU(N1)=Q/(2.*N)
      ENDIF
      IF  (C1.LT.0.)      THEN
      QU(N1)=0.
      ENDIF

 4       A1=PHI*R1
      A2=PHI*R1/2.
      B1=2.*3.1416*R2
      B2=2.*3.1416*R2
      DT(M,1)=DTT(M,1)
      DT(M,J)=DTT(M,J)
      DT(M,N1)=DTT(M,N1)
      DT(I,J)=DTT(I,J)
      DT(I,1)=DTT(I,1)
      DT(I,N1)=DTT(I,N1)
      DT(1,1)=DTT(1,1)
      DT(1,J)=DTT(1,J)
      DT(1,N1)=DTT(1,N1)

      DTT(M,1)=DT(M1,1)+2.*DR(M,1)*(DT(M1,1)-DT(M1,2))/DRC(M1,1)
      DTT(M,1)=DTT(M,1)-DR(M,1)*QU(1)
      DTT(M,1)=DTT(M,1)+(DR(M,1)/DR(M1,1))*(DT(M1,1)-Tins(1))
      DTT(M,J)=DT(M1,J)+DR(M,J)*(DT(M1,J)-DT(M1,J+1))/DRC(M1,J)
      DTT(M,J)=DTT(M,J)+DR(M,J)*(DT(M1,J)-DT(M1,J-1))/DRC(M1,J-1)
      DTT(M,J)=DTT(M,J)-DR(M,J)*QU(J)
      DTT(M,J)=DTT(M,J)+(DR(M,J)/DR(M1,J))*(DT(M1,J)-Tins(J))
      DTT(M,N1)=DT(M1,N1)+2.*DR(M,N1)*(DT(M1,N1)-DT(M1,N))/DRC(M1,N)
      DTT(M,N1)=DTT(M,N1)-DR(M,N1)*QU(N1)
      DTT(M,N1)=DTT(M,N1)+(DR(M,N1)/DR(M1,N1))*(DT(M1,N1)-Tins(N1))
      DTT(I,1)=DT(I+1,1)+2.*DR(I,1)*(DT(I+1,1)-DT(I+1,2))/DRC(I+1,1)
      DTT(I,1)=DTT(I,1)+DR(I,1)*(DT(I+1,1)-DT(I+2,1))/DR(I+1,1)
      DTT(I,J)=DT(I+1,J)+DR(I,J)*(DT(I+1,J)-DT(I+1,J+1))/DRC(I+1,J)
      DTT(I,J)=DTT(I,J)+DR(I,J)*(DT(I+1,J)-DT(I+1,J-1))/DRC(I+1,J-1)
      DTT(I,J)=DTT(I,J)+DR(I,J)*(DT(I+1,J)-DT(I+2,J))/DR(I+1,J)
      DTT(I,N1)=DT(I+1,N1)+DR(I,N1)*(DT(I+1,N1)-DT(I+1,N))/DRC(I+1,N)
      DTT(I,N1)=DTT(I,N1)+DR(I,N1)*(DT(I+1,N1)-DT(I+1,N))/DRC(I+1,N)
      DTT(I,N1)=DTT(I,N1)+DR(I,N1)*(DT(I+1,N1)-DT(I+2,N1))/DR(I+1,N1)
      DTT(1,1)=DT(2,1)+2.*DR(1,1)*(DT(2,1)-DT(2,2))/DRC(2,1)
```

```
      DTT(1,1)=DTT(1,1)+DR(1,1)*(DT(2,1)-DT(3,1))/DR(2,1)
      DTT(1,J)=DT(2,J)+DR(1,J)*(DT(2,J)-DT(2,J+1))/DRC(2,J)
      DTT(1,J)=DTT(1,J)+DR(1,J)*(DT(2,J)-DT(2,J-1))/DRC(2,J-1)
      DTT(1,J)=DTT(1,J)+DR(1,J)*(DT(2,J)-DT(3,J))/DR(2,J)
      DTT(1,N1)=DT(2,N1)+2.*DR(1,N1)*(DT(2,N1)-DT(2,N))/DRC(2,N)
      DTT(1,N1)=DTT(1,N1)+DR(1,N1)*(DT(2,N1)-DT(3,N1))/DR(2,N1)
35      CONTINUE
30      CONTINUE

      DO  40  I1=2,M
      DO  45  J=2,N
      I=M1-I1
      IF  (ABS(DTT(M,1)-DT(M,1)).GT.E)          GOTO  25
      IF  (ABS(DTT(M,J)-DT(M,J)).GT.E)          GOTO  25
      IF  (ABS(DTT(M,N1)-DT(M,N1)).GT.E)          GOTO  25
      IF  (ABS(DTT(I,1)-DT(I,1)).GT.E)          GOTO  25
      IF  (ABS(DTT(I,J)-DT(I,J)).GT.E)          GOTO  25
      IF  (ABS(DTT(I,N1)-DT(I,N1)).GT.E)          GOTO  25
      IF  (ABS(DTT(1,1)-DT(1,1)).GT.E)          GOTO  25
      IF  (ABS(DTT(1,J)-DT(1,J)).GT.E)          GOTO  25
      IF  (ABS(DTT(1,N1)-DT(1,N1)).GT.E)          GOTO  25
45      CONTINUE
40      CONTINUE
      WRITE(*,*)(DTT(1,J),          J=1,N1)
      WRITE(*,*)(DTT(2,J),          J=1,N1)
*       WRITE(*,*)(QU(J),          J=1,N1)

*       DO  22  J=1,N1
*       IF  (DTT(1,J).GT.(Tsat+273.15))          THEN
*       TF(J)=Tsat
*       ENDIF
* 22    CONTINUE

      DO  33  J=2,N
      Dh(1)=2.*(DTT(1,1)-DTT(1,2))/DRC(1,1)
      Dh(1)=(DTT(1,1)-DTT(2,1))/DR(1,1)+Dh(1)
      Dh(1)=Dh(1)/(DTT(1,1)-TF(1))
      Dh(1)=-Dh(1)/(LEN*A1)
      Dh(J)=(DTT(1,J)-DTT(2,J))/DR(1,J)
      Dh(J)=(DTT(1,J)-DTT(1,J-1))/DRC(1,J-1)+Dh(J)
      Dh(J)=(DTT(1,J)-DTT(1,J+1))/DRC(1,J)+Dh(J)
      Dh(J)=Dh(J)/(DTT(1,J)-TF(J))
      Dh(J)=-Dh(J)/(LEN*A1)
      Dh(N1)=(DTT(1,N1)-DTT(2,N1))/DR(1,N1)
      Dh(N1)=2.*(DTT(1,N1)-DTT(1,N))/DRC(1,N)+Dh(N1)
      Dh(N1)=Dh(N1)/(DTT(1,N1)-TF(N1))
      Dh(N1)=-Dh(N1)/(LEN*A1)
33      CONTINUE
      WRITE(*,*)'LOCAL        H.T.   COEFFICIENTS'
      WRITE(*,*)(Dh(J),          J=1,N1)

      DPrea=0.
      DO  56  J9=1,N1
      DPrea=DPrea+QU(J9)
56      CONTINUE
      DPPPA=2.*DPrea-QU(1)-QU(N1)-Qloss

      DPreslB=0.
      DO  66  J=1,N1
      DPre(J)=A1*LEN*Dh(J)*(DTT(1,J)-TF(J))
*       DPre(1)=A1*LEN*Dh(1)*(DTT(1,1)-TF(1))*0.5
*       DPre(N1)=A1*LEN*Dh(N1)*(DTT(1,N1)-TF(N1))*0.5
```

```
      DPrealB=DPrealB+DPre(J)
 66     CONTINUE
      DPrealB=2.*DPrealB-DPre(1)-DPre(N1)
*       WRITE(*,*)'     Q  =  ',Qq
*       WRITE(*,*)'Preal1        =  ',DPPPA,'      POWER   SUPPLIED    TO  COPPER'
*       WRITE(*,*)'Preal2        =  ',DPrealB,'      POWER   OBTAINED    BY  LIQUID'

      DhavgM=(Dh(1)+3.*(Dh(1+N/4)+Dh(1+3*N/4))+Dh(N1))/8.
      DTavg=(DTT(1,1)+3*(DTT(1,1+N/4)+DTT(1,1+3*N/4))+DTT(1,N1))/8.
      DhavgA=DPrealB/(3.1416*R1*LEN*(DTavg-Tb))
      WRITE(*,*)'     AVERAGE    H.T.   COEFFICIENT(M)       =',  DhavgM
*       WRITE(*,*)'     AVERAGE    H.T.   COEFFICIENT(A)       =',  DhavgA
*       WRITE(*,*)'     AVERAGE    WALL   TEMP.   =  ',DTavg
      POWER=6.*Q
      WRITE(7,*)POWER,DhavgM,DTavg

      RR(1)=R1*100.
      RR(M1)=R2*100.
      DO  85  N3=2,M
      RR(N3)=RR(1)+(N3-1)*Drr*100.
 85     CONTINUE
*       WRITE(*,*)(RR(N4),        N4=1,M1)
      DO  80  J=1,M1
      DO  90  I=1,M1
*       WRITE(3,*)RR(I),DTT(I,J),I,J
 90     CONTINUE
 80     CONTINUE

      DO  95  J=1,M1
      WRITE(5,*)'     HEAT   TRANSFER    COEFFICIENT'
      WRITE(5,*)J,Dh(J)
 95     CONTINUE
 100    CONTINUE
 101    CONTINUE
      STOP
      END


      subroutine     FLUID(i1,tb)
      real   i1,i(15),t(15)
      data   t(1),t(2),t(3),t(4)/10.,16.,22.,28./
      data   t(5),t(6),t(7),t(8)/34.,38.,42.,46./
      data   t(9),t(10),t(11),t(12)/50.,54.,58.,70./
      data   t(13),t(14),t(15)/90.,110.,130./
      data   i(1),i(2),i(3),i(4)/508.8,514.1,519.4,524.7/
      data   i(5),i(6),i(7),i(8)/530.1,533.7,537.3,540.9/
      data   i(9),i(10),i(11),i(12)/544.6,548.2,551.9,563.1/
      data   i(13),i(14),i(15)/582.1,601.9,622.6/
      do  9  k=1,15
      if  (i1.le.i(k))        then
      goto   3
      endif
 9        continue
 3        tb=t(k)+(i1-i(k))/(i(k)-i(k-1))*(t(k)-t(k-1))
      return
      end
```

APPENDIX B.2

List of program EPOX.FOR for Freon-11 data reduction in Domain II.

```
*     PROGRAM    FOR  H.T.  COEFFI.    INSIDE    OF  COPPER.
      REAL   K,iZ,iIN,A,A1,A2,Kins,L1,LEN
      DIMENSION     RR(45),TS(30),TF(30),QU(30),Tins(30),PH(30)
      DOUBLE    PRECISION     Dh(45),DT(30,30),DTT(30,30),DR(30,30)
      DOUBLE    PRECISION     DRC(30,30),Dhh(30),DPre(30),drc1(30,30)
      DOUBLE    PRECISION     DPrealB,DhavgA,DhavgM,DTavg,drc2(30,30)
      DOUBLE    PRECISION     DPrea,DPPPA
       OPEN(1,FILE='A:INC1.DAT',STATUS='OLD')
       OPEN(2,FILE='A:EPO2.DAT',STATUS='OLD')
      OPEN(3,FILE='B:AS31.DAT',STATUS='NEW')
      OPEN(4,FILE='A:INSHC.DAT',STATUS='NEW')
      OPEN(5,FILE='A:AS33.DAT',STATUS='NEW')
      OPEN(6,FILE='A:TOLE.DAT',STATUS='OLD')

      READ(6,*)M,N,E,LLL
      READ(2,*)R2,R1,K,Kins,WOT,iIN,G,L1
      Ac=3.1416*(R1**2.)
      AS=2.*3.1416*R2*L1/100.
      Tsat=41.65
      N1=N+1
      M1=M+1
      DO  101   MM=1,5
      DO  100   II=1,LLL
*     WRITE(*,*)'POWER       LEVEL   =  ',II,'          LOCATION    =  ',MM
      READ(1,*)Qq,DRins,Preal,LEN,Qloss,Z
      READ(1,*)(TS(I),        I=1,N1)
      READ(1,*)(Tins(I),        I=1,N1)
      IT=0
      Q=Qq
      Q1=Qq*6.

      iZ=iIN+(Q1*Z/(1000.*G*Ac*L1))
      CALL   FLUID(iZ,Tb)
      IF  (Tb.GT.Tsat)      THEN
      Tb=Tsat
      ENDIF
*     WRITE(*,*)'FLUID       TEMP   =  ',Tb+273.15
      DO  11   J=1,N1
      TF(J)=Tb+273.15
 11      CONTINUE
*     WRITE(*,*)(TF(J),        J=1,N1)
      Drr=(R2-R1)/M
      PHI=3.1416/N
      COUNT=WOT/(2.*R2*PHI)
      A1=PHI*R1
      A2=PHI*R1/2.
      RR(1)=R1
      RR(M1)=R2

      WRITE(4,*)'        INPUT   CHECK   LIST   FOT  COPPER   PROGRAM'
      WRITE(4,*)
      WRITE(4,*)
      WRITE(4,*)'      OUTSIDE   COPPER   RADIUS   (R2):   ',R2,'   m'
      WRITE(4,*)'      INSIDE   COPPER   RADIUS   (R1):   ',R1,'   m'
      WRITE(4,*)'      CONDUCTIVITY      OF  INSULATION     (Kins):    ',Kins,'W/mK'
```

```
      WRITE(4,*)'       CONDUCTIVITY      OF  COPPER    (Kcop):    ',K,'   W/mK'
      WRITE(4,*)'       FLOWRATE     OF  FREON-11     (G):   ',G,'   Kg/m*m   s'
      WRITE(4,*)'       POWER    SUPPLIED     TO  TEST   SECTION    (Q):   ',Qq,'    W'
      WRITE(4,*)'       REAL   POWER   CALCULATED      (Preal):    ',Preal,'     W'
      WRITE(4,*)'       INLET   ENTHALPY     AT  Tin=22.2     C:  ',IIN,'KJ/Kg'
      WRITE(4,*)'       WIDTH   OF  THE  HEATING     TAPE:    ',WOT,'m'
      WRITE(4,*)'       LENGTH    OF  THE  TEST   SECTION:     ',L1,'    cm'
      WRITE(4,*)'       LOCAL   Z  OF  THE  TEST   SECTION:     ',Z,'    cm'
      WRITE(4,*)


      DO  5  I=1,M1
      DO  8  J=1,N1
      DT(I,J)=23.5+273.15
      DT(M1,J)=TS(J)
      DTT(M1,J)=TS(J)
8        CONTINUE
5        CONTINUE

      DO  20  N2=2,M
      RR(N2)=RR(1)+(N2-1)*Drr
20       CONTINUE

      DO  10  JJ=1,M
      J=M1-JJ
      DO  15  J1=1,N1
      P=1.0
      IF  (J1.EQ.N1)     THEN
      P=0.5
      ENDIF
      IF  (J1.EQ.1)     THEN
      P=0.5
      ENDIF
        P=1.0
      DR(J,J1)=Drr/(PHI*P*(R1+(J-0.5)*Drr)*K*LEN)
      DR(J,N1)=Drr/(PHI*P*(R1+(J-0.5)*Drr)*K*LEN)
      DR(M1,J1)=DRins/(PHI*P*(R2+0.5*DRins)*Kins*LEN)
      DRC(J,J1)=(PHI*RR(J))/(K*Drr*LEN)
      DRC(1,J1)=(PHI*RR(1))/(K*0.5*Drr*LEN)
      drc1(m1,j1)=1./(2.*dr(m1,j1)+(phi*rr(m1))/(.5*kins*drins))
      drc2(m1,j1)=1./(2.*dr(m,j1)+(phi*rr(m1))/(.5*k*drr))
      drc(m1,j1)=1./(drc1(m1,j1)+drc2(m1,j1))
*     DRC(M1,J1)=(PHI*RR(M1))/((K*0.5*Drr+Kins*0.5*DRins)*LEN)
15       CONTINUE
10       CONTINUE
*        WRITE(*,*)(RR(J),        J=1,M1)
         DO  1  K1=1,M1
         DO  2  K2=1,N1
*         WRITE(4,*)DR(K1,K2),DRC(k1,k2),'              M=',k1,'       N=',k2
2        CONTINUE
1        CONTINUE

25       IT=IT+1
      DO  30  I1=2,M
      I=M1-I1
*        QU(1)=Q*PHI
      QU(1)=Q/(2.*N)
      DO  35  J=2,N
*        QU(J)=Q*PHI
      C1=(0.5*WOT)/(R2*(J-0.5)*PHI)
      IF  (C1.GE.0.5)     THEN
*        QU(J)=Q*C1*PHI
```

```
      QU(J)=Q*C1/(2.*N)
      ENDIF
      IF  (C1.GE.1.)     THEN
*       QU(J)=Q*PHI
      QU(J)=Q/(2.*N)
      ENDIF
      IF  (C1.LT.0.)     THEN
      QU(J)=0.
      ENDIF
*       QU(N1)=Q*PHI
      CN1=(0.5*WOT)/(R2*N*PHI)
      IF  (CN1.GE.0.5)      THEN
*       QU(N1)=Q*CN1*PHI
      QU(N1)=Q*CN1/(2.*N)
      ENDIF
      IF  (CN1.GE.1.)      THEN
*       QU(N1)=Q*PHI
      QU(N1)=Q/(2.*N)
      ENDIF
      IF  (C1.LT.0.)     THEN
      QU(N1)=0.
      ENDIF

 4      A1=PHI*R1
      A2=PHI*R1/2.
      B1=2.*3.1416*R2
      B2=2.*3.1416*R2
      DTT(M,1)=DT(M,1)
      DTT(M,J)=DT(M,J)
      DTT(M,N1)=DT(M,N1)
      DTT(I,J)=DT(I,J)
      DTT(I,1)=DT(I,1)
      DTT(I,N1)=DT(I,N1)
      DTT(1,1)=DT(1,1)
      DTT(1,J)=DT(1,J)
      DTT(1,N1)=DT(1,N1)

      DT(M,1)=DT(M1,1)+2.*DR(M,1)*(DT(M1,1)-DT(M1,2))/DRC(M1,1)
      DT(M,1)=DT(M,1)-DR(M,1)*QU(1)
      DT(M,1)=DT(M,1)+(DR(M,1)/DR(M1,1))*(DT(M1,1)-Tins(1))
      DT(M,J)=DT(M1,J)+DR(M,J)*(DT(M1,J)-DT(M1,J+1))/DRC(M1,J)
      DT(M,J)=DT(M,J)+DR(M,J)*(DT(M1,J)-DT(M1,J-1))/DRC(M1,J-1)
      DT(M,J)=DT(M,J)-DR(M,J)*QU(J)
      DT(M,J)=DT(M,J)+(DR(M,J)/DR(M1,J))*(DT(M1,J)-Tins(J))
      DT(M,N1)=DT(M1,N1)+2.*DR(M,N1)*(DT(M1,N1)-DT(M1,N))/DRC(M1,N)
      DT(M,N1)=DT(M,N1)-DR(M,N1)*QU(N1)
      DT(M,N1)=DT(M,N1)+(DR(M,N1)/DR(M1,N1))*(DT(M1,N1)-Tins(N1))
      DT(I,1)=DT(I+1,1)+2.*DR(I,1)*(DT(I+1,1)-DT(I+1,2))/DRC(I+1,1)
      DT(I,1)=DT(I,1)+DR(I,1)*(DT(I+1,1)-DT(I+2,1))/DR(I+1,1)
      DT(I,J)=DT(I+1,J)+DR(I,J)*(DT(I+1,J)-DT(I+1,J+1))/DRC(I+1,J)
      DT(I,J)=DT(I,J)+DR(I,J)*(DT(I+1,J)-DT(I+1,J-1))/DRC(I+1,J-1)
      DT(I,J)=DT(I,J)+DR(I,J)*(DT(I+1,J)-DT(I+2,J))/DR(I+1,J)
      DT(I,N1)=DT(I+1,N1)+DR(I,N1)*(DT(I+1,N1)-DT(I+1,N))/DRC(I+1,N)
      DT(I,N1)=DT(I,N1)+DR(I,N1)*(DT(I+1,N1)-DT(I+1,N))/DRC(I+1,N)
      DT(I,N1)=DT(I,N1)+DR(I,N1)*(DT(I+1,N1)-DT(I+2,N1))/DR(I+1,N1)
      DT(1,1)=DT(2,1)+2.*DR(1,1)*(DT(2,1)-DT(2,2))/DRC(2,1)
      DT(1,1)=DT(1,1)+DR(1,1)*(DT(2,1)-DT(3,1))/DR(2,1)
      DT(1,J)=DT(2,J)+DR(1,J)*(DT(2,J)-DT(2,J+1))/DRC(2,J)
      DT(1,J)=DT(1,J)+DR(1,J)*(DT(2,J)-DT(2,J-1))/DRC(2,J-1)
      DT(1,J)=DT(1,J)+DR(1,J)*(DT(2,J)-DT(3,J))/DR(2,J)
      DT(1,N1)=DT(2,N1)+2.*DR(1,N1)*(DT(2,N1)-DT(2,N))/DRC(2,N)
      DT(1,N1)=DT(1,N1)+DR(1,N1)*(DT(2,N1)-DT(3,N1))/DR(2,N1)
```

```
 35       CONTINUE
 30       CONTINUE

      DO  40  I1=2,M
      DO  45  J=2,N
      I=M1-I1
      IF  (ABS(DTT(M,1)-DT(M,1)).GT.E)            GOTO   25
      IF  (ABS(DTT(M,J)-DT(M,J)).GT.E)            GOTO   25
      IF  (ABS(DTT(M,N1)-DT(M,N1)).GT.E)            GOTO   25
      IF  (ABS(DTT(1,1)-DT(I,1)).GT.E)            GOTO   25
      IF  (ABS(DTT(I,J)-DT(I,J)).GT.E)            GOTO   25
      IF  (ABS(DTT(I,N1)-DT(I,N1)).GT.E)            GOTO   25
      IF  (ABS(DTT(1,1)-DT(1,1)).GT.E)            GOTO   25
      IF  (ABS(DTT(1,J)-DT(1,J)).GT.E)            GOTO   25
      IF  (ABS(DTT(1,N1)-DT(1,N1)).GT.E)            GOTO   25
 45       CONTINUE
 40       CONTINUE
*     WRITE(*,*)(DTT(1,J),          J=1,N1)
*     WRITE(*,*)(DTT(2,J),          J=1,N1)
*        WRITE(*,*)(QU(J),          J=1,N1)


      RR(1)=R1*100.
      RR(M1)=R2*100.
      DO  85  N3=2,M
      RR(N3)=RR(1)+(N3-1)*Drr*100.
 85       CONTINUE
*        WRITE(*,*)(RR(N4),          N4=1,M1)

      WRITE(5,*)Qq,Drr,preal,len,Qloss,Z
      WRITE(5,*)(DTT(1,J),          J=1,N1)
      WRITE(5,*)(DTT(2,J),          J=1,N1)
 100      CONTINUE
 101      CONTINUE
      WRITE(*,*)'POWER       LEVELS    =  ',LLL
      STOP
      END


      subroutine     FLUID(i1,tb)
      real   i1,i(15),t(15)
      data   t(1),t(2),t(3),t(4)/10.,16.,22.,28./
      data   t(5),t(6),t(7),t(8)/34.,38.,42.,46./
      data   t(9),t(10),t(11),t(12)/50.,54.,58.,70./
      data   t(13),t(14),t(15)/90.,110.,130./
      data   i(1),i(2),i(3),i(4)/508.8,514.1,519.4,524.7/
      data   i(5),i(6),i(7),i(8)/530.1,533.7,537.3,540.9/
      data   i(9),i(10),i(11),i(12)/544.6,548.2,551.9,563.1/
      data   i(13),i(14),i(15)/582.1,601.9,622.6/
      do  9  k=1,15
      if  (i1.le.i(k))       then
      goto   3
      endif
 9        continue
 3        tb=t(k)+(i1-i(k))/(i(k)-i(k-1))*(t(k)-t(k-1))
      return
      end
```

APPENDIX B.3

Nodal Equations Derivation.

The differential heat conduction equation in cylindrical coordinates can be expressed as

$$k\frac{\partial}{\partial r}(r\frac{\partial T}{\partial r}) + \frac{k}{r}\frac{\partial^2 T}{\partial \varphi^2} + kr\frac{\partial^2 T}{\partial Z^2} + q'''r = r\rho C_p\frac{\partial T}{\partial t} \qquad (B.3.1)$$

Applying following assumptions:

(1) steady state

(2) temperature distributed in radial and circumferential directions

(3) constant heat conductivity

(4) no inner heat resouces

(5) unit length in axial direction

Equation (B.3.1) becomes

$$kr\frac{\partial^2 T}{\partial r^2} + \frac{\partial T}{\partial r} + \frac{k}{r}\frac{\partial^2 T}{\partial \varphi^2} = 0 \qquad (B.3.2)$$

From Taylor series expension and using the notation in figure B.3.1,

$$\frac{\partial T(i,j)}{\partial r} = \frac{T(i+1,j) - T(i-1,j)}{2\Delta r} \qquad (B.3.3)$$

$$\frac{\partial^2 T}{\partial r^2} = \frac{T(i+1,j) - 2T(i,j) + T(i-1,j)}{(\Delta r)^2} \qquad (B.3.4)$$

$$\frac{\partial T(i,j)}{\partial \varphi^2} = \frac{T(i,j+1) - 2T(i,j) + T(i,j-1)}{(\Delta\varphi)^2} \qquad (B.3.5)$$

Inserting equations (B.3.3), (B.3.4), and (B.3.5) into equation (B.3.2),

$$kr_i \frac{T(i+1,j) - 2T(i,j) + T(i-1,j)}{(\Delta r)^2} + \frac{T(i+1,j) - T(i-1,j)}{2\Delta r}$$
$$+ \frac{k}{r_i} \frac{T(i,j+1) - 2T(i,j) + T(i,j-1)}{(\Delta\varphi)^2} = 0 \qquad (B.3.6)$$

where r_i is the radius for the center of the "i" node.

Equation (B.3.6) can be written in form of

$$kr_i \frac{T(i+1,j) - T(i,j)}{(\Delta r)^2} + kr_i \frac{T(i-1,j) - T(i,j)}{(\Delta r)^2} + \frac{T(i+1,j) - T(i,j)}{2(\Delta r)}$$
$$- \frac{T(i-1,j) - T(i,j)}{2(\Delta r)} + \frac{k}{r_i} \frac{T(i,j+1) - T(i,j)}{(\Delta\varphi)^2} + \frac{k}{r_i} \frac{T(i,j-1) - T(i,j)}{(\Delta\varphi)^2} = 0$$

After combining the terms with similar coefficients of $T(i+1,j)$, $T(i-1,j)$, $T(i,j+1)$, and $T(i,j-1)$, the above equation becomes

$$k(r_i + \frac{\Delta r}{2}) \frac{T(i+1,j) - T(i,j)}{(\Delta r)^2} + k(r_i - \frac{\Delta r}{2}) \frac{T(i-1,j) - T(i,j)}{(\Delta r)^2}$$
$$+ \frac{k}{r_i} \frac{T(i,j+1) - T(i,j)}{(\Delta\varphi)^2} + \frac{k}{r_i} \frac{T(i,j-1) - T(i,j)}{(\Delta\varphi)^2} = 0$$

Then

$$\frac{T(i+1,j) - T(i,j)}{\frac{(\Delta r)^2}{k(r_i + \frac{\Delta r}{2})}} + \frac{T(i-1,j) - T(i,j)}{\frac{(\Delta r)^2}{k(r_i - \frac{\Delta r}{2})}}$$

$$+\frac{T(i,j+1)-T(i,j)}{\frac{r_i(\Delta\varphi)^2}{k}}+\frac{T(i,j-1)-T(i,j)}{\frac{r_i(\Delta\varphi)^2}{k}}=0 \qquad (B.3.7)$$

After multiplying by $(\Delta r\Delta\varphi)$ in equation (B.3.7),

$$\frac{T(i+1,j)-T(i,j)}{\frac{\Delta r}{k(r_i+\frac{\Delta r}{2})\Delta\varphi}}+\frac{T(i-1,j)-T(i,j)}{\frac{\Delta r}{k(r_i-\frac{\Delta r}{2})\Delta\varphi}}$$
$$+\frac{T(i,j+1)-T(i,j)}{\frac{r_i\Delta\varphi}{k\Delta r}}+\frac{T(i,j-1)-T(i,j)}{\frac{r_i\Delta\varphi}{k\Delta r}}=0 \qquad (B.3.8)$$

Equation (B.3.8) is the finite difference formulation for equation (B.3.2). The numerator of each term in this equation is the temperature difference between the central node, (i,j), and the neighboring nodes, $(i+1,j)$, $(i-1,j)$, $(i,j+1)$, and $(i,j-1)$. The denominators are the heat resistances between the nodes just mentioned.

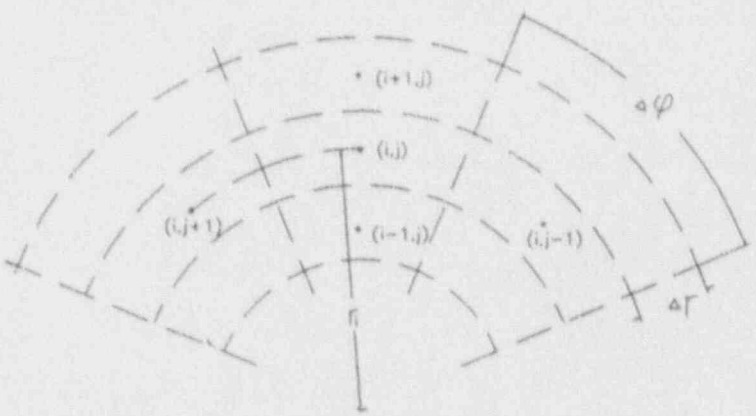

The beauty of this derivation is that it does not only give the finite difference formulation, but also gives the heat resistances. The four heat resistances in figure B.3 can be easily picked up from equation (B.3.8); i.e.,

$$R(i+1,j) = \frac{\Delta r}{k(r_i + \frac{\Delta r}{2})\Delta\varphi} \qquad (B.3.9)$$

$$R(i-1,j) = \frac{\Delta r}{k(r_i - \frac{\Delta r}{2})\Delta\varphi} \qquad (B.3.10)$$

$$R(i,j+1) = \frac{r_i \Delta\varphi}{k\Delta r} \qquad (B.3.11)$$

$$R(i,j-1) = \frac{r_i \Delta\varphi}{k\Delta r} \qquad (B.3.12).$$

When the convection boundary condition was applied, the heat resistance for inside wall was (see figure B.3.2)

$$R(j)_{conv} = \frac{1}{h(j)A(j)} = \frac{1}{h(j)R_1\Delta\varphi_n} \qquad (B.3.13)$$

Note that $\Delta\varphi_n$ will vary when applying equation (B.3.13) to full node, half node, or quarter node. The index, n, denotes this change for this respective nodes.

Few of current books have discussed formulation in cylindrical coordinates. Holman[1], Ozisik[2], and Jaluria[3] gave the same expressions for heat resistances and heat balance equation, and the differencing equations from these books all agree with equation (B.3.$\mathcal{E}$).

References

1. Holman, J.P., "Heat Transfer", 5th Edition, McGraw-Hill, 1981, p85.

2. Ozisik, M.N., "Heat Transfer, A Basic Approach", McGraw-Hill, 1985, p181-182.

3. Jaluria, Y., K. Torrance, "Computational Heat Transfer", Hemisphere Publication, 1986, p96.

4. Myers, G.E., "Analytical Methods in Conduction Heat Transfer", McGraw Hill, 1971, p10.

APPENDIX C

In the present analysis, the sample applications and numerical solutions were necessary in order to get: (1) verify the typical numerical difference equations and boudary conditions needed for data reduction, (2) obtain estimates of the largest radial and circumferential allowable numerical iteration tolerence which would result in acceptable accuracy. Based on what has been learned from these sample applications, the final numerical procedure was developed for the data reduction of wall temperature measurements[36,39] made from the configuration shown in Figure 4.2.

Sample Application 1

The first sample problem involves a one-dimensional conduction numerical solution in cylindrical coordinates, for given outside and inside surface temperatures. The purpose of this applicatoin is to determine allowable tolerances and mesh sizes. The equation to be solved can be written as:

The simple closed-form solution of this problem is:

$$T(r) = T(R_1) - \frac{q ln \frac{r}{R_1}}{2\pi k} \qquad (C.2)$$

where:

$$q = \frac{T_1 - T_2}{\frac{ln \frac{R_1}{R_2}}{2\pi k}}$$

For a simple computation k was selected to be 100 W/mK.

For a one dimensional problem, the outside supplied rate of heat flow per unit length, $q"$, remains the same throughout the radial direction. The numerical $q"$ solutions should be constant for each pair neighboring nodes as well. Therefore, this equality of the computed

$q^{"}$ with the supplied $q^{"}$ will be the basis to check the accuracy. Equality of temperature is usually not enough.

The numerical and exact temperature profiles are shown in figures C.1 to C.3 for different node numbers and tolerances. In these three figures, tolerance are 0.1, 0.05, 0.01, 0.005 and 0.001 for 10, 30 and 60 nodes, respectively. In figure C.1, the tolerances do not affect the accuracy very much for 10 nodes. For all cases, the computed temperatures were almost identical to that for the exact solution. In figure C.2 with 30 nodes, the temperature variations from the exact line were visable when the tolerance was large, e.g. 0.1, and 0.05. But, when the tolerance was reduced (below $0.01^{o}C$), the agreement between the numerical temperatures and the exact ones was excellent. In figure C.3 with 60 nodes, the temperatures deviated significant from the exact solution when tolerance was larger than 0.05. Clearly, as the number of nodes increase, the tolerance must correspondingly reduced.

As is well known, the apperance of apparent accuracy in local numerical temperatures does not imply similar accuracy in local heat flux. In this same sample problem, one can readily examine accuracy in the heat flux between each two nodes, because the heat flux should be constant for all radii. Figures C.4, C.5 and C.7 are the heat flux distributions for the three previously mentioned cases.

Figure C.4 shows the heat flux distribution between each two neighboring nodes in 10 nodes for tolerance 0.1, 0.05, 0.01, 0.005 and 0.001. The largest variaton in $q^{"}$ in figure C.4 was about 4% which is much larger than the 0.1% for temperatures (Figure C.5.1). As the number of nodes increases with constant tolerance, in figure C.5 (30 nodes)

shows large variations in q'' than that shown for 10 nodes in figure C.4. This trend becomes progressively werse as shown in figure C.6 (60 nodes). Therefore, when the numerical temperatures are close to the exact solution, it does not mean that the q'' solutions are completely accurate. Only when the accuracy has been veried with respect to both temperature and q' (and heat flux) can one be assured of acceptable solutions.

The result of this study is summarized based on a large number compter runs in figure C.7. The cross-hatched area in Figure C.7 is the suggested tolerance range for a desived or selected number of nodes. The computational results were fitted and resulted in the following exponential shown in figure C.7, which express the tolerance, ϵ (^{o}C), as a function of N, the number of nodes:

$$\epsilon = 103.621 N^{-3.83}. \qquad (C.3)$$

The corresponding tolerance to a certain number of nodes will help to give not only accurate temperatures but also local heat flux. In the latter cases, the suggested curve will be used as a guide to choose the appropriate tolerances and mesh sizes for the numerical data reduction.

In the cases with large conductivity material or very small tube thickness and anticipated ΔT, the accuracy of the temperature and heat flux becomes even more important. The reason for this is that the heat resistance, $R = \frac{\Delta r}{kA}$, is very small. Since $\frac{1}{R}$ is very large, the heat flux, which equals $\frac{\Delta T}{R}$, will be controlled by the factor of $\frac{1}{R}$, but, ΔT is controlled by the factor of R. Hence, for these special attention must be given to both the number of nodes and the corresponding tolerance.

Sample Application 2

The second problem involves one-dimensonal radial heat transfer with known outside surface temperature and heat flux. The solution will present the temperature, the heat transfer coefficient inside the tube.

The governing equation will be same as in Sample 1,

$$\frac{1}{r}\frac{d}{dr}(r\frac{dT}{dr}) = 0 \tag{C.4}$$

The exact solution is identical to that for the previous sample problem; i.e.

$$T(r) = T(R_2) - \frac{q_0}{\frac{ln\frac{R_2}{r}}{2\pi k}} \tag{C.5}$$

where, the rate of heat flow per unit length, q_o, maintains constant between R_2 and R_1.

The governing equation can be presented in finite difference form as:

$$\frac{T(I+1)-T(I)}{R(I)} + \frac{T(I)-T(I-1)}{R(I-1)} = 0 \tag{C.6}$$

Using the notation in figure 5.1 and 5.2, the boundary conditions are:

Assuming that we have $M+1$ nodes, $T(M+1)$ will be known as $T_2 = 100°C$. From equation (C.6), one can compute the temperature next to $T(M+1)$, $T(M)$, directly since q_0 and $T(M+1)$ are known. After $T(M)$ has been computed, $T(M-1)$ can be computed directly from $T(M+1)$ and $T(M)$, and so on. Hence, the inside surface temperature, $T(1)$, can be obtained without iteration. Once $T(1)$ is obtained, for known bulk temperature, the heat transfer coefficient can be obtained from

$$\frac{T(2)-T(1)}{R(1)} = \frac{T(1)-T_f}{\frac{1}{2\pi R_1 h}} \tag{C.7}$$

Figure C.8 shows the temperature distribution in radial direction from numerical and exact solutions. The numerical solutions are at node number of 10, 20, 30, 40, 50, 60, 70 and 80. The largest temperature difference from exact solution is taken place at inside surface and the value is 0.001^0C, which is 0.001% relative error compared with theoretical results. As mentioned in sample application 1, accurate temperatures do not always mean that the solutions are ideal. The heat flux must be cheched also to verify the overall accuracy.

It took long time to figure this phenomena out, because the temperatures were sought of accurate, but heat fluxes had large variations to exact solution. This indicates the problems. One of the reason was that the problem consisted small thickness and large conductivity, which made the temperature difference from outside surface to inside surface extremely small. Therefore, the temperater must be accurate enough in order to get accurate heat flux. The question is that is 0.001% accurate enough? The answer is not for this particular problem. After many times of checking carefully with the FORTRAN program, the question mark finally was turned to the digital computer.

The program for figures C.8 and C.9 was in single precision mode which gave maximum six dicimal digits for any parameters given in program. The double precision mode, which gives forteen decimal digits for parameter was used in the same program, so that the same parameters were plotted to prove the idea. Figure C.10 shows the temperature distribution in radial direction but in double precisoin mode. The temperatures do not have very much difference in figures C.8 and C.10. Figure C.11 shows the same plot as figure C.9 but in double precision mode for heat flux distribution. As it shows, the heat flux for numerical results was same as the supplied heat flux which is $100W/m$. Now, the temperature

solutions are accurate.

The results from Sample 2 can be expressed as that when small thickness and large conductivity involved, the numerical accuracy is strongly affected by thickness and conductivity. In FORTRAN 77, the double precision may be employed for some cases. When the condition is changed for different problems, other method should be developed to double secure the physical accuracy of the numerical solutions.

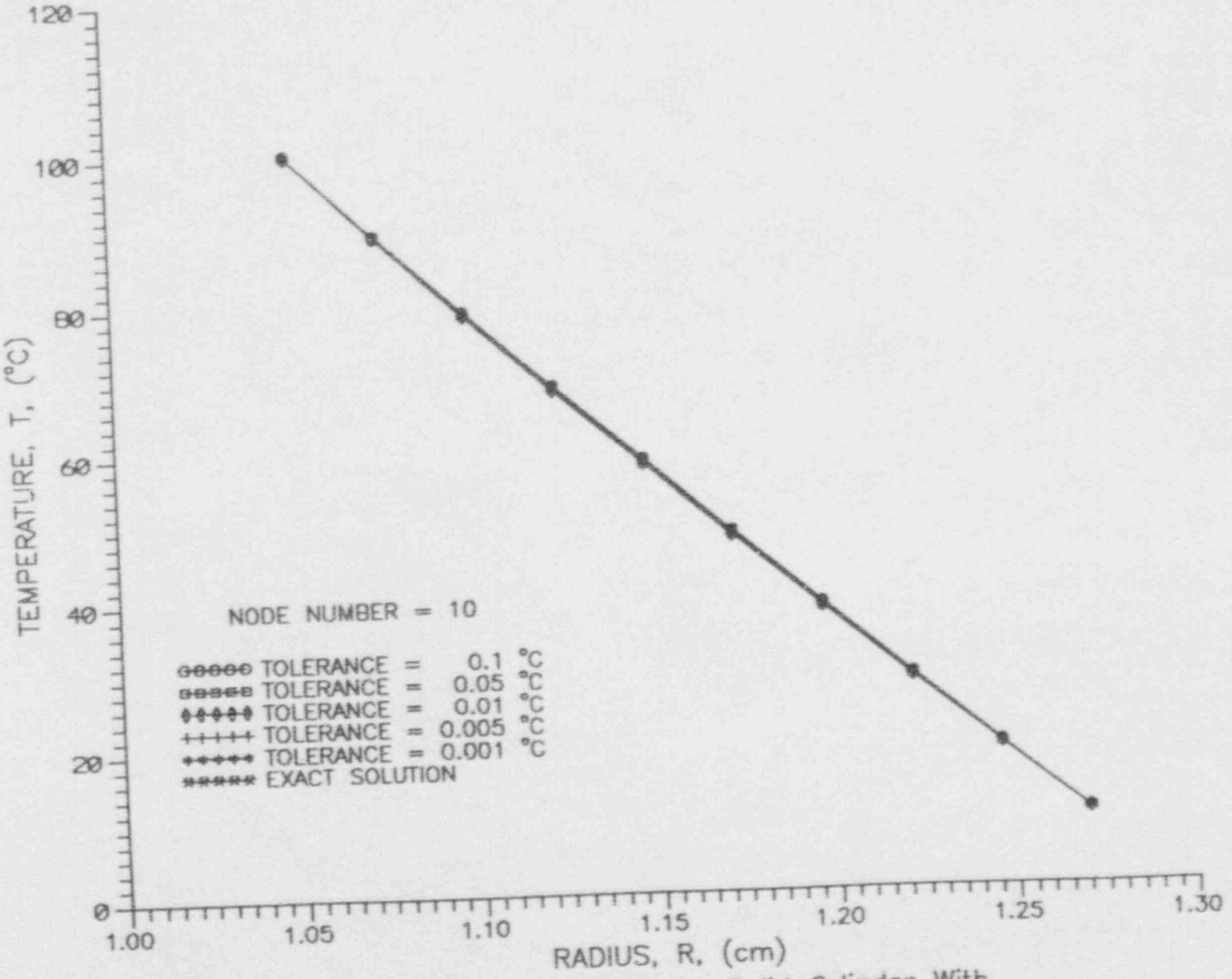

Fig. C.1 1–D Temperature Profile for a Solid Cylinder With Isothermal Boundaries (10 nodes).

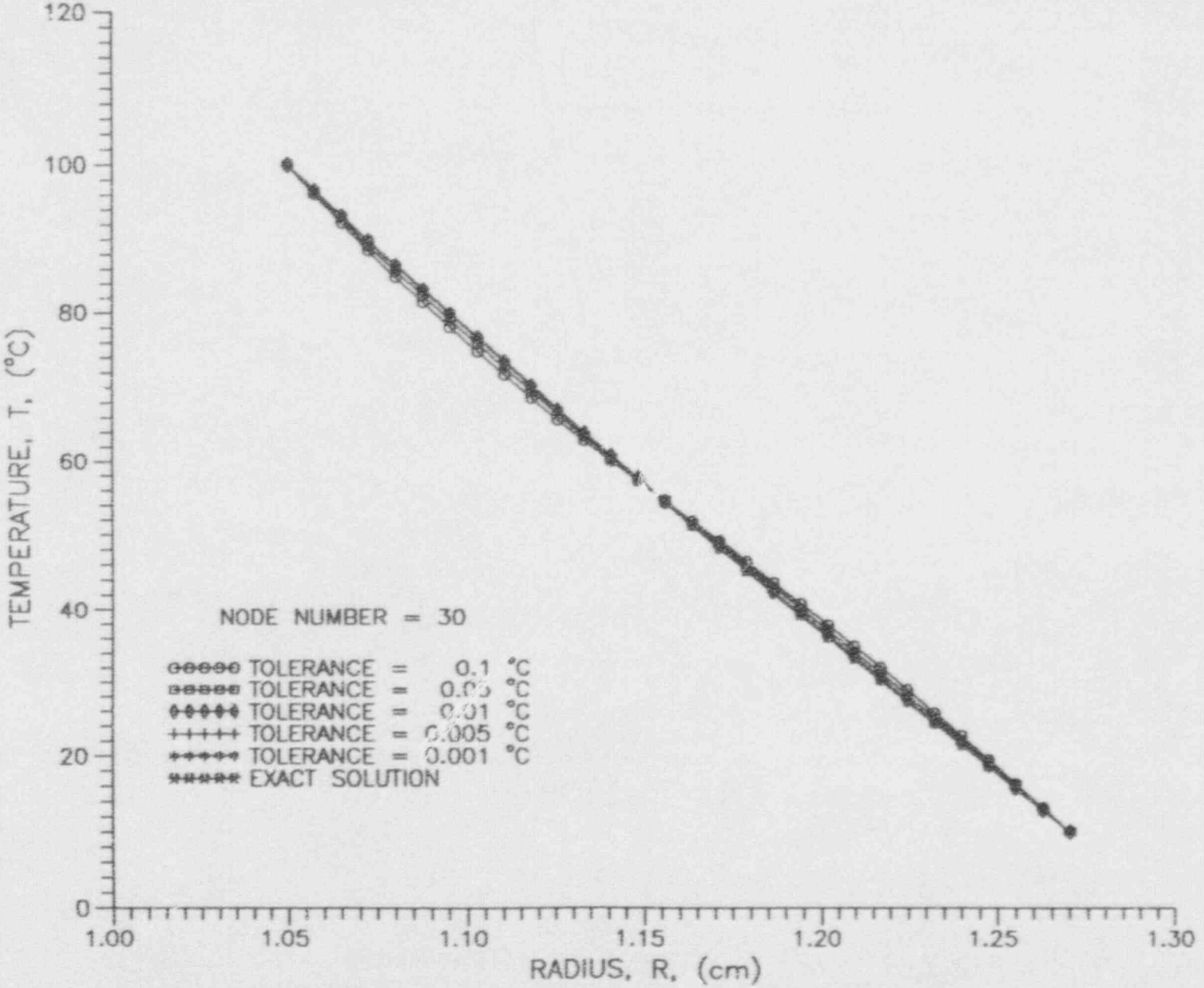

Fig. C.2 1-D Temperature Profile for a Solid Cylinder With Isothermal Boundaries (30 nodes).

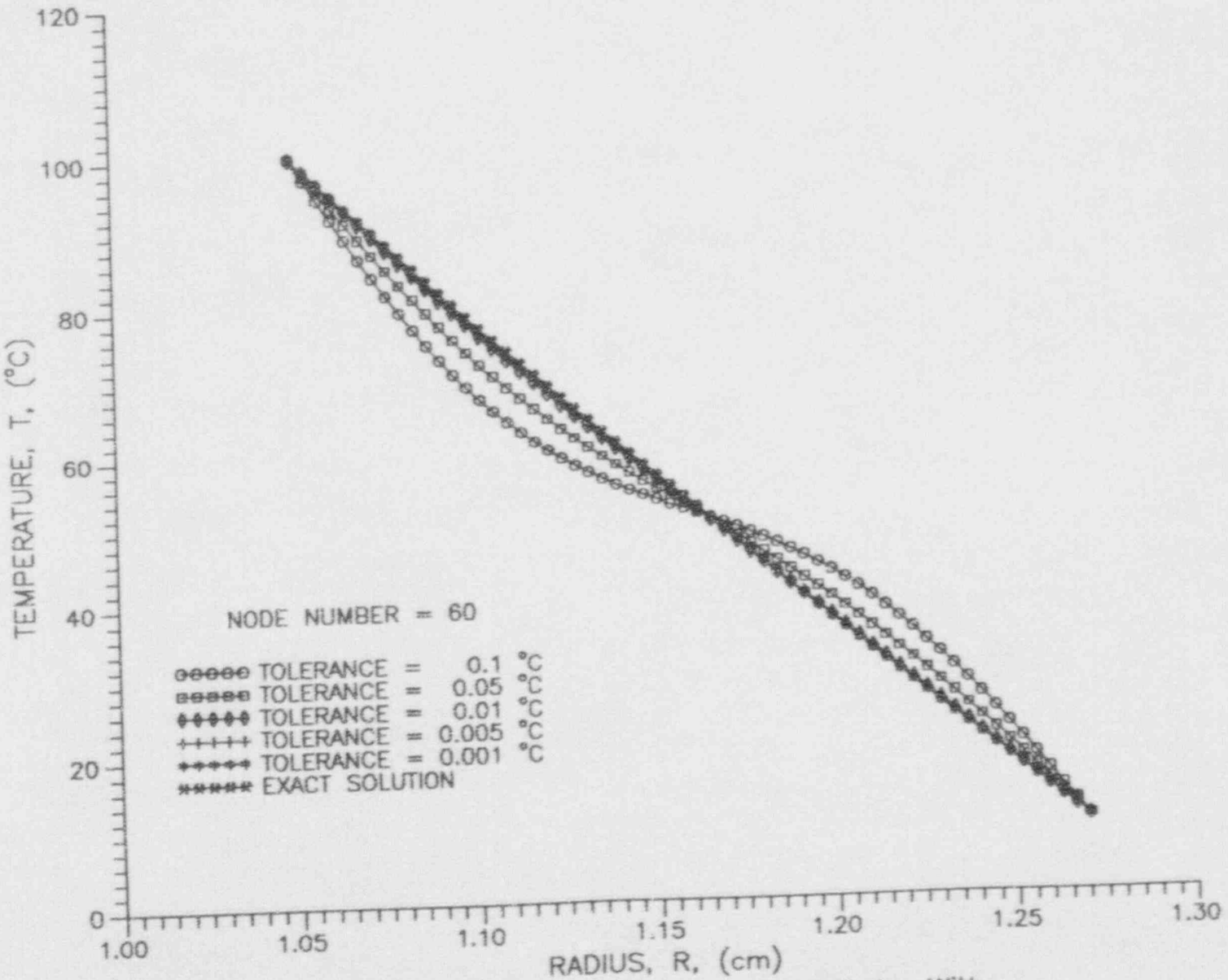

Fig. C.3 1–D Temperature Profile for a Solid Cylinder With Isothermal Boundaries (60 nodes).

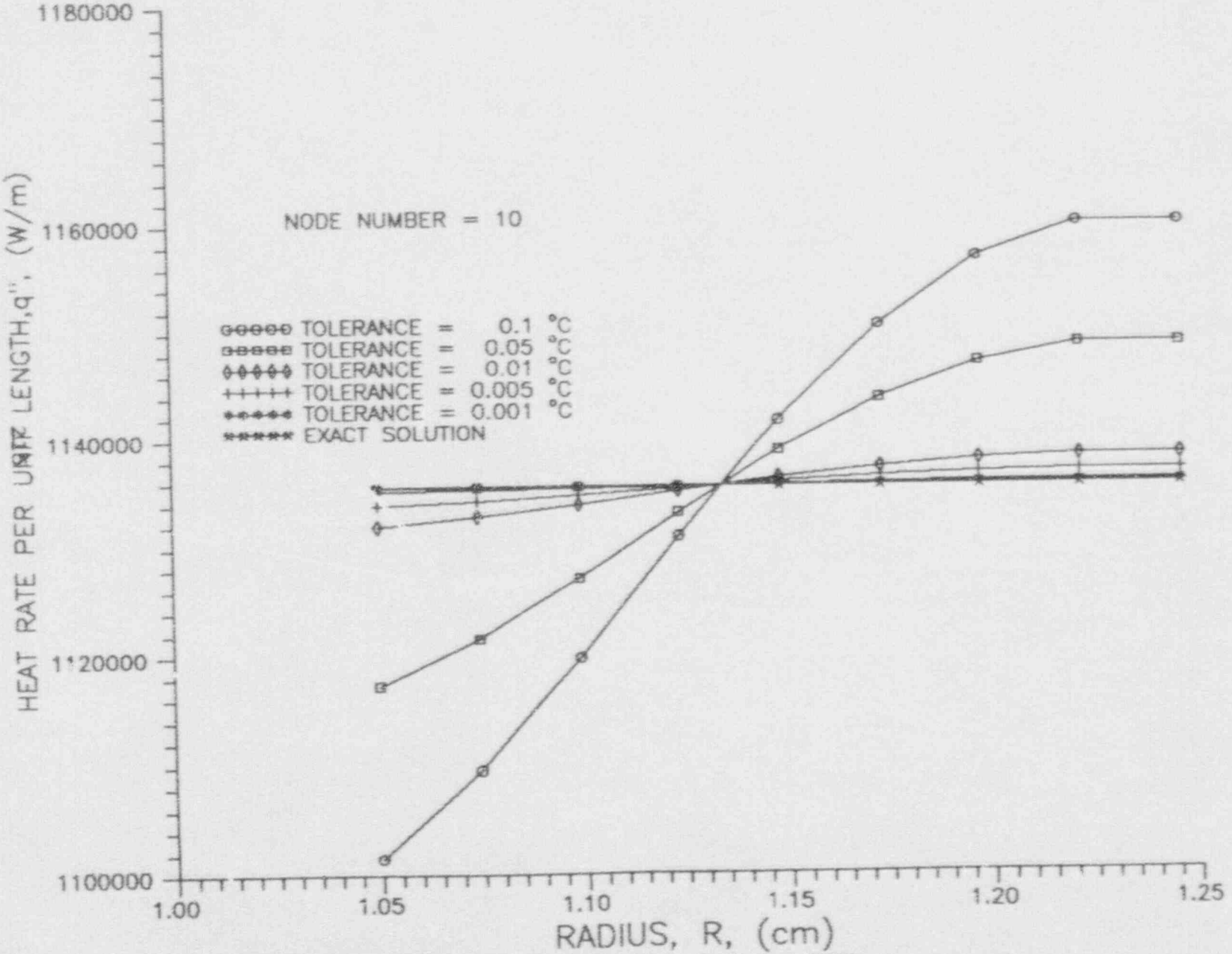

Fig. C.4 1–D Heat Flux for a Solid Cylinder With Isothermal Boundaries (10 nodes).

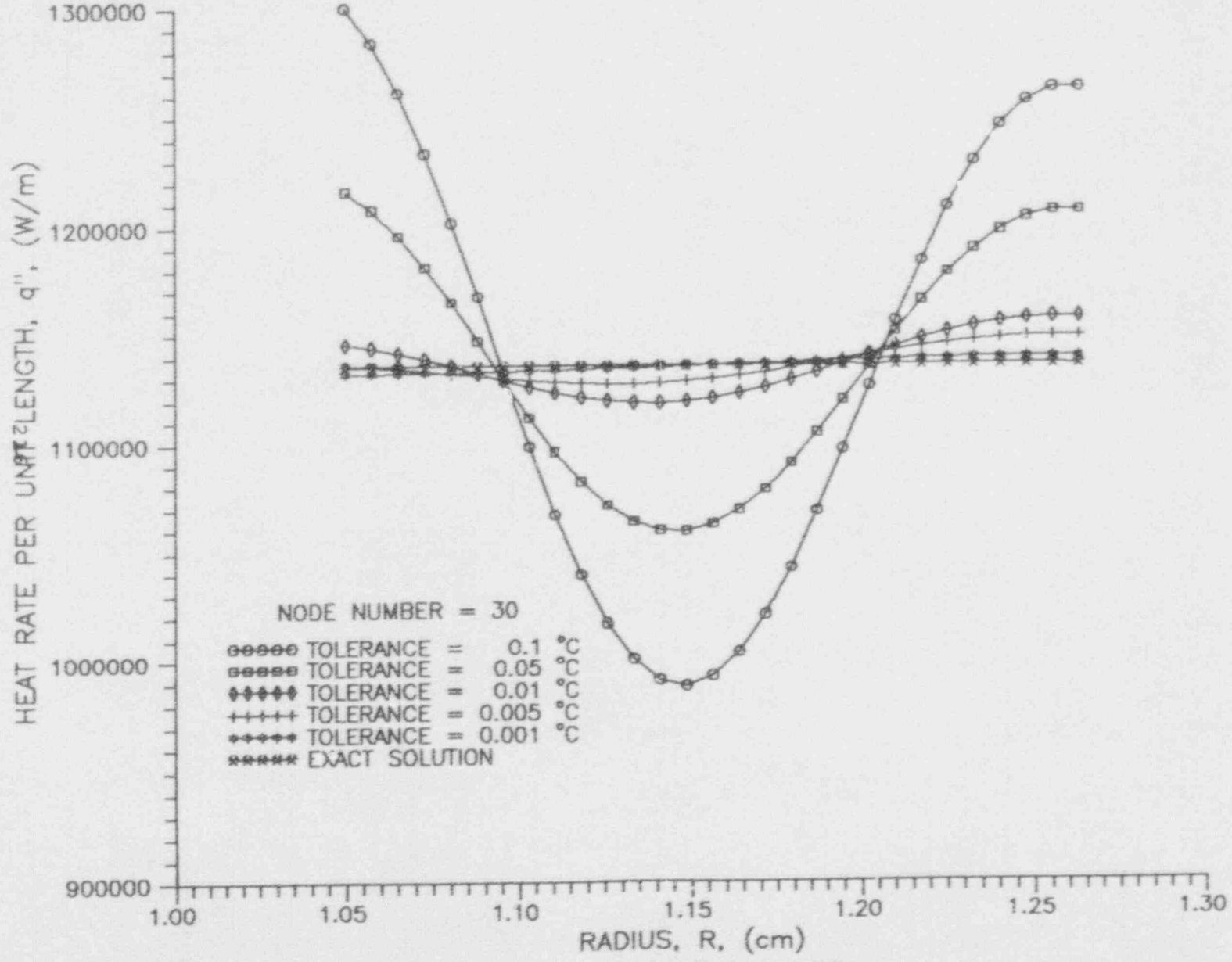

Fig. C.5 1-D Heat Flux for a Solid Cylinder With Isothermal Boundaries (30 nodes).

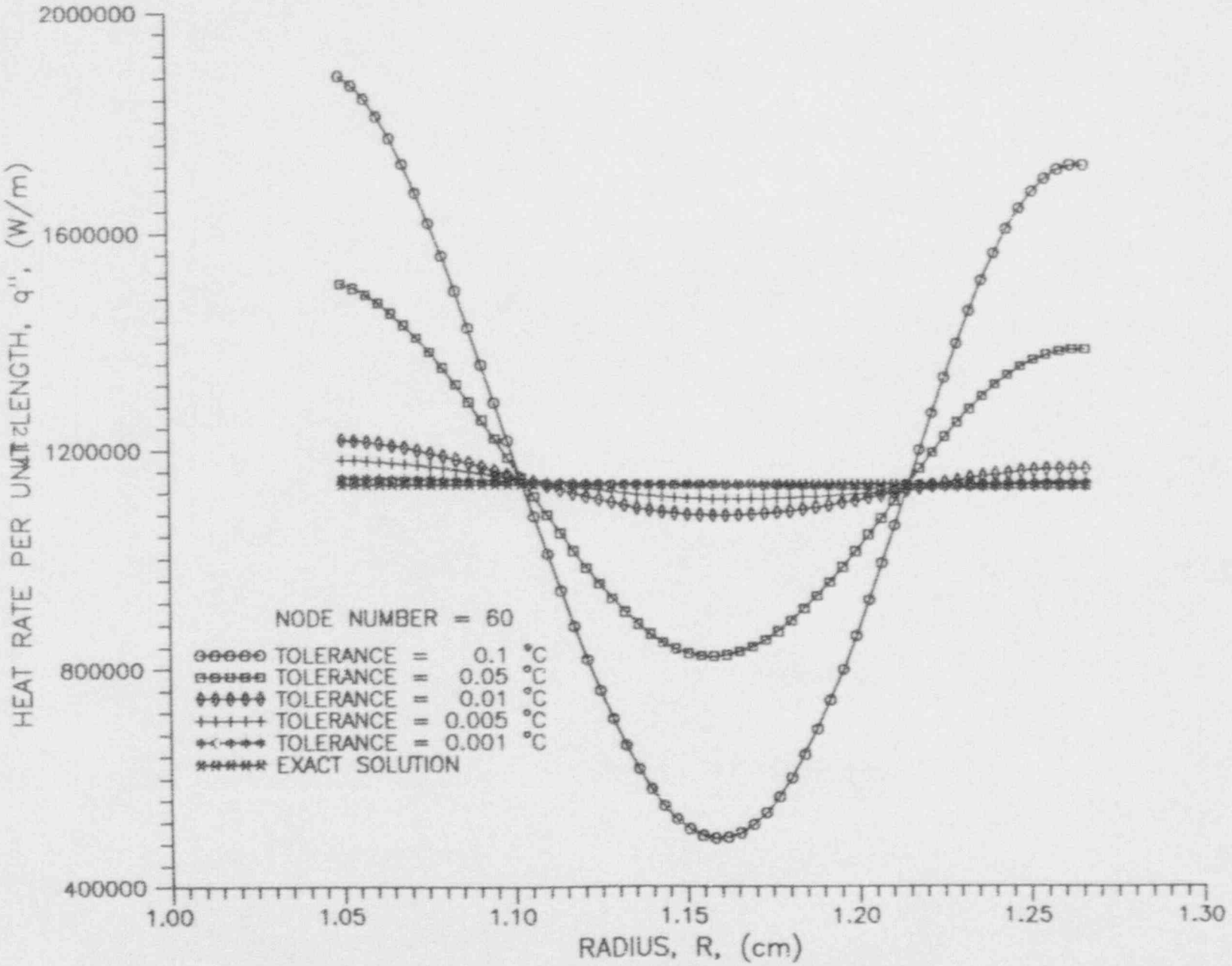

Fig. C.6 1–D Heat Flux for a Solid Cylinder With Isothermal Boundaries (60 nodes).

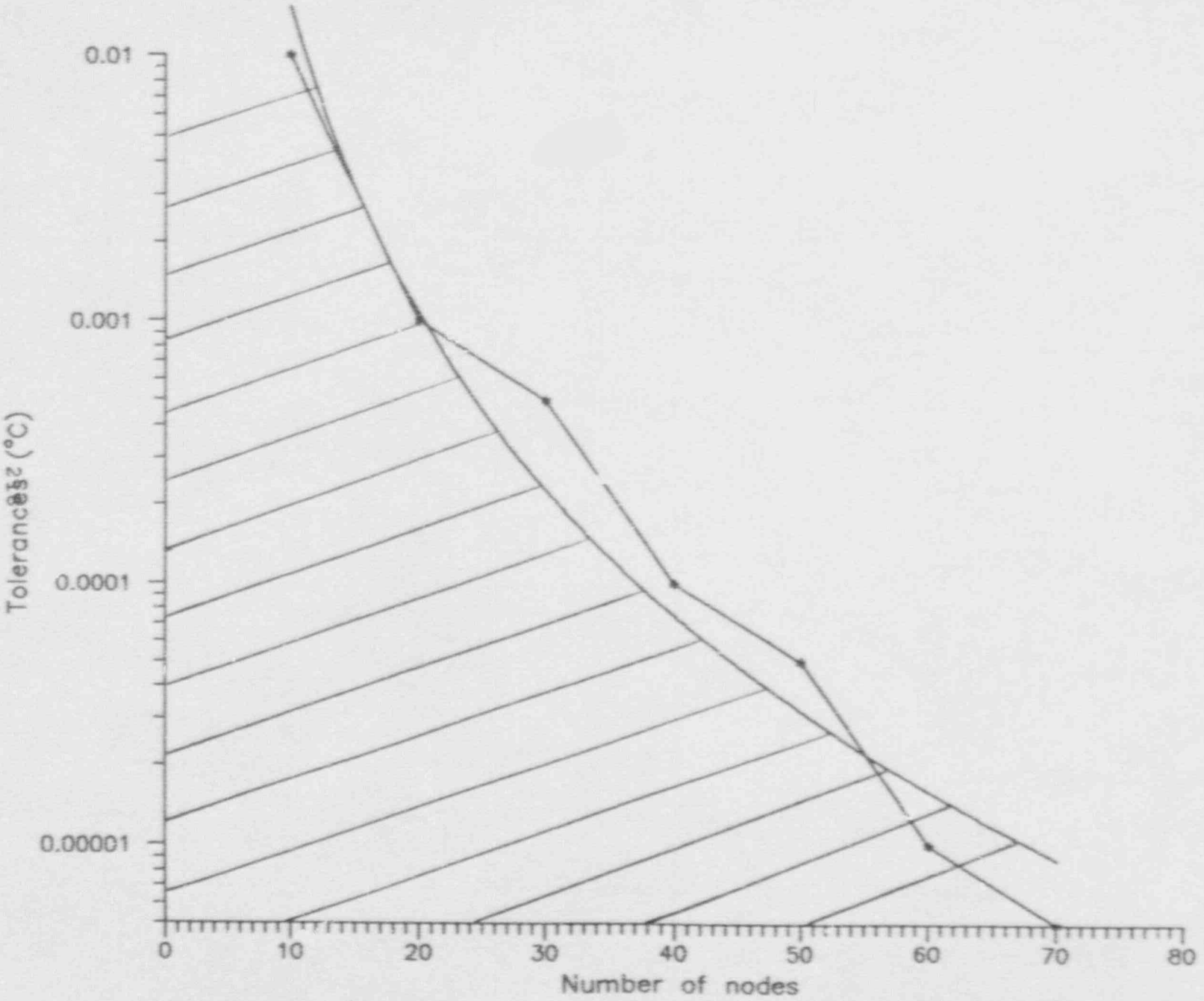

Fig. C.7 Suggested Tolerances for 1–D Radial Conduction With Constant Temperature Boundaries and Constant k.

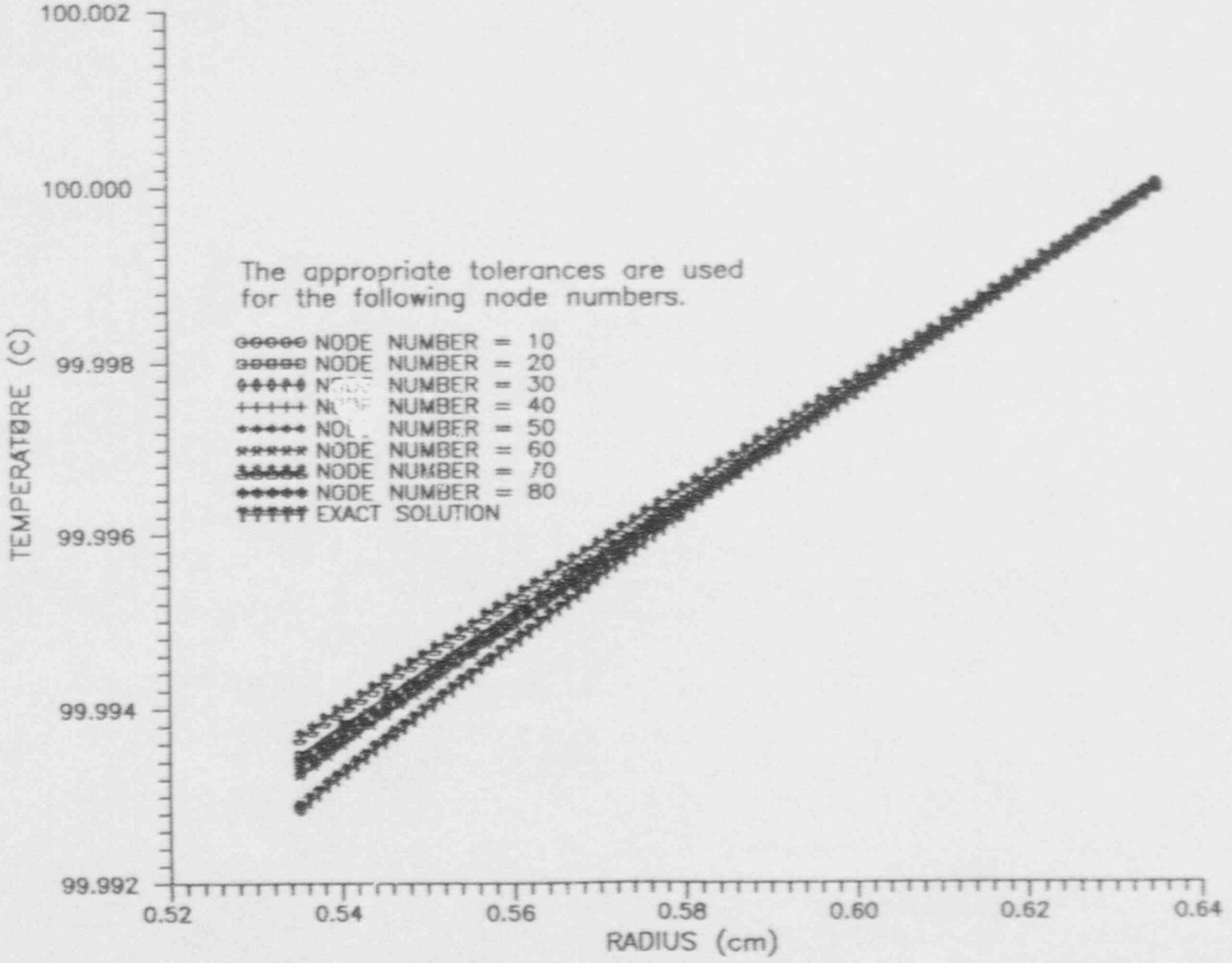

Fig. C.8 Temperature distribution of single precision.

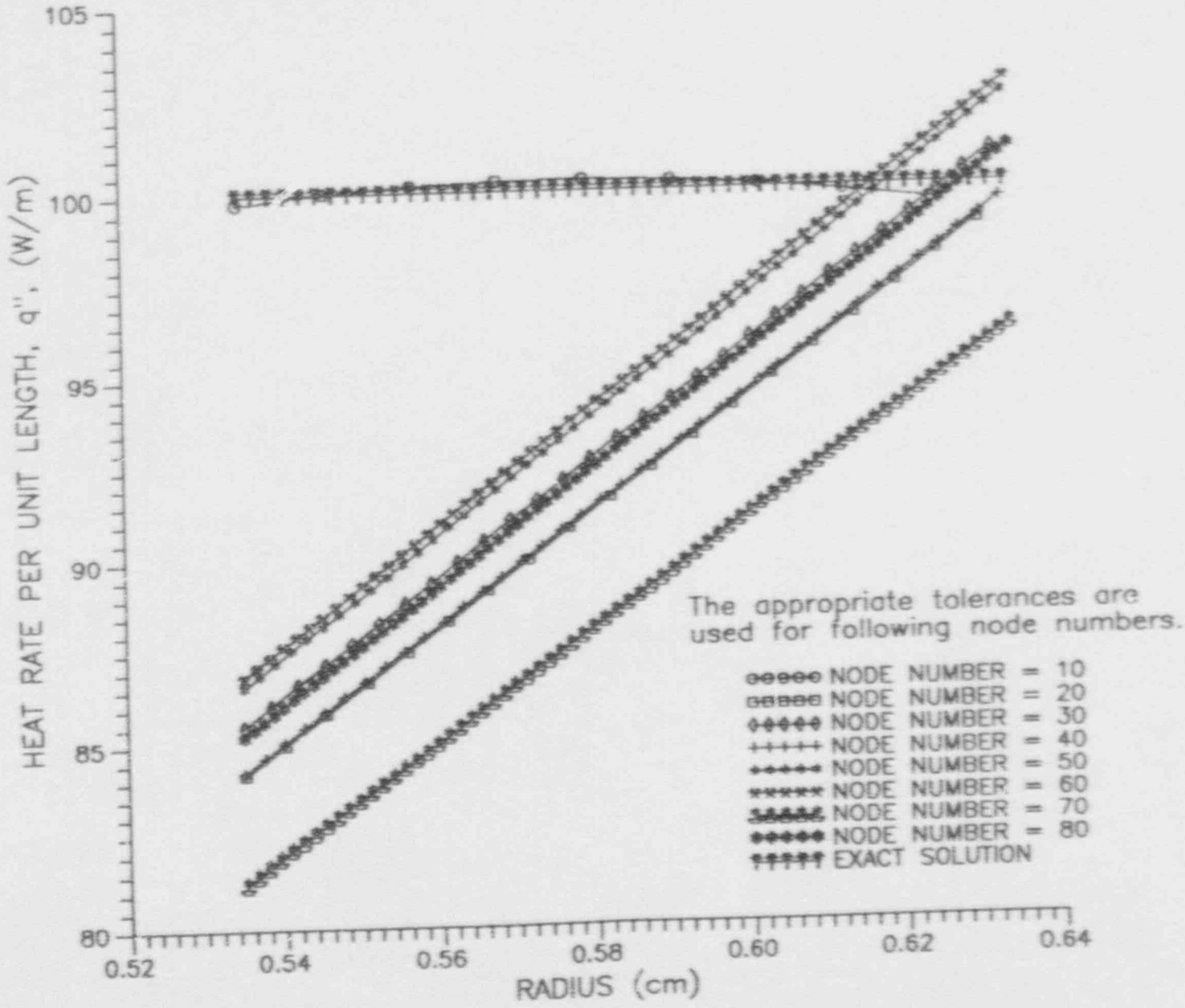

Fig. C.9 Heat Flux Distribution of Single Precision.

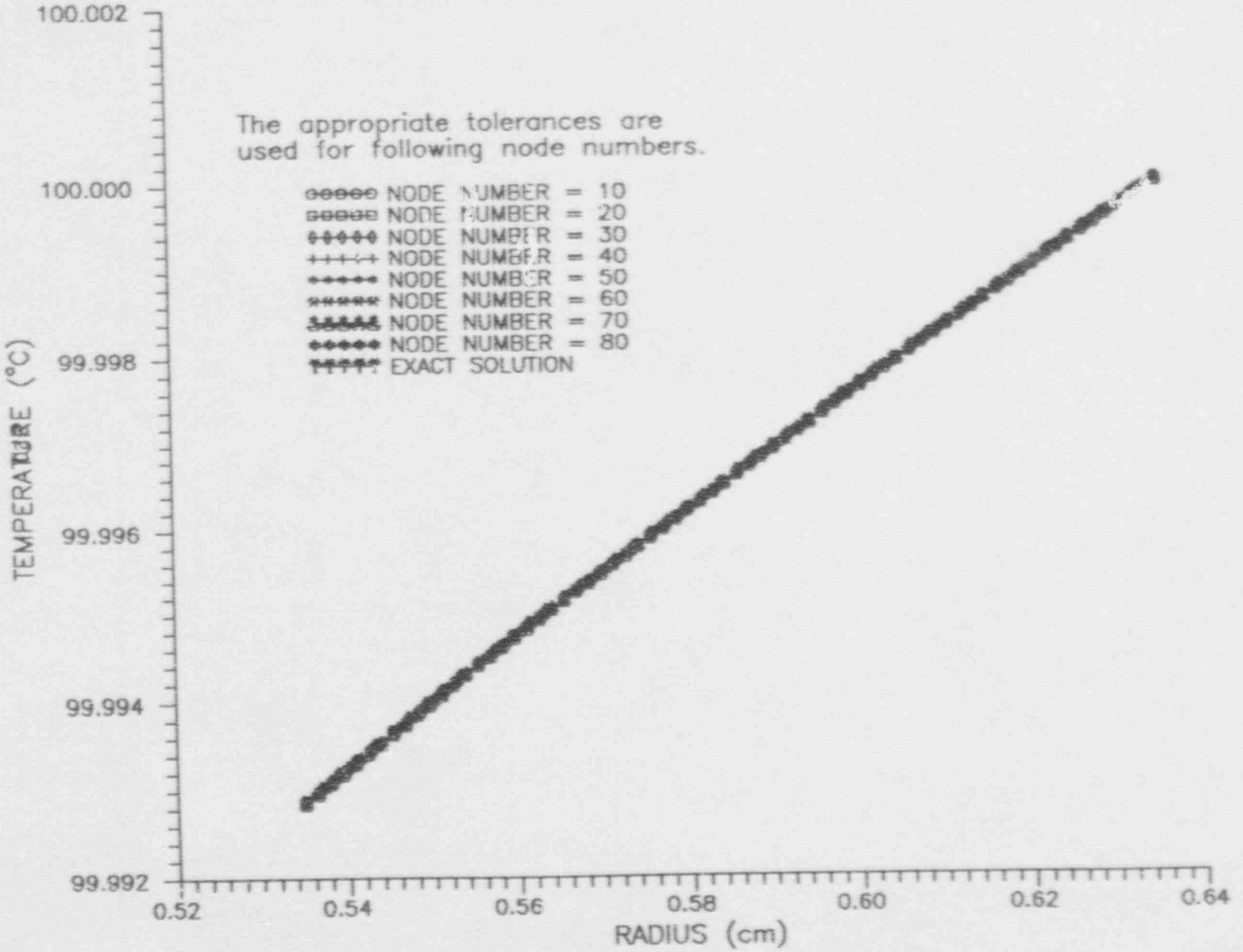

Fig. C.10 Temperature Distribution of Double Precision.

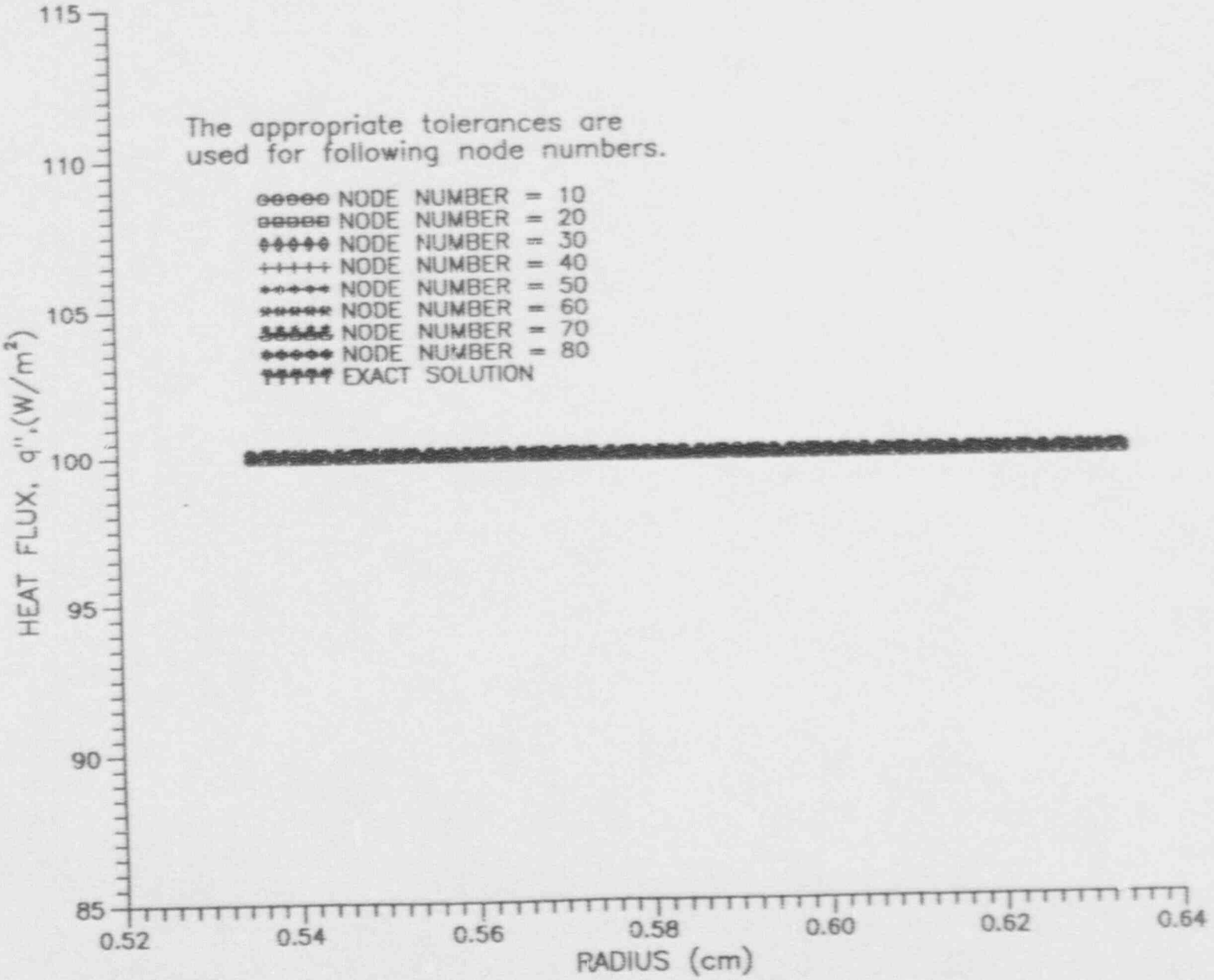

Fig. C.11 Heat flux distribution of double precision.

APPENDIX D

SUBCOOLED FLOW BOILING MODEL ASSESSMENT AND DEVELOPMENT

Performance Report: October 23, 1992

Project # NRC-04-91-364

Submitted to U.S. Nuclear Regulatory Commission

Ronald D. Boyd
Honeywell Endowed Professor of Engineering and
Director of the Thermal Science Research Center
P.O. Box 397
Prairie View A&M University
Prairie View, Texas 77446
Phone: (409) 857-4811 or 4023

Summary:

This is the third performance report for our subcooled flow boiling model assessment and development. The objectives of this research is to improve our present ability to predict both local heat transfer and the critical heat flux (CHF) in the subcooled flow boiling regime for the case of uniformly heated coolant channels. Although water is presumed to be the primary fluid, comparisons may be with data for other fluids.

During this funding period, more emphasis has been placed on local predictions of heat transfer using the "patched" model referred to in item #3 of part I of the milestones. This model will be referred to here after as the "modified model" (MM). This emphasis involved: (1) MM development, and (2) data reduction model development (DRMD). The MM development included model: (1) development, (2) implementation, (3) comparison, and (4) verification. The DRMD is an additional task which was found necessary to be added to the Part I milestones (local heat transfer).

PROGRESS:

As our work progressed, we have found it necessary to alter the previously submitted milestones. This became obvious when work began on item #4, 7, 9, and 10 of Part I of the Milestones. In these items, the preliminary correlation and the MM were to be compared with data other than but including the 0.77 MPa water data, which were used in comparisons summarized in the last progress report (April 28, 1992). However before the rationale for the need of the DRMD in discussed, some results associated with MM development will be summarized.

The MM development is a continuation of efforts to refine and imm-prove the "new (preliminary)" correlation (NPC) discussed in the last progress report. The worst agreement between predictions and the data was noted to be in the partial nucleate boiling regime. The need for the MM resulted from an attempt to improve and possibly simpify the NPC. Although there was an improvement in the overall accuracy, the improvement amounted to less than 1.0%. However, these results show that the basis or premise for making the improvement was sound and should result in greater improvement. The MM provides an approximation for the asymptotic limit. However, the scope of the present contract does not allow for

finding the "true" limit. If additonal funding becomes available, this "true" asymptotic limit condition can be determined. This should result in additional improvements in the predictive accuracy inn the partial nucleate boiling region and possibly wider applicability of the correlation to other fluids. Presently, the MM employs a "patching" condition which approximates the "true" asymptotic limit. This was accomplished by requiring the transition from single-phase to partial nucleate boiling to occur when the wall temperature reached the saturation temperature. In particular, the following conditions were required by the NPC but are not by the MM: (1) the slope, m, of the subcooled boiling curve linearly increases with heat flux in the partial nucleate boiling regime, (2) accurate prediction of the onset to nucleate boiling (ONB) is essential, (3) $m = 1.0$ at ONB, and (4) $m = 2.0$ at the onset of fully developed boiling. In addtion, no arbitrary assumptions for the values of m were made as the heat flux changes for the MM. Further, there **are no** empirical constants in the MM and the form of the correlation appears to make it applicable to water and other fluids.

As a result, the slope, m, for the MM will have a different non-linear variation for different fluids in the partial nucleate boiling region. Prediction of the ONB is not needed for the MM. Finally, the lower and upper limits

of m will vary from fluid to fluid, and will also be related to the flow and fluid thermodynamic specifications.

The MM correlation parameters for the partial nucleate boiling region have a specified, closed-form relationship with: (1) the local heat flux, and (2) the thermodynamic state of the fluid. Both the MM and the NPC require the flow to be fully-developed hydrodynamicallyy and thermally. Although this is a definite limitation, this limitation is less severe near the exit of the channel where the greatest prediction accuracy occurs. If additonal funding becomes available, the present correlations could likely be improved by accouting for the flow development nature.

The results show that although the MM is not simpler, it is based on less assumptions and has more accurate predictions of the heat transfer coefficient in some cases than the NPC. The MM has the potential to apply to many fluids (with a preliminary Prandtl number range of 0.5 to 200), but the NPC applies only to water.

For the present, both correlations apply in the region where the Stanton number is less than 0.006 and the Peclet number is greater than 10^5, which corresponds to high velocity and high subcooled flows. Thus far, comparisons have been made for both models with 354 water data points at 0.77

MPa and 1.66 MPa. The MM had better accuracy, relative to the NPC, of 12.5% compared to 13.5% at 1.66 MPa for 185 data points. However at 0.77 MPa the NPC had 18.6% and the MM 19.0% standard deviation.

Comparisons of the NPC and Kandlikar's model with the water data at 0.77 MPa showed that the NPC and the MM consistently have better comparisons with the data. There are two basic reasons for this. First, Kandlikar used the Dittus-Boelter equation (DBE) for all single-phase computations. As reported in the literature, the DBE uses the bulk temperature as the characteristic temperature. Since the correlations for all regions (partial nucleate and fully developed boiling regions) rely indirectly on a single-phase correlation, all Kandlikar's predictions fall significantly below the data. Finally, there are severe discontinuities in Kandlikar's correlation at ONB and the onset to fully developed boiling. These discontinuities do not exist in either the NPC or the MM.

Improved predictions can be obtained with Kandliker's correlation provided the DBE is modified by using the film temperature as the characteristic tempertature. However, the discontinuities remain. The improvement in agreement results in most cases due to his correlation crossing the data at a point. Of course, the predictions are "perfect" at the point of intersection

with the data and "poor" elsewhere. By contrast, both the MM and NPC have the same trends and curve slope variations as the data.

We are preparing to make additional comparisons with freon-11 data. Preliminary comparisons with some freon data at 0.187 MPa showed favorable trends. However this data, and possibly other data which will be found in the literature, was obtained from local measurements of the outside wall temperature. At a given axial location, investigators computed a circumferentially averaged outside wall temperature. This averaged wall temperature was then used to compute inside wall temperature and heat transfer coefficient using the total heat flux and fluid conditons. The accuracy of the resulting heat transfer data, based on this data reduction approach may not always be acceptable especially if there are circumferential variations in the measured wall temperatures. Any heat transfer coefficient data must result from accurate values of the inside wall temperature. Since it is not possible to measure this latter temperature, its' accurate determination may be possible from the former by employing a finite-different formulation to relate the two. This formulation is refered in this report as the data reduction model development (DRMD).

As a result of the above noted deficiency in the way the freon-11 data

was reduced, the DRMD was added to the Part I milestones. This finite difference model will be used to accurately reduce and relate the outside wall temperature measurements to inside wall temperatures and the heat transfer coefficient. These indirectly measured heat transfer coefficients will provide an improved data base for freon-11, which we will be able to use to make comparisons with both the MM and NPC. The DRMD has been developed, programmed, and is being implemented. Preliminary testing of the routine is in process.

STATUS

The work is proceeding well. As noted above, our current progress necessitated a change in the milestone for Part I. Another task had to be added in order to complete tasks 4,7,9 and 10. This new task involved developing a data reduction model. With this inclusion, greater emphasis has been placed on part I of the milestones. All CHF correlations except Lee and Mudawar, and Vandervort have been obtained. A CHF data source has been identified and will be requested.

As of now, no other additions are anticipated. Due to the above noted addition, some of the original milestone tasks may have to be redistributed

or eliminated.

DISTRIBUTION:

1. Division of Contracts
   US Nuclear Regulatory Commission
   Office of Nuclear Regulatory Research
   Washington, D.C. 20555

2. U.S. Nuclear Regulatory Commission (3)
   Office of Nuclear Regulatory Research
   Attn: Dr. Frank Odar, Mail Stop NLS-353
   Washington, DC 20555

3. U.S. Nuclear Regulatory Commission (2)
   Division of Technical Information and Document Control
   Document Management Branch
   Washington, D.C. 20555

4. S. Crampton, ADM/CABI
   U.S. Nuclear Regulatory Commission
   Washington, D.C. 20555

5. Dr. Ronald D. Boyd (3)
   Honeywell Professor of Engineering and
   Director of the Thermal Science Research Center
   Prairie View A&M University
   Prairie View, Texas 77446

6. Mr. Bruce Cunningham
   Prairie View A&M Resear . Foundation
   P.O. Box 3578

College Station, Texas 77343

SUBCOOLED FLOW BOILING MODEL ASSESSMENT AND DEVELOPMENT

Performance Report: April 28, 1992

Project # NRC-04-91-364

Submitted to U.S. Nuclear Regulatory Commission

Ronald D. Boyd
Honeywell Endowed Professor of Engineering and
Director of the Thermal Science Research Center
P.O. Box 397
Prairie View A&M University
Prairie View, Texas 77446
Phone: (409) 857-4811 or 4023

Summary:

This is the second performance report for our subcooled flow boiling model assessment and development. The objectives of this research is to improve our present ability to predict both the critical heat flux (CHF) and local heat transfer in subcooled flow boiling regime for the case of uniformly heated coolant channels. Although water is presumed to be the primary fluid, comparisons may be made with data for other fluids.

Because of many dimensionless parameters affecting local heat transfer and contributing to aspects of CHF, we are proceeding with our assessment of both CHF and local heat transfer simultaneously. In these efforts, a graduate student has been used to assist in the local heat transfer assessment, and an undergraduate has been assisting in the CHF assessment.

Summaries of the milestones for both the local heat transfer and CHF work are enclosed. The actual accomplishments compare well with the anticipated work outlined for the local heat transfer assessment. However, our anticipated progress on CHF was hampered. This occurred because more time than anticipated was needed to work with the undergraduate student. Nevertheless, a comparison of the work described below with the milestones shows that all milestones were met.

The literature survey is proceeding. An example of some of the important work was noted in the last performance report. The literature survey will include: (1) local and mean heat transfer correlations which may or may not have a theoretical basis, (2) CHF phenomenological and empirical correlations, and (3) supportive literature for model development.

The anticipated local heat transfer work (see item # 1,2, and 3 from the heat transfer milestones) was completed during this past funding period. Using existing correlations where possible, much of our work has been devoted to developing a preliminary heat transfer correlation by matching the single-phase, partial nucleate boiling, and developed flow boiling regimes. Comparisons, made with 186 data points for water at 0.77 MPa, have resulted in an overall standard deviation of less than 14%. We now seek to compare this new (preliminary) correlation with a different published correlation by Kandlikar for the partial subcooled nucleate boiling region. Comparisons will be made with other subcooled data and correlations if they are found in the literature. The present comparisons show that the worst agreement between the predictions and data is in the partial nucleate boiling region. We will be attempting to alter the present matching conditions to improve the predictions in this region. We will also make

local heat transfer predictions in the regions near the anticipated CHF so that any thermophysical parametric relationships can be identified.

The CHF work has focused on a reexamination and verification of Gambill correlation (item #1 of the CHF milestones) for both very high heat flux levels and very large channel length-to-diameter ratios. Based on temperature-dependent properties, sample predictions at 1.66 MPa were used as a basis to develop a computer program for CHF (item #2 of CHF milestone) predictions. The preliminary interactive predictions agreed, qualitatively, with data reported in the literature. We anticipated completing the CHF computer program based on Gambill's correlation. However, more time than anticipated was needed for the sample prediction. After the program has been completed, predictions will be used to make quantitative comparisons with available subcooled CHF data as well as other CHF correlations. Additional work is proceeding to debug and test the program.

There may be a cost overrun up to this point. The main reason for this is as follows: We were able to identify two students (both undergraduate and graduate students) who we thought were capable and who would benefit from this experience. We will attempt to make other adjustments to compensate for any apparent overrun.

Distribution:

1. Division of contracts (1)
U.S. Nuclear Regulatory Research
Office of Nuclear Regulatory Research
Washington, D.C. 20555

2 U.S. Nuclear Regulatory Commission (3)
Office of Nuclear Regulatory Research
Attn: Dr. Frank Odar, Mail Stop NLS-353
Washington, D.C. 20555

3 U.S. Nuclear Regulatory Commission (2)
Division of Technical Information and Document Control
Document Management Branch
Washington, D.C. 20555

4 S. Crampton, ADM/CABI (1)
U.S. Nuclear Regulatory Commission
Washington, D.C. 20555

5 Dr. Ronald D. Boyd (6)
Honeywell Professor of Engineering and
Director of the Thermal Science Research Center
Prairie View A&M University
Prairie View, Texas 77446

Attachments:
(1) Local Heat Transfer Milestones for 1991-1992 and 1992-1993, and
(2) CHF Milestones for 1991-1992 and 1992-1993.

FUNDING SOURCE: NUCLEAR REGULATORY COMMISSION (NRC)

Part I: Local Heat Transfer Milestones

Project Title: Subcooled Flow Boiling Model Assessment and Development	Number NRC-04-91-364

Milestones	1991 J F M A M J J A S O N D	1992 J F M A M J J A S O N D
1. Literature Survey (Local and Mean Correlations): Theoretical and Empirical Correlations.		
2. Selection of Preliminary Correlations for Characterizing Single Phase, Partial Nucleat Boiling, and Fully Developed Boiling		
3. Initial "Patching"/"Matching" of Preliminary Correlations and Assessment of Agreement With Subcooled Water Data at 0.77 MPa.		
4. Comparison of Preliminary Correlation with Available Freon-II Data from Lab Experiments.		
5. Improved Matching, if needed using suitable Asymptotic Limits.		
6. Accuracy Assessment of Results		
7. Identification of Other Data and/or Correlations--and Comparison With Previous Results.		
8. Preliminary Selection of Theoretical Approaches Based on Literature and Correlational Data Comparisons (Preliminary Model).		
9. Develop Data Base for Subcooled Heat Transfer for Other Water and Nonaqueous Data.		
10. Comparisons of Recommended Correlations With Data Base.		
(a) Heat flux vs h.		
(b) Heat flux vs Tw.		
11. Formulation of the Theoretical Model-- Correlational Approach.		
(a) Inclusion of Normal Convective Effects.		
(b) Assessment and/or Inclusion of Viscous Dissipation Effects.		
(c) Laminar Formulation.		
(d) Tubulent Formulation.		
(e) Possibility of Single-Side Heat Flux Inclusion Using the Existing Formulation.		
12. Reporting and Technical Paper Development.		

FUNDING SOURCE: NUCLEAR REGULATORY COMMISSION (NRC)

Part I: Local Heat Transfer Milestones

Project Title: Subcooled Flow Boiling Model Assessment and Development	Number NRC-04-91-364

Milestones	1992 J F M A M J J A S O N D	1993 J F M A M J J A S O N D
1. Literature Survey (Local and Mean Correlations): Theoretical and Empirical Correlations.	———	———
2. Selection of Preliminary Correlations for Characterizing Single Phase, Partial Nucleate Boiling, and Fully Developed Boiling.		
3. Initial "Patching"/"Matching" of Preliminary Correlations and Assessment of Agreement With Subcooled Water Data at 0.77 MPa.		
4. Comparison of Preliminary Correlation with Available Freon-II Data from Lab Experiments.		
5. Improved Matching, if needed using suitable Asymptotic Limits.		
6. Accuracy Assessment of Results		
7. Identification of Other Data and/or Correlations--and Comparison With Previous Results.		
8. Preliminary Selection of Theoretical Approaches Based on Literature and Correlational Data Comparisons (Preliminary Model).		
9. Develop Data Base for Subcooled Heat Transfer for Other Water and Nonaqueous Data.	———	———
10. Comparisons of Recommended Correlations With Data Base.	———	———
(a) Heat flux vs h. (b) Heat flux vs Tw.		
11. Formulation of the Theoretical Model--Correlational Approach.	———	———
(a) Inclusion of Normal Convective Effects. (b) Assessment and/or Inclusion of Viscous Dissipation Effects. (c) Laminar Formulation. (d) Tubulent Formulation. (e) Possibility of Single-Side Heat Flux Inclusion Using the Existing Formulation.	———	———
12. Reporting and Technical Paper Development.	———	———

FUNDING SOURCE: NUCLEAR REGULATORY COMMISSION (NRC)

Part II: CHF Milestones

Project Title: Subcooled Flow Boiling Model Assessment and Development			Number NRC-04-91-364
Milestones	1991 J F M A M J J A S O N D	1992 J F M A M J J A S O N D	
1. Verification of Gambill's Correlation at Isolated Points.			
2. Development of a Computer Program for Gambill's Correlation and Comparison With Data at 0.77, 1.66, and 0.45 MPa, and Documentation of Results.			
3. Compare CHF Water data at 0.77 MPa With Preliminary Heat Transfer Correlation at the Point of the Onset of Fully Developed Boiling.			
4. Repeat items # 1-3 with other CHF Correlations: (a) Weisman (b) Katto (c) Lee and Mudawar (d) Vandervort, and (e) Tong-75			
5. Identify Other Data Suitable for use in Above Correlations.			
6. Literature Survey.			
7. Adaptation of Tong-75 and Other Correlations to Single Side Heating and Comparison to Available Data: Sandia, Japanese, Italian, etc.			
8. Proposed Mechanism(s) and Model for Identity or Correlation of CHF & Describe Basis.			
9. Investigate the Fundamental Thermodynamic Definition of Work and Add Surface Tension into the Fundamental Thermodynamics. Does the Definition of Enthalpy Need Redefining to Include the Contribution From the Extra Work Term?			

FUNDING SOURCE: NUCLEAR REGULATORY COMMISSION (NRC)

Part II: CHF Milestones

Project Title: Subcooled Flow Boiling Model Assessment and Development	Number NRC-04-91-364

Milestones	1992 J F M A M J J A S O N D	1993 J F M A M J J A S O N D
1. Verification of Gambill's Correlation at Isolated Points.		
2. Development of a Computer Program for Gambill's Correlation and Comparison With Data at 0.77, 1.66, and 0.45 MPa; and Documentation of Results.		
3. Compare CHF Water data at 0.77 MPa With Preliminary Heat Transfer Correlation at the Point of the Onset of Fully Developed Boiling.		
4. Repeat items # 1-3 with other CHF Correlations: (a) Weisman (b) Katto (c) Lee and Mudawar (d) Vandervort, and (e) Tong-75		
5. Identify Other Data Suitable for use in Above Correlations.		
6. Literature Survey.		
7. Adaptation of Tong-75 and Other Correlations to Single Side Heating and Comparison to Available Data: Sandia, Japanese, Italian, etc.		
8. Proposed Mechanism(s) and Model for Identity or Correlation of CHF & Describe Basis.		
9. Investigate the Fundamental Thermodynamic Definition of Work and Add Surface Tension into the Fundamental Thermodynamics. Does the Definition of Enthalpy Need Redefining to Include the Contribution From the Extra Work Term?		

SUBCOOLED FLOW BOILING MODEL ASSESSMENT AND DEVELOPMENT

Performance Report: January 30, 1992

Project # NRC-04-91-364

Ronald D. Boyd
Honeywell Endowed Professor of Engineering and
Director of the Thermal Science Research Center
P.O. Box 397
Prairie View A&M University
Prairie View, Texas 77446
Phone: (409) 857-4811 or 4023

RE: Performance Report #1: "Subcooled Flow Boiling Model Assessment".

In accordance with your previous request, I am submitting a summary of our work on contract NRC-04-91-364. The objectives of this work are to make comparisons and assessments of both local heat transfer and critical heat flux for the subcooled flow boiling regime.

Summary:

Although there are numerous two-phase heat transfer and CHF correlations, many of these correlations are severely restricted to specific parameter ranges, fluids, and flow regimes.

After an initial review of the literature and preliminary calculations, we have chosen to use a combination of correlations to examine the local heat transfer in the non-boiling and subcooled flow boiling regimes for a uniformly heated circular coolant channel. Initial comparisons will be made with data for water under conditions of high velocity and subcooling, and with an exit channel pressure of 0.77 MPa.

Although comparisons with other local heat transfer correlations will be made later, those correlations that are summarized below are the ones that we are including in our assessment computer program. For the single-phase flow, we will use Petuhkov's[1] correlation. The onset of nucleate boiling (ONB) will be initially examined using the Bergles and Rohsenow[2] correlation, but will later be compared with correlations by Frost and Dzakowic[2], Davis and Anderson[3], and others. A simple matching criteria is being used to describe the partial nucleate boiling region in terms of the ONB, the point at which fully developed nucleate boiling occurs, and the slopes

of the boiling curves at these two points. Shah's work[4] is being used for the fully developed flow boiling regime. With these correlations, we should be able to reproduce the entire subcooled flow boiling curve.

As far as subcooled CHF is concerned, we are presently verifying previous assessments which recommended correlations by Gambill[5] and Tong for CHF in highly subcooled and high velocity flows. One of our students is now examining Gambill's correlation to verify CHF predictions and data comparisons at 0.77 MPa. Other correlations and data sets will be added to this assessment later.

We are also making some efforts to look at previous fundamental theoretically-based models, which may provide insight in correlation improvement.

REFERENCES :

1. B. S. Petukhov, "Heat Transfer and Friction in Turbulent Pipe Flow with Variable Physical Properties," Advances in Heat Transfer, Vol. 6, Academic Press, 1970, pp 503-564.

2. J. G. Collier, Convective Boiling and Condensations, McGraw-Hill Inc.,

New York, 1981.

3. E. J. Davis, and G. H. Anderson, "The Incipience of Nucleate Boiling in Forced Convection Flow," A.I.Ch.E. J., (July) 1966, Vol. 12 (# 4), pp. 774-780.

4. M. M. Shah, "A Genaral Correlation for Heat Transfer During Subcooled Boiling in Pipes and Annuli," ASHRAE Transactions, 83, pp. 202-215, 1977.

5. W. R. Gambill, "Generalized Prediction of Burnout Heat Flux for Flowing, Subcooled Wetting Liquids," 1963 Chemical Engineering Progress Symposium Series, 1963, vol. 59 (H41), pp. 71-87.

APPENDIX E

2-D Numerical Freon-11 Data Reduction with Epoxy Layer for Uniformly-Heated Smooth Tubes.

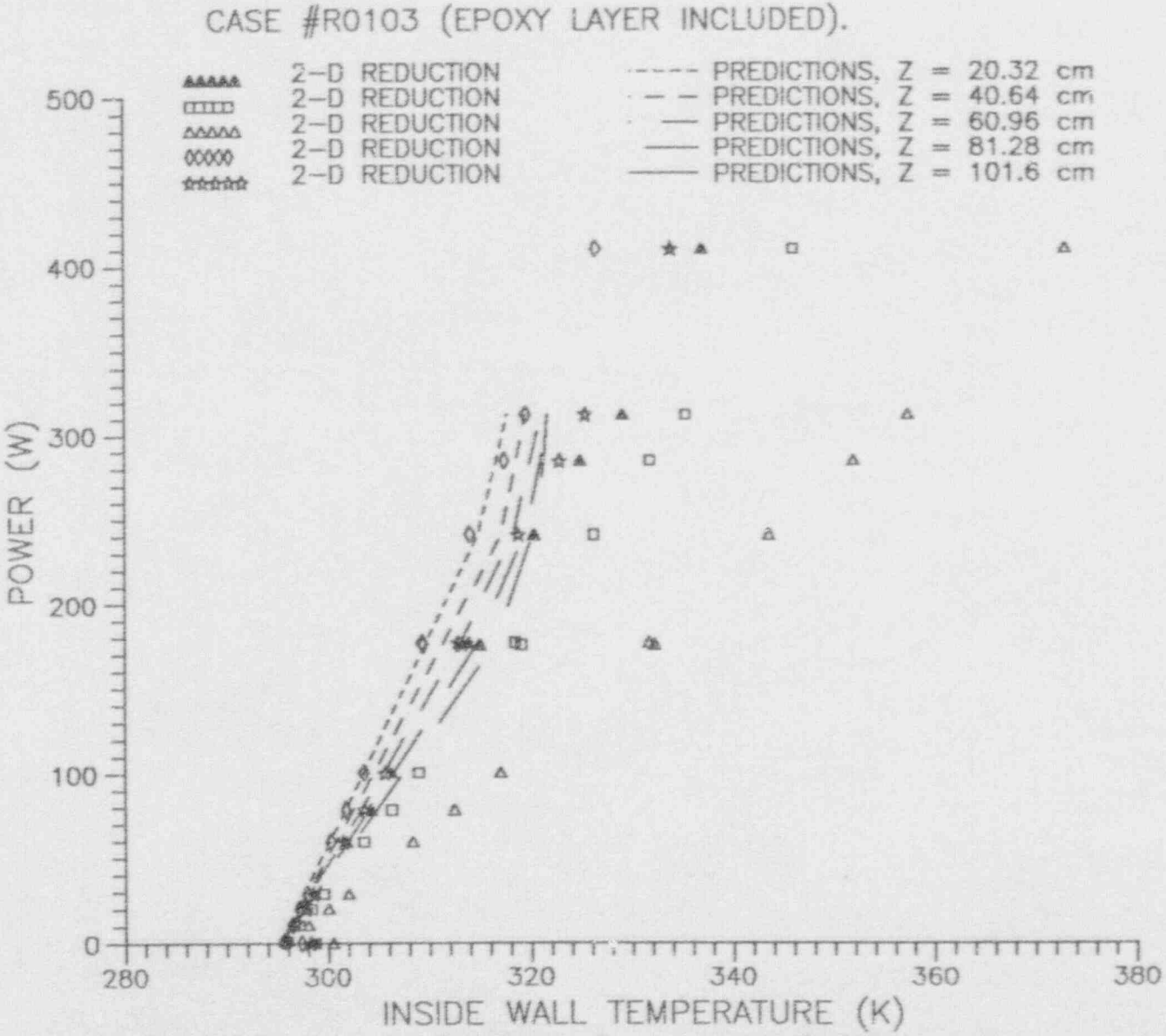

Figure 6.2.1 Inside Wall Temperature Comparisons for 2-D Reduced Data With Predictions for Case #R0103 (Epoxy Layer Included).

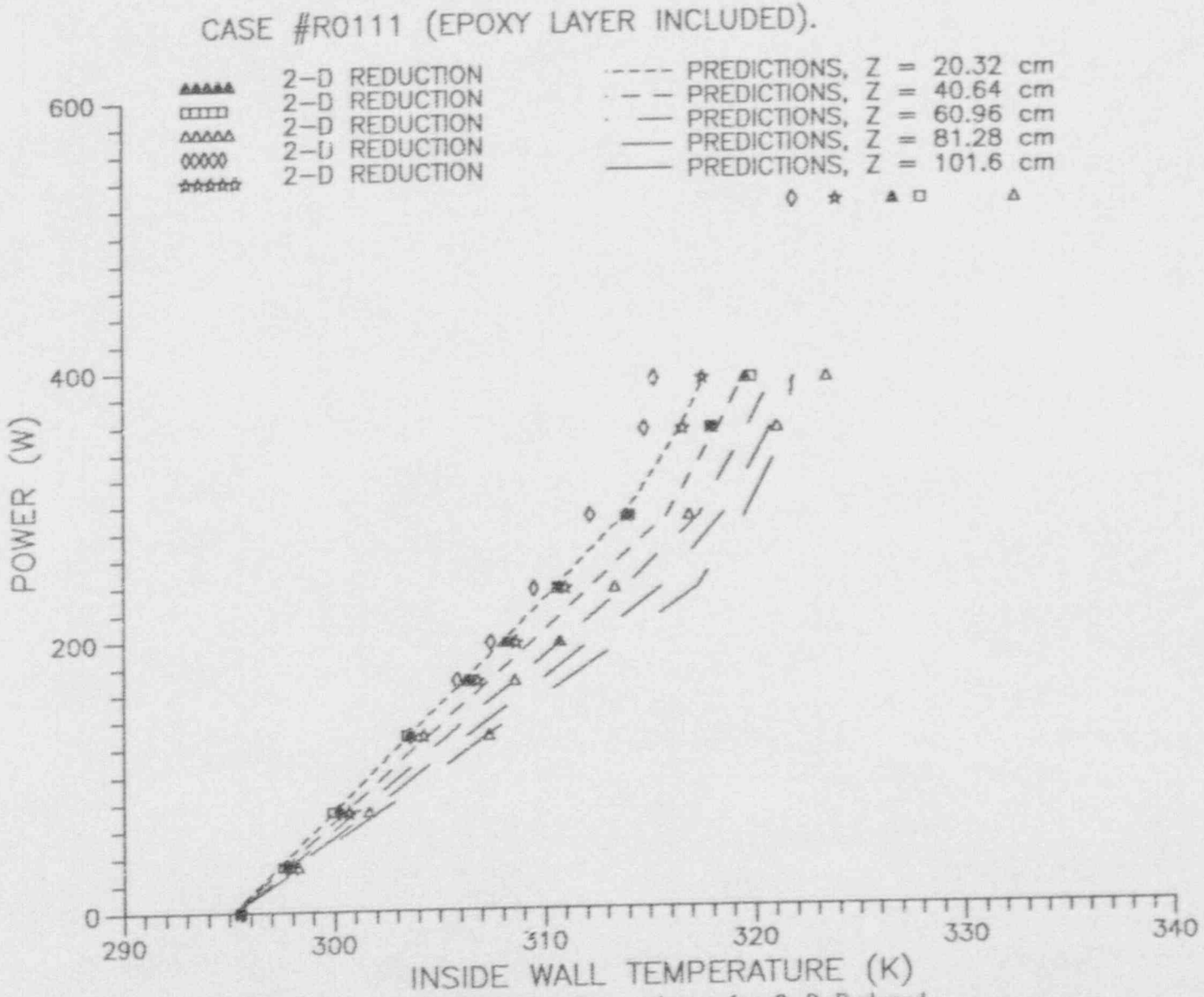

Figure 6.2.2 Inside Wall Temperature Comparisons for 2-D Reduced Data With Predictions for Case #R0111 (Epoxy Layer Included).

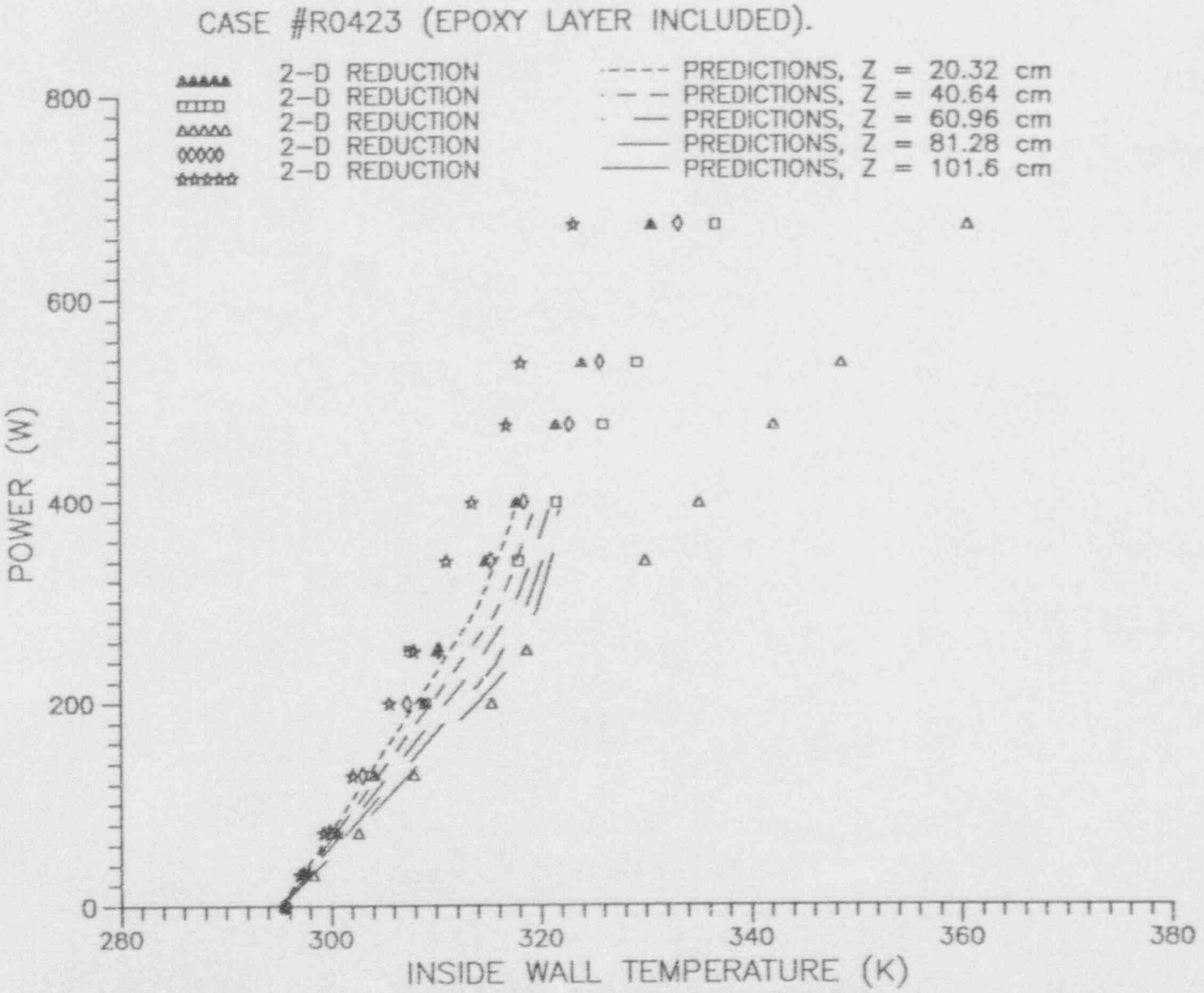

Figure 6.2.3 Inside Wall Temperature Comparisons for 2-D Reduced Data With Predictions for Case #R0423 (Epoxy Layer Included).

APPENDIX F

2-D Reduced Heat Transfer Data for 22 cases.

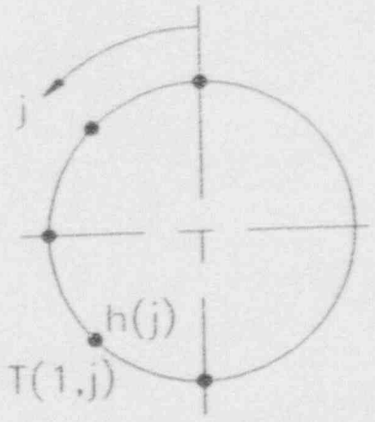

$j=1,2,\cdots 5$

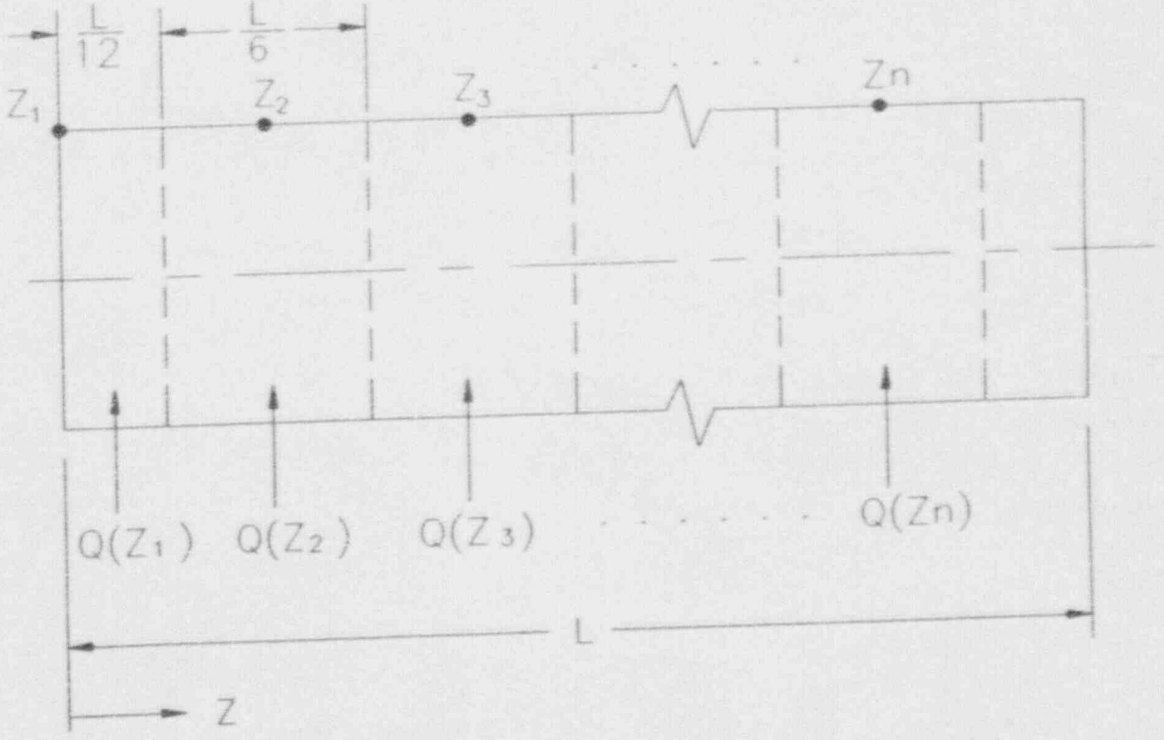

$Q_{Total}=\Sigma Q(Zn)$

$n=1,2,\cdots 7$

2-D Numerical Reduced Circumferential Heat Transfer Coefficients (Epoxy Layer Included) for Case #R0103 (Freon-11)

Z	PHI	Q(Z)	Ql(Z)	hr	hinf	Tb	T(1,j)	h(j)
cm	degree	W	W	-W/mmC-		C	K	W/mmC
20.32	0.	.00	.06	5.92	7.35	22.19	295.03	-879682.20
20.32	45.	.00	.06	5.92	7.50	22.19	301.18	-29642.91
20.32	90.	.00	.06	5.92	7.48	22.19	299.50	933.47
20.32	135.	.00	.06	5.92	7.38	22.19	298.15	831.22
20.32	180.	.00	.06	5.92	7.29	22.19	296.83	40227.84
20.32	0.	3.35	-.02	6.09	7.35	22.39	296.44	98902.97
20.32	45.	3.35	-.02	6.09	7.24	22.39	298.39	-8848.41
20.32	90.	3.35	-.02	6.09	7.20	22.39	298.20	8581.98
20.32	135.	3.35	-.02	6.09	7.28	22.39	298.18	-14461.79
20.32	180.	3.35	-.02	6.09	7.38	22.39	296.37	99107.59
20.32	0.	13.07	.22	5.93	7.88	22.97	299.49	97472.84
20.32	45.	13.07	.22	5.93	7.96	22.97	306.76	-16636.74
20.32	90.	13.07	.22	5.93	7.97	22.97	305.81	1142.47
20.32	135.	13.07	.22	5.93	7.92	22.97	305.48	-14621.11
20.32	180.	13.07	.22	5.93	7.83	22.97	298.71	118740.50
20.32	0.	29.32	.50	5.95	8.32	23.95	304.78	94357.51
20.32	45.	29.32	.50	5.95	8.42	23.95	320.83	-16839.75
20.32	90.	29.32	.50	5.96	8.42	23.95	318.35	1140.41
20.32	135.	29.32	.50	5.95	8.36	23.95	317.20	-13834.37
20.32	180.	29.32	.50	5.94	8.26	23.95	302.90	111984.00
20.32	0.	52.06	.88	5.96	8.68	25.31	311.92	90759.80
20.32	45.	52.06	.88	5.97	8.78	25.31	338.94	-16626.15
20.32	90.	52.06	.88	5.97	8.79	25.31	334.72	1148.60
20.32	135.	52.06	.88	5.96	8.72	25.31	332.74	-13681.83
20.32	180.	52.06	.88	5.95	8.60	25.31	308.56	108898.30
20.32	0.	68.41	.95	6.34	9.05	26.29	317.46	76023.90
20.32	45.	68.41	.95	6.35	9.16	26.29	347.69	-15272.36
20.32	90.	68.41	.95	6.35	9.18	26.29	343.53	1152.94
20.32	135.	68.41	.95	6.34	9.10	26.29	342.00	-13868.68
20.32	180.	68.41	.95	6.33	8.97	26.29	312.53	102488.90
20.32	0.	47.51	.75	6.00	8.61	25.04	310.91	76375.39
20.32	45.	47.51	.75	6.01	8.71	25.04	332.37	-15192.16
20.32	90.	47.51	.75	6.01	8.72	25.04	329.59	1142.89
20.32	135.	47.51	.75	6.01	8.66	25.04	328.69	-14064.18
20.32	180.	47.51	.75	6.00	8.55	25.04	307.52	103162.70
20.32	0.	40.23	.54	6.22	8.60	24.60	308.41	76947.06
20.32	45.	40.23	.54	6.23	8.70	24.60	326.52	-15167.40
20.32	90.	40.23	.54	6.23	8.71	24.60	324.26	1148.02
20.32	135.	40.23	.54	6.22	8.65	24.60	323.58	-14223.87
20.32	180.	40.23	.54	6.21	8.53	24.60	305.56	104953.10
20.32	0.	29.52	.27	6.46	8.44	23.96	304.98	76994.53
20.32	45.	29.52	.27	6.46	8.56	23.96	318.34	-14906.92
20.32	90.	29.52	.27	6.47	8.58	23.96	316.92	1144.20
20.32	135.	29.52	.27	6.46	8.51	23.96	316.69	-14680.28
20.32	180.	29.52	.27	6.46	8.36	23.96	302.92	107579.20
20.32	0.	16.78	.29	5.87	7.97	23.20	300.88	78263.59
20.32	45.	16.78	.29	5.88	8.04	23.20	308.71	-14683.41
20 32	90.	16.78	.29	5.88	8.06	23.20	308.05	1133.47
20.32	135.	16.78	.29	5.88	8.02	23.20	308.10	-15269.52
20.32	180.	16.78	.29	5.87	7.94	23.20	299.73	111971.70
20.32	0.	9.92	.13	5.97	7.71	22.78	298.65	74847.03
20.32	45.	9.92	.13	5.98	7.78	22.78	303.13	-13996.34
20.32	90.	9.92	.13	5.98	7.80	22.78	302.89	1151.10

20.32	135.	9.92	.13	5.98	7.76	22.78	305.06	-15808.97
20.32	180.	9.92	.13	5.97	7.68	22.78	297.96	113947.80
20.32	0.	4.78	.05	5.97	7.34	22.48	297.01	75430.40
20.32	45.	4.78	.05	5.97	7.43	22.48	299.31	-13900.52
20.32	90.	4.78	.05	5.97	7.45	22.48	299.20	1117.53
20.32	135.	4.78	.05	5.97	7.41	22.48	299.32	-15794.56
20.32	180.	4.78	.05	5.97	7.31	22.48	296.71	108860.40
20.32	0.	1.82	-.02	6.02	7.28	22.30	296.04	71081.35
20.32	45.	1.82	-.02	6.02	7.22	22.30	296.95	-11233.21
20.32	90.	1.82	-.02	6.02	7.20	22.30	296.91	3625.93
20.32	135.	1.82	-.02	6.02	7.23	22.30	296.96	-15138.20
20.32	180.	1.82	-.02	6.02	7.30	22.30	295.94	94540.46
20.32	0.	.21	-.10	6.14	7.79	22.20	295.62	19761.24
20.32	45.	.21	-.10	6.14	7.78	22.20	295.73	-39563.09
20.32	90.	.21	-.10	6.14	7.78	22.20	295.73	-32670.48
20.32	135.	.21	-.10	6.14	7.78	22.20	295.73	-6494.22
20.32	180.	.21	-.10	6.14	7.79	22.20	295.62	19396.65
40.64	0.	.00	.06	5.92	7.15	22.19	295.50	792018.80
40.64	45.	.00	.06	5.92	7.29	22.19	298.39	-19496.86
40.64	90.	.00	.06	5.92	7.37	22.19	297.85	2128.28
40.64	135.	.00	.06	5.92	7.49	22.19	297.01	141632.20
40.64	180.	.00	.06	5.93	7.68	22.19	306.91	-38265.25
40.64	0.	3.35	-.01	6.09	7.15	22.59	299.27	-24509.89
40.64	45.	3.35	-.01	6.09	7.25	22.59	297.31	37989.55
40.64	90.	3.35	-.01	6.09	7.23	22.59	297.51	5049.43
40.64	135.	3.35	-.01	6.09	6.90	22.59	297.36	80556.30
40.64	180.	3.35	-.01	6.09	7.31	22.59	303.12	-34820.87
40.64	0.	13.07	.26	5.93	8.01	23.76	310.06	-25132.81
40.64	45.	13.07	.26	5.93	7.94	23.76	302.58	31476.28
40.64	90.	13.07	.26	5.93	7.95	23.76	303.08	-1834.97
40.64	135.	13.07	.26	5.93	8.05	23.76	302.27	94521.58
40.64	180.	13.07	.26	5.94	8.23	23.76	324.41	-35897.38
40.64	0.	29.32	.60	5.96	8.47	25.71	327.65	-24871.58
40.64	45.	29.32	.60	5.95	8.39	25.71	311.46	29899.90
40.64	90.	29.32	.60	5.95	8.39	25.71	312.08	-1887.41
40.64	135.	29.32	.60	5.96	8.52	25.71	309.86	102279.50
40.64	180.	29.32	.60	5.98	8.74	25.71	358.55	-36363.71
40.64	0.	52.06	1.03	5.98	8.85	28.42	350.60	-24729.92
40.64	45.	52.06	1.03	5.97	8.75	28.42	323.19	28616.63
40.64	90.	52.06	1.03	5.96	8.73	28.42	323.37	-1927.74
40.64	135.	52.06	1.03	5.98	8.88	28.42	318.70	113693.10
40.64	180.	52.06	1.03	6.01	9.15	28.42	402.05	-36969.36
40.64	0.	68.41	1.17	6.36	9.28	30.35	366.16	-24583.30
40.64	45.	68.41	1.17	6.35	9.16	30.35	331.34	27582.72
40.64	90.	68.41	1.17	6.34	9.13	30.35	330.75	-1936.25
40.64	135.	68.41	1.17	6.36	9.30	30.35	323.99	121786.60
40.64	180.	68.41	1.17	6.40	9.60	30.35	430.03	-37334.68
40.64	0.	47.51	.91	6.02	8.81	27.89	345.91	-24629.36
40.64	45.	47.51	.91	6.01	8.71	27.89	320.94	27801.81
40.64	90.	47.51	.91	6.01	8.69	27.89	320.64	-2007.26
40.64	135.	47.51	.91	6.02	8.83	27.89	315.83	123856.80
40.64	180.	47.51	.91	6.05	9.11	27.89	393.89	-37461.64
40.64	0.	40.23	.68	6.23	8.81	27.01	338.21	-24791.34
40.64	45.	40.23	.68	6.23	8.70	27.01	316.90	28286.24
40.64	90.	40.23	.68	6.22	8.69	27.01	316.70	-2046.53
40.64	135.	40.23	.68	6.24	8.84	27.01	312.64	125955.60
40.64	180.	40.23	.68	6.26	9.11	27.01	379.60	-37569.54
40.64	0.	29.52	.38	6.47	8.69	25.73	327.31	-24980.77
40.64	45.	29.52	.38	6.47	8.57	25.73	311.26	29007.27
40.64	90.	29.52	.38	6.46	8.55	25.73	311.25	-2077.61
40.64	135.	29.52	.38	6.47	8.73	25.73	308.32	124936.90
40.64	180.	29.52	.38	6.49	9.02	25.73	358.77	-37543.61

40.64	0.	16.78	.36	5.88	8.12	24.20	314.06	-24908.02
40.64	45.	16.78	.36	5.88	8.05	24.20	304.66	28971.18
40.64	90.	16.78	.36	5.88	8.04	24.20	304.72	-2083.14
40.64	135.	16.78	.36	5.88	8.15	24.20	303.06	121817.90
40.64	180.	16.78	.36	5.89	8.35	24.20	332.85	-37414.97
40.64	0.	9.92	.17	5.98	7.86	23.38	306.52	-24892.42
40.64	45.	9.92	.17	5.98	7.79	23.38	300.90	28995.62
40.64	90.	9.92	.17	5.98	7.79	23.38	300.95	-2068.22
40.64	135.	9.92	.17	5.98	7.89	23.38	299.96	121570.50
40.64	180.	9.92	.17	5.99	8.08	23.38	317.85	-37409.16
40.64	0.	4.78	.07	5.97	7.51	22.76	301.05	-24713.75
40.64	45.	4.78	.07	5.97	7.44	22.76	298.18	38554.59
40.64	90.	4.78	.07	5.97	7.44	22.76	298.26	6292.10
40.64	135.	4.78	.07	5.97	7.54	22.76	297.82	107804.70
40.64	180.	4.78	.07	5.97	7.71	22.76	306.70	-36705.55
40.64	0.	1.82	-.01	6.02	7.15	22.41	297.60	-22359.56
40.64	45.	1.82	-.01	6.02	7.19	22.41	296.57	23485.81
40.64	90.	1.82	-.01	6.02	7.19	22.41	296.62	-2678.93
40.64	135.	1.82	-.01	6.02	7.07	22.41	296.47	87855.50
40.64	180.	1.82	-.01	6.02	6.87	22.41	299.93	-35332.81
40.64	0.	.21	-.09	6.14	7.78	22.22	295.95	-17559.35
40.64	45.	.21	-.09	6.14	7.77	22.22	295.72	-20200.29
40.64	90.	.21	-.09	6.14	7.77	22.22	295.73	-35785.76
40.64	135.	.21	-.09	6.14	7.77	22.22	295.70	48079.95
40.64	180.	.21	-.09	6.14	7.76	22.22	296.39	-30160.14
60.96	0.	.00	.11	5.92	7.56	22.19	294.93	**********
60.96	45.	.00	.11	5.93	7.70	22.19	304.69	-30051.64
60.96	90.	.00	.11	5.93	7.67	22.19	301.75	923.26
60.96	135.	.00	.11	5.92	7.56	22.19	299.31	5236.73
60.96	180.	.00	.11	5.92	7.47	22.19	297.71	31385.78
60.96	0.	3.35	.03	6.09	7.33	22.79	298.37	51440.44
60.96	45.	3.35	.03	6.09	7.45	22.79	301.15	-14086.23
60.96	90.	3.35	.03	6.09	7.44	22.79	300.56	755.72
60.96	135.	3.35	.03	6.09	7.35	22.79	300.17	-7545.33
60.96	180.	3.35	.03	6.09	7.21	22.79	298.26	37394.50
60.96	0.	13.07	.41	5.94	8.24	24.54	306.34	54179.50
60.96	45.	13.07	.41	5.95	8.30	24.54	316.77	-14642.13
60.96	90.	13.07	.41	5.95	8.29	24.54	314.37	772.04
60.96	135.	13.07	.41	5.94	8.24	24.54	312.75	-7699.98
60.96	180.	13.07	.41	5.94	8.17	24.54	305.58	41333.88
60.96	0.	29.32	.91	5.98	8.74	27.46	318.82	56928.00
60.96	45.	29.32	.91	5.99	8.82	27.46	341.89	-15059.07
60.96	90.	29.32	.91	5.99	8.81	27.46	336.43	794.29
60.96	135.	29.32	.91	5.98	8.74	27.46	332.66	-7665.12
60.96	180.	29.32	.91	5.97	8.66	27.46	317.11	42939.23
60.96	0.	52.06	1.55	6.01	9.15	31.49	334.60	59478.86
60.96	45.	52.06	1.55	6.02	9.24	31.49	374.27	-15494.62
60.96	90.	52.06	1.55	6.02	9.23	31.49	364.41	813.15
60.96	135.	52.06	1.55	6.01	9.14	31.49	357.41	-7131.15
60.96	180.	52.06	1.55	6.00	9.05	31.49	332.20	41745.23
60.96	0.	68.41	1.80	6.40	9.60	34.37	345.79	57215.74
60.96	45.	68.41	1.80	6.41	9.70	34.37	394.51	-15433.84
60.96	90.	68.41	1.80	6.41	9.68	34.37	381.59	812.56
60.96	135.	68.41	1.80	6.40	9.59	34.37	372.10	-6269.19
60.96	180.	68.41	1.80	6.38	9.48	34.37	342.77	38085.71
60.96	0.	47.51	1.39	6.05	9.10	30.68	331.70	56868.05
60.96	45.	47.51	1.39	6.06	9.19	30.68	366.95	-15172.44
60.96	90.	47.51	1.39	6.06	9.18	30.68	358.23	804.13
60.96	135.	47.51	1.39	6.05	9.10	30.68	352.06	-7113.83
60.96	180.	47.51	1.39	6.04	9.01	30.68	329.30	40778.91
60.96	0.	40.23	1.09	6.26	9.11	29.40	326.26	56711.75
60.96	45.	40.23	1.09	6.27	9.20	29.40	356.17	-15058.52

60.96	90.	40.23	1.09	6.27	9.19	29.40	348.99	804.13
60.96	135.	40.23	1.09	6.26	9.11	29.40	344.00	-7400.38
60.96	180.	40.23	1.09	6.25	9.02	29.40	324.23	41591.89
60.96	0.	29.52	.69	6.49	9.02	27.50	318.55	56166.87
60.96	45.	29.52	.69	6.50	9.11	27.50	340.92	-14885.95
60.96	90.	29.52	.69	6.50	9.10	27.50	335.75	796.13
60.96	135.	29.52	.69	6.49	9.02	27.50	332.22	-7641.81
60.96	180.	29.52	.69	6.49	8.92	27.50	317.12	41773.21
60.96	0.	16.78	.55	5.89	8.35	25.21	309.14	55028.49
60.96	45.	16.78	.55	5.90	8.42	25.21	322.35	-14648.37
60.96	90.	16.78	.55	5.90	8.41	25.21	319.41	780.20
60.96	135.	16.78	.55	5.89	8.36	25.21	317.46	-7935.45
60.96	180.	16.78	.55	5.89	8.29	25.21	308.27	42178.07
60.96	0.	9.92	.29	5.99	8.09	23.97	303.69	53137.79
60.96	45.	9.92	.29	5.99	8.15	23.97	311.44	-14294.03
60.96	90.	9.92	.29	5.99	8.14	23.97	309.80	767.48
60.96	135.	9.92	.29	5.99	8.10	23.97	308.73	-8014.54
60.96	180.	9.92	.29	5.98	8.03	23.97	303.23	40931.89
60.96	0.	4.78	.13	5.97	7.72	23.05	299.68	50391.39
60.96	45.	4.78	.13	5.98	7.78	23.05	303.61	-14055.75
60.96	90.	4.78	.13	5.98	7.78	23.05	302.76	762.05
60.96	135.	4.78	.13	5.97	7.73	23.05	302.20	-7874.48
60.96	180.	4.78	.13	5.97	7.67	23.05	299.40	39892.47
60.96	0.	1.82	.01	6.02	6.88	22.52	297.08	51604.81
60.96	45.	1.82	.01	6.02	7.09	22.52	298.70	-6394.24
60.96	90.	1.82	.01	6.02	7.08	22.52	298.37	8101.47
60.96	135.	1.82	.01	6.02	6.95	22.52	298.15	-7757.68
60.96	180.	1.82	.01	6.02	6.74	22.52	297.03	37464.55
60.96	0.	.21	-.09	6.14	7.75	22.23	295.90	30154.42
60.96	45.	.21	-.09	6.14	7.74	22.23	296.25	-22120.95
60.96	90.	.21	-.09	6.14	7.75	22.23	296.08	-13496.39
60.96	135.	.21	-.09	6.14	7.76	22.23	295.92	2365.52
60.96	180.	.21	-.09	6.14	7.77	22.23	295.82	11273.08
81.28	0.	.00	.03	5.92	7.20	22.19	296.62	52796.25
81.28	45.	.00	.03	5.92	7.26	22.19	298.15	-15050.38
81.28	90.	.00	.03	5.92	7.22	22.19	297.35	-263.34
81.28	135.	.00	.03	5.92	7.17	22.19	296.55	45108.11
81.28	180.	.00	.03	5.92	7.21	22.19	298.19	-25555.51
81.28	0.	3.35	-.04	6.09	7.45	22.99	296.64	64327.65
81.28	45.	3.35	-.04	6.09	7.42	22.99	297.34	-12982.03
81.28	90.	3.35	-.04	6.09	7.42	22.99	297.05	2384.64
81.28	135.	3.35	-.04	6.09	7.41	22.99	296.72	82652.97
81.28	180.	3.35	-.04	6.09	7.36	22.99	298.47	-33260.49
81.28	0.	13.07	.16	5.92	7.74	25.32	299.88	87549.53
81.28	45.	13.07	.16	5.92	7.78	25.32	302.58	-20212.57
81.28	90.	13.07	.16	5.92	7.77	25.32	301.36	665.88
81.28	135.	13.07	.16	5.92	7.78	25.32	299.98	119353.90
81.28	180.	13.07	.16	5.93	7.85	25.32	306.56	-35836.74
81.28	0.	29.32	.37	5.94	8.15	29.20	305.45	86510.40
81.28	45.	29.32	.37	5.94	8.19	29.20	311.31	-20301.47
81.28	90.	29.32	.37	5.94	8.18	29.20	308.60	700.82
81.28	135.	29.32	.37	5.94	8.19	29.20	305.53	120906.80
81.28	180.	29.32	.37	5.95	8.28	29.20	319.53	-35835.72
81.28	0.	52.06	.65	5.94	8.48	34.55	312.43	100930.00
81.28	45.	52.06	.65	5.95	8.52	34.55	322.86	-21230.51
81.28	90.	52.06	.65	5.95	8.51	34.55	318.12	800.72
81.28	135.	52.06	.65	5.95	8.52	34.55	312.80	128970.30
81.28	180.	52.06	.65	5.95	8.62	34.55	336.57	-36199.20
81.28	0.	68.41	.70	6.32	8.85	38.40	317.72	97508.93
81.28	45.	68.41	.70	6.32	8.90	38.40	330.84	-21057.86
81.28	90.	68.41	.70	6.32	8.89	38.40	324.79	894.37
81.28	135.	68.41	.70	6.32	8.90	38.40	318.04	124749.80

81.28	180.	68.41	.70	6.33	9.01	38.40	347.04	-35877.70
81.28	0.	47.51	.57	5.99	8.45	33.48	311.26	91682.64
81.28	45.	47.51	.57	5.99	8.49	33.48	320.51	-20653.24
81.28	90.	47.51	.57	5.99	8.48	33.48	316.24	823.53
81.28	135.	47.51	.57	5.99	8.49	33.48	311.47	119762.40
81.28	180.	47.51	.57	6.00	8.58	33.48	332.32	-35654.71
81.28	0.	40.23	.39	6.21	8.42	31.77	308.91	87527.27
81.28	45.	40.23	.39	6.21	8.47	31.77	316.53	-20408.82
81.28	90.	40.23	.39	6.21	8.45	31.77	312.96	813.61
81.28	135.	40.23	.39	6.21	8.47	31.77	308.94	122422.80
81.28	180.	40.23	.39	6.22	8.57	31.77	326.73	-35825.68
81.28	0.	29.52	.16	6.45	8.21	29.24	305.43	86691.98
81.28	45.	29.52	.16	6.45	8.27	29.24	311.17	-20271.96
81.28	90.	29.52	.16	6.45	8.26	29.24	308.52	778.15
81.28	135.	29.52	.16	6.45	8.27	29.24	305.54	117190.00
81.28	180.	29.52	.16	6.46	8.41	29.24	318.84	-35553.79
81.28	0.	16.78	.23	5.87	7.86	26.21	301.27	78916.58
81.28	45.	16.78	.23	5.87	7.89	26.21	304.55	-19518.54
81.28	90.	16.78	.23	5.87	7.89	26.21	303.05	724.89
81.28	135.	16.78	.23	5.87	7.90	26.21	301.35	109125.50
81.28	180.	16.78	.23	5.87	7.96	26.21	309.23	-35143.20
81.28	0.	9.92	.10	5.97	7.59	24.57	298.87	79403.59
81.28	45.	9.92	.10	5.97	7.62	24.57	300.86	-19296.15
81.28	90.	9.92	.10	5.97	7.62	24.57	299.99	670.70
81.28	135.	9.92	.10	5.97	7.63	24.57	298.99	102884.50
81.28	180.	9.92	.10	5.97	7.70	24.57	303.81	-34806.38
81.28	0.	4.78	.03	5.97	7.23	23.34	297.33	44481.87
81.28	45.	4.78	.03	5.97	7.28	23.34	298.16	-6493.79
81.28	90.	4.78	.03	5.97	7.27	23.34	297.75	8127.81
81.28	135.	4.78	.03	5.97	7.28	23.34	297.29	79211.08
81.28	180.	4.78	.03	5.97	7.35	23.34	299.64	-32824.76
81.28	0.	1.82	-.03	6.02	7.32	22.63	296.18	39496.79
81.28	45.	1.82	-.03	6.02	7.29	22.63	296.53	-17195.38
81.28	90.	1.82	-.03	6.02	7.29	22.63	296.41	-6861.82
81.28	135.	1.82	-.03	6.02	7.29	22.63	296.27	43819.13
81.28	180.	1.82	-.03	6.02	7.27	22.63	297.10	-27420.98
81.28	0.	.21	-.10	6.14	7.78	22.24	295.73	225.28
81.28	45.	.21	-.10	6.14	7.78	22.24	295.73	-36755.01
81.28	90.	.21	-.10	6.14	7.78	22.24	295.73	-36732.13
81.28	135.	.21	-.10	6.14	7.78	22.24	295.73	505.48
81.28	180.	.21	-.10	6.14	7.79	22.24	295.73	21.96
101.60	0.	.00	.05	5.92	7.37	22.19	297.75	21573.40
101.60	45.	.00	.05	5.92	7.40	22.19	298.93	-4964.71
101.60	90.	.00	.05	5.92	7.37	22.19	298.30	5078.45
101.60	135.	.00	.05	5.92	7.33	22.19	297.71	9128.72
101.60	180.	.00	.05	5.92	7.32	22.19	298.08	-5864.80
101.60	0.	3.35	-.02	6.09	7.37	23.19	296.92	72535.50
101.60	45.	3.35	-.02	6.09	7.30	23.19	297.84	-1695.34
101.60	90.	3.35	-.02	6.09	7.27	23.19	297.85	12504.24
101.60	135.	3.35	-.02	6.09	7.29	23.19	297.94	-9801.78
101.60	180.	3.35	-.02	6.09	7.34	23.19	297.27	33365.03
101.60	0.	13.07	.20	5.93	7.85	26.11	300.80	109428.10
101.60	45.	13.07	.20	5.93	7.89	26.11	304.48	-15872.83
101.60	90.	13.07	.20	5.93	7.91	26.11	304.21	1336.36
101.60	135.	13.07	.20	5.93	7.90	26.11	304.19	-6832.24
101.60	180.	13.07	.20	5.93	7.87	26.11	302.45	25604.10
101.60	0.	29.32	.46	5.95	8.28	30.92	307.53	111389.80
101.60	45.	29.32	.46	5.95	8.33	30.92	315.97	-17740.29
101.60	90.	29.32	.46	5.95	8.34	30.92	314.45	1352.90
101.60	135.	29.32	.46	5.95	8.32	30.92	313.40	-1543.39
101.60	180.	29.32	.46	5.95	8.30	30.92	311.25	14708.92
101.60	0.	52.06	.79	5.95	8.62	37.61	316.59	104530.80

101.60	45.	52.06	.79	5.96	8.67	37.61	329.90	-17702.90
101.60	90.	52.06	.79	5.96	8.68	37.61	327.17	1429.26
101.60	135.	52.06	.79	5.96	8.65	37.61	325.15	273.96
101.60	180.	52.06	.79	5.95	8.63	37.61	322.52	11432.28
101.60	0.	68.41	.88	6.33	9.02	41.65	323.49	83699.03
101.60	45.	68.41	.88	6.34	9.08	41.65	339.36	-16568.49
101.60	90.	68.41	.88	6.34	9.08	41.65	335.89	1390.04
101.60	135.	68.41	.88	6.34	9.05	41.65	333.22	1861.59
101.60	180.	68.41	.88	6.33	9.03	41.65	331.08	7225.13
101.60	0.	47.51	.70	6.00	8.58	36.27	314.94	97915.66
101.60	45.	47.51	.70	6.01	8.64	36.27	326.74	-17155.46
101.60	90.	47.51	.70	6.01	8.64	36.27	324.45	1422.15
101.60	135.	47.51	.70	6.00	8.62	36.27	322.79	-515.81
101.60	180.	47.51	.70	6.00	8.60	36.27	320.11	12628.60
101.60	0.	40.23	.50	6.22	8.58	34.13	311.77	106052.40
101.60	45.	40.23	.50	6.22	8.63	34.13	322.18	-17461.16
101.60	90.	40.23	.50	6.22	8.64	34.13	320.26	1431.11
101.60	135.	40.23	.50	6.22	8.62	34.13	318.92	-1520.83
101.60	180.	40.23	.50	6.22	8.59	34.13	316.17	15254.94
101.60	0.	29.52	.25	6.46	8.41	30.98	307.46	106334.00
101.60	45.	29.52	.25	6.46	8.48	30.98	315.20	-16959.88
101.60	90.	29.52	.25	6.46	8.50	30.98	314.02	1416.41
101.60	135.	29.52	.25	6.46	8.47	30.98	313.30	-3524.06
101.60	180.	29.52	.25	6.46	8.44	30.98	310.68	19311.98
101.60	0.	16.78	.28	5.87	7.96	27.22	302.36	103134.20
101.60	45.	16.78	.28	5.87	8.00	27.22	306.86	-16212.42
101.60	90.	16.78	.28	5.88	8.01	27.22	306.35	1375.34
101.60	135.	16.78	.28	5.87	8.00	27.22	306.12	-5604.94
101.60	180.	16.78	.28	5.87	7.98	27.22	304.19	23969.56
101.60	0.	9.92	.13	5.97	7.69	25.16	299.51	101303.90
101.60	45.	9.92	.13	5.97	7.74	25.16	302.16	-15603.36
101.60	90.	9.92	.13	5.98	7.75	25.16	301.94	1400.31
101.60	135.	9.92	.13	5.97	7.74	25.16	301.89	-6868.87
101.60	180.	9.92	.13	5.97	7.72	25.16	300.59	26906.38
101.60	0.	4.78	.05	5.97	7.33	23.62	297.61	63252.71
101.60	45.	4.78	.05	5.97	7.38	23.62	298.75	1435.05
101.60	90.	4.78	.05	5.97	7.40	23.62	298.70	15652.10
101.60	135.	4.78	.05	5.97	7.39	23.62	298.74	-8324.49
101.60	180.	4.78	.05	5.97	7.35	23.62	297.97	29899.95
101.60	0.	1.82	-.03	6.02	7.29	22.74	296.27	54350.90
101.60	45.	1.82	-.03	6.02	7.25	22.74	296.73	-10718.71
101.60	90.	1.82	-.03	6.02	7.24	22.74	296.71	2296.05
101.60	135.	1.82	-.03	6.02	7.25	22.74	296.73	-8384.00
101.60	180.	1.82	-.03	6.02	7.28	22.74	296.40	30081.76
101.60	0.	.21	-.10	6.14	7.78	22.25	295.73	233.99
101.60	45.	.21	-.10	6.14	7.78	22.25	295.73	-38180.83
101.60	90.	.21	-.10	6.14	7.78	22.25	295.73	-37920.21
101.60	135.	.21	-.10	6.14	7.78	22.25	295.73	-7485.81
101.60	180.	.21	-.10	6.14	7.79	22.25	295.62	23924.27

2-D Numerical Reduced Circumferential Heat Transfer Coefficients (Epoxy layer included) for Case #R0111 (Freon-11)

Z	PHI	Q(Z)	Ql(Z)	hr	hinf	Tb	T(1,j)	h(j)
cm	degree	W	W	-W/mmC-		C	K	W/mmC
20.32	0.	.00	-.01	5.90	6.86	22.19	295.45	-533.94
20.32	45.	.00	-.01	5.90	6.81	22.19	295.45	-134801.60
20.32	90.	.00	-.01	5.90	6.79	22.19	295.50	-93593.68
20.32	135.	.00	-.01	5.90	6.79	22.19	295.55	-5609.38
20.32	180.	.00	-.01	5.90	6.83	22.19	295.55	292.40
20.32	0.	5.50	.05	5.91	7.31	22.44	297.00	18983.28
20.32	45.	5.50	.05	5.91	7.35	22.44	297.56	7178.70
20.32	90.	5.50	.05	5.91	7.38	22.44	297.90	10547.88
20.32	135.	5.50	.05	5.91	7.39	22.44	298.32	-11968.22
20.32	180.	5.50	.05	5.91	7.36	22.44	297.19	32144.95
20.32	0.	12.17	.11	5.94	7.60	22.74	298.78	16817.17
20.32	45.	12.17	.11	5.94	7.64	22.74	299.77	665.25
20.32	90.	12.17	.11	5.94	7.68	22.74	300.67	1184.33
20.32	135.	12.17	.11	5.94	7.70	22.74	301.74	-14150.05
20.32	180.	12.17	.11	5.94	7.66	22.74	298.91	42680.58
20.32	0.	21.28	.22	5.93	7.85	23.14	301.32	11016.85
20.32	45.	21.28	.22	5.93	7.89	23.14	302.37	4540.86
20.32	90.	21.28	.22	5.94	7.95	23.14	304.32	1136.92
20.32	135.	21.28	.22	5.94	7.98	23.14	306.51	-14026.71
20.32	180.	21.28	.22	5.94	7.94	23.14	301.97	36466.56
20.32	0.	28.13	.28	5.95	7.99	23.45	303.19	11759.54
20.32	45.	28.13	.28	5.95	8.03	23.45	304.68	3605.32
20.32	90.	28.13	.28	5.95	8.09	23.45	307.03	1122.30
20.32	135.	28.13	.28	5.95	8.12	23.45	309.66	-12707.68
20.32	180.	28.13	.28	5.95	8.09	23.45	304.47	30267.29
20.32	0.	32.84	.34	5.95	8.08	23.66	304.42	12320.47
20.32	45.	32.84	.34	5.95	8.12	23.66	306.24	3599.29
20.32	90.	32.84	.34	5.96	8.18	23.66	309.04	1126.63
20.32	135.	32.84	.34	5.96	8.22	23.66	312.19	-12928.76
20.32	180.	32.84	.34	5.96	8.18	23.66	305.97	31080.57
20.32	0.	39.41	.40	5.97	8.18	23.96	306.12	12247.76
20.32	45.	39.41	.40	5.97	8.22	23.96	308.25	3860.18
20.32	90.	39.41	.40	5.98	8.29	23.96	311.66	1141.92
20.32	135.	39.41	.40	5.98	8.33	23.96	315.51	-13317.73
20.32	180.	39.41	.40	5.98	8.29	23.96	307.82	32865.05
20.32	0.	48.29	.49	5.98	8.30	24.35	308.53	12511.53
20.32	45.	48.29	.49	5.98	8.34	24.35	311.21	3467.90
20.32	90.	48.29	.49	5.99	8.42	24.35	315.22	1143.09
20.32	135.	48.29	.49	5.99	8.45	24.35	319.77	-13042.58
20.32	180	48.29	.49	5.99	8.42	24.35	310.61	31980.54
20.32	0.	59.05	.61	5.99	8.43	24.84	311.51	12266.39
20.32	45.	59.05	.61	5.99	8.47	24.84	314.72	3441.95
20.32	90.	59.05	.61	6.00	8.55	24.84	319.55	1152.49
20.32	135.	59.05	.61	6.00	8.59	24.84	325.03	-13244.38
20.32	180.	59.05	.61	6.00	8.55	24.84	313.61	33433.73
20.32	0.	65.21	.65	5.99	8.48	25.11	313.13	8790.96
20.32	45.	65.21	.65	6.00	8.52	25.11	315.50	5678.21
20.32	90.	65.21	.65	6.00	8.60	25.11	321.21	1168.75
20.32	135.	65.21	.65	6.01	8.64	25.11	327.57	-13706.89
20.32	180.	65.21	.65	6.00	8.60	25.11	315.01	34301.45
20.32	0.	86.97	.86	6.01	8.67	26.09	318.80	8768.99
20.32	45.	86.97	.86	6.02	8.71	26.09	321.90	5225.48
20.32	90.	86.97	.86	6.02	8.79	26.09	328.94	1232.59
20.32	135.	86.97	.86	6.03	8.83	26.09	336.93	-14893.24
20.32	180.	86.97	.86	6.02	8.77	26.09	318.48	43780.35
40.64	0.	.00	.00	5.90	6.80	22.19	295.55	3.80

40.64	45.	.00	.00	5.90	6.74	22.19	295.55	-71216.82
40.64	90.	.00	.00	5.90	6.74	22.19	295.55	-71170.74
40.64	135.	.00	.00	5.90	6.78	22.19	295.55	351.42
40.64	180.	.00	.00	5.90	6.82	22.19	295.55	8.27
40.64	0.	5.50	.05	5.91	7.30	22.68	297.12	13018.81
40.64	45.	5.50	.05	5.91	7.33	22.68	297.46	7570.26
40.64	90.	5.50	.05	5.91	7.35	22.68	297.65	10113.16
40.64	135.	5.50	.05	5.91	7.36	22.68	297.88	-6409.87
40.64	180.	5.50	.05	5.91	7.34	22.68	297.45	12723.05
40.64	0.	12.17	.11	5.94	7.59	23.28	298.89	17967.04
40.64	45.	12.17	.11	5.94	7.62	23.28	299.79	-2556.38
40.64	90.	12.17	.11	5.94	7.64	23.28	300.12	1239.37
40.64	135.	12.17	.11	5.94	7.65	23.28	300.53	-5937.81
40.64	180.	12.17	.11	5.94	7.64	23.28	299.68	12647.79
40.64	0.	21.28	.21	5.93	7.87	24.10	301.47	19530.41
40.64	45.	21.28	.21	5.93	7.90	24.10	303.16	-2648.95
40.64	90.	21.28	.21	5.93	7.93	24.10	303.82	1216.90
40.64	135.	21.28	.21	5.93	7.94	24.10	304.63	-6778.28
40.64	180.	21.28	.21	5.93	7.92	24.10	302.91	14530.19
40.64	0.	28.13	.29	5.95	8.05	24.71	303.30	42365.77
40.64	45.	28.13	.29	5.95	8.09	24.71	308.30	-12696.57
40.64	90.	28.13	.29	5.95	8.09	24.71	306.93	1152.89
40.64	135.	28.13	.29	5.95	8.07	24.71	305.75	6446.24
40.64	180.	28.13	.29	5.95	8.07	24.71	306.46	-2666.66
40.64	0.	32.84	.34	5.96	8.14	25.13	304.49	43140.23
40.64	45.	32.84	.34	5.96	8.18	25.13	310.29	-12553.12
40.64	90.	32.84	.34	5.96	8.18	25.13	308.84	1164.46
40.64	135.	32.84	.34	5.96	8.16	25.13	307.61	5531.58
40.64	180.	32.84	.34	5.96	8.16	25.13	308.24	-1810.39
40.64	0.	39.41	.40	5.97	8.24	25.72	306.13	43564.90
40.64	45.	39.41	.40	5.97	8.28	25.72	312.97	-12501.45
40.64	90.	39.41	.40	5.97	8.28	25.72	311.31	1188.25
40.64	135.	39.41	.40	5.97	8.27	25.72	309.93	5034.95
40.64	180.	39.41	.40	5.97	8.26	25.72	310.51	-1144.77
40.64	0.	48.29	.49	5.99	8.36	26.52	308.01	49993.48
40.64	45.	48.29	.49	5.99	8.41	26.52	317.04	-13304.10
40.64	90.	48.29	.49	5.99	8.41	26.52	314.98	1214.66
40.64	135.	48.29	.49	5.99	8.39	26.52	313.29	4549.74
40.64	180.	48.29	.49	5.99	8.39	26.52	313.71	-265.86
40.64	0.	59.05	.60	5.99	8.48	27.48	309.68	61254.29
40.64	45.	59.05	.60	6.00	8.54	27.48	321.71	-14358.69
40.64	[illegible]	59.05	.60	6.00	8.54	27.48	319.25	1264.68
40.64	[illegible]	59.05	.60	6.00	8.52	27.48	317.33	3591.62
40.64	180.	59.05	.60	6.00	8.51	27.48	317.26	1278.53
40.64	0.	65.21	.66	6.00	8.53	28.03	310.12	74315.69
40.64	45.	65.21	.66	6.00	8.60	28.03	324.61	-15900.64
40.64	90.	65.21	.66	6.00	8.60	28.03	321.36	1302.67
40.64	135.	65.21	.66	6.00	8.58	28.03	318.72	5256.46
40.64	180.	65.21	.66	6.00	8.57	28.03	319.31	-299.99
40.64	0.	86.97	.89	6.02	8.74	29.95	315.15	73189.20
40.64	45.	86.97	.89	6.03	8.81	29.95	334.39	-15788.33
40.64	90.	86.97	.89	6.03	8.81	29.95	330.09	1331.84
40.64	135.	86.97	.89	6.02	8.78	29.95	326.69	3392.08
40.64	180.	86.97	.89	6.02	8.76	29.95	325.64	3328.75
60.96	0.	.00	.00	5.90	6.80	22.19	295.55	3.80
60.96	45.	.00	.00	5.90	6.74	22.19	295.55	-71216.82
60.96	90.	.00	.00	5.90	6.74	22.19	295.55	-71170.74
60.96	135.	.00	.00	5.90	6.78	22.19	295.55	351.42
60.96	180.	.00	.00	5.90	6.82	22.19	295.55	8.27
60.96	0.	5.50	.07	5.91	7.27	22.93	296.61	38907.31
60.96	45.	5.50	.07	5.91	7.33	22.93	297.01	22780.66
60.96	90.	5.50	.07	5.91	7.44	22.93	298.25	711.66

60.96	135.	5.50	.07	5.91	7.53	22.93	299.48	-3490.27
60.96	180.	5.50	.07	5.91	7.56	22.93	300.15	-7279.04
60.96	0.	12.17	.15	5.93	7.55	23.83	297.89	44923.43
60.96	45.	12.17	.15	5.94	7.62	23.83	298.67	32664.07
60.96	90.	12.17	.15	5.94	7.77	23.83	301.68	786.58
60.96	135.	12.17	.15	5.94	7.88	23.83	304.69	-7021.42
60.96	180.	12.17	.15	5.95	7.92	23.83	305.21	-2764.24
60.96	0.	21.28	.30	5.93	7.82	25.05	299.67	52020.53
60.96	45.	21.28	.30	5.93	7.91	25.05	301.11	38190.45
60.96	90.	21.28	.30	5.94	8.09	25.05	307.08	558.68
60.96	135.	21.28	.30	5.95	8.24	25.05	312.94	-2903.74
60.96	180.	21.28	.30	5.95	8.30	25.05	316.82	-9342.21
60.96	0.	28.13	.34	5.95	7.95	25.97	301.30	55992.82
60.96	45.	28.13	.34	5.95	8.02	25.97	303.75	9600.18
60.96	90.	28.13	.34	5.96	8.15	25.97	307.68	450.61
60.96	135.	28.13	.34	5.96	8.28	25.97	311.25	13670.44
60.96	180.	28.13	.34	5.97	8.37	25.97	322.17	-21037.64
60.96	0.	32.84	.40	5.95	8.03	26.60	302.21	60392.28
60.96	45.	32.84	.40	5.95	8.10	26.60	305.21	8756.35
60.96	90.	32.84	.40	5.96	8.24	26.60	309.75	492.80
60.96	135.	32.84	.40	5.97	8.37	26.60	313.89	12673.08
60.96	180.	32.84	.40	5.98	8.47	26.60	325.96	-20442.25
60.96	0.	39.41	.46	5.97	8.13	27.49	303.60	57425.71
60.96	45.	39.41	.46	5.97	8.20	27.49	307.02	8888.62
60.96	90.	39.41	.46	5.98	8.34	27.49	312.27	561.24
60.96	135.	39.41	.46	5.99	8.48	27.49	317.11	11426.71
60.96	180.	39.41	.46	5.99	8.57	27.49	330.23	-19651.69
60.96	0.	48.29	.56	5.98	8.26	28.67	305.46	61163.54
60.96	45.	48.29	.56	5.98	8.33	28.67	309.98	7119.81
60.96	90.	48.29	.56	5.99	8.47	28.67	316.23	770.80
60.96	135.	48.29	.56	6.00	8.60	28.67	322.24	5092.11
60.96	180.	48.29	.56	6.01	8.67	28.67	332.61	-14848.89
60.96	0.	59.05	.68	5.99	8.38	30.09	307.69	62014.92
60.96	45.	59.05	.68	5.99	8.46	30.09	313.30	6343.79
60.96	90.	59.05	.68	6.00	8.60	30.09	320.71	902.35
60.96	135.	59.05	.68	6.01	8.72	30.09	328.00	1529.65
60.96	180.	59.05	.68	6.02	8.78	30.09	336.56	-11227.54
60.96	0.	65.21	.74	5.99	8.45	30.90	308.98	62403.52
60.96	45.	65.21	.74	6.00	8.52	30.90	315.26	5679.47
60.96	90.	65.21	.74	6.01	8.66	30.90	323.22	946.42
60.96	135.	65.21	.74	6.02	8.78	30.90	331.10	603.49
60.96	180.	65.21	.74	6.02	8.84	30.90	339.22	-10041.25
60.96	0.	86.97	.99	6.01	8.64	33.77	313.91	52517.88
60.96	45.	86.97	.99	6.02	8.72	33.77	321.29	8361.55
60.96	90.	86.97	.99	6.03	8.87	33.77	332.50	1017.58
60.96	135.	86.97	.99	6.05	9.00	33.77	343.77	-2578.95
60.96	180.	86.97	.99	6.05	9.06	33.77	350.05	-6214.45
81.28	0.	.00	.00	5.90	6.79	22.19	295.55	-270.54
81.28	45.	.00	.00	5.90	6.72	22.19	295.55	-62691.35
81.28	90.	.00	.00	5.90	6.69	22.19	295.60	-52106.45
81.28	135.	.00	.00	5.90	6.69	22.19	295.65	-3824.45
81.28	180.	.00	.00	5.90	6.75	22.19	295.65	195.72
81.28	0.	5.50	.05	5.91	7.22	23.18	296.51	116262.20
81.28	45.	5.50	.05	5.91	7.27	23.18	296.95	20169.83
81.28	90.	5.50	.05	5.91	7.35	23.18	297.40	14545.15
81.28	135.	5.50	.05	5.91	7.44	23.18	297.72	54146.52
81.28	180.	5.50	.05	5.91	7.53	23.18	301.41	-32302.63
81.28	0.	12.17	.11	5.93	7.48	24.37	297.59	613318.60
81.28	45.	12.17	.11	5.93	7.53	24.37	298.46	6866.15
81.28	90.	12.17	.11	5.94	7.63	24.37	299.43	-89.84
81.28	135.	12.17	.11	5.94	7.75	24.37	300.06	67268.20
81.28	180.	12.17	.11	5.94	7.87	24.37	308.37	-34047.41

81.28	0.	21.28	.21	5.93	7.73	26.00	299.07	-940760.00
81.28	45.	21.28	.21	5.93	7.79	26.00	300.71	4484.40
81.28	90.	21.28	.21	5.93	7.89	26.00	302.32	33.87
81.28	135.	21.28	.21	5.94	8.02	26.00	303.42	64997.89
81.28	180.	21.28	.21	5.94	8.15	26.00	316.93	-33777.30
81.28	0.	28.13	.27	5.94	7.86	27.23	300.12	-421988.40
81.28	45.	28.13	.27	5.95	7.92	27.23	302.32	2384.08
81.28	90.	28.13	.27	5.95	8.02	27.23	304.28	201.34
81.28	135.	28.13	.27	5.96	8.15	27.23	305.60	65530.11
81.28	180.	28.13	.27	5.96	8.29	27.23	322.25	-33792.73
81.28	0.	32.84	.32	5.95	7.94	28.07	300.95	-463205.70
81.28	45.	32.84	.32	5.95	7.99	28.07	303.49	1389.18
81.28	90.	32.84	.32	5.95	8.10	28.07	305.64	244.80
81.28	135.	32.84	.32	5.96	8.23	28.07	307.07	67500.44
81.28	180.	32.84	.32	5.97	8.38	28.07	326.15	-33974.89
81.28	0.	39.41	.37	5.96	8.03	29.23	301.94	-334968.90
81.28	45.	39.41	.37	5.96	8.09	29.23	304.92	329.57
81.28	90.	39.41	.37	5.97	8.19	29.23	307.32	231.76
81.28	135.	39.41	.37	5.98	8.34	29.23	308.84	74878.55
81.28	180.	39.41	.37	5.99	8.49	29.23	331.97	-34699.21
81.28	0.	48.29	.45	5.97	8.14	30.79	303.55	-449547.50
81.28	45.	48.29	.45	5.98	8.20	30.79	307.11	-3459.27
81.28	90.	48.29	.45	5.98	8.30	30.79	309.43	190.10
81.28	135.	[illegible]	.45	5.99	8.45	30.79	310.64	92508.07
81.28	180.	48.29	.45	6.00	8.61	30.79	339.59	-36024.89
81.28	0.	59.05	.53	5.98	8.25	32.68	305.30	-406370.40
81.28	45.	59.05	.53	5.98	8.31	32.68	309.68	-7805.85
81.28	90.	59.05	.53	5.99	8.40	32.68	311.81	538.09
81.28	135.	59.05	.53	6.00	8.54	32.68	312.74	99725.13
81.28	180.	59.05	.53	6.01	8.70	32.68	344.41	-36365.29
81.28	0.	65.21	.55	5.98	8.30	33.77	306.33	-396222.20
81.28	45.	65.21	.55	5.98	8.36	33.77	311.06	-9933.90
81.28	90.	65.21	.55	5.99	8.43	33.77	312.96	1357.66
81.28	135.	65.21	.55	6.00	8.55	33.77	313.94	80155.04
81.28	180.	65.21	.55	6.01	8.68	33.77	339.81	-34702.79
81.28	0.	86.97	.74	6.00	8.50	37.59	310.31	-731393.80
81.28	45.	86.97	.74	6.00	8.55	37.59	316.74	-10285.28
81.28	90.	86.97	.74	6.01	8.63	37.59	319.09	1495.47
81.28	135.	86.97	.74	6.02	8.75	37.59	320.[illegible]	71723.79
81.28	180.	86.97	.74	6.03	8.89	37.59	351 [illegible]	-33796.36
101.60	0.	.00	.00	5.90	6.80	22.19	295.55	6.43
101.60	45.	.00	.00	5.90	6.75	22.19	295.55	-71213.98
101.60	90.	.00	.00	5.90	6.75	22.19	295.55	-70806.90
101.60	135.	.00	.00	5.90	6.79	22.19	295.55	-11983.99
101.60	180.	.00	.00	5.90	6.85	22.19	295.44	52233.18
101.60	0.	5.50	.06	5.91	7.27	23.42	296.83	40707.53
101.60	45.	5.50	.06	5.91	7.32	23.42	297.01	55116.27
101.60	90.	5.50	.06	5.91	7.42	23.42	298.15	1502.02
101.60	135.	5.50	.06	5.91	7.48	23.42	299.36	-18473.95
101.60	180.	5.50	.06	5.91	7.47	23.42	298.19	32391.92
101.60	0.	12.17	.12	5.93	7.55	24.92	298.22	169408.90
101.60	45.	12.17	.12	5.94	7.60	24.92	298.69	73452.66
101.60	90.	12.17	.12	5.94	7.71	24.92	300.97	1736.52
101.60	135.	12.17	.12	5.94	7.79	24.92	303.37	-18300.40
101.60	180.	12.17	.12	5.94	7.78	24.92	301.28	9433.86
101.60	0.	21.28	.23	5.93	7.80	26.96	300.00	-595697.90
101.60	45.	21.28	.23	5.93	7.86	26.96	301.21	54391.45
101.60	90.	21.28	.23	5.94	7.97	26.96	304.72	1836.20
101.60	135.	21.28	.23	5.94	8.05	26.96	308.42	-17654.85
101.60	180.	21.28	.23	5.94	8.04	26.96	305.30	27324.74
101.60	0.	28.13	.30	5.95	7.94	28.48	301.57	**********
101.60	45.	28.13	.30	5.95	7.99	28.48	303.20	43117.19

101.60	90.	28.13	.30	5.95	8.11	28.48	307.38	1901.98
101.60	135.	28.13	.30	5.96	8.19	28.48	311.78	-16805.77
101.60	180.	28.13	.30	5.96	8.19	28.48	308.22	24754.45
101.60	0.	32.84	.35	5.95	8.02	29.52	302.49	-593244.90
101.60	45.	32.84	.35	5.95	8.08	29.52	304.56	38352.61
101.60	90.	32.84	.35	5.96	8.19	29.52	309.29	1910.15
101.60	135.	32.84	.35	5.96	8.28	29.52	314.28	-16149.62
101.60	180.	32.84	.35	5.96	8.28	29.52	310.49	22210.72
101.60	0.	39.41	.41	5.97	8.11	30.96	303.78	-375972.90
101.60	45.	39.41	.41	5.97	8.17	30.96	306.16	42299.35
101.60	90.	39.41	.41	5.98	8.30	30.96	311.71	1960.34
101.60	135.	39.41	.41	5.98	8.38	30.96	317.56	-15804.52
101.60	180.	39.41	.41	5.98	8.39	30.96	313.44	20368.17
101.60	0.	48.29	.49	5.98	8.23	32.91	305.57	-334970.20
101.60	45.	48.29	.49	5.98	8.29	32.91	308.85	26737.44
101.60	90.	48.29	.49	5.99	8.41	32.91	314.63	2033.45
101.60	135.	48.29	.49	5.99	8.49	32.91	320.68	-13069.92
101.60	180.	48.29	.49	5.99	8.50	32.91	317.65	12395.02
101.60	0.	59.05	.57	5.98	8.34	35.28	307.59	-264620.30
101.60	45.	59.05	.57	5.99	8.40	35.28	312.05	11065.19
101.60	90.	59.05	.57	5.99	8.50	35.28	317.30	2321.02
101.60	135.	59.05	.57	6.00	8.58	35.28	322.84	-10497.25
101.60	180.	59.05	.57	6.00	8.59	35.28	320.93	7706.84
101.60	0.	65.21	.61	5.99	8.40	36.63	308.63	-247907.90
101.60	45.	65.21	.61	5.99	8.46	36.63	314.51	-2619.03
101.60	90.	65.21	.61	6.00	8.54	36.63	318.75	2772.09
101.60	135.	65.21	.61	6.00	8.60	36.63	323.50	-14931.77
101.60	180.	65.21	.61	6.00	8.58	36.63	318.23	29503.46
101.60	0.	86.97	.79	6.01	8.60	41.42	313.36	-328601.40
101.60	45.	86.97	.79	6.01	8.66	41.42	321.55	-9117.41
101.60	90.	86.97	.79	6.02	8.73	41.42	325.49	3033.75
101.60	135.	86.97	.79	6.02	8.77	41.42	330.08	-14446.60
101.60	180.	86.97	.79	6.02	8.75	41.42	323.49	35323.45

2-D Numerical Reduced Circumferential Heat Transfer Coefficients (Epoxy Layer Included) for Case #R042(Freon-11)

Z	PHI	Q(Z)	Ql(Z)	hr	hinf	Tb	T(1,j)	h(j)
cm	degree	W	W	-W/mmC-		C	K	W/mmC
20.32	0.	.00	.01	5.87	6.79	22.19	295.55	6.09
20.32	45.	.00	.01	5.87	6.84	22.19	295.55	-70882.84
20.32	90.	.00	.01	5.87	6.84	22.19	295.55	-70833.55
20.32	135.	.00	.01	5.87	6.82	22.19	295.55	339.47
20.32	180.	.00	.01	5.87	6.77	22.19	295.55	-2.01
20.32	0.	5.10	.06	5.88	7.27	22.42	296.43	30255.95
20.32	45.	5.10	.06	5.88	7.32	22.42	296.96	19772.09
20.32	90.	5.10	.06	5.89	7.40	22.42	297.88	13934.05
20.32	135.	5.10	.06	5.89	7.43	22.42	298.92	-20247.14
20.32	180.	5.10	.06	5.88	7.39	22.42	296.84	73474.20
20.32	0.	12.04	.16	5.84	7.59	22.73	297.66	38157.66
20.32	45.	12.04	.16	5.84	7.65	22.73	299.04	7403.29
20.32	90.	12.04	.16	5.85	7.73	22.73	301.23	1312.55
20.32	135.	12.04	.16	5.85	7.78	22.73	303.71	-20978.57
20.32	180.	12.04	.16	5.85	7.73	22.73	298.63	82843.27
20.32	0.	21.36	.23	5.91	7.80	23.15	299.28	42153.39
20.32	45.	21.36	.23	5.92	7.87	23.15	301.86	5344.23
20.32	90.	21.36	.23	5.92	7.98	23.15	305.36	1316.68
20.32	135.	21.36	.23	5.92	8.04	23.15	309.34	-20612.37
20.32	180.	21.36	.23	5.92	7.98	23.15	300.94	81502.95
20.32	0.	33.20	.36	5.93	8.03	23.68	301.57	44246.53
20.32	45.	33.20	.36	5.93	8.11	23.68	305.92	2750.52
20.32	90.	33.20	.36	5.94	8.22	23.68	310.76	1310.91
20.32	135.	33.20	.36	5.94	8.27	23.68	316.32	-19710.84
20.32	180.	33.20	.36	5.94	8.21	23.68	304.15	75049.91
20.32	0.	41.81	.35	6.06	8.08	24.06	303.53	405.58
20.32	45.	41.81	.35	6.07	8.15	24.06	303.13	36859.56
20.32	90.	41.81	.35	6.07	8.32	24.06	311.73	1348.62
20.32	135.	41.81	.35	6.08	8.43	24.06	320.96	-21824.25
20.32	180.	41.81	.35	6.08	8.38	24.06	306.38	71511.81
20.32	0.	56.69	.49	6.08	8.35	24.73	305.38	48894.93
20.32	45.	56.69	.49	6.08	8.42	24.73	313.12	-4640.38
20.32	90.	56.69	.49	6.09	8.51	24.73	316.71	1375.52
20.32	135.	56.69	.49	6.09	8.54	24.73	321.09	-13260.63
20.32	180.	56.69	.49	6.09	8.50	24.73	310.86	36213.27
20.32	0.	66.51	.59	6.05	8.44	25.17	307.07	48682.64
20.32	45.	66.51	.59	6.06	8.51	25.17	316.05	-4962.55
20.32	90.	66.51	.59	6.06	8.59	25.17	319.96	1388.97
20.32	135.	66.51	.59	6.07	8.63	25.17	324.76	-12902.50
20.32	180.	66.51	.59	6.06	8.59	25.17	313.31	35125.94
20.32	0.	79.19	.70	6.07	8.56	25.74	309.38	49790.19
20.32	45.	79.19	.70	6.07	8.64	25.74	320.44	-6225.98
20.32	90.	79.19	.70	6.08	8.71	25.74	324.14	1401.17
20.32	135.	79.19	.70	6.08	8.74	25.74	328.89	-11972.87
20.32	180.	79.19	.70	6.08	8.70	25.74	316.39	32996.77
20.32	0.	89.50	.77	6.07	8.64	26.20	310.75	54240.06
20.32	45.	89.50	.77	6.08	8.72	26.20	323.92	-8030.68
20.32	90.	89.50	.77	6.08	8.78	26.20	326.75	1435.15
20.32	135.	89.50	.77	6.09	8.80	26.20	330.69	-10541.67
20.32	180.	89.50	.77	6.08	8.76	26.20	318.53	29495.49
20.32	0.	112.24	.96	6.11	8.84	27.22	313.50	80513.00
20.32	45.	112.24	.96	6.12	8.93	27.22	336.41	-14410.17
20.32	90.	112.24	.96	6.12	8.96	27.22	334.21	1466.89
20.32	135.	112.24	.96	6.12	8.94	27.22	333.43	-4750.63
20.32	180.	112.24	.96	6.11	8.90	27.22	323.95	19380.37

40.64	0.	.00	.01	5.87	6.85	22.19	295.65	186.80
40.64	45.	.00	.01	5.87	6.88	22.19	295.65	-49408.33
40.64	90.	.00	.01	5.87	6.86	22.19	295.60	-57202.54
40.64	135.	.00	.01	5.87	6.83	22.19	295.55	6425.94
40.64	180.	.00	.01	5.87	6.78	22.19	295.55	-282.47
40.64	0.	5.10	.06	5.89	7.41	22.65	297.49	28808.59
40.64	45.	5.10	.06	5.89	7.42	22.65	298.57	-12258.98
40.64	90.	5.10	.06	5.88	7.37	22.65	297.53	413.56
40.64	135.	5.10	.06	5.88	7.28	22.65	296.52	43278.36
40.64	180.	5.10	.06	5.88	7.26	22.65	296.84	-11157.51
40.64	0.	12.04	.15	5.85	7.74	23.27	299.95	36685.62
40.64	45.	12.04	.15	5.85	7.76	23.27	302.82	-18131.70
40.64	90.	12.04	.15	5.85	7.69	23.27	300.33	1204.07
40.64	135.	12.04	.15	5.84	7.60	23.27	297.95	47301.76
40.64	180.	12.04	.15	5.84	7.57	23.27	298.61	-10820.13
40.64	0.	21.36	.23	5.92	8.01	24.10	303.00	48476.03
40.64	45.	21.36	.23	5.92	8.04	24.10	309.19	-20086.87
40.64	90.	21.36	.23	5.92	7.95	24.10	304.36	1253.15
40.64	135.	21.36	.23	5.91	7.82	24.10	299.76	53681.65
40.64	180.	21.36	.23	5.91	7.78	24.10	300.82	-10318.59
40.64	0.	33.20	.36	5.94	8.27	25.17	306.81	60869.13
40.64	45.	33.20	.36	5.94	8.31	25.17	318.32	-21560.43
40.64	90.	33.20	.36	5.94	8.21	25.17	310.06	1266.87
40.64	135.	33.20	.36	5.93	8.05	25.17	302.25	56404.48
40.64	180.	33.20	.36	5.93	8.00	25.17	303.77	-9370.59
40.64	0.	41.81	.29	6.07	8.28	25.94	310.44	1385.39
40.64	45.	41.81	.29	6.07	8.26	25.94	310.58	-5491.64
40.64	90.	41.81	.29	6.07	8.19	25.94	307.43	1380.58
40.64	135.	41.81	.29	6.06	8.12	25.94	304.22	23464.02
40.64	180.	41.81	.29	6.06	8.10	25.94	305.82	-8396.38
40.64	0.	56.69	.56	6.10	8.67	27.27	313.25	72561.98
40.64	45.	56.69	.56	6.10	8.72	27.27	333.97	-22617.58
40.64	90.	56.69	.56	6.09	8.59	27.27	319.92	1331.07
40.64	135.	56.69	.56	6.08	8.40	27.27	306.67	60449.72
40.64	180.	56.69	.56	6.08	8.34	27.27	309.29	-10014.69
40.64	0.	66.51	.68	6.08	8.76	28.15	315.96	74016.91
40.64	45.	66.51	.68	6.08	8.81	28.15	340.10	-22705.78
40.64	90.	66.51	.68	6.07	8.69	28.15	323.86	1349.64
40.64	135.	66.51	.68	6.06	8.49	28.15	308.56	59731.70
40.64	180.	66.51	.68	6.05	8.43	28.15	311.47	-9508.46
40.64	0.	79.19	.80	6.09	8.88	29.26	319.29	75638.30
40.64	45.	79.19	.80	6.10	8.94	29.26	347.69	-22774.25
40.64	90.	79.19	.80	6.09	8.81	29.26	328.80	1378.69
40.64	135.	79.19	.80	6.07	8.61	29.26	311.03	57190.29
40.64	180.	79.19	.80	6.07	8.54	29.26	313.92	-7791.14
40.64	0.	89.50	.90	6.10	8.97	30.17	321.66	78005.88
40.64	45.	89.50	.90	6.11	9.03	30.17	353.49	-22965.20
40.64	90.	89.50	.90	6.09	8.89	30.17	332.46	1409.88
40.64	135.	89.50	.90	6.08	8.68	30.17	312.70	58170.79
40.64	180.	89.50	.90	6.07	8.61	30.17	315.75	-7424.53
40.64	0.	112.24	1.11	6.14	9.12	32.17	323.94	99476.31
40.64	45.	112.24	1.11	6.14	9.19	32.17	365.08	-23821.11
40.64	90.	112.24	1.11	6.13	9.06	32.17	340.82	1471.27
40.64	135.	112.24	1.11	6.11	8.86	32.17	318.21	48992.26
40.64	180.	112.24	1.11	6.10	8.80	32.17	321.90	-6739.80
60.96	0.	.00	.01	5.87	6.85	22.19	295.65	2.06
60.96	45.	.00	.01	5.87	6.89	22.19	295.65	-43569.31
60.96	90.	.00	.01	5.87	6.89	22.19	295.65	-43289.45
60.96	135.	.00	.01	5.87	6.86	22.19	295.65	-8161.45
60.96	180.	.00	.01	5.87	6.81	22.19	295.54	25778.46
60.96	0.	5.10	.08	5.88	7.35	22.88	296.94	22235.47
60.96	45.	5.10	.08	5.89	7.40	22.88	297.33	20015.58

60.96	90.	5.10	.08	5.89	7.49	22.88	298.78	1363.15
60.96	135.	5.10	.08	5.89	7.53	22.88	300.42	-27249.69
60.96	180.	5.10	.08	5.89	7.47	22.88	296.59	301966.50
60.96	0.	12.04	.20	5.85	7.70	23.81	298.98	27642.84
60.96	45.	12.04	.20	5.85	7.75	23.81	300.07	20485.70
60.96	90.	12.04	.20	5.85	7.86	23.81	303.74	1352.37
60.96	135.	12.04	.20	5.85	7.91	23.81	307.89	-28113.96
60.96	180.	12.04	.20	5.85	7.84	23.81	298.03	410132.70
60.96	0.	21.36	.32	5.92	7.94	25.06	301.40	35079.16
60.96	45.	21.36	.32	5.92	8.02	25.06	303.62	19704.33
60.96	90.	21.36	.32	5.93	8.16	25.06	310.12	1399.95
60.96	135.	21.36	.32	5.93	8.22	25.06	317.50	-28831.48
60.96	180.	21.36	.32	5.93	8.12	25.06	299.54	606050.90
60.96	0.	33.20	.51	5.94	8.19	26.65	304.66	44150.55
60.96	45.	33.20	.51	5.94	8.28	26.65	309.01	15235.26
60.96	90.	33.20	.51	5.95	8.44	26.65	318.87	1392.59
60.96	135.	33.20	.51	5.96	8.51	26.65	330.16	-28584.14
60.96	180.	33.20	.51	5.95	8.39	26.65	301.89	604903.30
60.96	0.	41.81	.56	6.07	8.30	27.81	307.45	-821.47
60.96	45.	41.81	.56	6.08	8.38	27.81	306.71	67140.24
60.96	90.	41.81	.56	6.09	8.61	27.81	322.34	1385.95
60.96	135.	41.81	.56	6.10	8.73	27.81	339.46	-29447.32
60.96	180.	41.81	.56	6.09	8.61	27.81	305.02	378921.80
60.96	0.	56.69	.85	6.10	8.65	29.78	310.05	105204.60
60.96	45.	56.69	.85	6.11	8.77	29.78	326.21	-4775.60
60.96	90.	56.69	.85	6.12	8.90	29.78	336.08	1379.21
60.96	135.	56.69	.85	6.12	8.94	29.78	348.42	-25240.49
60.96	180.	56.69	.85	6.11	8.80	29.78	308.12	347990.30
60.96	0.	66.51	1.00	6.08	8.74	31.07	312.52	104759.70
60.96	45.	66.51	1.00	6.09	8.86	31.07	331.27	-5220.84
60.96	90.	66.51	1.00	6.10	9.00	31.07	342.17	1390.45
60.96	135.	66.51	1.00	6.10	9.03	31.07	355.91	-25106.94
60.96	180.	66.51	1.00	6.09	8.89	31.07	310.11	348992.70
60.96	0.	79.19	1.19	6.09	8.87	32.75	315.20	111256.30
60.96	45.	79.19	1.19	6.11	8.99	32.75	337.51	-5146.19
60.96	90.	79.19	1.19	6.12	9.14	32.75	350.71	1421.94
60.96	135.	79.19	1.19	6.13	9.17	32.75	367.37	-25869.63
60.96	180.	79.19	1.19	6.11	9.02	32.75	311.09	485937.00
60.96	0.	89.50	1.36	6.10	8.99	34.10	317.13	138559.40
60.96	45.	89.50	1.36	6.12	9.12	34.10	346.84	-8951.14
60.96	90.	89.50	1.36	6.14	9.25	34.10	358.62	1430.09
60.96	135.	89.50	1.36	6.14	9.27	34.10	374.43	-25170.76
60.96	180.	89.50	1.36	6.12	9.11	34.10	312.53	526987.40
60.96	0.	112.24	1.67	6.15	9.20	37.10	321.65	173907.70
60.96	45.	112.24	1.67	6.16	9.34	37.10	364.99	-13785.21
60.96	90.	112.24	1.67	6.18	9.44	37.10	372.04	1405.45
60.96	135.	112.24	1.67	6.18	9.43	37.10	383.69	-21462.55
60.96	180.	112.24	1.67	6.16	9.29	37.10	322.38	228090.60
81.28	0.	.00	.01	5.87	6.80	22.19	295.55	-287.17
81.28	45.	.00	.01	5.87	6.85	22.19	295.55	-62383.43
81.28	90.	.00	.01	5.87	6.86	22.19	295.60	-51898.61
81.28	135.	.00	.01	5.87	6.86	22.19	295.65	-3819.23
81.28	180.	.00	.01	5.87	6.83	22.19	295.65	189.98
81.28	0.	5.10	.05	5.88	7.28	23.10	296.75	33664.98
81.28	45.	5.10	.05	5.88	7.31	23.10	297.09	6296.90
81.28	90.	5.10	.05	5.88	7.34	23.10	297.23	10982.75
81.28	135.	5.10	.05	5.88	7.37	23.10	297.33	25408.57
81.28	180.	5.10	.05	5.89	7.40	23.10	298.63	-23852.31
81.28	0.	12.04	.14	5.84	7.60	24.35	298.40	48728.44
81.28	45.	12.04	.14	5.84	7.63	24.35	299.31	-4779.46
81.28	90.	12.04	.14	5.84	7.66	24.35	299.64	1171.64
81.28	135.	12.04	.14	5.85	7.70	24.35	299.87	27385.33

81.28	180.	12.04	.14	5.85	7.74	24.35	302.93	-24630.20
81.28	0.	21.36	.21	5.91	7.81	26.02	300.57	55245.42
81.28	45.	21.36	.21	5.91	7.84	26.02	302.16	-5974.06
81.28	90.	21.36	.21	5.92	7.88	26.02	302.61	1328.18
81.28	135.	21.36	.21	5.92	7.93	26.02	302.92	30095.41
81.28	180.	21.36	.21	5.92	7.98	26.02	308.10	-25358.15
81.28	0.	33.20	.32	5.93	8.04	28.14	303.43	59229.06
81.28	45.	33.20	.32	5.93	8.07	28.14	306.03	-6465.37
81.28	90.	33.20	.32	5.93	8.11	28.14	306.76	1332.42
81.28	135.	33.20	.32	5.93	8.17	28.14	307.29	26320.99
81.28	180.	33.20	.32	5.94	8.23	28.14	314.61	-23955.83
81.28	0.	41.81	.36	6.07	8.20	29.65	305.33	67431.02
81.28	45.	41.81	.36	6.07	8.24	29.65	308.84	-7316.24
81.28	90.	41.81	.36	6.07	8.29	29.65	309.74	1394.61
81.28	135.	41.81	.36	6.08	8.35	29.65	310.42	24023.39
81.28	180.	41.81	.36	6.08	8.41	29.65	318.94	-22958.59
81.28	0.	56.69	.50	6.08	8.39	32.27	307.63	155996.20
81.28	45.	56.69	.50	6.08	8.45	32.27	314.97	-15098.77
81.28	90.	56.69	.50	6.08	8.49	32.27	314.97	1569.51
81.28	135.	56.69	.50	6.09	8.53	32.27	314.84	26488.08
81.28	180.	56.69	.50	6.09	8.59	32.27	325.33	-22807.49
81.28	0.	66.51	.60	6.06	8.49	34.00	309.59	172266.50
81.28	45.	66.51	.60	6.06	8.54	34.00	318.55	-16286.61
81.28	90.	66.51	.60	6.06	8.58	34.00	318.16	1634.68
81.28	135.	66.51	.60	6.07	8.62	34.00	317.66	27619.18
81.28	180.	66.51	.60	6.07	8.68	34.00	329.50	-22877.24
81.28	0.	79.19	.73	6.07	8.61	36.23	312.07	198030.40
81.28	45.	79.19	.73	6.08	8.67	36.23	323.46	-17557.90
81.28	90.	79.19	.73	6.08	8.71	36.23	322.55	1663.60
81.28	135.	79.19	.73	6.08	8.74	36.23	321.54	28842.94
81.28	180.	79.19	.73	6.09	8.80	36.23	335.45	-23007.73
81.28	0.	89.50	.81	6.08	8.69	38.04	314.05	199488.40
81.28	45.	89.50	.81	6.08	8.75	38.04	326.24	-17197.16
81.28	90.	89.50	.81	6.09	8.79	38.04	325.46	1736.70
81.28	135.	89.50	.81	6.09	8.82	38.04	324.56	28079.14
81.28	180.	89.50	.81	6.09	8.88	38.04	339.56	-22776.91
81.28	0.	112.24	1.02	6.11	8.85	41.65	316.74	424935.60
81.28	45.	112.24	1.02	6.12	8.93	41.65	334.47	-19816.84
81.28	90.	112.24	1.02	6.12	8.97	41.65	332.97	1741.99
81.28	135.	112.24	1.02	6.12	9.01	41.65	331.38	30752.79
81.28	180.	112.24	1.02	6.13	9.08	41.65	351.51	-23662.71
101.60	0.	.00	.01	5.87	6.82	22.19	295.66	-16106.69
101.60	45.	.00	.01	5.87	6.85	22.19	295.54	-59720.03
101.60	90.	.00	.01	5.87	6.84	22.19	295.55	-71099.11
101.60	135.	.00	.01	5.87	6.82	22.19	295.55	341.50
101.60	180.	.00	.01	5.87	6.78	22.19	295.55	-2.02
101.60	0.	5.10	.05	5.88	7.24	23.33	296.32	-199482.70
101.60	45.	5.10	.05	5.88	7.28	23.33	297.01	-14936.05
101.60	90.	5.10	.05	5.88	7.30	23.33	297.03	13349.67
101.60	135.	5.10	.05	5.88	7.31	23.33	297.06	24664.97
101.60	180.	5.10	.05	5.88	7.32	23.33	297.67	-21846.39
101.60	0.	12.04	.13	5.84	7.55	24.89	297.21	-110221.70
101.60	45.	12.04	.13	5.84	7.59	24.89	299.16	-31145.57
101.60	90.	12.04	.13	5.84	7.63	24.89	299.33	2932.90
101.60	135.	12.04	.13	5.84	7.65	24.89	299.53	22328.98
101.60	180.	12.04	.13	5.85	7.68	24.89	301.10	-21898.29
101.60	0.	21.36	.18	5.91	7.74	26.97	298.51	-99295.66
101.60	45.	21.36	.18	5.91	7.80	26.97	301.94	-35715.43
101.60	90.	21.36	.18	5.91	7.84	26.97	302.11	3375.08
101.60	135.	21.36	.18	5.92	7.87	26.97	302.30	29939.78
101.60	180.	21.36	.18	5.92	7.91	26.97	305.20	-24415.97
101.60	0.	33.20	.28	5.92	7.96	29.60	300.41	-103001.90

101.60	45.	33.20	.28	5.93	8.02	29.60	305.57	-35873.50
101.60	90.	33.20	.28	5.93	8.06	29.60	305.66	3466.50
101.60	135.	33.20	.28	5.93	8.09	29.60	305.78	34497.99
101.60	180.	33.20	.28	5.93	8.13	29.60	310.25	-25456.72
101.60	0.	41.81	.30	6.06	8.09	31.49	301.60	-95035.72
101.60	45.	41.81	.30	6.07	8.16	31.49	307.78	-37384.98
101.60	90.	41.81	.30	6.07	8.21	31.49	308.03	3797.85
101.60	135.	41.81	.30	6.07	8.25	31.49	308.35	30785.12
101.60	180.	41.81	.30	6.07	8.29	31.49	313.33	-24370.01
101.60	0.	56.69	.40	6.07	8.27	34.76	303.90	-89824.38
101.60	45.	56.69	.40	6.07	8.33	34.76	311.58	-42115.24
101.60	90.	56.69	.40	6.08	8.37	34.76	311.46	5231.10
101.60	135.	56.69	.40	6.08	8.40	34.76	311.51	28404.82
101.60	180.	56.69	.40	6.08	8.42	34.76	315.46	-21365.78
101.60	0.	66.51	.49	6.05	8.36	36.92	305.50	-89667.69
101.60	45.	66.51	.49	6.05	8.42	36.92	314.22	-42834.54
101.60	90.	66.51	.49	6.05	8.46	36.92	313.95	5560.65
101.60	135.	66.51	.49	6.06	8.48	36.92	313.86	32928.57
101.60	180.	66.51	.49	6.06	8.51	36.92	318.58	-22637.54
101.60	0.	79.19	.58	6.06	8.48	39.71	307.67	-91538.20
101.60	45.	79.19	.58	6.07	8.54	39.71	317.77	-42138.05
101.60	90.	79.19	.58	6.07	8.58	39.71	317.39	5721.01
101.60	135.	79.19	.58	6.07	8.60	39.71	317.24	30707.26
101.60	180.	79.19	.58	6.07	8.62	39.71	322.16	-21314.41
101.60	0.	89.50	.64	6.07	8.55	41.65	309.37	-93088.86
101.60	45.	89.50	.64	6.07	8.61	41.65	320.10	-45473.25
101.60	90.	89.50	.64	6.07	8.63	41.65	318.69	7314.75
101.60	135.	89.50	.64	6.07	8.64	41.65	317.48	72474.10
101.60	180.	89.50	.64	6.07	8.67	41.65	323.91	-28710.95
101.60	0.	112.24	.79	6.10	8.74	41.65	313.30	-494054.60
101.60	45.	112.24	.79	6.10	8.80	41.65	329.23	-29401.35
101.60	90.	112.24	.79	6.10	8.79	41.65	324.50	3987.84
101.60	135.	112.24	.79	6.10	8.77	41.65	320.28	42764.21
101.60	180.	112.24	.79	6.10	8.77	41.65	325.05	-17400.90